PH.D. THESIS IN CHEMICAL ENGINEERING

XXIVth Cycle

Ignition Process in Non-Conventional Combustion System

Scientific Committee

Prof. Antonio Cavaliere
Eng. Maria Rosaria de Joannon
Eng. Pino Sabia

Candidate

Eng.Antonio Picarelli

IGNITION PROCESS IN NON-CONVENTIONAL COMBUSTION SYSTEM

Table of Contents

Introduction

The main pollutants responsible for the global and local environmental impact, are species such as NOx, soot particles and solid polycyclic aromatic hydrocarbons (PAHs) formed during combustion processes. The interest of the scientific community is focused on identifying new technologies that enable more efficient energy production and a simultaneous reduction of the pollutants emission. In particular, the trend established in recent years regarding the identification of operating conditions, different from those of traditional systems, which may allow the achievement of these objectives.

In this context, the use of new combustion processes, which use high levels of diluent species, such as nitrogen, water vapor or gas exhaust, seems to be promising. The high degree of dilution greatly increases the heat capacity of the system and consequently lowers adiabatic flame temperature. These characteristics allow to control the production of pollutant such as NOx, soot and aromatic compounds. In particular, in order to reach working temperatures lower than the critical value that causes the production of these pollutants, the composition of the mixture must be outside the flammability limits. Under these conditions, the oxidative process can evolve only in the presence of a pre-heating of reagents leading to an inlet temperature higher than the auto-ignition of the mixture.

Different definitions are present in the scientific literature concerning such or similar technologies. Each definitions differs for some aspects and sometimes seems to be difficult to distinguish among them. The topic of such thesis work is focused on a specific technology known in literature as MILD combustion. The word “MILD” is both an acronym (Moderate or intense low-oxygen dilution) and also a slavish definition relating to the characteristics of the process that will be widely discussed in this thesis.

MILD combustion is a technology of interest in many applications, from industrial furnaces for the processing of raw materials to gas turbine combustors, but also in afterburners as a process of pollutants abatement. For instance, for gas turbine, the diluents used (such as recycled flue gases and/or steam) are fed in concentrations such that the maximum temperature reached is lower than the maximum temperature relating to mechanical resistance of the blades. The initial temperature of the mixtures used is high and the working range of temperatures in which the process evolves, allows to achieve both high thermodynamic efficiency and a good preservation of the turbine blades.

It also eliminates the effects of combustion instability, such as noise and fluctuation of the pressure that could lead to resonance phenomena, responsible for the break of some mechanical parts. Studies based on this type of process, were conducted on typical chemical reactors models.

The peculiarity of this approach is due to the opportunity of highlighting combustion peculiarities process using different elementary configurations. The behavior of these reactors has been extensively modeled by means of conservation equations needed to describe these systems, which, under ideal conditions, are functions of a single parameter, such as time or space. This configuration allows to study the evolution of the oxidation process as a function of one spatial coordinate, and therefore represents an optimal configuration for the evaluation of the characteristic times of the process. Moreover such systems are often indicated as zero or one dimensional approach.

This optimal aspect has promoted the development of several software suitable to simulate the behavior of ideal reactors and the development of new models on the oxidative process. Although there are numerous studies in scientific literature, both numerical and experimental, this new type of combustion, there is a need to characterize the process by further basic studies.

The lack of fundamental investigations depends on the difficulty of creating a laboratory-scale plant suitable for working with the high operating temperatures typical of MILD combustion. These working conditions imply difficulties in the choice of materials and sealing problems of the reactor. These problems can be solved more easily in a pilot-scale plant or industrial.

During this thesis work, the attention was focused on the study of the ignition process of different fuel blends in working conditions typical of MILD combustion. An experimental work was carried out in a tubular flow reactor, at atmospheric pressure, high temperatures and degree of dilution, typical working conditions of industrial burners operating in MILD combustion. The ignition process was analyzed and auto-ignition times were evaluated on the basis of temperature profile acquired. A criterion based on the increment of temperatures observed in the experimental reactor was used to evaluate the ignition times. Moreover, the contribution of this thesis is important according to the absence of experimental data available in literature at atmospheric pressure.

Some crucial working parameters were changed in order to characterize the ignition process. The degree of dilution, the feed ratio as well as the initial temperatures of the system and chemical nature of the fuel were widely investigated.

Two fuel blends were tested in order to create a rich database concerning the ignition process in MILD conditions. Methane blends were used as a benchmark fuel in the scientific research and the simplest hydrocarbon. It is widely used in several fields of application both in industrial or pilot-scale plants. Moreover, several studies are available in literature concerning the oxidation processes of pure methane blends or mixed with different hydrocarbons. In addition, methane oxidation process follows reaction pathways which are well know and hence also the kinetic scheme is widely characterized by now.

Nevertheless, further studies are necessary in order to deepen the knowledge of the oxidation process in highly diluted and preheated conditions.

Afterwards, further study were also carried out with different fuel blends denoted as *biogas*. The growing interest in new energy carriers derived from biomass treatment leads to the opportunity of testing such experimental facility with different fuels. In particular the composition of the fuel was made on the basis of literature evidences and obtained by subjecting the biomass to a slow/conventional pyrolytic process. Moreover, the intrinsic peculiarities of such mixture, make it suitable for being used in combustion system operating in MILD conditions. The low calorific value of the blends along with the large amount of diluent species made it as an ideal candidate for combustion system that evolves in MILD conditions.

Several experimental tests were also carried out for *biogas* and different crucial parameters were investigated. The overall reactivity of the system was analyzed and auto-ignition times were also evaluated. Different phenomenologies were observed and reactivity maps were delineated in function of the different working parameters.

In order to deepen the knowledge about the kinetic pathways follow by the mixtures, a sampling system was implemented on the experimental plant. The characterization of the exhaust gases were carried out by means of a micro gas chromatograph. The concentration of different species allows to understand the kinetic scheme in highly diluted and preheated conditions.

A numerical study was also carried out in parallel. This work is mandatory in order to tune and validate, in these new combustion conditions, all the kinetic mechanisms available in literature. Such mechanisms are actually used to evaluate the combustion processes in working condition typical of traditional combustion system. In addition, the possibility to implement such mechanisms in CFD commercial software make necessary a deepen study

also on basic aspects of the combustion process, such as characteristic times etc. In combustion processes that evolves in MILD conditions, the highly diluted and pre-heated mixtures follow different chemical oxidation pathways due to the intrinsic characteristics of the process far from being a traditional combustion.

Chapter I

MILD Combustion

I.1 - Problem identification

In the century of global warming causes by greenhouse gases emissions, one of the main targets in energy production systems development has been to obtain a combustion process that allows to reduce pollutants emission, to increase the process efficiency, and consequently to reduce fuel consumption and hence CO_2 emission.

However, in processes involving combustion, the abatement, of pollutants often comes at the price of efficiency losses. In other words, the existing combustion system remains to be difficult to simultaneously satisfy the requirements for both high efficiency and low pollution.

For instance, although application of the swirl burner (N. Syred 2006) and the oxy-fuel burner can increase the flame temperature, stability and combustion intensity, they yield a great deal of pollutants. On the contrary, the technology of cooling flame (J. A. Wunning 1997) may cause combustion instability problems, due to the temperature reduction, leading to incomplete combustion of fuels and high CO emission. Moreover reduce NO_x emissions by creating fuel-lean and oxygen-lean combustion regions leading to a decrease in the combustion intensity and efficiency under certain conditions. Another example is the fluidized bed combustion technology (J. Koornneef 2007). It is able to use various kinds of low-grade solid fuels and low NO_x emissions but cannot overcome the problem of relatively low combustion efficiency due to low combustion temperature. A combustion chamber using a higher range of temperatures than the traditional one, obtained through a

pre-heating of reactants, could allow an higher fuel conversion in CO_2 and H_2O and the possibility to maximize the enthalpy content exhausted gases to pre-heat air and/or reactants coming inside combustion chamber. This operation may need other fuel to feed burners in pre-combustion chamber and could cause a higher production of pollutants emissions that originate greenhouse effect. On the other side, the possibility to raise work temperature is fought by drastic increasing NO_x production.

MILD (Moderate or intense low-oxygen dilution) combustion processes evolve in a temperature and concentration range outside the sphere of interest of standard combustion processes and is one of the credible candidate to simultaneously meet thermal efficiency need and pollutant emission restriction. Moreover it represents a trade-off between optimizing fuel conversion in terms of energy saving and pollutant abatement, and maintaining the configurations of traditional processes. MILD combustion regime operates using contemporaneously high temperatures and high dilution of reacting mixture with inert gases, in order to make use of temperature positive effects and, at the same time, to keep under control their gradients. In fact dilution allows increasing thermal capacity of the system and thus contain adiabatic flame temperature in a range that keeps NO_x emission under control. In order to smother the adiabatic flame temperatures reached during combustion process is necessary to use high mixture dilution levels, so that the composition falls out from LFL-UFL (Lower Flammable Limit – Upper Flammable Limit). To realize the process combustion is hence necessary to keep the pre-heating temperature higher than the auto-ignition temperature of mixture. Heat and flue gas recirculation allow to attain the task about pre-heating temperature. The recirculation of hot combustion products decreases oxygen concentration locally and increases the temperature of the reactants. This slows the reactions and leads to a distributed reaction zone, combustion occurs in homogeneous conditions and in combustion chamber uniform concentration and

temperature profiles of the chemical species can be realized. Various advantages derive from using high preheating temperatures. Higher temperature allows an higher efficiency of oxidation process. This induced an higher speed oxidation in the first part of the process of combustion, for liquids and solids fuel, and an acceleration in the physical process of atomization, vaporization and gasification. This means that the use of high initial temperatures implies a higher flexibility in the choice of the fuel. Working temperatures should determine an important reduction in the production of NO_x and soot.

As a matter of fact, in the Fig I.1 and I.2 soot yield is reported as function of temperature during experiments realized in a shock tube for several mixtures in pyrolysis and oxidation conditions (G. L. Agafonov 2011).

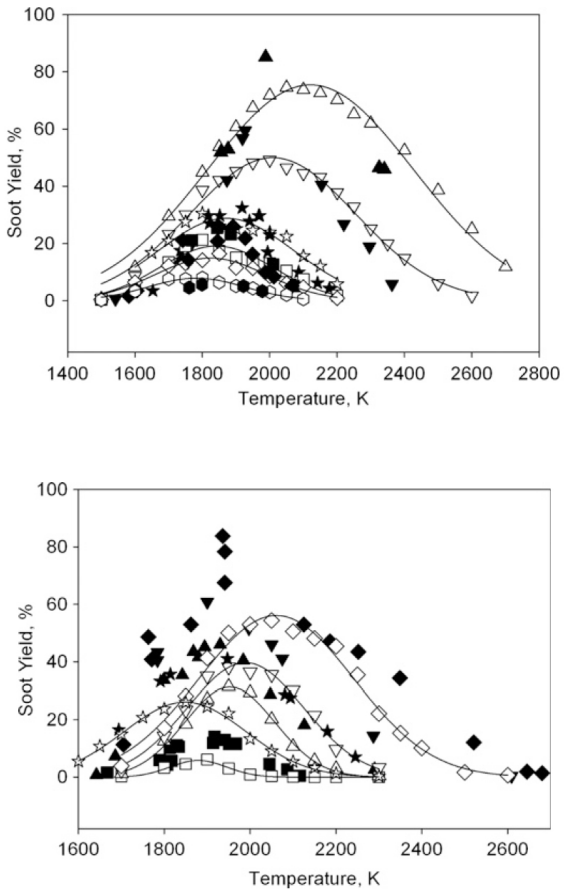

Fig. I.1 - Temperature dependences of the experimentally and numerically measured and calculated soot yields for various toluene/Ar mixtures (upper figure) and benzene/Ar (lower figure) in a shock tube: P = 3.0 bar.

A number of aromatic (benzene, toluene, and ethylbenzene) and aliphatic (methane, propane and propylene) hydrocarbons were tested. Although they have different chemical structures, the reported data identify a range of temperature, independently from the type of fuel, in which production of particulate matter is relevant.

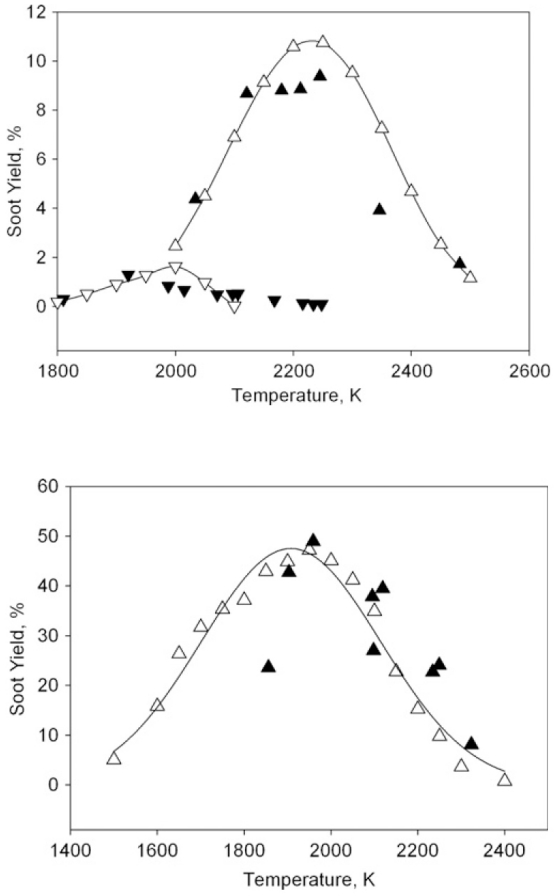

Fig. I.2 - Temperature dependences of the experimentally and numerically measured and calculated soot yields for various methane/Ar mixtures (upper figure) and ethylbenzene/Ar (lower figure) in a shock tube: P = 3.0 bar.

In particular, the maximum value of yield soot is obtained using toluene (Fig. I.1 on the left) for values of temperature of 2100 K while lower values are obtained for temperature lower than 1800 K or higher than 2400 K. The same trend is observable for different fuel even if soot yield are lower and (for ethylbenzene) with the curve maximum shifted along lower temperature values (from 1700 K to 2100 K).

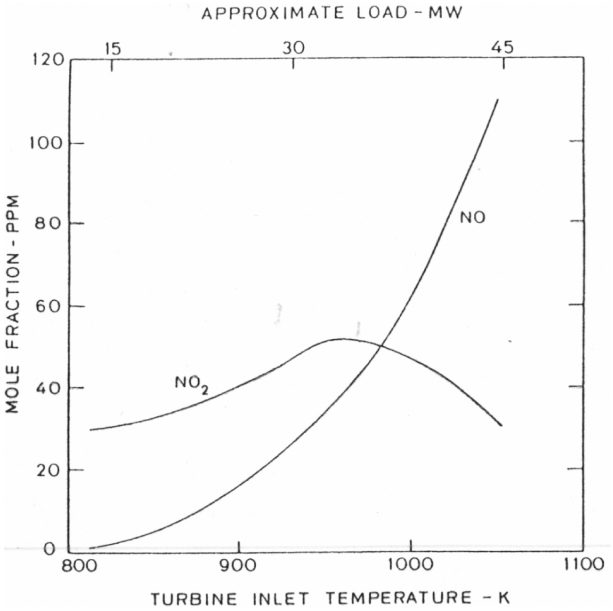

Fig.I.3 - Concentrations of NO and NO2 versus the initial temperature in a gas- turbine burner.

The Fig I.3 shows the dependence of the production of NO_x from the temperature in a flame in a gas turbine burner (Y. H. Song 1981) . In particular it is possible to see how the production of NO is extremely dependent on the temperature. Considering temperature values lower than 1000 K, the NO_x class is represented by NO_2. Its molar concentration is almost constant as function of the temperature. For temperatures values higher of 1000 K the NO concentration increases abruptly with the temperature.

The production of this class of pollutants goes by through three kinetic mechanisms; the most important of them is the following one:

(1) $$O + N_2 \rightarrow NO + N$$

(2) $$N + O_2 \rightarrow NO + O$$

(3) $$N + OH \rightarrow NO + H$$

In steady-state the rate of production of NO is expressed by the equation:

(4) $$\frac{\delta(NO)}{\delta t} = K \cdot [N_2] \cdot [O]$$

Where *K* is the kinetic constant end express the dependence of the reaction velocity from the temperature. A decrease of temperature and of O radicals concentration implies a minor production of NO. The dilution of the system, for example with gas or exhausted gas recycled in the combustion chamber, should bring to an increase of the thermal capacity of the mixture and so to lower temperatures and concentration of the O radicals, limiting the NO production. The Fig I.4 shows the variation of the NO_x production in a premixed flame in dependence of the feed fuel/combustive R on curves normalized on the dilution rate αN_2.

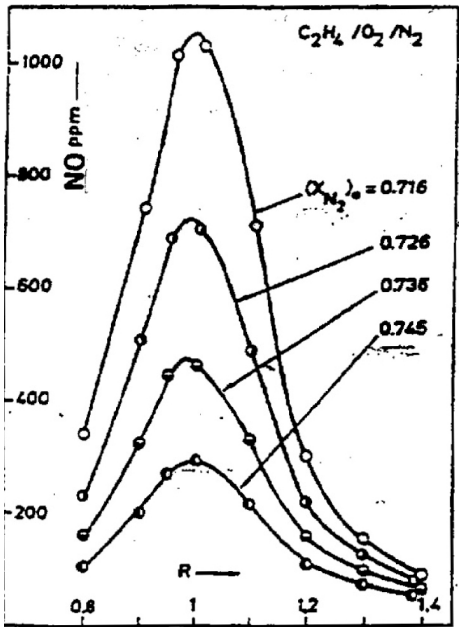

Fig I.4 - NO concentration in a premixed flame normalized to of the feed fuel/combustive R and on the dilution rate α_{N_2} .

The NO production reaches a maximum value in correspondence of the stoichiometric ratio feed R=1, that implies the system reaches the maximum flame adiabatic temperature, meanwhile an increase of the dilution degree αN_2 lowers the production of NO_x. In fact, increasing the dilution rate of the system, the thermal capacity of the system increases and the adiabatic temperature decreases leading to a reduction of NO_x production. The heat capacity of the system can be enhanced using inert species, such as hydrogen, or recycling

exhaust gases that have a high content of steam water and carbon dioxide. This last solution is very attractive since it assures high dilution level and meanwhile pre-heating of reactants up to temperature necessary to sustain the oxidation process.

I.2 - Definition

Features of combustion processes, such as maximum temperature, structure of the pyrolytic and oxidative region, species distribution and pollutant formation, are the effects of complex interleaved heat and mass transport phenomena and kinetics. The initial and boundary conditions have a significant influence on the evolution of the whole process. However, they become even more significant when the process evolves in conditions that can be considered as occurring at the boundary of an admissible range of parameters. This is the case of MILD combustion processes which, by definition, evolve in different temperatures and concentration ranges from those of standard combustion processes.

In order to define the conditions in which MILD combustion evolves, we may start by considering a homogeneous charge of fuel, such as methane, and air at stoichiometric conditions and at a temperature of 300 K. The temperature increase ΔT related to complete fuel conversion can be computed by the following heat balance relation:

$$m_{in} \cdot Y_{CH_4} \cdot \Delta H_r = m_{out} \cdot c_p \cdot \Delta T \qquad (5)$$

where $m_{in} = m_{out}$ is the mass flow, Y_{CH_4} the fuel mass fraction, ΔH_r the heat of reaction, c_p the specific heat capacity at constant pressure and ΔT the temperature increase during oxidation. The relation between temperatures and mixture compositions, given by relation (5), is represented schematically in Fig I.5, where a plane $T_{inlet} - X_{O_2}$ is reported. On this plane the iso-concentration lines can be associated to a well identified temperature

increase, such as expressed by relation (5) and reported for a representative number of X_{O_2}. All the values on this plane are obtained by considering the thermodynamic properties constant with temperature. With such an approximation ΔT corresponding to a fixed X_{O_2} is independent of the initial temperature of the mixture. The final temperature T reached by system will be $T = T_{inlet} + \Delta T$.

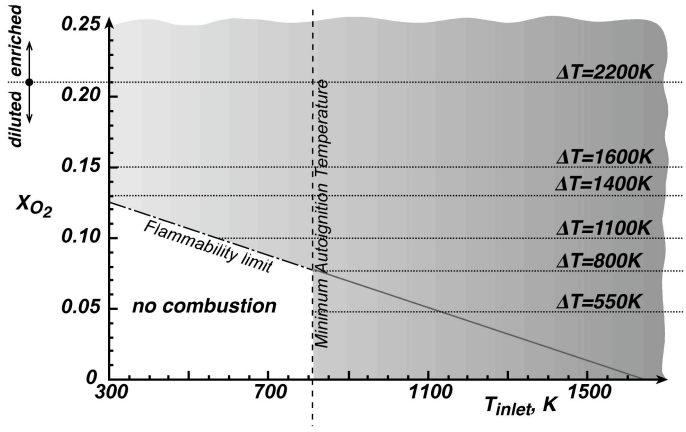

Fig. I.5 - $T_{inlet} - X_{O_2}$ plane identifying the region at different temperature increases during oxidation

The temperature increase corresponding to stoichiometric standard conditions ($X_{O_2} = 0.21$) is about 2200 K. It can be straightaway seen that a decrease in the oxygen molar fraction, while keeping the fuel/oxygen ratio constant, corresponds to a decrease in ΔT. For instance, the temperature increase related to $X_{O_2} = 0.15$ is about 1600K. Starting from X_{O_2} of about 0.125 (ΔT =1400K) the iso-concentration lines intersect a dashed-dotted line. This represents the flammability limit associated with the maximum dilution level allowable for a stoichiometric methane/oxygen/diluent for the propagation of a deflagration structure. It is well known from the literature that this is possible only when the temperature increase due to the oxidative process is high enough to ensure a feedback

of radicals and heat so that fresh mixture can reach the ignition temperature and then autoignite. The flammability limit intersects a vertical dashed line, drawn at the minimum auto-ignition temperature $T_{ign}^{\min}$, at T_{inlet} = 800K(M. G. Zabetakis 1965). For $T_{inlet} < T_{ign}^{\min}$ and X_{O_2} below the flammability limit, a deflagration structure cannot be sustained and no combustion occurs without an external permanent source. In contrast, for the same dilution levels the oxidation process can evolve if T_{inlet} is higher than $T_{ign}^{\min}$. In these conditions, very low temperature increases with respect to standard combustion processes are obtained.

It should be pointed out that the minimum auto-ignition temperature is independent of the dilution of the fuel/oxidant mixture (M. G. Zabetakis 1965). In such a case, dilution affects the ignition time, as will be discussed below.

On the basis of these indications MILD combustion is defined by Cavaliere A. and de Joannon M. (A. Cavaliere 2004) as follows:"A combustion process is termed "mild" when the inlet temperature of a reactant mixture is higher than the self-ignition temperature of the mixture, whereas the maximum allowable temperature increase with respect to the inlet temperature during combustion is lower than self ignition temperature "

As clearly shown in Fig I.5, the process evolves in a narrow temperature range, which could be placed in an intermediate region between the very fast kinetics of the oxidative undiluted conditions and the relatively slow kinetics linked to low-temperature self-ignition regimes.

By defining $\Delta T_{inlet} = T_{inlet} - T_{ign}^{\min}$ it is possible to summarize the different combustion regimes on the basis of the main macro area of possible processes. They are illustrated in Fig I.6 in which ΔT and ΔT_{inlet} are reported on the ordinate and abscissa axis respectively.

In this diagram four main categories are identified. Below the abscissa are processes with a negative maximum temperature increase. They are identified as pyrolysis processes because they are endothermic in nature and are subdivided into two categories, *auto-incepted pyrolysis* and *assisted pyrolysis*. The first needs no external source to make the processes effective and is located in the lower-right quadrant, for $\Delta T_{inlet} > 0$. The second is called *assisted pyrolysis*, because it needs external heating or a catalytic device in order to develop. It is located in the lower-left quadrant, where the inlet temperature is lower than the ignition temperature ($\Delta T_{inlet} < 0$), which in the case of pyrolysis should be called *inception temperature*. In principle and in a rigorous way the maximum temperature should always be higher than the frozen temperature. Therefore, the lower quadrants should not exist. In practice, pyrolytic conditions are obtained for high mixture fraction values.

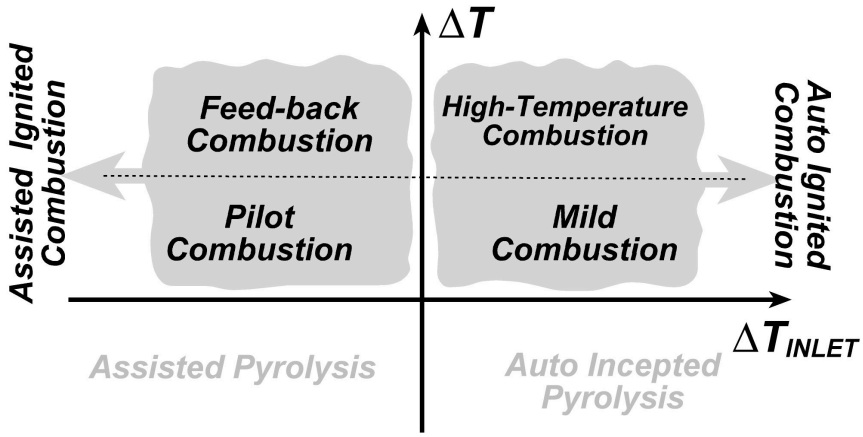

Fig. I.6 - Combustion categories as a function of ΔT and ΔT_{inlet}

The upper-left quadrant is the region of assisted ignited combustion for which the maximum temperature difference is positive, whereas the inlet ignition differential is negative. This is the classical, standard combustion condition, in which the first ignition of the mixture is ensured by heat (or other source) by an external source, since reactants do

not carry enough sensitive enthalpy to incept the process. This region corresponds to the region on the left side of $T_{ign}^{\min}$ on the plane in Fig I.5. This region is also divided in two parts. Feed-back combustion is associated to the region above the flammability line, pilot combustion to the region below it.

Spontaneous inception of oxidation occurs in the processes in the upper-right quadrant and are classified as *auto ignited combustion*. In this case the differential inlet temperature is positive and auto-ignition should occur with no external energy input. Also in this case two regions can be identified. The first, known as *high-temperature combustion*, is the region where the system can increase its temperature up to values comparable to air/fuel systems in stoichiometric condition. In contrast, in the second region the maximum ΔT is lower than a certain value, as shown in Fig I.6. This region has been termed *MILD combustion* (A. Cavaliere 2004) both because the temperature increase is quite mild and because reference is made to diluted conditions according to the acronym, Moderate or Intense Level of Dilution. The definition is rigorous in the sense that it is not ambiguous and is based on a conservative criterion identifying approximate conditions in which oxidation is more controlled by auto ignition rather than by the heat released by the oxidation itself. Figs I.5 and I.6 are only indicative of the range of MILD combustion and are used to clarify the basic concept behind it. A more precise boundary of the region in which it occurs can be obtained only if specific processes have to be analyzed in detail, in terms of fuel type, system composition and configuration considered.

Categorization of possible processes occurring in MILD combustion is not trivial due to the particular characteristics that distinguish it from standard combustion, which make it difficult to associate the processes occurring in different configurations and conditions to the well-known identified categories of standard processes, such as deflagration or

diffusion flames. This consideration will be clear after the analysis of the main features of oxidation evolving in MILD conditions that are reported in the following section.

It is possible to give other definitions, available in literature, of the MILD combustion that stresses the peculiar characteristics of such a process. In particular (N. Peters 2000) has suggested an analytic definition basing on the absence of ignition and of extinction of oxidation process that occurs for highly diluted and pre-heated mixtures. In particular the authors speak about a fuel-comburent-diluent system perfectly mixed, in flow and in adiabatic system considering a kinetic of reaction of the first order with a reaction rate defined by the following equation:

$$\omega = \frac{B}{\Omega \cdot \phi \cdot \varepsilon \cdot \xi \cdot \pi \cdot \left(-E/P \cdot T\right)} \tag{6}$$

In a-dimensional terms the representative equations of the system are:

$$\frac{dY}{dt} = 1 - Y - Da \cdot Y \cdot \exp(-E/T) \tag{7}$$

$$\frac{dT}{dt} = 1 - T + Q \cdot Da \cdot Y \cdot \exp(-E/T) \tag{8}$$

where:

$$Y = Y_{Fu}/Y_F \tag{9}$$

$$Da = B \cdot t \tag{10}$$

$$T = T/T_u \tag{11}$$

$$E = E/R \cdot T_u \tag{12}$$

$$Q = \frac{Q \cdot Y_{Fu}}{c_p \cdot W_F \cdot T_u} \tag{13}$$

In these correlations Y represents the mass fractions, T the temperatures, *Da* is the Damkoehler number. The subscript F regards the fuel while the subscript *u* concerns about the starting condition of the systems. The behaviour of the system can be characterized on the basis of the time reaction B^{-1} and on the permanence time $\tau = m/M$.

In steady state the following relations represent the solutions of the system:

$$1 - T_s + Da \cdot (1 + Q - T_s)\exp(-E/T_s) = 0 \qquad (14)$$

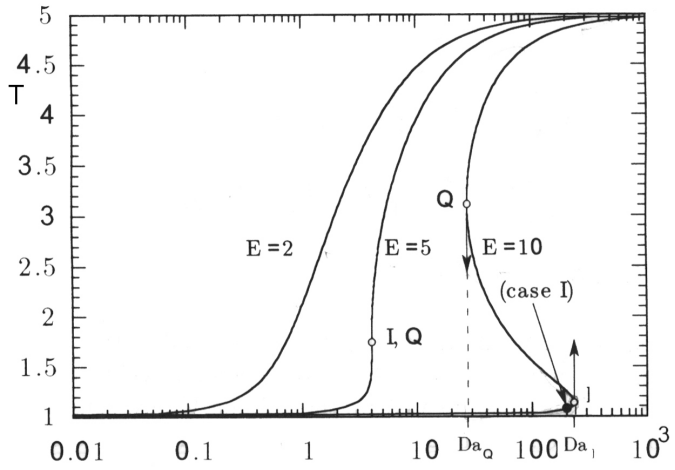

Fig. I.7 - Temperature (a-dimensional) of work in a CSTR in dependence of the Damkoehler number .

The Fig I.7 reports the system temperature in dependence of the Damkoehler number on curves parametric in the a-dimensional parameter E. The value of the parameter Q in this case graph is 4, $T_u = 1$ for $Y = 1$ while $T_u = 1 + Q$ for $Y = 0$. Changing the value E the curve assumes a characteristic "S" shape, hence three solutions can be obtained. The described curve indicates a hysteresis behaviour and the points Q and I are bifurcation points of the system. In particular the I point is an ignition point: for values of Damkoehler number is equal to Da_I the solutions moves up to the superior branch; the point Q is a

turn-off point of the reactor and so the solution of the superior branch falls down to the inferior branch.

It possible to analytically find the vertical tangent to the curve by setting the following condition:

$$\frac{\delta Da}{\delta Ts} = 0 \tag{15}$$

and the roots of the equation obtained are:

$$T_I = (2+Q)\cdot E + [(E\cdot Q - 4\cdot(1+Q)\cdot E\cdot Q]^{1/2} \tag{16}$$

$$T_Q = (2+Q)\cdot E + [(E\cdot Q - 4\cdot(1+Q)\cdot E\cdot Q]^{1/2} \tag{17}$$

The condition for which the ignition point and the extinction point are the same implies:

$$E = \frac{4\cdot(1+Q)}{Q} \tag{18}$$

If it is set the condition $E \geq 4\cdot(1+Q)/Q$ it is not possible that the two points are real and distinct solutions and so curves like “S” with multiple solutions are not possible solutions. In these conditions it is to possible to have ignitions or extinguishments but just a soft passage from the conditions of turn-off reactor to that one of turn-on reactor. This is the condition for which the combustion is named MILD. Peters associates the absence of ignition and extinguishment of the oxidation reaction to the peculiar absence of noise of the MILD process. For this particular feature this new combustion process is also referred in literature with the angles axon term “noiseless”.

I.3 - Characteristics

On the basis of the definition given above several peculiarities of such combustion mode could be highlighted. The classification reported in the previous section places MILD combustion in an atypical range of temperatures with respect to all other oxidation processes associated with combustion.

One of the peculiarities of this combustion mode is the absence of a flame front. Actually in the conventional burners the real chemical reactor is the steady front flame, an area stretched by turbulence, on which typical reactions of combustion processes occur. Although the thickness of the front of flame is very tight, it hosts great temperature and species concentration gradients. The location of this chemical rector (flame front) and its stability in the combustion chamber depends on many fluidynamic parameters, thus the design of system geometry is very important and complicated, in fact it is necessary a preliminary study in order to maximize combustion efficiency. If mixture is highly diluted (beyond flammability limits) and preheated to temperatures that allow auto-ignition, there will not be a front flame but a reaction volume that extends to the whole combustion chamber. Furthermore in these operative conditions, there are no problems related to flame instability, hence this results in a simplification of reactants mixing and flame stabilization devices. This is what happens in MILD combustion processes.

Combustors working in MILD combustion conditions have been developed and studied in industry and academia (J. Yuan 1999; B. Özdemir 2001; A. Cavigiolo 2003; C. Galletti 2007; M. Fantuzzi 2008; P. R. Medwell 2008) . In literature there are different jobs that ensure the existence of a homogeneous combustion zone within the combustion chamber and assert that one of the most remarkable characteristics of such combustors is that they develop oxidation processes with negligible “visible” emission. When MILD combustion

happens the entire furnace is bright and transparent, i.e. no flame is visible (J. A. Wunning 1997; M. Katsuki 1998; H. Tsuji 2003; A. Cavaliere 2004), so that it is often called "flameless combustion" or "flameless oxidation" (FLOX) (J. A. Wunning 1997). An example of such a unique phenomenology is shown in the pictures reported in Fig I.8. On the left-hand side a flame obtained in a 40MW natural gas burner working in standard conditions is reported (A. Saponaro 2009), where the fuel is fed by a central nozzle. In this case a diffusion-controlled flame with both shape and visible emission of traditional characteristics was stabilized. The compact yellow region develops around the burner axis and extends throughout the combustion chamber.

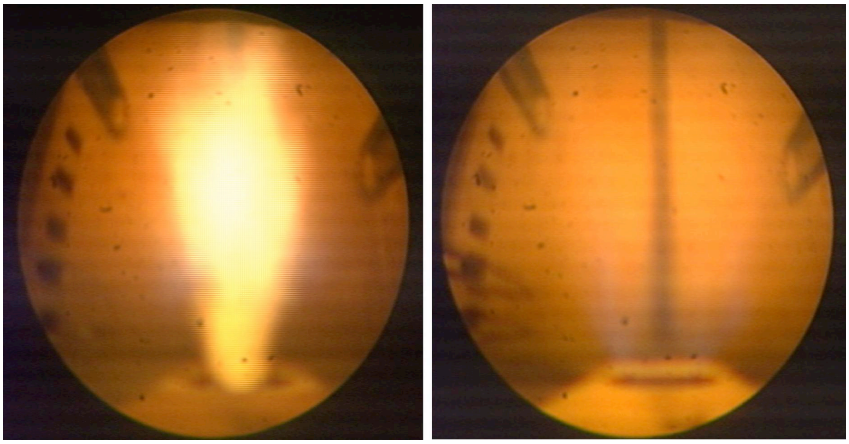

Fig. I.8 - Image of a natural gas traditional flame (left) and natural gas flameless combustion (right)

The image reported on the right-hand side of Fig. I.8 was obtained by changing the fluid-dynamic configuration. In this case, natural gas was injected by lateral nozzles into the exhaust gas flow of the internal recirculation drawn into the inlet air flow. A very imperceptible bluish emission is present in the first zone of the combustion chamber. The most relevant characteristic of the new combustion regime is revealed by visual observation of the combustion chamber. The image shows details of its internal part: it is possible to observe the hopper at the bottom of the chamber, which is emitting due to the heating of the refractory coating by radiative heat transfer from the reaction region. This

latter is not delimited to a portion of the combustion chamber but extends into most of this, as testified by the extension of the hopper's emitting region. This is the basis on which MILD is referred to as distributed combustion or a volumetric combustion regime instead of a flame front combustion regime (A. Milani 2001) as written before.

There have been several experiments that allow to characterize combustion properties by means of optical analyses. Gupta (A. K. Gupta 17-18 January 2000) has investigated the light emission coming by flames of several fuels using pre-heated up to 900°C-1100°C and oxygen concentration comprised between 5% and 21%. In this work author demonstrated that flame presents several colors in dependence of dilution degrees of mixture: from yellow to blue, from blue to light green, to green and in some conditions the flame does not present any emission in the visible spectrum. Different luminous emission characteristics have been detected in other conditions that cause a faint chemiluminescence in particular, in the blue and or green spectral range. For instance, Yasuda (T. Yasuda 1999) observed emission in the green band from propane flames. Similar behavior was also reported by de Joannon et al. (M. De Joannon 2000; M. de Joannon 2000) for auto-ignition of tetradecane in diluted high-temperature, high-pressure conditions that recall the previous findings of Gaydon (A. Gaydon 1955) for methane auto-ignition.

The dimension and the colour of flames depend on several parameters such as the pre-heating temperature, the oxygen concentration and the fuel and diluent nature. In particular, the reaction volume grows up with temperature and with the going-down of oxygen concentration. This trend was confirmed considering the combustion of propane as function of varying the oxygen concentration and temperature. Flames showed a blue colour for temperatures in the range 900°C-950°C and oxygen concentrations between 5% and 15%. For high temperatures around 1100°C and low reactants feed rates the flame emission was too high. At the same temperatures and for an oxygen concentration equal to

21% the flame was completely yellow. At higher temperatures and lower oxygen concentrations (2-5%) flame was green. This colour indicates high concentration of the compounds C_2 in the flame in this condition. When the concentration is lower than 2%, there is not any light emission in the visible spectrum. . The green flame observed for the propane at the low percentages of oxygen has not been identified for the methane. This demonstrates that flames light emission depends also on fuel. Shimo et al. (N. Shimo 2000) showed that the kerosene at high pre-heating temperatures and low oxygen concentration (5%) emits a green flame whether diluted with nitrogen, blue-orange whether diluted with argon and a different colour in presence of CO_2. The difference in light emissions is probably due to the different thermal capacities of diluents and to the different interaction with the oxidation process.

This characteristic is generally related to a high level of homogeneity immediately after the near field of injection regions. Temperature and species concentration profiles measured in burners working in diluted high-temperature condition show a fairly uniform distribution. For instance in Fig I.9, the wall temperature of a furnace where natural gas is burnt in MILD conditions (S. Orsino 2001) is reported on the left axis as a function of axial coordinate. It is evident that temperature is quite constant along the whole furnace (A. Milani 17-18 January 2000). This testifies that there is no main reaction zone, associated with strong gradients, localized in a limited region of the combustion chamber, as would be generally expected for a standard furnace . In this case, the reaction zone extends to most of the available volume, thus often leading to the statement that such systems work in almost “well-stirred” conditions (S. Orsino 2001). The presence of substances beaming as like as H_2O and CO_2 makes the thermal gradient be constricted. Distributing heat release to a larger volume results in a nearly uniform temperature distribution with reduced peak temperatures. As a consequence the net radiation flux can be enhanced by as much as 30%

(H. Tsuji 2003) and emissions of some pollutants are lower than from conventional combustion system in which combustion zone is concentrated on a flame front. Nevertheless combustion chamber temperature, in a process based on this new combustion mode, is comparable to the average temperature of a traditional combustion chamber; this implies that materials used for combustion chambers are the same of a traditional system but, because of the homogeneity of MILD processes, material will undergo lower thermal stresses.

In the same diagram (Fig. I.9) a third characteristic is highlighted, which seems to conflict with the flameless feature, namely the relatively high radiative heat flux in the order of 300-350KW/m2 (S. Orsino 2001) measured in the same furnace. Such a high radiative flux is due to high concentrations of species strongly emitting in the infrared region, such as CO_2 and H_2O. Because the whole combustor is filled with such species, the whole medium becomes more emitting with respect to a traditional combustion furnace. This is the most puzzling characteristic and is also of great practical interest because it positively affects heat transfer and contributes to keeping the average temperature low.

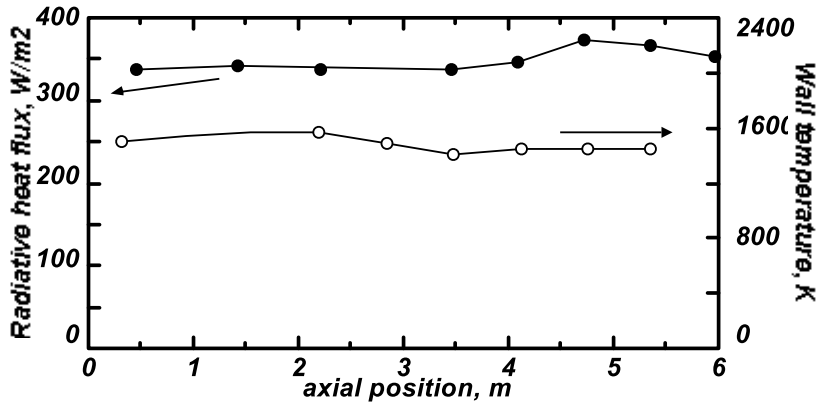

Fig.I.9 - Radiative heat flux (left axis) and wall temperature profile (right axis) in the burner in a mild combustion regime

Because of this almost homogeneous distribution of heat, “hot spots” are eliminated and product quality can be improved in some applications.

In practice, MILD combustion should not be confused with other emission control strategies proven to work in conventional systems, such as staged combustion and flue or exhaust gas recirculation (FGR or EGR). Although there are similarities, the MILD regime operates with dilution rates well beyond the critical limits for conventional flame stabilization. Therefore, in order to sustain the oxidation reactions in such diluted conditions, MILD burners are often coupled with air preheating. The recycling of exhausted gases implies the use of minor amount of fuel, that would be employed to pre-heat the fresh gases, and consequently a lower emission of pollutants and a lower exercise cost; furthermore the minor number of pollutants abatement devices imply a meaningful reduction of plant costs. Heat exchangers are used to recover energy from the exhaust gases, before they are discharged into the atmosphere, and preheat the incoming combustion air. This not only increases the temperature of the mixture of gases and helps to maintain the combustion reactions, but also improves thermal efficiency. A better understanding of this innovative combustion technology will enable its implementation in a variety of combustion devices. At this regard, in order to understand how this mode of combustion has gained importance over the years it is necessary an historical review which will be presented below.

I.4 - Historical Review

The German and Japanese researchers (H. Tsuji 2003) found in early 1990's that preheating air to about 1600K and injecting approximately at 90 m/s could not be observable a typical flame. At first they thought that no reaction take place, but the found that O_2 concentration in the flue gas was very low, as low as that of the flue gas when complete combustion reaction occurred. This means that although no flame is visible, chemical reactions took place. In that experiment, very low NOx emissions were

measured, the maximum was 80 ppmv, or even almost zero (H. Tsuji 2003). It was further confirmed that under the conditions of highly preheated air and high injection momentum, the combustion reaction occurs uniformly throughout the furnace, the in-furnace thermal distribution is uniform, the radiation heat transfer increases by more than 30% , and also there is no audible combustion noise. All this confirms what has already been pointed out previously, the MILD combustion conditions has the advantages of energy savings and low pollutant emissions.

With the end of doing an historical review of this combustion mode, in literature there are a lot of works concerning this argument. Investigators from Germany (J. A. Wunning 1997; T. Plessing 1998; M. Mancini 2002; **M. Mancini** 2007; P. J. Kim 2008; M. Zieba 2010), Japan (M. Katsuki 1998; J. Yuan 1999; H. Tsuji 2003), Sweden (W. Yang 2005; W. Yang 2005; W. Yang 2005; W. Yang 2005; W. Yang 2006; A. Ponzio 2009), Italy ,(S. Orsino 2001; M. Mancini 2002; A. Cavigiolo 2003; A. Cavaliere 2004; M. Galbiati 2004; C. Galletti 2007; M. de Joannon 2009) Netherlands (R. Weber 2000), France, Australia, United States (G. M. Choi 2001; A. K. Gupta 2004) and China (H. Y. Qi 2001; J. T. Wang 2003; X. J. Xing 2006; H. Zhang 2007; J. Mi 2010; P. Li 2010; Y. Yu 2010; Z. Tang 2010) conduct the research and development on the MILD combustion.

These studies lead to say that there are specific conditions to obtain MILD combustion:

1. High temperature preheat of combustion air and high-speed injections of air and fuel are the main requirements of achieving MILD combustion;
2. Strong entrainment of high-temperature exhaust gases, which dilute fuel and air jets, are the key technology of maintaining MILD combustion;
3. Local oxygen concentration must be less than 5 % – 10 % while local temperature is greater than that for fuel self-ignition in the reaction zone. These must be achieved by strong dilution of reactants with the flue gas (N2 and CO2-rich exhaust gas);

4. When using the regenerator to recycle the waste heat of flue gases, the thermal efficiency of MILD combustion can increase by more than 30%, while reducing more than 70 % NOx emission (H. Tsuji 2003)

Degree of dilution of reactants by the flue gas was defined by Wünning et al.(J. A. Wunning 1997) . A relative internal recirculation rate that is the ratio of the mass flow rate of the internal recirculation gas (M_E) to that of initial fuel and air jet ($M_F + M_A$), namely:

$$K_V = \frac{M_E}{(M_F + M_A)} = \frac{(M_J - M_F - M_A)}{(M_F + M_A)} \tag{19}$$

where $M_E = M_J \cdot (M_F + M_A)$ and M_J is the total mass flow rate of flue gases entrained by both fuel and air jets.

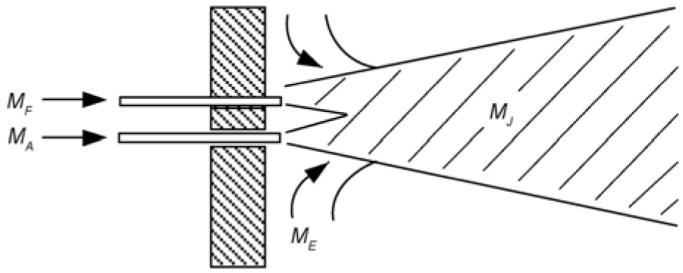

Fig. I.10 - Stability limits of the non-premixed MILD combustion of methane by Wünning & Wünning.

This parameter is crucial in defining the influence of gas recirculation on MILD combustion. Fig II.10 illustrates the axial evolution and radial spread of the fuel-air jet, which results from the entrainment of the surrounding flue gas by the jets and their mixing. The reactants are gradually diluted by the flue gases (e.g., CO_2 and H_2O) and inert gas (N_2).

Wünning et al. obtained by experiment the relationship between K_V and the furnace temperature in diffusion combustion, from which a stability limit diagram was constituted

for the non-premixed MILD combustion of methane (CH_4) in a particular furnace system (Fig. I.10).

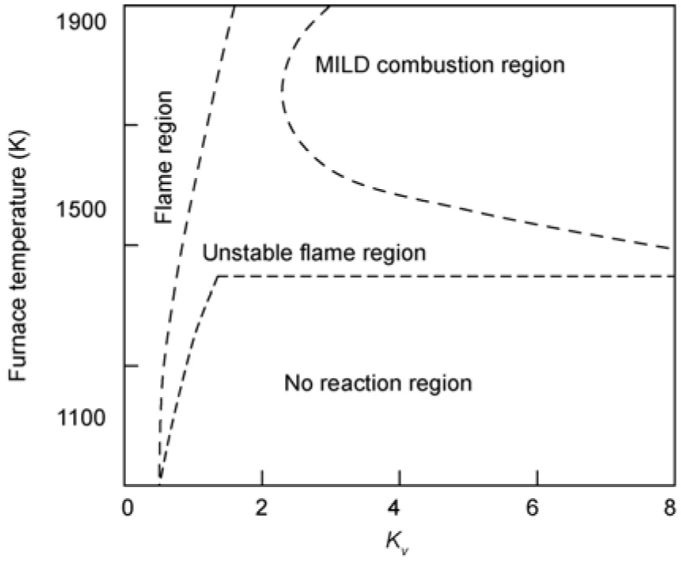

Fig. I.11 - The relationship between Kv and temperature in methane non-premixed combustion .

The majority of previous investigations on MILD combustion was carried out by examining the influence of K_V on combustion and sometimes by comparing it with the diagram.

Fig. I.11 shows that in the MILD combustion zone, the internal recirculation rate (K_V) is greater than 2.5, and the furnace temperature is greater than 1100 K. Based on this definition there are many works that attempt to classify the conditions under which you can get a MILD combustion as a function of parameters. Cavigiolo et al. (A. Cavigiolo 2003) carried out a detailed study on the influence of K_V on the reaction temperature and formations of NOx and CO in the natural gas combustion process. They found that MILD combustion is extremely stable because the characteristics of NOx and CO emissions reduction do not change with the furnace temperature, fuel type or fuel heat value. They also found that due to differences in the burning point and the calorific value between

different fuels, the critical values of Kv are different for different fuels to establish the MILD combustion. For example, for firing methane to obtain MILD combustion, K_V must be greater than 2.3 and the furnace temperature must be greater than 800°C–850°C. An important result was achieved by Galletti et al. (C. Galletti 2007). They found by experiments and CFD simulations that to save the computation time for engineering applications, the 3-D simulation of the MILD combustion should be simplified to the 2-D case. They found quite small differences between the 2-D and 3-D calculations. This consideration allows to assess the spatial uniformity of this combustion mode. Galletti et al. also found that reducing air inlet area can increase the jet momentum, enhance the mixing and entrainment between the reactant jet and the flue gas, and increase the uniformity of the furnace temperature, hence reducing the reaction peak temperature and NOx emissions. Effuggi et al. and Derudi et al. (M. Derudi 2007; M. Derudi 2007; A. Effuggi 2008) revealed that the MILD combustion of biomass gas with low calorific value can be achieved under the condition of high recirculation rate at $K_V > 5$ and high furnace temperature at > 800°C. They analyzed the difference between the MILD combustions of natural gas and biomass gas according to the magnitudes of K_V and the furnace temperatures of different fuels. Moreover, the combustion region was divided into the mixing zone (Mixed Zone) and pure MILD combustion zone (Clean MILD Combustion Zone). Dally et al. (B. B. Dally 2002; B. B. Dally 2004; G. G. Szegö 2008; G.G. Szegö 2009) found that the reaction peak temperature decreases due to the initial fuel dilution that can increase jet scalar dissipation rate, and influence flame front structure and combustion reaction. Krishnamurthy et al. (N. Krishnamurthy 2009) found that if using pure oxygen as the oxidizer, the establishment of MILD combustion requires a much higher recirculation rate of flue gas. The above results show that Kv and temperature are two key parameters

for the study of the MILD combustion. Same consideration were made by Dally et al. (B. B. Dally 2002). They found that increasing the dilution of oxidants can increase the flame volume and lower the intensity of reaction. They also investigated the relationship between OH and temperature under different oxygen concentrations. Dally found that the mass fraction of OH in MILD combustion is more uniform than that of conventional combustion. Moreover Medwell et al. (P. R. Medwell 2007; P. R. Medwell 2008) also measured the oxygen concentration in different reaction regions between OH and the temperature component, and found that the MILD combustion occurred over a much larger space so that the mass fraction of OH was lower and more uniformly distributed in the reaction zone than that from conventional combustion. These studies thus point to the importance of diluting reactants on MILD combustion.

On the numerical simulation side, based on , Christo and Dally et al. (B. B. Dally 2002; F. C. Christo 2005) carried out numerical simulation on the similar conditions. That study provided detailed assessments on several turbulence models (such as standard $k-\varepsilon$ model, RNG $k-\varepsilon$ model and $k-\varepsilon$ model), numerous combustion models, including mixture fraction/probability density function model (ξ/PDF), the flamelet model, eddy dissipation model (EDM), eddy dissipation/finite reaction rate Model (EDM/FR) and the eddy dissipation concept model (EDC). Christo and Dally found that the simulation of MILD combustion need to consider flame lift up and the in-furnace slow reaction caused by the high speed jet. The EDC combustion model with the GRI-3.0 detailed chemical reaction mechanism was found to perform the best, relative to the experimental results. The simulated average velocity and furnace temperature were different from the measurements by less than 5%.

Further studies have to evaluate the use of different fuels under MILD condition. In particular the use of firing oil and coal was studied (M. Derudi 2007; M. Derudi 2007; S. R. Wu 2007; A. Parente 2008; C. Galletti 2009; Y. Yu 2010). This suggests that the MILD combustion may be realized broadly by using any types of fuel no matter it is a gas, liquid or solid fuel. For example, the studies on the MILD combustion of hydrogen fuel (M. Derudi 2007; M. Derudi 2007; S. R. Wu 2007; A. Parente 2008; C. Galletti 2009) found that as the hydrogen concentration in natural gas increases, the greater initial velocity (>70m/s) and higher flue gas re- circulation (Kv>9) must be used to achieve MILD combustion. Yu et al. (Y. Yu 2010) found that the increase of the reactant dilution will decrease the reaction temperature and that when reactants are highly diluted with the flue gas (Kv>10), NOx and CO emissions are not sensitive to the dilution level. Weber et al. (R. Weber 2005)and Zhang et al. (H. Zhang 2007) investigated the MILD combustion of the pulverized-coal fuel and confirmed the possibility of occurrence of coal MILD combustion. Stadler et al. (H. Stadler 2009; H. Stadler 2009) investigated the formation mechanisms of NOx for coal combustion under the MILD mode and, especially, the influence of char combustion and gasification on NOx formation. Recently Dally et al. (B. B. Dally 2010)have successfully achieved MILD combustion of firing sawdust in a lab-scale furnace.

Lou et al. tried to achieve the MILD combustion of firing the biomass fuel. They found that when firing rice husk, the NOx emission increased with increasing air preheat temperature, and when the temperature > 1000°C–1050°C, the NOx emission increased with temperature at a higher rate but was still lower than that from the conventional combustion mode. The reason for lower NOx emissions is that the slower reaction of MILD combustion reduces both the fuel and thermal NO emissions. The MILD combustion can

decrease the thermal NO emission by 70% and fuel NOx by 40%–60%. This is why NOx emissions can be reduced when coal combustion takes place the MILD mode.

In conclusion, we can say that this combustion mode has the characteristics to be considered one of the most promising within the development of new technologies. Therefore it is necessary a detailed study of the intrinsic characteristics of such technology in order to the complete characterization of the same.

I.5 - Aim of the thesis

The dynamic development of production systems for energy production, are focused on some major objectives, inevitably tied to a high thermal efficiency and to the abatement of pollutant species, such as NO_x, CO_2, SO_x, soot particulates, PAH, etc.. These constraints are necessarily defined by some issues of global concern, such as public health (especially since those pollutants are directly related to the incidence of new human diseases), the so-called "global warming" (the phenomenon of raising the average temperature of Earth's atmosphere) as well as by declining fossil fuel resources. This last constraint implies the need to reduce the specific consumption of fuel in existing energy production systems and, simultaneously, to develop new technologies to achieve these goals. In this context, on the one hand it is necessary a study of improvement and optimization of existing resources of energy production (by making changes economically attractive to existing installations) and on the other the development of new combustion technologies that will inevitably require a phase of verification and feasibility for a first significant use in industry.

In this complex perspective, one of the "unconventional" technologies and perhaps, the most promising is the so-called MILD combustion (Moderate or Intense Low-oxygen Dilution). This combustion mode involves the use of high degrees of dilution and high

inlet temperature, necessarily more than self-ignition temperature of the combustion air-fuel mixture used.

The thesis concerns the study of the behavior of model reactors in working conditions typical of a MILD Combustion process. These operative conditions allow for a reducing of pollutants formation, such as NOx and soot, and save energy. Hence this is a very promising process in the framework of the development of new combustion technologies aimed to reduce the environmental impact of combustion systems. Although in literature there are many works on this new combustion mode, there is still the necessity to characterize the process by means of basic studies. This depends on the difficulty to realize in a laboratory scale plants able to work with the extreme high inlet temperatures typical of MILD condition. These extreme conditions imply a difficult choice of materials and problems of sealing of the reactor. These problems can be more easily overcome in pilot or industrial plant. Basic studies usually carried out by means of model reactors typical of chemical engineering. The strength of this approach is the opportunity to highlight particular features of combustion process using different elementary configurations. In fact the combustion process is characterized by very short characteristic time, i.e. for instance reaction time, and by the interaction between fluid-dynamic and chemistry. Model reactions allow simplifying the study of oxidation reactions since they permit to emphasize particular aspects of the process. Furthermore their complementary allow for a global and structured characterization of the process itself. These features justify their wide spread use in the research field.

Moreover the behavior of model reactors has been widely modeled since the equations, such as mass or energy conservation, necessary to describe such systems, in ideal conditions, are function of just one coordinate. This aspect has promoted the development of numerous numerical codes able to simulate the behavior of ideal reactors and the

development of a modeling activity of the oxidation process. Hence they allow for a good comprehension of physical and chemical phenomenology and meanwhile for a validation and tuning of predictive models supported by experimental data obtained in precise operative conditions.

In this thesis the attention has been focused on the plug flow configuration because it allows for an accurate and structured analysis of the kinetic and the dynamic evolution of the combustion process. Hence the aim of the thesis has been the characterization of the effect of the high dilution degree and of the high inlet temperature on the evolution of the oxidation process of mixtures and the identification of combustion regimes that establish in MILD combustion conditions. Moreover, the effect of different fuels and different diluent species were considered. On the basis of the sampling of the gas feed up to the reactor, it would be possible know the oxidation path of the mixture.

Based on these samples of the gases has been possible to assess the composition of the mixture at the exit of the experimental plant as well as to verify the presence of oxygen species or low molecular weight hydrocarbons (C_1 and C_2). These samples have allowed us to verify the successful oxidation of the mixture as well as to assess their progress in order to return an organic database of results that would allow to give detailed information on the oxidation of different fuels in MILD conditions. On the other hand, a numerical study has been carried out in parallel. The availability of different kinetic mechanisms available in literature has been tested. These mechanisms were developed mainly in standard working conditions and require verification and validation in conditions of high dilution. Using simple numerical tools it was possible to evaluate the characteristics of ignition of combustible mixtures by varying the characteristic parameters of work.

Chapter II

Auto-ignition of gaseous fuels. State of the art

The self-ignition is a spontaneous process in which a combustible mixture, in response to a chemical reaction, quickly free a quantity of heat sufficient to support the combustion process in the absence of external energy sources, like a flame or spark.

The self-ignition is a fundamental problem in the study of combustion and is relevant in many industrial applications (D. B. Spalding 1979; L. Spadaccini 1994; A. Lefebvre 1999). An important property associated with this process is the ignition delay time. Depending on the initial conditions this time could vary from a few hundred microseconds to several seconds.

The ignition delay is not an absolute property of the fuel mixture and therefore all experimental data must be interpreted carefully keeping in mind the experimental and the criterion used for the determination of this characteristic time. Ideally, the evaluation of the delay to the ignition of a combustible mixture under certain conditions should be independent of the experimental configuration choice and not influenced by wall effects. In addition, the mixing between fuel and oxidizer should be almost instantaneous and the temperature gradients and pressure should be negligible. Over the years, different experimental setups were used for the evaluation of ignition delay.

In the first part of this chapter presents the main experimental apparatus used for the evaluation of ignition delay focusing on the flow reactors. The second part is, instead, a state of the art about auto-ignition of methane.

II.1 - Auto-ignition into bombs, shock tube and RCM

Early studies on the auto-ignition of gaseous fuels have been made into bombs. A bomb is a container at constant volume (usually spherical or cylindrical), quartz or other transparent material. Initially, fuel and oxidizer are introduced at low temperature, after which the temperature is increased gradually until it made the phenomenon of self-ignition does not occur. The flammability limits may be raised going to plot the values of temperature and pressure for which ignition took place.

The results obtained with this technique are strongly influenced by the configuration of the vessel (form, surface and volume) and the material used to build the bomb. For this reason only a limited number of data on the auto-ignition of methane were obtained with this technique and can be taken into account for applications (L. Spadaccini 1994).

Another technique for studying the process of self-ignition of a fuel and evaluation of ignition delay under certain conditions is the shock tube. The Fig below shows a diagram of a shock tube and its operation.

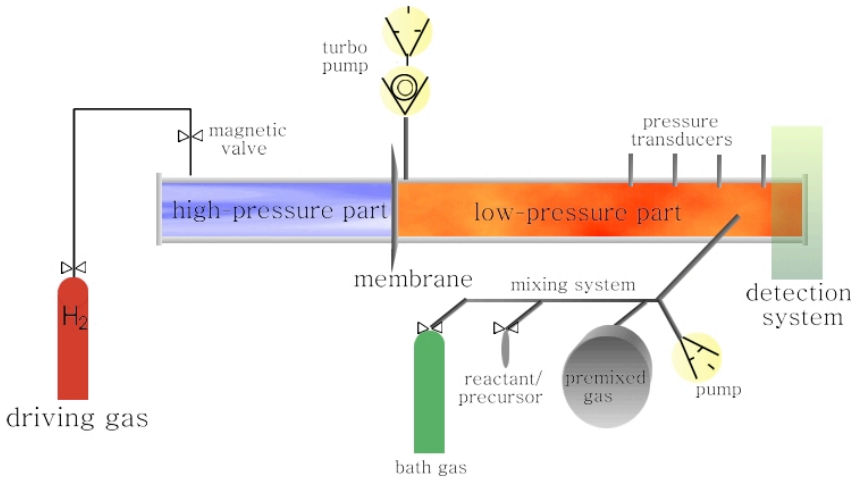

Fig. II.1 - Schematic of a shock tube and its operation

This tube consists of two different areas. The first contains the fuel mixture at room temperature and ambient pressure while the second has a carrier gas (usually argon or helium) at high pressure. The two zones are separated by a membrane. The test begins when the membrane is broken. The rupture of the membrane involves the formation of a shock wave that propagates through the combustible mixture. After reaching the back wall the wave is reflected back through the mixture. Following the passage of this wave, the temperature and pressure of the mixture increases rapidly. In these new conditions, fuel and oxidizer could ignite. In a shock tube ignition delay is defined as the period of time between the passage of the reflected wave through the mixture and the onset of the ignition process. In the case of a shock-wave strong, however, the test is started at the passage of the incident wave (G. Schott 1958).

To measure the wave velocity corresponding to auto-ignition time using pressure transducers and the test ends when the reflected wave passes through a second time the mixture .(D. J. Beerer 2009)

The test time is then defined as the period of time between the first and last passage of the wave through the mixture. One limitation of this technique, therefore, is that it is only suitable for the study of self-ignition processes with characteristic times much shorter (order of ten microseconds. In addition, the test conditions are well controlled for less than 5 ms (A. G. Gaydon 1963). In a shock tube is very important that the gradients of temperature, pressure and species are spatially homogeneous wave upstream. For example, if the membrane breaks asymmetrically, upstream wave gradients may exist that influence the process of self-ignition and thus the ignition delay. A more detailed description of a shock tube and problems related to the use of this technique can be found in the work of Meyer and Oppenheim (J. Meyer 1971) and Spadaccini and Colket (1994) (L. Spadaccini 1994).

Another device used for the study of ignition delay is the rapid compression machine (RCM). The fuel mixture is placed inside a cylinder temperature and pressure. A piston compresses quickly controlled mechanically. This compression results in a sharp rise in pressure and temperature of the mixture. After the compression stroke of the piston, the mixture may ignite. The ignition delay time, in this case, is rated as the time between the end of the compression stroke and the onset of the ignition process. To reveal the ignition uses a pressure transducer and a photo-detector. Fig II.2 illustrates the pattern of operation of a rapid compression machine.

A rapid compression machine has the advantage, compared to a shock tube, to be able to sustain pressure and temperature for longer than 10 ms. However, the time needed to compress the fuel mixture limits the time of investigation than 1 ms.

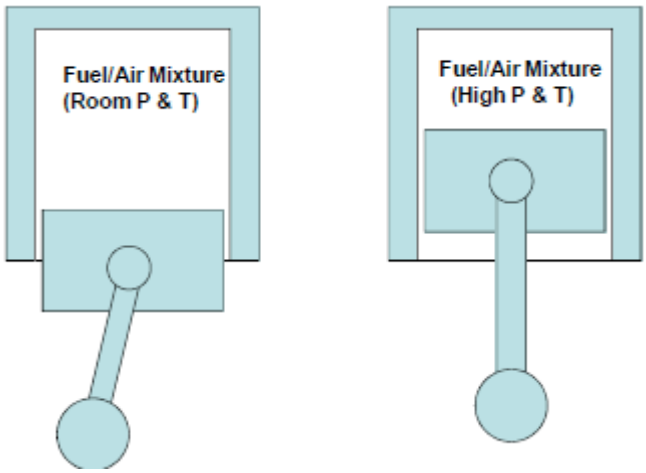

Fig II.2 - Schematic of a rapid compression machine

This equipment represents a simple method to simulate the processes that occur in engines and homogeneous charge compression ignition (HCCI).

A difficulty met with in the use of RCM is to obtain spatially homogeneous conditions before compression. The presence of a boundary layer and the presence of heat losses to

the wall result in a change of the temperature field inside the cylinder and affecting, therefore, the ignition delay measurements.

II.2 - Auto-ignition in flow reactors

The devices described until now studied the process of auto-ignition of a fixed mass under iso-volumetric by simulating what occurs in a diesel engine. These conditions, however, are very different from what happens in a gas turbine, a ramjet or within a re-burner instead are systems in turbulent flow in isobaric condition. In addition, both units work under high pressure and the results are related to these conditions. Kinetic data used for modeling and development of a process that evolves at atmospheric pressure, could be obtained by extrapolation from experimental measurements obtained with these devices, but these extrapolated data require validation to be used. This point is crucial, for example, in the case of furnaces that operate under MILD condition and VOC oxidation systems that evolve under HDDI.

Using a flow reactor allows to obtain relevant kinetic data in typical working conditions of these systems.

To obtain a quasi-one-dimensional flow, the reactor must be operated in turbulent conditions, ensuring, thus, a nearly flat velocity profile outside the boundary layer and consequently a well defined correspondence between the residence time and the spatial position along the reactor. As an alternative to turbulent flow conditions, could be operated under laminar or transitional condition. In these cases the mixture may ignite fuel inside the reactor at a longer time. Hereinafter are summarized main laboratory studies conducted on the process of auto-ignition in a flow reactor.

The first to use a flow reactor for the evaluation of delayed ignition of combustible mixtures was B. P. Mullins (B. Mullins 1953) at the National Gas Turbine Establishment in

Great Britain. In a period of six years he has studied the effect of fuel composition, the diluent and other factors on the ignition delay. The latter has been evaluated for more than thirty different fuels, including methane, in the sub-atmospheric or atmospheric conditions and temperatures of 1300 K in order to reproduce the operating conditions of a gas turbine. In the configuration used by Mullins there is only one fuel injector places in the opening section of the reactor, and the ignition delay is estimated by dividing the distance at which the flame is observed for the speed of the main flow. The flame is observed through the windows of silica and is stabilized by a divergence (divergence angle of 3 degrees) placed downstream of the input section.

In addition to tests with different fuels, Mullins has studied the effect of variation of the injectors, carbon-oxygen ratio, the intensity of turbulence and the fuel injection strategy on the ignition delay. The results obtained showed that the latter is not influenced by these parameters, and is heavily dependent on fuel type and conditions of pressure and temperature.

E.D. Taback (E. Taback 1971) has conducted studies on the process of self-ignition of the fuel JP-4 under high pressure (from 18 to 28.2 atm) and temperatures from 650 to 770K in a tubular reactor in a flow very similar to that used by Mullins. The main difference is the presence of photodiodes distributed along the wall of the reactor to measure the intensity and position of the flame. Taback also rated the ignition delay in a real premixer for aircraft engines and found that the delays measured in these conditions are in good agreement with those measured in its flow reactor. He also studied the effect that a metal obstacle, which can disturb the main flow, can have on the ignition delay by noting that the presence of a jamming of the flow, although small, may cause a reduction of up to 50% of the ignition delay time.

Spadaccini (1976) (L. Spadaccini 1976) carried out additional studies, using Taback facility, of liquid oils for temperatures from 671 to 866K and pressures from 7 atm to 16.3 atm. Then he developed a new type of flow reactor to study the process of auto-ignition under more controlled condition. New facility has some differences with the oldest reactor. It consists of an initial straight section followed by an expansion at the end of the reactor and a new type of injector to minimize the flow disturbance. In addition, the walls of the reactor is cooled, so that the reactions of self-ignition will not occur in the boundary layer adjacent to the walls where the residence time of the flow is significantly higher than the core of the flow.

Lefebvre has measured the ignition delay times using dry air at a pressure of 1-10 atm and at a temperature of 670-1020 K. The fuels tested were methane, propane, ethylene and acetylene. To prevent flashbacks and formation of the flame in the opening section of the reactor was inserted a nozzle that could increase the speed of the mixture to a value higher than that of the turbulent flame speed.

A unique method for measuring the speed of reaction of induction and post-induction in a flow reactor was developed at Princeton in 1950 and is still used today. In the reactor at Princeton developed a mobile sensor that has the task of measuring the temperature and collecting gas samples along the axis of reactor. In this way you can get the temperature profiles and species to be used for determining the reaction rate. In the work of Princeton the fuel mixture was highly diluted in order to have a low concentration of reagents and then the reaction rate more manageable for the measurement.

Swigart (R. Swigart 1958) was one of the first to study the process of auto-ignition of mixtures hydrogen / oxygen / nitrogen in a tubular flow reactor operating at atmospheric pressure (APFR). In this reactor the temperature profile is measured by using thermocouples placed axially. Applying the assumption of plug flow, the measures can be

converted into spatial temporal profiles. The ignition delay time, in this case, was defined as the time between fuel injection and the time for which the temperature increases by 10 K compared to the initial one. The high levels of dilution involve a maximum increase in temperature of the order of 100 degrees.

Swigart has studied the effect of certain physical aspects of the reactor on the ignition delay. For example, he found that the ignition delay decreases significantly with decreasing diameter of the tube, probably due to catalytic effects or heat transfer. Following Sawyer (R. Sawyer 1965) examined the effect of wall material (quartz and steel) on the kinetics of reaction and Papas (P. Papas 1994) , by taking gas samples, studied the performance of the main species during the induction period.

A latest study on the process of self-ignition of a combustible mixture in a reactor in a flow, that should be mentioned, is to Brokaw and Jackson (R. Brokaw 1955).

They carried out experiments on mixtures of propane / air at a pressure of 0.3 to 1 bar and in the temperature range 800-1013 K. In the reactor used by Brokaw and Jackson is used to control a solenoid opening valve of the fuel. In this way it can be possible determine accurately the time of injection. A pressure recorder measure the onset (which occurs with a peak). The ignition delay is defined as the difference between the time of ignition and the injection.

Recently Gokulakrishnan (P. Gokulakrishnan July 2007) and Holton (M. Holton 2009) have been working on a flow reactor based on the reactor used by Brokaw and Jackson and have used the same method for the evaluation of ignition delay. The first studied the process of auto-ignition of the kerosene while the second of methane, ethane and propane.

II.3 - Auto-ignition of Methane

The availability, low cost and reduced emissions have made methane a primary fuel in many technological applications. For this reason, the process of auto ignition of methane has long been studied over the years. Despite the richness of experimental data obtained in previous studies, in some cases there are differences between the various data and also there is a lack in relevant working conditions for some industrial applications.

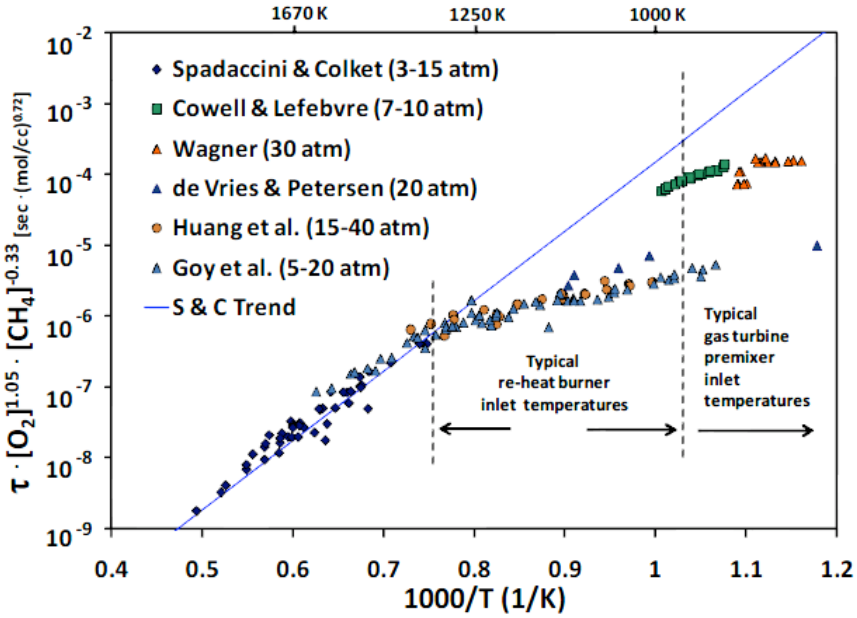

Fig II.3 - Trend of ignition delay time against 1000 / T

That scarcity is documented in non-traditional combustion processes. Therefore it is necessary to fill the data gaps in working conditions (pressure, temperature, dilution, etc..) completely different from traditional combustion processes.

Fig II.1 shows the trend of ignition delay time versus 1000/T reproduced by Spadaccini and Colket (L. Spadaccini 1994) for many studies. The vertical axis is normalized to the concentration of oxygen and methane to to obtain a comparison of all data.

Spadaccini and Colket have measured ignition delay of mixtures methane / oxygen diluted in argon in a shock tube for pressures between 3 and 15 atm, temperatures varying from 1350 up to 2000 K and equivalence ratios between 0.45 and 1.25.

The results are reproduced by the equation:

$$\tau = 2.21 \cdot 10^{-14} \exp\left(\frac{22659}{T}\right)\left[O_2\right]^{-1.05}\left[CH_4\right]^{0.33} \quad (20)$$

The Fig also presented to the ignition delays measured in a flow reactor at moderate temperatures (up to 1000 K) for mixtures methane / air obtained from Cowell and Lefebvre (L. Cowell 1986) and Wagner (T. Wagner 1990) . The experimental data obtained from Cowell and Lefebvre were obtained for pressures of 7-10 atm, temperatures of 920-1000 K and equivalence ratios between 0.2 and 0.5. The measures obtained from Wagner at 30 atm, temperatures between 763 and 917 K and equivalence ratios between 0.83 and 2.5. In both studies, the ignition delay times are of the order of 100-200 milliseconds. The temperature dependency obtained in the work of Spadaccini and Colket (22.659 / T) corresponds to activation energy of 45 kcal / mol, while that measured in the work with flow reactors is significantly lower and approximately 25 kcal / mol. In addition to the ignition delays measured in flow reactors are much smaller than those obtained by extrapolating data obtained in shock tubes at lower temperatures. The reason for these differences is not yet well understood. For example Spadaccini and Colket suggests that this difference in the evaluation of activation energy may be due to the presence of impurities (nitrogen, ethane) in the sample of fuel used. It 'important to note that the measurements obtained with a shock tube for temperatures up to 1000 K overestimate those obtained in a flow reactor under an order of magnitude.

Based on the work of Spadaccini and Colket have been recently made new measurements of ignition delay in shock tubes at lower temperatures (850-1000 K) for methane and

natural gas (C. Goy 2001; J. Huang 2004; J. de Vries 2007; C. Aul 2009). In all these works, the ignition delay times measured were the order of 10 ms, smaller than those measured in flow reactors. Dryer and Chaos (F. Dryer 2008) have hypothesized that this difference may be due to the effect of mixing time and / or catalytic effects of the wall. Aul and Petersen have observed a continuous increase of pressure in the shock tube, after a long time since the shock wave passed through the mixture. They also observed the presence of chemiluminescence before the primary ignition. Aul and Petersen consider that this phenomenon lead to a decrease in ignition delay due to further crushing the mixture after the shock wave. This behavior has been observed in other works. For example, Pang (G. Pang 2009) described this behavior as "pre-ignition event" to highlight the increased reactivity of the system and the decrease of ignition delay. Recently, unusual behaviors were observed during the process of auto ignition of methane. In particular there was a typical phenomenology of the high molecular weight hydrocarbons (C5-C7), known as NTC (Negative Temperature Coefficient). Huang et al. (J. Huang 2004) have observed this behavior by performing tests in a shock tube with mixtures of methane / air diluted with nitrogen and argon in the typical working conditions of a gas turbine (16-40 atm pressure and temperature 1000-1350 K). In the same way Petersen et al. (E. Petersen 1999) in a previous paper have observed substantial variation in activation energy with temperature in the range 1040-1500 K at high pressures (40-260 atm) for mixtures methane/oxygen diluted in argon, nitrogen or helium in a shock tube. Sokolov et al.(O. V. Sokolov 1996) have studied the process of auto-ignition of the mixture methane/oxygen rich conditions at inlet temperatures between 740 K and 820 K and low pressures in a completely mixed reactor. In the region of high temperature have observed the typical behavior of cool flames and then the phenomenology of the NTC. Bendtsen et al. (A. B. Bendtsen 2000) have identified a region of NTC studying the process of oxidation of methane in the presence of

NOx in a plug flow reactor for inlet temperatures between 750 and 1250 K. In many of the cited articles, the authors have carried out numerical analysis modifying the kinetic models available in the literature, although in some cases it is not a satisfactory correspondence between experimental and numerical data. For example, Huang et al. (J. Huang 2004), have reached a good agreement between experimental and numerical data only in stoichiometric and poor fuel conditions adding some reactions and modifying some rate coefficients in the mechanism of Petersen. In particular, in this work, sensitivity analysis and reaction path diagrams showed that the oxidation reaction of methyl radical (to form the methoxy radical) is a limiting reaction in the kinetic of pre-ignition of stoichiometric methane/air mixtures at 1250 K. For lower temperatures the activation energy decreases due to the rapid increase in the rate of reaction of the following reactions:

(21) $$CH_3 + O_2 \rightleftharpoons CH_3O_2$$

(22) $$CH_3 + CH_3O_2 \rightleftharpoons CH_3O + CH_3O$$

These reactions promote the ignition in these conditions. For lower temperatures (less than 1100 K) the decrease in the concentration of hydroxyl and methyl radicals and implies a re-increase of activation energy. The model developed by Huang et al. is not, however, able to predict experimental results under fuel-rich. In turn, Petersen et al. (E. Petersen 1999), have expanded the mechanism GRI-Mech 1.2 by adding the important reactions in the kinetics of oxidation of methane at low temperature. By implementing this new mechanism, they observed that at a temperature of 1400 K and a pressure of 100 atm of ignition primary reactions are:

(23) $$CH_3 + O_2 \rightleftharpoons CH_3O + O$$

(24) $$CH_3 + HO_2 \rightleftharpoons CH_3O + OH$$

However, the recombination reaction of methyl radical with ethane, appears to be the main termination reaction and the primary sink for the radical CH_3. At 1100 K and 100 atm the main branching reactions were as follows:

(25) $$H_2O_2 + M \rightleftharpoons OH + OH$$

(26) $$CH_3 + CH_3O_2 \rightleftharpoons CH_3O + CH_3O$$

These two reactions promote the formation of radicals H and OH, which explains the decrease of ignition delay for lower temperatures (the activation energy is 19 kcal / mol at 1100 K and is equal to 32.7 kcal / mol at 1400 K).

Over the years it has been long been investigated the effect that the addition of other hydrocarbons involves on the methane auto-ignition times. The presence of even a small amount of different hydrocarbon species from methane can have a marked influence on the process of auto-ignition. Methane has a primary C-H bond with higher energy than a secondary or tertiary. Therefore, the methyl radical formed from the decomposition of methane, is relatively stable and hardly oxidized. However, the radicals that are formed by hydrocarbons with higher molecular weight (weaker bond), are more reactive and can activate the system more quickly with a consequent decrease of the ignition delay time. This effect was confirmed in several experimental studies. For example Burcat et al. (A. Burcat 1971) have carried out a systematic study of ignition delay in a shock tube for mix air / hydrocarbon from methane to pentane, noting that methane has an ignition delay of about an order of magnitude longer than these hydrocarbons. Westbrook et al. (C. K. Westbrook 1979; C. K. Westbrook 1984) and afterwards Simmie (J. M. Simmie 2003) have studied the induction period of blends methane / hydrocarbon / air using numerical techniques. In particular, using a kinetic mechanism of 75 reactions developed to describe the oxidation of the system methane / ethane, have observed that the addition of small

amounts of ethane (5-10%) to the mixture of methane / air results in a significant reduction of the delay ignition than that observed for a pure mixture. This phenomenon is due to increased production of radicals by ethane. In addition in subsequent works, Westbrook et al. have observed that the mixture methane / ethane / air is sensitive to a small addition (less than 10%) of an additive (propane), while this sensibility decreases drastically for higher volumes.

Bornside and Frenklach (M. Frenklach 1984) measured the ignition delays of mixtures methane / oxygen / argon in the presence and absence of propane (up to 20% of the volume of methane) finds a decrease of the ignition delay for mixtures rich in propane. Petersen et al. (J. de Vries 2007) have investigated the oxidation of mixtures methane / propane in the pressure conditions typical of gas turbines (5.3-31.4 atm) in a shock tube. In this paper, the experimental study was accompanied by a numerical work. In particular it has been observed that reactions involving species CH_3O, CH_3O_2 and chemistry of $CH_3 + O_2/HO_2$ system are essential to reproduce the correct kinetic behavior of the system.

Healy et al. (D. Healya 2008) have studied the oxidation blends of methane / propane in the air in the temperature range 740-1550 K, pressure varying between 10 and 30 atm and equivalence ratios from 0.3 to 3 in a shock tube and a rapid compression machine. The data obtained are in agreement with those reported in the literature and also for mixtures containing a high percentage of propane (30%) was observed a region of NTC.

The kinetic mechanism used for numerical simulations has been able to reproduce the effect of the change of pressure and equivalence ratio and the presence of a region of NTC.

More recently, Holton et al. (M. Holton 2009) have studied the process of auto ignition in a flow reactor at atmospheric pressure for different mixtures (methane/ethane/air, methane/ propane/air and methane/ethane/propane/air) for temperatures of 930-1140 K and equivalence ratio variable from 0.5 up to 1.25. In agreement with previous studies, they

observed that an increase in inlet temperature and equivalence ratio results in a reduction of ignition delays under these conditions. Moreover, the addition of 5-10% of ethane or propane to a mixture of methane / air drops to the ignition delay by 30-50%. This work has also studied the effect of adding CO_2 to fuel mixture, and found that the presence of carbon dioxide in the system slightly reduces the delay to the ignition. It was used the correlation of the Arrhenius to derive activation energy of the ignition of individual hydrocarbons and hydrocarbon blends. The results showed a reduction of activation energy at high temperatures, suggesting a change in the chemistry of ignition in these conditions. Beerer et al. (D. J. Beerer 2009) have investigated the ignition delay of mixtures of alkanes in a tubular reactor in a flow in turbulent conditions, high pressures (7-15 atm) and moderate temperatures (785-935 K). In this work the results were compared with those at the highest temperature available in literature. In particular, for these conditions, the process of ignition is controlled by reactions involving RO_2 and H_2O_2.

A thorough review of experimental and numerical results related to the process of auto ignition of mixtures methane / hydrocarbon and natural gas can be found in the work of Spadaccini and Colket (L. Spadaccini 1994).

II.4 - On the effects of wall. State of the art.

A fundamental aspect to establish the reliability of the measurements and then estimate the time of self-ignition of the blends considered is the evaluation of potential catalytic or inhibiting effects of the reactor wall.

In the literature this problem has been dealt for various combustion processes. First, are reported the conclusions on the influence of kinetic heterogeneous processes in partial oxidation of methane to methanol, specifying that the operating conditions are substantially different from those adopted in the process of MILD combustion.

Nevertheless, the presence of a wide literature on the partial oxidation of paraffins is a useful source of information for understanding the heterogeneous kinetics. Arutyunov et al. evaluated the effect of initial temperature, the composition of the mixture, the pressure and materials on the yield and selectivity of methane to methanol to carry out experiments in two tubular flow reactor (made of quartz and stainless steel) in a pressure range between 15 and 80 bar and temperatures between 480 °C - 600 °C. The typical residence time in the reactor is 3 - 4 s.

In the experimental conditions examined, the yields of products depend strongly on the fact that the surface of the reactor is steel or quartz. These differences are dictated by the onset of heterogeneous oxidation processes on the surface of the reactor in parallel with the homogeneous oxidation. Other experiments have been made introducing a single grain of a supported platinum catalyst (~ 1 mm in diameter) in the flow of methane (O. V. Sokolov 1996). The experimental data show that in this way not only accelerates the reaction rate but also increases the percentage of complete oxidation products. An increase in pressure of the system produces a positive effect on the degree of oxidation of methane to methanol because the radical branching reactions are accelerated (O. V. Sokolov 1996) and the spread of the species to the wall is slowed down. The extent of heterogeneous processes on the surface of the reactor is therefore reduced. This implies an increase in the yield of complete oxidation products while accelerates homogeneous reactions oxidation. Pressure effect is also verified by changing the dilution of the mixture and then the partial pressure of methane. Experiments were carried out in addition to mixtures in which 75% of methane was replaced with nitrogen keeping constant the ratio carbon / oxygen. The concentration of methanol in the liquid phase was found to be considerably higher than in experiments on pure methane gas. The most plausible explanation of this effect is that

increasing the partial pressure of nitrogen slows down the diffusion of the reactants on the surface of the reactor, restricting heterogeneous reactions.

Yarlagadda et al. (P. S. Yarlagadda 1988) studied the partial oxidation of methane at high pressure in the reactor tube steel internally coated Pyrex. The residence time of 2 min were considered and examined the temperatures are 400-500 ° C. Experimental data show that the methanol yield of 70-80% can be achieved by conversion of methane equivalent to 8-10% using the reactor under appropriate conditions. The selectivity to methanol obtained is significantly higher due to the use of a Pyrex glass covering of the reactor in such a way as to minimize surface reactions. Hunter et al. (T. B. Hunter 1994) have carried out a study on the oxidation of natural gas to methanol partial. In the first part, the effect of wall composition of the reactor (Pyrex, Teflon, stainless steel, silver and copper) on this process has been determined for a pressure of 30 atm and temperatures of 350-400 ° C. In the second part, has been characterized the effect of solid catalysts (Cu/SiO2, Co/A12O3 etc..). Finally, was evaluated (p = 10 atm) the effect of various species that can promote the formation of radical species or characterized by the presence of H radicals easily removed from their system.

The results show that compositions of the wall does not have significant consequences for the productivity of methanol. This is coherent with the homogeneity of the reaction and slow diffusion of intermediary free radicals to the wall in high pressure systems. The differences observed at low temperatures but may be due to the composition of the wall which acts by promoting the radical chain branching reactions.

Onsager et al. (O. T. Onsager 1989) have studied the process of partial oxidation of methane in a tubular reactor made of stainless steel 316SS internally coated in Alsint (A12O3) for pressures between 3 and 40 bar and temperatures from 500 ° C up to 750 ° C. The typical residence time of the mixture are 0.1-1 s. The yield of methanol has been

characterized as a function of system parameters (pressure, temperature). In addition various catalysts have been introduced into the reactor (SrCO3, Bacos, and 7% Li / MqO). They found that the presence of fillers leads to an increase of CO2 to the detriment of CO and pointed out that the inert surfaces increase the rate of termination of the radical species. Mahajan et al. (1977) have published three articles on the homogeneous partial oxidation of methane to methanol. They (1977) conducted a systematic partial oxidation of methane and propane in reactors made of different materials (glass, aluminum, steel and copper).

All the reactors were in steady state exercise using propane or methane and oxygen, for temperatures between 300 °C and 500 °C and pressures from 1 up to 4 atm. The feed ratio of hydrocarbon / oxygen varies from 0.5:1 up to 10:1, while the residence time in the reactor are from 0.6 up to 3.6 min. They found that the surfaces of the reactor to catalyze the reaction surface. In particular, the decomposition and oxidation reactions occur significantly on the inner surface of the reactors reactors especially in steel and copper. These reactors contain respectively oxides of iron and copper on the surface because their reactions occur between the surface and oxygen during the partial oxidation processes. These metal oxides act as catalysts in a very effective manner; oxides also act as oxidizing agents for oxygenated compounds, carbon monoxide, and paraffin at the temperatures used. However, the heterogeneous kinetics are of much less importance, when aluminum or Pyrex glass are used. For these two materials, the surfaces are mainly alumina and silica, respectively. Both are very stable and have little or no oxidative capacity. Thus the relative importance of these reactions varies for different materials as follows:

copper > *steel* > *alumimum* > *pyrex* (Mahajan et al., 1977b)

Mahajan et al. have also found a variation in the influence of heterogeneous processes on the yield of methanol compared to the hours of operation of the reactors especially for metallic materials because their morphological structure changes due to corrosion.

In particular, Mahajan et al. assert that the main effect of the surface evolution of the oxidation process is primarily concerned with the catalytic decomposition of aldehydes especially in metal reactors. The reaction surface of a Pyrex glass surfaces are of minor importance, but they are still significant. They also conducted experiments using only methanol and acetaldehyde in nitrogen in different reactors. Experimental tests were conducted after pretreatment of oxidation of the walls of the reactor made directly during the process of partial oxidation of methane or by passing a stream of oxygen for a few minutes up to forty hours.

The main reaction products were carbon monoxide, hydrogen, water and carbon (deposited on the walls).

Mahajan et al. conclude that the reactions taking place during the partial oxidation of methane are as follows:

A. oxidation of hydrocarbons and the products of partial oxidation on the surface of all the reactors investigated, the inner surfaces are reduced as a result of this oxidation
B. the decomposition of oxygenates with the production of carbon monoxide, hydrogen and carbon (coke)
C. oxidation of the inner surface of the reactor with oxygen, the coke deposited on the surface is oxidized
D. adsorption and desorption of water vapor, oxygen compounds, etc..

In addition, the water-gas shift reaction with the destruction and / or the possible initiation of radical reactions on the surface of the reactors are conceivable.

In a third work (Mahajan et al (1977c)) they propose a mechanism that explains the main differences of the experimental results for the partial oxidation of light paraffins in various reactors. Summarizing the chemical kinetics of oxidation is divided into homogeneous and heterogeneous reactions:

Oxidation in gas phase:

$$paraffins + oxygen \rightarrow oxygenates + CO + CO_2 + H_2O + olefins + CH_4 + hydrogen$$

Surface reactions:

A. The oxidation of internal surfaces with oxygen to form metal oxides.

B. Reduction of oxidized surfaces (often metal oxides) with oxygenated compounds, paraffins, olefins, CO and hydrogen to produce CO_2, CO, and H_2O.

C. The decomposition of oxygenated products on the surfaces and production of CO, H_2, coke and by-products.

D. Oxidation of coke (or carbon deposits) with oxygen to produce mainly CO_2, CO, H_2O and H_2 can be produced in small quantities.

Zhang et al. (H. Zhang 2007) have conducted experiments homogeneous partial oxidation of methane at 380-500 ° C and 5 MPa in a tubular reactor. They found that the material composition of the reactor has a large effect on the yield partial oxidation of methane to methanol. In particular, the reactor in stainless steel has lower yield in methanol, but form CO and CO_2. Consequently, this material is not suitable for the partial oxidation. It is well-known that the oxygen in the oxides of iron and other metal oxides is very efficient in the complete oxidation of the fuel. In particular, methanol is more unstable of methane and is more easily adsorbed and activated on metal surfaces and metal oxides because of its high molecular polarity. The effects of heterogeneous catalysis have been evaluated in other processes of industrial interest. Marengo et al. (2010) have carried out a systematic study

of oxidation of hydrogen in the presence of different materials in order to evaluate the effect of hydrogen on the structural properties of metallic materials. The experimental campaigns were carried out in a reactor tube made of sapphire, 145 mm long and with an internal diameter of 8 mm. Sapphire was chosen because it chemically inert and also for its mechanical and optical techniques to implement optical diagnostics. Mixtures highly diluted hydrogen in air (2-3% v / v) were used in order to maintain the oxidation process under controlled conditions and safe. The residence time of the mixture in the reactor is 22 s. The role of different materials was evaluated by placing into the reactor tube strips or sheets of the lining of the reactor of different materials (platinum, steel, 304 stainless steel and quartz. Platinum is used because it is known to be a good catalyst and then acts as a reference material for the evaluation of experimental evidence. The tests performed with steel showed a promotion of the oxidation of steel in a temperature range (300 and 400 ° C) in which the reactions occur in the gas phase in a limited way. This effect is emphasized by the surface changes of the material induced by corrosion. In general it was found that the steel entails the dissociation of molecular hydrogen, followed by a strong interaction of H atoms with the metal. This is the initial step of a mechanism that forms an active species that can easily combine with oxygen, leading finally to the formation of water.

In contrast, the experimental tests made with stainless steel 304 show that it assumes a role of inhibition of oxidation in H_2. The surface of the metal has an effect on the mechanism of switching off the gas phase, by blocking the radicals who promote branching chain reactions. Crynes et al. (B. L. Crynes 1969) studied the pyrolysis of propane in a reactor tube made of 304 stainless steel with low content of carbon and nickel. The internal surfaces of the reactor have been treated with oxygen, hydrogen bromide and water vapor. The pyrolysis process was characterized in terms of species produced, for temperatures between 600 and 750 ° C at atmospheric pressure with a residence time of the mixture

equal to 2.8 s. Some materials have been very efficient in promoting secondary reactions, including propylene and ethylene to carbon, hydrogen and methane. This conclusion is obvious, according to the concentrations of olefins at low and high carbon content and the formation of hydrogen occurred during the experimental tests in the reactors pretreated with oxygen, hydrogen bromide, and steam and steel reactors low carbon. However the walls of the reactor have a role in initiation of radical reactions and/or termination during the pyrolysis of propane although these effects are minor and, under the operating conditions for these experiments can not be determined precisely. No effect was observed in the untreated stainless steel reactors, when the surface to volume ratio was increased. The surface effects observed after pretreatment with oxygen reactors are caused by adsorption of oxygen and / or by the reaction of oxygen with the reactor walls. Stainless steel 304 is attacked by oxygen at temperatures above 700 ° C (Lymar, 1961), and complex metal oxides are formed. The walls of the reactor will coarsen if the corrosion is severe enough. Heterogeneous catalysis decreases during the experimental evidence due to loss of oxygen from the walls and because of the overlap of the metal oxides of carbon and carbonaceous materials. The pretreatment of walls with hydrogen and hydrocarbons leads to a lower activity of the walls. The results of this study showed unequivocally that the current reactors treated with oxygen are effectively reduced by the presence of hydrogen. The treatments made with hydrogen sulfide for 35 to 66 minutes at 700 ° C eliminated the effects of oxygen treatment reactors because it forms a durable protective layer of sulfide. Shree (1963) says that a film of sulphide, depending on its structure, may be "more or less protective." In this case, the oxide layer is completely converted to sulfides or at least to a depth sufficient to isolate the oxides on the surface of the walls of the reactor against the gas stream (Farber and Ehrenberg, 1952). Although metal sulfides resist to short-term oxygen treatment, the contact with the steam slowly oxidizes the walls of the reactor or at

least prepare them to additional oxidation. Robinson and Smith (1984) have analyzed the delay to the ignition of methane in a spherical container made of stainless steel. Their work shows that the ignition of methane is significantly influenced by the nature of the vessel wall. Thompson (1929) and Townend et al. (1936) argue that metal surfaces result in a higher ignition temperature than glass. This is probably due to reactions that occur on the walls, which destroy the reactive species necessary for the evolution of the oxidation process. These reactions occur more easily on metal than on glass (Hoare et al, 1967). In order to overcome these problems, Robinson and Smith have treated the reactor with boric acid to reduce the efficiency of termination reactions on the wall (Bamford et al., 1977). For propane and butane, the experimental data are consistent with the values commonly found, while for ethane the value is slightly lower (490-500 ° C instead of 515 ° C) (Zabetakis et al., 1965))

Konnov et al. studied the non-catalytic partial oxidation of methane to syngas in a wide temperature range (823 - 1531 K) and atmospheric pressure (1.2 atm) using two tubular flow reactors. The residence time was varied from 1 to 164 sec. They have also modeled the process of partial oxidation using the CHEMKIN code and their kinetic mechanism. They assert that modeling of the experiments in the flow reactor has some problems due to the mixing time, with the effects of mass diffusion and reaction of the wall surface. The common problem of flow reactors is the difficulty in converting experimental profiles of axial distance in the time profiles (Yetter et al., 1991). This problem is usually overcome by shifting the experimental data to fit the numerical results in a benchmark of 50% consumption of the main reagent. The effects of mass diffusion and reaction of the wall surface are found to be important in assessing the speed of chemical reactions in laminar flow reactors (Lee et al.). In addition, flow reactors are neither completely adiabatic nor isothermal, and heat transfer can greatly complicate the modeling, especially in conditions

close to the flammability limits (Kim et al., 1994). Scire et al. (2001) argue that there is significant uncertainty in the determination of rate constants from the data of reactor. A combined effect of mixing time, time of mass diffusion, of the heterogeneous reactions on the walls of the reactor and the exchange of heat can result in the leveling of the spatial profiles of temperature and concentration of species compared to the calculated values (Konnov, 2003). In experiments with long residence times, Konnov et al. argue that the heterogeneous reactions have an inhibitory impact on the chemical kinetics. It is well known that the results vary significantly in the partial oxidation reactor built with different materials or with different pre-treatment (Mahajan et al. 1977, Thomas et al., 1992). Konnov et al. use the application software plug CHEMKIN to model the heterogeneous reactions on the surfaces of the reactors. They proposed a simplified mechanism. It includes the following reactions: adsorption of O and H on the surface, the reaction of CH3 with H adsorbed on the surface, and the reaction of O with O adsorbed on the surface. The last two reactions of methane and oxygen involves the return of the species under discussion in the gas phase. In this way they are able to get a better agreement between experimental data and numerical results. Potter et al. (2008) have implemented a kinetic model with heterogeneous reactions to study the inhibitory effect of surfaces in which the reactor walls have been treated with acid or metal oxides on the auto-ignition phenomena at low temperature. The heterogeneous reactions considered involve HO2, RO2 and H2O2. These reactions have been incorporated into the kinetic mechanism of oxidation of n-butane. The simulations were performed considering the spatially uniform system, in order to assess the effect of heterogeneous reactions on the ignition delay times. The reaction rate constants are defined on the wall and depend on the geometry of the system, the activity of the surface and the temperature. Analysis carried out for auto-ignition of low temperature has shown that there is a loss of OH radicals, O, H on the wall, but that the termination

reactions of peroxides are much more influential, probably because of their slower reaction and therefore longer life in the system, so that they can spread up the wall and promote heterogeneous reactions. Consequently, only the radical HO2 reactions are interesting for the wall, while at lower temperatures are RO2 radicals in sufficient quantities to be potentially important for surface reactions. Cheaney et al. (1959) studied the effects of surfaces on the combustion of methane and divided the surfaces into two classes, each connected to a specific mixed reaction. The category I includes the acid-treated surfaces.

Reactions are the following:

$$HO_2(g) + H^+(s) \rightarrow \tfrac{1}{2} H_2O_2(g) + \tfrac{1}{2} O_2(g) + H^+(s)$$

Category II is related to surfaces covered with metal oxides or salts.

The kinetics of the surface is as follows:

$$HO_2(g) + e^-(s) \rightarrow \tfrac{1}{2} H_2O(g) + \tfrac{3}{4} O_2(g) + e^-(s)$$

Whereas for the hydroperoxides kinetics are these:

$$RO_2(g) + e^-(s) \rightarrow \tfrac{1}{2} RH(g) + \tfrac{1}{2} Olefins + e^-(s) + O_2(g)$$

The comparison with experimental data shows that the model is able to predict the main features of the process of ignition. In particular, the results show that for temperatures below 700 K the heterogeneous reactions related to RO2 radicals influence the ignition temperature of the mixture, while for temperatures higher than 650 K the reactions involving radicals HO2 and H2O2 affect the minimum pressure which occurs ignition. Egerton et al. 1957 studied the slow oxidation of methane by focusing on the effects of reactions on surfaces, for temperatures between 450 ° to 500 ° C and pressures from 100 to 400 mm Hg. Soo been determined yields of methane to formaldehyde, the reaction intermediates and hydrogen peroxide. The reactions are faster in containers of silica or

Pyrex treated with hydrofluoric acid and washed with water. In glass containers coated with potassium chloride or alkali, the reaction proceeds much more slowly and with a long induction period. In the vessels treated, the order of reaction and activation energy were 2.3 kcal and 39.3 respectively. was also evaluated the effect of the size of the container on the reaction rate. Tripling the surface / volume ratio did not notice a substantial change in the order of the reaction rate or of the maximum formaldehyde, although the maximum production of hydrogen peroxide is slightly increased. Experiments were also made in containers coated with lead oxide, boric oxide, silver and gold in a reactor. The lead monoxide strongly inhibits the formation of peroxide and thus strongly limits the reactions. The reactor treated with boric acid behaves in a similar manner to that of Pyrex treated with hydrofluoric acid. The gold surface prevents the reactions, even at 500 ° C and 600 mm pressure. The effects of diluents such as nitrogen, argon and helium have been studied. The reaction rate and the rate of formaldehyde increases slightly with an increase in the percentage of diluent. The water vapor has a slight effect of promotion of heterogeneous reactions, which appears to be stronger than carbon dioxide. They concluded that formaldehyde as well as other intermediate products control the speed and, as in hydrogen-oxygen reaction, HO2 plays an important role through the reaction:

(5) $$CH_4 + HO_2 \rightarrow H_2O_2 + CH_3$$

The surfaces covered with alkali and lead monoxide are especially active in destroying HO2. Finally, David and Schmidt (1999) studied numerically the process of partial oxidation of methane to syngas using code CHEMKIN II and different kinetic mechanisms. They focus attention on the impact of heterogeneous reactions on the time of auto-ignition of the mixture and products selectivity. In particular introduce radicals O, H, OH and species such as H2O2 and CH3OH in the mixture of methane and oxygen, characterized by a feed ratio CH_4/O_2 of 1.7, for different initial temperatures (1000 K,

1400 K) at atmospheric pressure. The insemination of these chemical species ideally simulates the presence of radicals or molecules produced by any catalytic reactions. The first case study at 1000 K clearly shows that insemination reduces the time delay auto-ignition of homogeneous reactions. With an initial concentration of O by about 3.7%, it decreases by about 80%, ie from a value of 1.1 to 0.2 s. All other introduced species, both molecular radical, showed similar results. They argue that a percentage equal to 3.7% of all radical and / or molecule produced by catalytic reactions in a system is impossible. Percentage of 0.1% in real systems are credible. Using these percentages, the ignition delay decreases slightly. In the event that instead the inlet temperature is equal to 1400 K even a high percentage of introduced species do not have a significant effect on the ignition delay. For both temperatures considered, the insemination of chemical species in the main stream does not change the yield of products. In conclusion, the literature suggests that the chemical kinetics is greatly affected by heterogeneous reactions on the surface of the reactors. Such reactions may have a role thus inhibiting or catalysis. It 'important to note, however, that the kinetics of surface plays a fundamental role in systems at low pressure and low temperature, ie in operating conditions for which the homogeneous gas phase kinetics is very slow while the diffusion processes are significant and radical species can migrate to the vessel walls and promote the surface kinetics. The processes previously reported because they relate to oxidation of methane or partial processes of auto-ignition of hydrocarbons to which the temperatures of interest are relatively low and relatively slow kinetics of homogeneous oxidation. It 'may be said therefore that the problems are relevant in the case of catalysis in which the characteristic times of homogeneous and heterogeneous kinetics are comparable with each other. So the possible occurrence of heterogeneous reactions is to be excluded in the system used in this thesis because the temperatures of interest are significantly high and homogeneous oxidation is relatively fast.

To confirm this point you may notice that the residence times of the mixtures in the systems discussed above are relatively long, so the impact on the evolution of the heterogeneous kinetics of the oxidation process is relevant just because the characteristic times of the kinetics of the surface are compatible with those of residence. By contrast in the tubular reactor used in this thesis the residence time of the mixture is very small (thousandths of a second) to ensure that the evolution of the oxidation process is greatly influenced by the surface kinetics, which is notoriously slow. In fact, the kinetics of heterogeneous processes involving adsorption on active sites of the wall configurations of reactors, chemical reactions and desorption.

Chapter III

Methodologies for the study of MILD combustion process

This thesis may be included within the broad context of the studies on combustion processes connected to the large class of MILD or HTAC combustion technologies. In this respect the thesis deals with numerical and experimental studies of the kinetics of oxidation of different fuels at high dilution and high inlet temperatures. In particular the attention was focused on the determination of ignition delay time and the identification of main kinetic pathways active, at different stages of the oxidation process and for different fuels.

Experimental measurements were carried out using a reactor already available in the laboratories of the Institute for Research on Combustion of the National Research Committee in Naples. The core of the experimental reactor is a tubular flow reactor, similar to a PFR. The feeding section of the reactor has been designed with the intent to ensure optimum mixing of the charge in order to create a premixed feed. A thorough description of the plant layout will be given in the next paragraph. The choice of a tubular flow reactor, is justified by some intrinsic characteristic of such configuration that allows for following the temporal evolution of the oxidative process along the axis in a continuous fashion and to separate the mixing phase from the reactive one. In addition, in this case the combustion process is independent of transport phenomena, differently to what occurs, for example, in a counter diffusion flame. Other advantages include the possibility to easily perform sampling and measurements within the reactor itself at different position along the axial

coordinate or at the end of the reactor and the ease to adjust time, in a fairly wide range, resolution of measurements acting on the residence time (i.e. on flow velocity).

Along with the experimental work, a parallel numerical work aiming to deepen the understanding the phenomena observed in the experiment and to assess the availability of kinetic mechanisms available in literature was performed.

In this chapter experimental and numerical tools used during the thesis preparation work, for the characterization of mixtures of different fuels combustion in MILD conditions, are presented in detail. In particular, the first part of the chapter describes the experimental set-up, the diagnostics and the analytical procedures, while the second part describes the numerical tools.

III.1 - Description of the facility and testing procedures

Experimental facility used for the study of the process of ignition of different fuels combustion in MILD conditions is schematically represented in Fig. III.1.

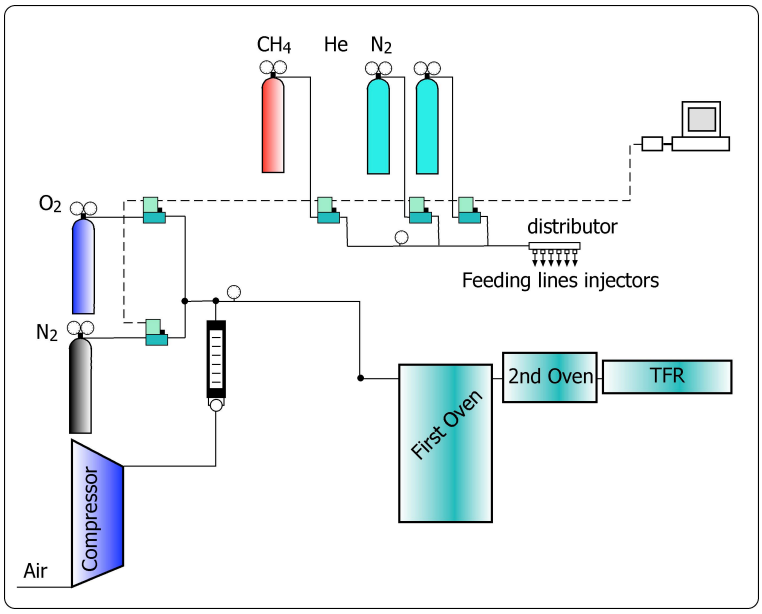

Fig.III.1 Experimental system layout.

The experimental set-up can be schematically divided in three main sections: A feeding section, a flow heating up system and the tubular flow reactor.

The gas feed to the tubular flow reactor can be divided in two main parts: a main gas flow, that is a mixture of inert gases, used as diluents, and oxygen, and a secondary gas flow, essentially made up of the fuel and an appropriate amount of inert gases to keep the optimize the mixing of the two flows in the reactor premixing section. Rate, pressure and composition of the main and secondary gas flows are regulated by means of a set of regulators/flowmeters by Bronkhorst (www.bronkhorst.com) controlled by a PC. The management and visualization of flow using during the data acquisition is monitored through a control panel developed in Labview. The automation of the plant management was a necessary step in order to regulate the flow rates needed, and the exact relationship between these and working temperatures and pressures.

The entire gas supply line and the reactor were built in 310 stainless steel as this material is able to withstand high operating temperatures and has reduced corrosion.

The heating up of the inlet gas flow up to the desired temperature is made by means of two heaters. A first heater (P_{max} = 14 kW) is placed immediately downstream of the inlet air supply line. The gas flow passes through a coil of stainless steel, whose specifications are shown in Fig III.2, placed inside a ceramic oven heated by four fiber heaters (Watlow®), controlled by means of a SSR actuator and a PID. The heat exchanger dimensioning and optimization have been made in order to maximize heat exchange efficiency while keeping the total volume as small as possible. This first heater is used to rise the inlet flow temperature up to about 800 K. The preheated gas is then sent to a second ceramic heater (P_{max} = 5 kW), with a similar design but with a much smaller size and, hence, thermal inertia, that is used to reach the final prefixed temperature.

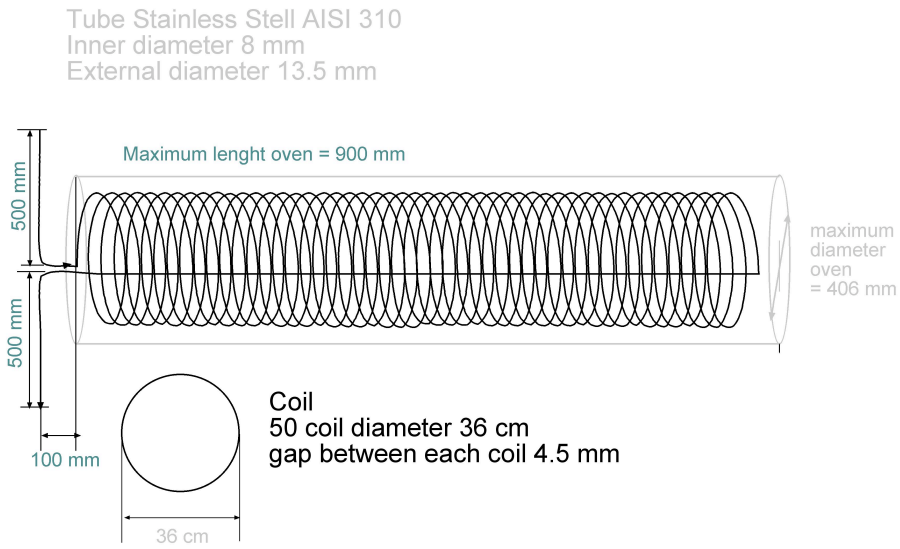

Fig III.2 Specifications of coil used in the main heater.

The core of the experimental system is a tubular reactor manufactured in steel AISI 310 with physical access to the temperature measurements. The axial dimension of the reactor is 150 cm while the inner diameter is equal to 1 cm. A singular unit of the reactor is shown in fig. III.3. Thermocouples are placed every 5 cm along the axis of the reactor and allow the acquisition of temperature profiles along the axial dimension of the reactor.

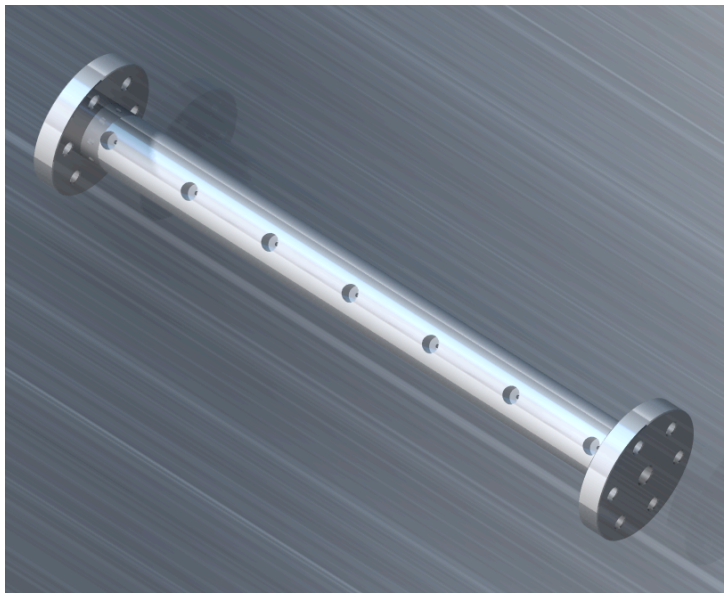

Fig III.3 Detail of a singular unit of the reactor .

The fuel is fed directly to the mixing zone, upstream of the test plans by 6 injectors placed on the walls of the same mixing zone. The optimum mixing is ensured by a flow injection configuration in crossflow with the main flow (fig. III.4).

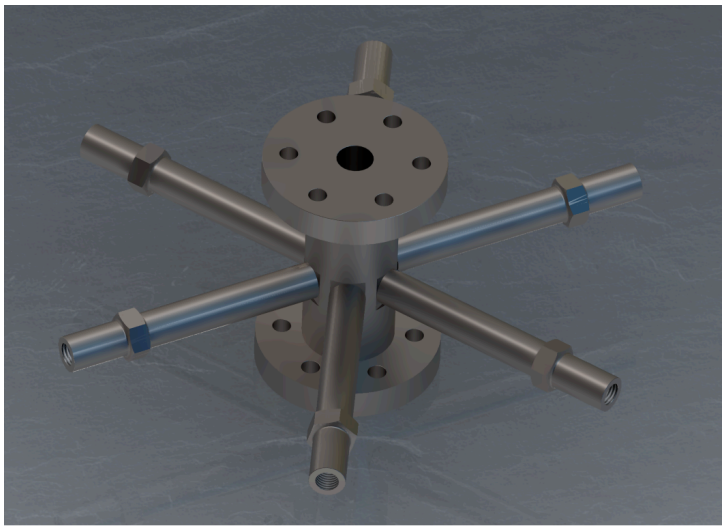

Fig III.4 Detail of the mixing section of the reactor.

At this regard, particular care was used in the design of the mixing section in which the mixture of oxygen / diluent is thoroughly mixed with the fuel. In the followings a detailed description of the design procedure of the pre-mixer is reported.

The execution of the experimental tests can be divided into several phases:

- Start-up of the experimental plant.
- Data Acquisition.
- Post-processing data.

During the first phase of preparation the reactor was fed up with air. The flow required is provided by a compressor (shown in blue in Fig III.1), and regulated by flowmeters placed on the feed line. This preparation is important for the achievement of the desired working temperature inside the test region. During data acquisition the main flow is replaced with a suitable mixture of nitrogen and oxygen at specific flow rates. The secondary flow composition is varied in dependence of the specific test being conducted.

In the following phase of post processing the acquired temperature profiles were elaborated to determine the ignition delay times and the temporal evolution of the ignition process.

The definition of ignition delay time requires the use of specific criteria. In general, τ_{ign} is correlated with the value or concentration of a chemical species or with the reference system ΔT . An analysis of various analytical criteria available in the literature for the definition of τ_{ign} mixture methane / air was carried out by Zhou et al. (G. Zhou 1994).

In this thesis τ_{ign} is defined as the time for the system to increase its temperature by 10 K compared to the T_{in} . The ignition delay is estimated by dividing the axial position for which $\Delta T = T_{reactor} - T_{in}$ is 10 K (M. De Joannon 2002) by the gas flow speed at 2 mm from the reactor wall. The values are interpolated linearly between two thermocouples in order to obtain a temperature value for each position while the maximum speed of 2 mm is provided by fluid dynamic simulations.

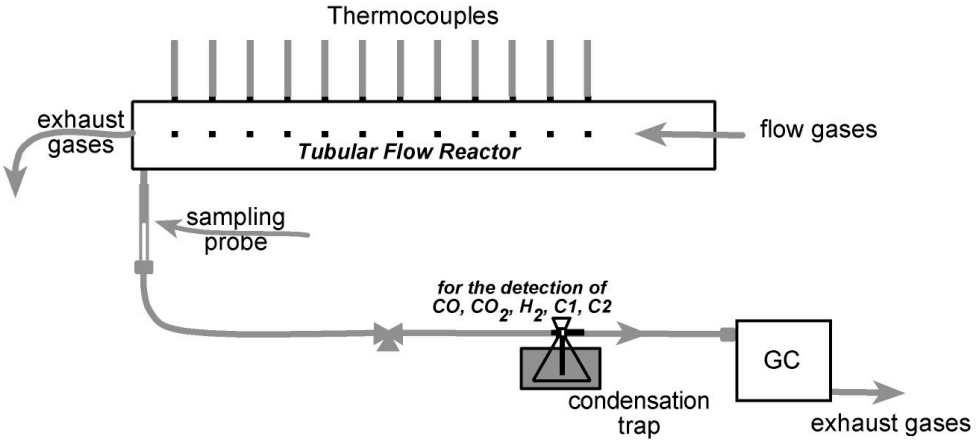

Fig III.4 - Layout of sampling system.

In order to understand the kinetic pathways follows by the mixtures used during the experimental tests, the experimental plant is equipped with a micro gas chromatograph (GC) made by Agilent Technologies Company. It is equipped with two columns. The

former is dedicated to the retention of H_2, N_2, O_2, CH_4, CO, while the latter to CO_2 and C_2 species (C_2H_2, C_2H_4, C_2H_6).

It is a compact and efficient analytical tool, using well established chemical separation and detection principles. The heart of the instrument is the GC module. It includes a heated injector, sample column, reference column, thermal conductivity detector (TCD), electronic pressure control (EPC) hardware, gas flow solenoids, and control board.

Operation can be better understood by examining what takes place during an analysis. The major steps include:

6. Injection
7. Separation
8. Detection

During the first step, the gaseous sample enters the Micro GC heated manifold. The manifold regulates the samples' temperature and directs it into the injector. The injector then drives the sample onto the column, while a vacuum pump helps draw the sample through the system.

After passing through the injector, the sample gas enters the column, which separates it into its component gases in typically less than 180 seconds (*separation*) . Gas chromatography works because different volatile molecules have unique partitioning characteristics between the column substrate and the carrier gas. These differences allow for component separation and eventual detection. In practice, achieving quality separations involves understanding and optimizing the effect of many variables including:

- Choice and thickness of column coating
- Column length and diameter
- Choice of carrier gas and flow rate
- Oven temperature

After separation on the column, the sample gas flows through a TCD. Carrier and sample gases separately feed this detector, each passing over different hot filaments (*detection*). The varying thermal conductivity of sample molecules causes a change in the electrical resistance of the sample filaments when compared to the reference or carrier filaments.

In fig. III.5 the layout of the sampling system is shown. Exhausted gases were sampled at the end of the reactor, throughout a dedicated pipeline. Gases are sucked out by means of vacuum pump and sent to the micro-GC for analyses on-line. The sampling AISI 316 stainless steel pipeline is long enough to cool down the exhausted gases up to environmental temperature. A silica-gel trap has been placed along the sampling line to remove condensed water.

The presence of oxygen species was evaluated by using a colorimetric technique developed for the identification of traces of formaldehyde in the atmosphere (T. Nash 1953; T. Salthammer 2008). This technique allows to evaluate the concentrations of formaldehyde in water and is based on the Hantzsch reaction. It is a cyclization reaction among formaldehyde, acetyl-acetone and ammonium acetate which leads to the formation of a compound di-idropiridina**,** 3-5 diacetyl 1,4 diidrolutidina (DDL). This compound has a specific factor in UV-visible has a maximum at a wavelength of 412 nm, whose position does not depend on dilution and therefore it is suitable for the determination of the compound concentration in the liquid phase.

Therefore an efficient sampling strategy for formaldehyde in water and a protocol for measuring the concentration of formaldehyde in the same aqueous solution was developed. Considering the high solubility of formaldehyde in water, the exhaust gas flow from the tubular reactor are sucked out by a vacuum pump (made by KNF laboport) at a flow rate equal to 12 Nl/min and got throw a known amount of distilled water for an appropriate time so that formaldehyde was adsorbed. In particular, the time must be enough such that

the concentration of formaldehyde adsorbed is the equilibrium concentration corresponding to the partial pressure of formaldehyde in the gas flow. In this way, the concentration of formaldehyde in the liquid phase is relating to the concentration of formaldehyde in the gas flow coming from the tubular flow reactor. In particular, the concentration of formaldehyde in the liquid phase can be calculated by means of the apparent Henry's constant reported in the literature by Seyfioglu (R. Seyfioglu 2006), according to which:

$$P = C \exp\left(\left(-\frac{1641{,}3}{T}\right) - 3{,}089\right) \tag{9}$$

where P is the partial pressure expressed in atm, C is the concentration of formaldehyde in the liquid phase, expressed in M and T is the temperature in K. For a temperature of 293 K the partial pressure dependence of the concentration is shown in fig. III.5.A.

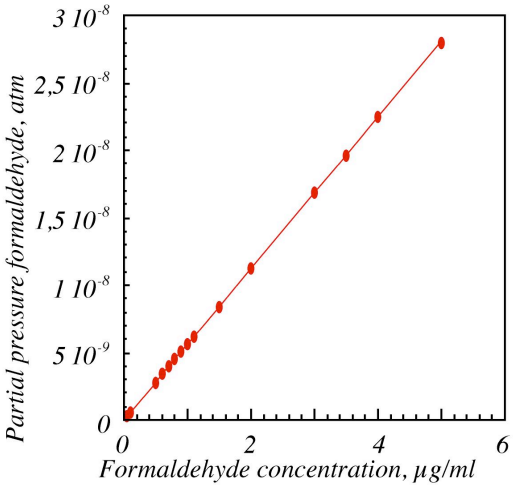

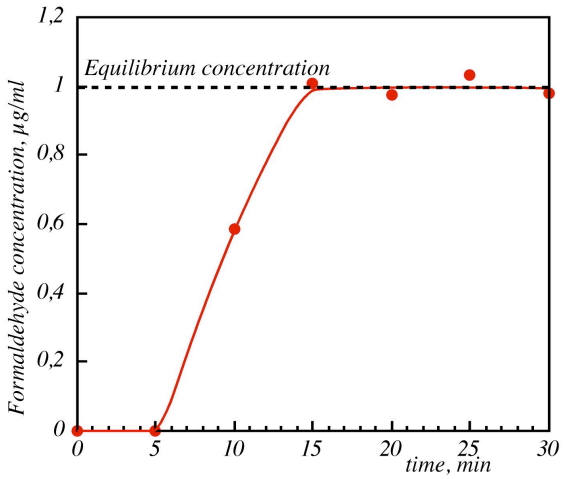

The estimation of the time necessary to achieve the equilibrium between the concentration of formaldehyde in the liquid phase and gas flow, adsorption tests were carried out in water using gas flows containing known partial pressures of formaldehyde. The range of potential concentrations of formaldehyde in the gases obtained in the working conditions

were used to assess the values of partial pressures and were obtained by means of kinetic evaluation done with the CHEMKIN software. Fig III.5 shows the time dependence of the concentration in the liquid phase considering a gas stream containing a partial pressure of formaldehyde equal to 5.6 atm and 9 atm. In this condition an aqueous solution contains 1μg/ml of formaldehyde.

The equilibrium concentration, indicated in the Fig by a dashed line, in the liquid phase is reached after a time of 15 min. Based on this results, the sampling time was set equal to 20 min.

For the evaluation of formaldehyde concentration in the liquid phase, the reaction of Hantzsch was done by following the method of Nash (T. Nash 1953). The aqueous solution was treated by using an equal volume of an aqueous solution of ammonium acetate, acetic acid and acetyl-acetone in concentrations equal to those reported in Table IV.1, which represent the optimal values identified by Nash relating to the speed of the reaction and the stability of the product.

Composition of Aqueous solution	
ammonium acetate	2M
acetic acid	0,05M
acetyl-acetone	0,02M

Tab. III.1 - Composition of the reactive aqueous solution for the reaction of Hantzsch

Afterwards, the solution was placed for 20 minutes in water at a temperature of 313 K. In this interval of time reaction of cyclization occurs and leads to the formation of DDL. The solution assumes a yellow color. The absorbance at 412 nm of the sample obtained was evaluated by measuring the absorption spectrum using a UV-visible spectrophotometer made by Agilent 8453A, as an example shown in Fig III.6.

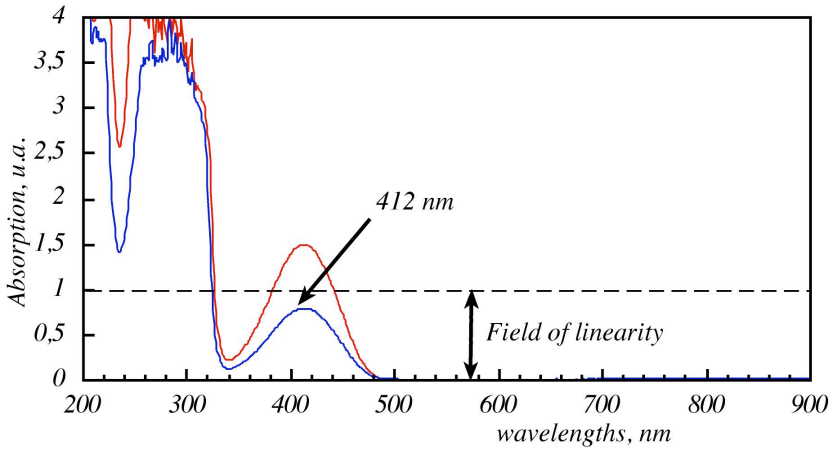

Fig. III.6 - UV-Visible absorption spectrum of DDL

The function of the instrument was obtained by measuring the absorbance of solutions at known concentrations. The calibration curve thus obtained is shown in Fig. III.7.

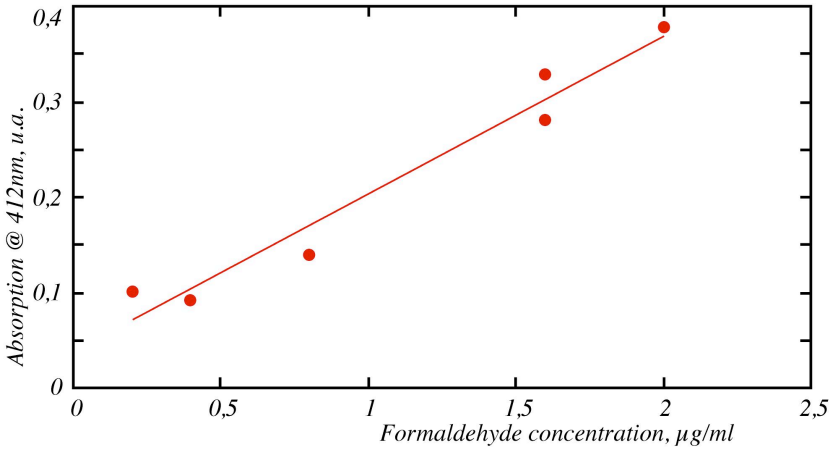

Fig. III.7 - Dependence of absorbance on the concentration of formaldehyde in the sample

The experimental plant was also equipped with an optical diagnostics system. Such system was implemented to make measurements of the light emitted spontaneously from the reaction volume, shown schematically in fig.III.8. A fiber-optic endoscope to collect the radiation from the reactor, optically accessible through the quartz window in the present at the output section of the reactor itself. The endoscope focuses on the two-dimensional image input section of an image intensifier (made by Hamamatsu). A camera fast (Nanosense Mk III made by Dantec Dynamics) was used to the acquisition and storage of

two-dimensional images (1280x1024 pixels) by means of Dynamic Software Studio. The images are sampled with a frequency of 30Hz and acquisition of a dynamic field of 8bit. Upstream of the endoscope, the light emitted spontaneously from the reaction volume was analyzed using bandpass filters, so you can make a rough estimate of the classes of species present in the volume control. In particular they have been used a filter that allows the collection of wavelengths below 400 nm and a filter that allows the harvest between 500 and 600nm. The fig. III.8 shows the layout of the system and a brief sketch of the subsequent procedure of the images post-processing. A small window was located at the end of the reactor and the light intensity was captured, filtered and amplified to the acquisition camera. Different filters were used in order to investigate a wide range of wavelengths. The frames collected were stored and post processed by means of a Labview routine. For each test condition a 1000-frame sample was collected. Moreover a background image was collected and then used to clean up the original images, reducing the electronic noise as well as the brightness of the bottom of the reactor, which operates at a very high temperature and emits a light beam similar to that of a blackbody at the same temperature.. A typical result was shown in fig. III.8 with false colors.

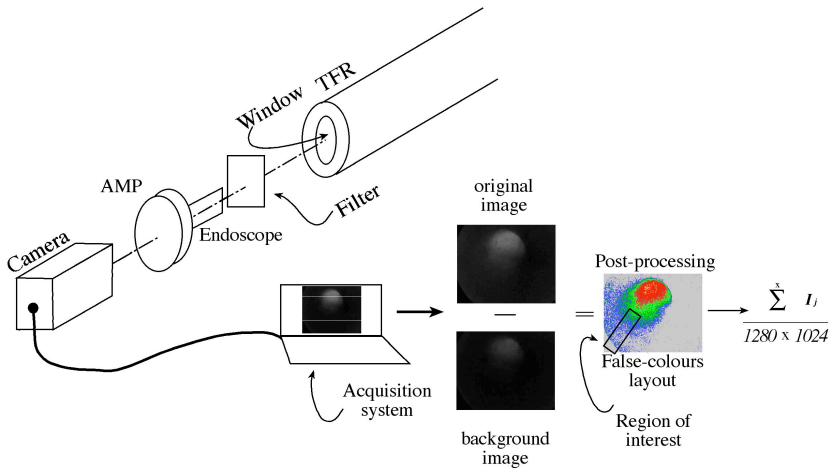

Fig. III.8 - Layout of the optical diagnostic system and sketch of the image acquisition procedure and post-processing.

III.2 - Numerical Tools

III.2.1 - Chemkin Software

The CHEMKIN is a software developed by Sandia National Laboratories for the solution of problems and interpretation of gas phase chemical kinetics with elementary. It 'a powerful and flexible tool for simulation of systems described by kinetic mechanisms detailed and complex. The software is widely used for the development and optimization of combustion processes. It allows also the study of systems not in thermal equilibrium, called plasma, where the reactions could be due to different temperatures and involve ions and electrons.

The CHEMKIN consists of four main parts: the thermodynamic database, the INTERPRETER, linking files, and the GAS-PHASE Soubroutines.

The thermodynamic database is a file that contains the declaration of many chemical species and their thermodynamic properties such as specific heat, enthalpy and entropy. These values are provided as constants which are the coefficients of polynomials in the independent variable temperature. The polynomial expression changes as a function of the temperature field analyzed. We recognize two fields, one for low temperatures and a high temperature. The cutoff between the two intervals, for most species, is 1000 K.

Thermodynamic information necessary for the study of a particular system can be declared in the file of the kinetic mechanism where are listed all the chemical reactions and rate coefficients. The reaction rate is expressed with the modified Arrhenius law:

$$K = A \cdot T^{b} \exp\left(\frac{-E \cdot a}{R \cdot T}\right) \quad (1)$$

The Interpreter is a program that can read information from the files of the kinetic mechanism and extract the necessary information from the thermodynamic database is added to a chemical species declared in the file of the reaction mechanism. It generates the files LINKING.

The latter is a binary file that contains all information relevant to the chemical species, elements and reactions that need to be sent CHEMKIN Subroutines running. Gas-phase Subroutines CHEMKIN consists of approximately 100 subroutines written in Fortran.

CHEMKIN software also has several applications designed to solve problems common chemicals.

Each of these applications can invoke the linking files and subroutines necessary for the numerical solution of the problem specified by the user.

For each sub-problem only a few, among all those available in the library of CHEMKIN, are used.

Some of the applications available are: a configuration OPPDIF to model jet opposed to plug flow reactors and piston SENKIN for batch reactors.

The user may define his alternative model through the set of equations governing the problem of interest. CHEMKIN software has also made planning somewhat simplified because the user has at his disposal routines in the Gas-Phase Library. The user only has to recall the right to define soubroutines equations, thermodynamics and combine them to define the system.

The application of the CHEMKIN used in this thesis is to simulate the reactor tube PLUG, which simulates the behavior of a PFR. More specifically, the application uses a non-dispersive model, consider the one-dimensional flow of a reactant species and the mixture is assumed ideal considered.

Plug solves the differential-algebraic set of equations that describe the reactor using an implicit numerical software DASSL. Plug solves the equations of the model to the stationary phase can be used in design, control and optimization of a tubular reactor in a flow.

III.2.2 - Cantera Software

Cantera is a software developed by prof. Dave Goodwin of the California Institute of Technology. And 'programmed in C + + and can be used in C + +, Python, Matlab and Fortran.

Cantera is a software for solving problems involving chemical kinetics, thermodynamics and transport problems. It can be used also for simulations of chemical kinetics reaction mechanisms with large, to calculate thermodynamic equilibrium, to evaluate the thermodynamic and transport properties of a mixture, to assess the rate of production of chemical species and make analysis of reaction pathways to simulate processes using series of CSTR and finally to model non-ideal fluids.

Cantera is an evolving software and its ability increase steadily over the years.

III.2.3 - Fluent Software

Fluent is a commercial software for computational fluid dynamics (CFD). It 'used to simulate, visualize and analyze such phenomena as the motion of a fluid, heat transfer, chemical reactions, turbulence and multiphase problems. It 's based on the finite volume method. The geometry and the mesh are defined using pre-processors or TGrid as Gambit.

III.3 - Fluid dynamics characterization of the reactor

In this section are the main tests carried out to feature a fluid dynamic point of view of the thermal reactor and the mixing section.

The mixing section, through which the fuel is injected into the system, was designed with an appropriate geometry to minimize the mixing time between the species.

In a first phase, a bibliographic research was made in order to evaluate the different mixing configuration. Then, further study were made in the evaluation of parameters such as shape, number, position and protrusion into the main channel of the injection orifices.

The configuration selected for an optimal mixing of stream of fuel and oxidizer / diluent consists of feeding a flow transverse jets.

The main parameter that influences the efficiency of mixing for a system with cross-flow jets is the ratio of the moments of J flows, defined as:

$$J = \frac{\rho_j v_j}{\rho_s v_s}$$

(2)

where ρ_j and v_j are respectively the density and velocity of incoming flow injected, and ρ_j and v_s are the density and speed of the main flow.

To the purpose of assessment of the configuration in terms of more efficient mixing of the main course and side parts, various tests were made on the mixing along the axial and radial coordinate system. The analysis carried out in particular have concentrated, for a given ratio of the moments of J streams, dependence of the degree of mixing on the variation of the converged, the number and radial position of the injectors.

Based on these studies was chosen the optimum configuration for the injection of the lateral flow within the mixing zone. This is guaranteed by six injection nozzles located along the walls and a convergent linear with a slope angle of 26 degrees. The nominal size of the injection diameter is 0.8 mm.

The mixing efficiency has been evaluated both experimentally and numerically.

The flow is injected into the reactor through six plane nozzles floors realized along the wall of the mixing zone and consists of the fuel and an equimolar flow of nitrogen and helium to make independently the efficiency of the mixing ratio C/O **.**

The numerical study on the efficiency of mixing was performed using Fluent's software. The geometry constructed in Gambit, shown in Fig III.3, consists of a first duct of 15 cm with a diameter of 1.4 cm, to obtain a fully developed flow before the mixing section. This is first duct is followed by a convergent linear with a slope angle of 26 ° and led by another 10 cm long.

In numerical simulations we used the K-ω turbulence model for multi-component equation.

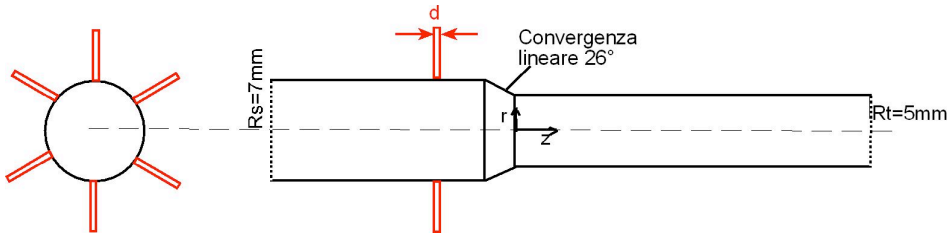

Fig. III.3 Geometry of mixing section

In order to highlight the efficiency of the mixing section, reports the results of a numerical test in which an equimolar mixture of methane / nitrogen / helium is fed into the reactor at 500 K. The final composition of the mixture is equal to a system fed at stoichiometric ratio and dilution level of 85%. In this test the main flow (oxygen / nitrogen) enters the first duct with a velocity of 13 m / s and a temperature of 1000 K.

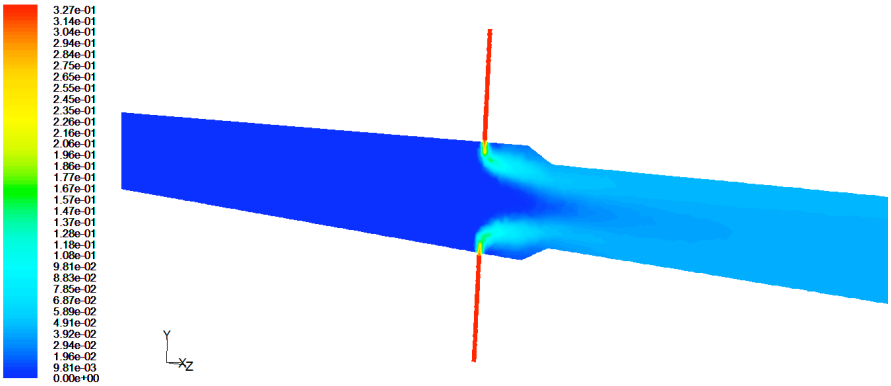

Fig. III.4 Distribution of molar fraction of methane for a side flow of methane / nitrogen / helium.

Fig III.4 presents the distribution of the mole fraction of methane, divided into 50 levels, along the axial direction in the plane z, for the numerical simulation described above.

To better analyze the efficiency of mixing of the mixing system, shown in Fig III.5 is the mole fraction of methane as a function of radius for three different sections of the reactor, respectively located at z = 0.1, 1 and 2 cm from the convergent duct.

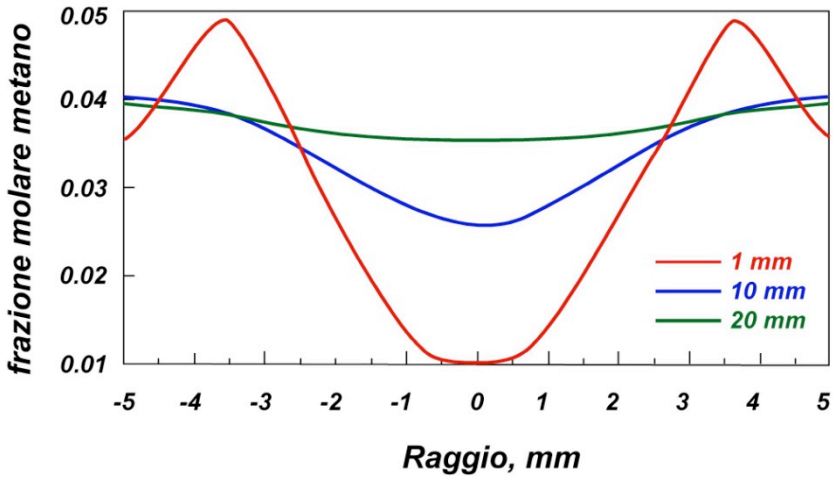

Fig. III.5 Molar fraction of methane as a function of radius for three different sections of the reactor

As can be seen from Fig III.5 the system reaches a level of complete mixing for z = 2 cm from the convergent and the final value of the molar fraction of methane is about 4%.

The mixing section is very flexible. It is possible to increase the value of J and thus the penetration of the jet, by varying the composition of the side flow or by using different gases.

This is important because this configuration will be used even with different fuels. To highlight this flexibility, in Figs III.6 and IV.7 are shown the distribution of the mole fraction of methane along the axial direction in the plane z as a function of radius for three different sections of the reactor, located respectively at z = 0.1, 1 and 2 cm from the convergent. This simulation is similar to that described above with the exception of the side flow made up of methane/nitrogen/argon in equimolar fractions.

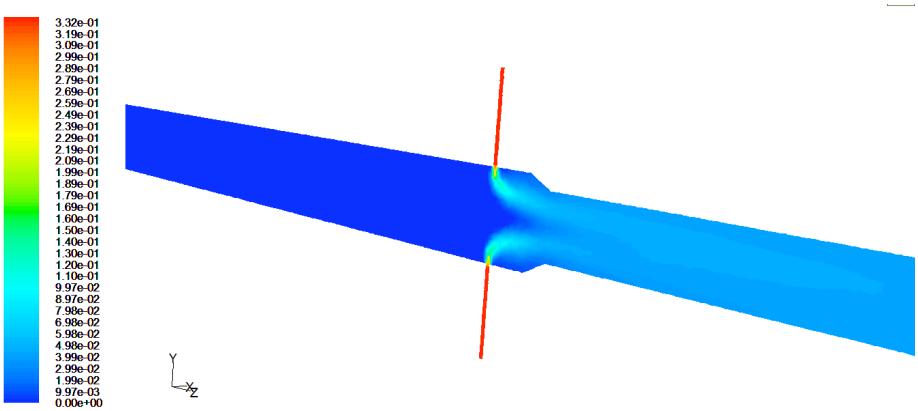

Fig. III.6 Distribution of molar fraction of methane for power supply side of methane / nitrogen

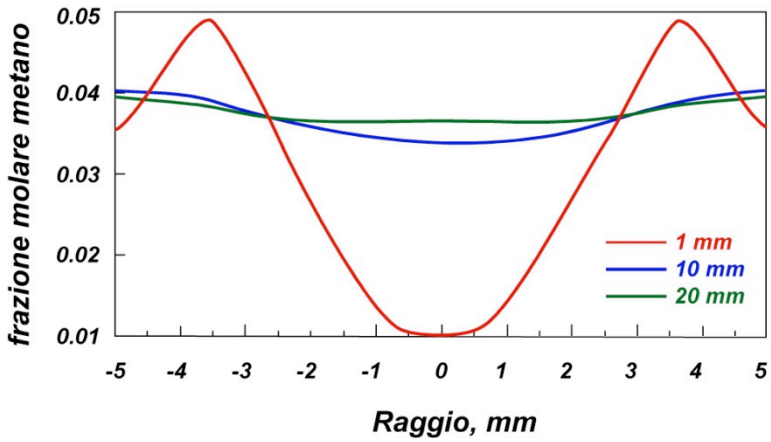

Fig. III.7 Molar fraction of methane as a function of radius for three different sections of the reactor

Optimum values of the main parameters (length and diameter of the reactor, etc..) were evaluated. so that the reactor could be approximated to a PFR.

Using a tubular flow reactor, similar to a PFR the MILD combustion process can be studied as a function of the axial coordinate. This allows to follow clearly the evolution of the process.

Based on these considerations, the length of the reactor was set equal to 1.5 m, the diameter of 1 cm and the input flow rate of 100 m/s. A study on the design of the reactor can be found in Sabia (2005).

However the preliminary tests have shown that for the power installed on the system, with a value of the input speed of 100 m/s, the residence time is too small to observe the ignition of the mixture under normal conditions of study.

The experimental evidence presented in the following chapter have been made with an inlet velocity of the flow (30 and 40 m/s). A slower velocity increases the residence time in reactor. In the following are a series of analytical approaches used to define the typical parameters (residence time, Reynolds number and etc.) of the reactor and to quantify some important characteristics of the flow.

An important parameter to evaluate the experimental evidence is the residence time t_{res} can be defined as the ratio between the length of the reactor and the average velocity of flow. Because of the presence of the walls the residence time of particles of fluid can be longer. However, the residence time defined previously is a good indication of the average time that a particle spends in the reactor.

Consider a particle of fluid that remains inside the reactor a time t^* making a number of convolutions n.

The time t^* is defined as:

$$t^* = \frac{\pi r n}{v}$$

(3)

where v is the average velocity of flow and r the radius characteristic of the convolution.

Based on these considerations, the length of the reactor L is equal to $2rn$ and, therefore, the residence time τ_{res} initially defined is equal to:

$$\tau_{res} = \frac{2rn}{v}$$

(4)

The relationship between the time t^* and time t_{res} is equal to $\pi / 2$, and then you make the mistake of considering the average speed is approximately 50%.

For an inlet velocity of the flow rate of 30 and 40 m/s the average residence time is respectively equal to 0.05 and 0.038 s.

By varying the speed, in addition to the residence time also varies the time resolution of the acquisition system is defined as:

$$\frac{\Delta x}{v}$$

(5)

where Δx is the distance between two thermocouples (5 cm) and v the average velocity of flow.

For an inlet velocity of the flow rate of 30 and 40 m/s time resolution is respectively equal to 0.00167 and 0.00125 s.

For the evaluation of ignition delay is important to know the velocity at 2 mm from the reactor wall. This value is numerically evaluated through the use of Fluent. In Fig III.8 are presented velocity profiles at z = 2 cm from the convergent duct obtained from numerical simulations with the software Fluent for a speed input flow of 30 m/s, for two different reactor T_{in} (1000 and 1300 K) and a degree of dilution of 85 %.

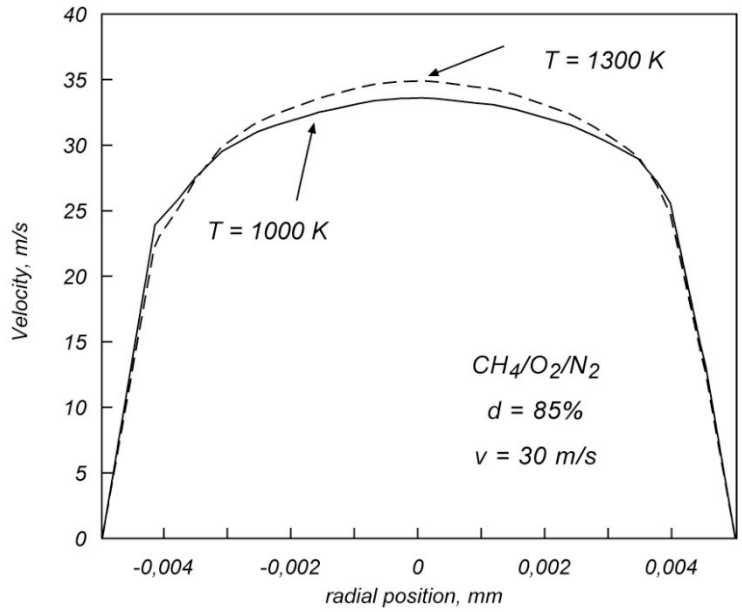

Fig. III.8 Profiles of velocity at z = 2 cm from the converging inlet velocity for a flow of 30 m / s for two different reactor Tin (1000 and 1300 K)

From Fig III.8 we observe that the velocity at 2 mm from the reactor wall is practically equal to the speed input to the system, regardless of the value of T_{in} , which is of fundamental importance for the evaluation of the main characteristic times is chemical and physical.

In addition, the Fig shows that the laminar boundary layer affected by the presence of the wall and that might be affected by catalytic effects is about 1 mm. For this reason, control measures have been placed at 2 mm from the walls of the reactor, so as to be outside of this layer.

A key parameter for the characterization of the flow is the Reynolds number, which represents the ratio between the forces of inertia and the viscous.

This dimensionless number is defined as:

$$\mathrm{Re} = \frac{\rho v d}{\mu} \tag{6}$$

The Reynolds number depends on the temperature through the density ρ and viscosity μ, and in particular for a gas it decreases the ρ and μ increases with increasing temperature. This means that the higher the temperature the smaller the Reynolds number.

Temperature (K)	***Velocity (m/s)***	***Re***
973	*30*	*2650*
1023	*30*	*2450*
1073	*30*	*2270*
1123	*30*	*2111*
1173	*30*	*1970*
1223	*30*	*1850*
1273	*30*	*1725*
1323	*30*	*1620*

Table IV.1 Values of the Reynolds number for a speed input to the system of 30 m / s as a function of T_{in}

Temperature (K)	***Velocity (m/s)***	***Re***
973	*40*	*3540*
1023	*40*	*3270*
1073	*40*	*3000*
1123	*40*	*2810*

Temperature (K)	Velocity (m/s)	Re
1173	40	2620
1223	40	2460
1273	40	2300
1323	40	2150

Table IV.2 Values of Reynolds number for a speed input to the system of 40 m / s as a function of T_{in}.

Depending on the value of the Reynolds number, we can distinguish three types of flow (values reported below refer to motion in tubes):

- for $Re < 2100$ the flow is laminar.
- for $2100 < Re < 3000$ the flow is transitional.
- for $Re > 3000$ the flow is turbulent.

In tables IV.1 and IV.2 are the values of the Reynolds number for a speed input to the system 30 and 40 m / s and varying the T_{in} . From the tables it is observed that for a speed input to the system of 40 m / s the flow regime is transitional, while a speed of 30 m / s regime is a transition not only for high T_{in} (up to 1150 K).

In relation to the fact that the Reynolds number decreases and kinetic times are shorter with increasing temperature in the future will be to conduct tests at fixed values of the Reynolds number, in order to better understand the effect of turbulence on ignition delay .

For a complete characterization of the reactor, as well as a simple assessment of the flow regime is important to assess the effects of dispersion of matter and heat both axial and radial.

The axial dispersion can be evaluated by introducing the Peclet number, which represents the ratio between the characteristic time of diffusion and the characteristic time of the axial convection. It is defined as:

$$Pe = \frac{\tau_{diff}}{\tau_{conv}} = \frac{vL}{D} \tag{7}$$

where D is the dispersion coefficient, v is the average velocity of flow and L is the length of the duct.

In particular:

- for $Pe \to \infty$ axial dispersion is negligible.
- for $Pe \to 0$ the dispersion is high.

To estimate the Peclet number you can use the diagram in Fig III.9 (O. Levenspiel 1958)) that shows the Reynolds number on the x-axis and the ratio D/vd_t on the y-axis, where d_t is the diameter of the tube. In literature is introduced the number of dispersion D defined as the reciprocal of the Peclet number rather than referring to the Peclet number. The axial dispersion is negligible for a value of D less than 0.01 (Levenspiel, 1958).

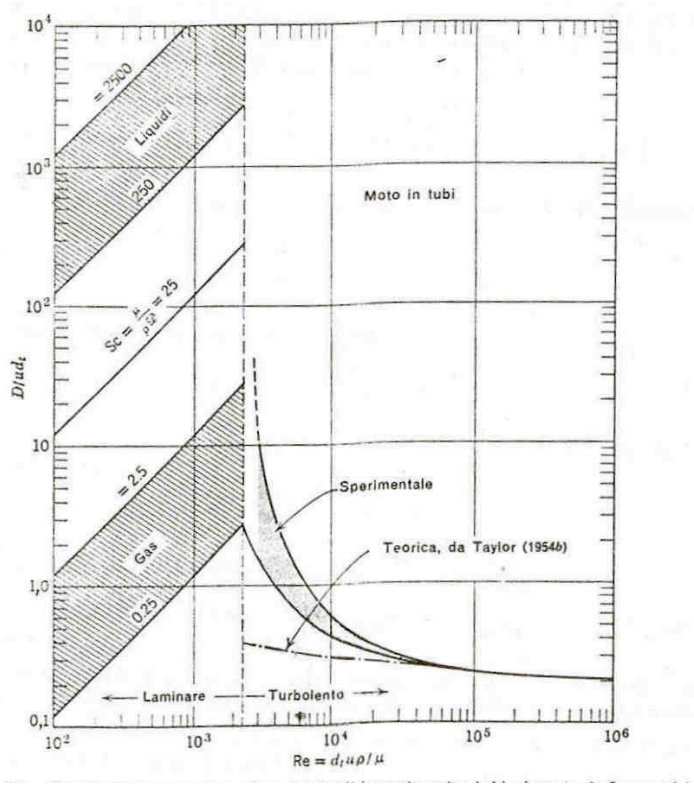

Fig. III.9 Diagram for the evaluation of the number of dispersion (Levenspiel, 1958)

Using the diagram above has a value for the speed input to the system of 30 and 40 m / s for a T_{in} of 1000 K gives a value of D respectively equal to 0.012 and 0.09. Therefore, for a speed value of 40 m / s, the axial dispersion is negligible while for a speed of 30 m / s the number of dispersion is slightly higher at 0.01 but also in this case it can neglect the effect of dispersion.

In order to assess the effect of axial dispersion due to turbulent diffusion must introduce the turbulent diffusivity, D_{turb} defined as the product of the turbulent fluctuation velocity v' and the size of the larger vortex. The larger vortex can have a maximum size of the tube while the fluctuation of the turbulent velocity v' is equal to the product of the average velocity of the turbulent flow intensity I .

The latter is equal to:

$I = 0.16 \cdot \mathrm{Re}^{-1/8}$

The characteristic time of convection is equal to the residence time τ_{res} as time characteristic of turbulent diffusion is equal to the ratio between the square of the length of the reactor and the value of turbulent diffusivity D_{turb}. Then:

$$Pe_{axial} = \frac{\tau_{diff}}{\tau_{conv}} = \frac{vL^2}{LD_{turb}} = \frac{vL}{D_{turb}}$$

(8)

For a speed value input to the system of 30 and 40 m / s for a T_{in} of 1000 K, the Peclet number is equal respectively to 2500 and 2700. This means that in both cases the axial dispersion due to turbulent diffusion alone is negligible.

In addition to an assessment of the axial dispersion is important to assess the effect of radial dispersion of the species and heat, which can be quantified by comparing the characteristic time of radial diffusion to the characteristic time of convection.

The characteristic time of diffusion is equal to the radial:

$$\tau_{diff} = r^2 \big/ Diff$$

(9)

Where with $Diff$ indicates the diffusivity of species that for the operating conditions is of the order of 10^{-4} m^2 / s.

For an initial temperature T_{in} equal to 1000 K, the diffusivity is equal to $1.8 \cdot 10^{-4}\, m^2/s$, and $d_t = 1cm$ is obtained that the characteristic time of radial diffusion is equal to 0.14. As mentioned previously, the characteristic time of the forced convection is none other than

the residence time is 0.05 s and for a speed input to the system of 30 m / s and is equal to 0.0375 for a speed of 40 m / s.

Therefore the characteristic time of convection is only 3 times smaller than the characteristic time of radial diffusion, while this factor is approximately 5 for a speed of 40 m / s. This result highlights the fact that the radial dispersion for the system under consideration can be neglected.

Chapter IV

Experimental Results

The experimental tests for the characterization of the oxidation process of fuel mixtures in condition typical of the MILD combustion, were carried out in the tubular flow reactor described in the chapter IV.

The experimental tests were performed by varying some characteristic parameters to characterize the oxidation of different fuel blends in working conditions typical of MILD combustion processes. As described in the previous chapter, due to the experimental facility having been purposely designed and set up, the working parameters can be varied independently from each other thus allowing to explore the effect of a single parameter on the whole process.

The experimental results will be presented by dividing them into paragraphs according to the investigated parameters considered. These are summarized in table IV.I which have been summarized in the table IV.1 below.

Fuel	*Dilution %*	*Velocity (v) m/s*	*Temperature (T) K*	*C/O*	*Ω*
Methane	*85-90-95*	*30-35*	*from 1150 to 1400*	*from 0.015 to 1*	*-*
Biogas	*90-95*	*30*	*from 950 to 1350*	*-*	*from 0.02 to 10*

Table IV.I Summary of experimental condition grid analyzed in the thesis

Thus, in the first session, tests were carried out for v=30 m/s, a degree of dilution of the mixture fed to the reactor equal to 90% and by using methane as fuel. The chemical nature

of the diluent is one of the most important parameters of the blend according to the chemical peculiarities of the potential species used. During the first session of tests the species for diluting the mixture was nitrogen.

Afterwards, further tests were made to evaluate the effect of the dilution parameter on the general behavior of the system as well as on the peculiarities of the oxidation process. In particular, during the second session test, the dilution degree was diminished and increased at 85% and 95% respectively, keeping the other parameters constant. The main flow rate is one of the crucial feeding parameter of the experimental plant, so supplementary tests were made by varying the velocity of main flow from 30 m/s to 35m/s. These tests are necessary for a full characterization of the oxidation process, and are also required to assess repeatability and validity of the characteristic oxidation times evaluated.

Further tests were carried out by varying the chemical nature of the fuel. The increasing industrial interest in alternative energy carriers with respect to the traditional ones is actually well-known. Among them, the ones derived from the thermal treatment of biomass, such as syngas and biofuel, occupy a central place. The usefulness of these fuels in industrial plants needed an evaluation of their oxidation process because their calorific value is generally low, thus making it very difficult to take advantage of their use in an efficient way. In this framework, the fifth session of tests was made by using a synthetic mixture of different hydrocarbons (denoted as *biogas* in the following). In order to characterize oxidation of fuels derived from biomass pyrolysis processes a mixture of fixed composition (chosen on the basis of evidence in literature) was selected. In particular, a gaseous mixture obtained from biomass slow conventional pyrolysis process (C. Branca 2003; P. Giudicianni 2005) was considered. As reported in Table IV.1, even for biogas, two degrees of dilution (90% and 95%) were investigated for a fixed velocity of main flow equal to 30m/s.

For each experimental test, the temperature profile along the reactor axis was measured and analyzed. On the basis of temperature increment during the process, different reactive and non reactive regimes were identified thus allowing for the build up working maps as function of operational parameters. At the same time, temperature profiles were also processed to obtain ignition delay times on the basis of the criterion reported in the chapter III, which relies on a minimum temperature increment of 10 K during the oxidation process.

In order to understand the reaction paths followed by the chosen fuels in the working condition considered, on line chemical sampling and analysis of gases were also made at the reactor exit. Concentration of supplied species as well as of species formed during the oxidation process of the mixture were measured.

IV.1 - Methane

As described in detail in chapter II, although several data are available in literature concerning auto-ignition of methane since it is a fuel widely known and used in industry and energy conversion plants working in standard conditions, nevertheless no data are available in regarding of conditions typical of MILD combustion.

In the following paragraphs, experimental results on highly diluted and preheated methane oxidation are thus presented. In particular, temperature profiles along the axial coordinate of the experimental plant were acquired. On the basis of these data, auto-ignition delay times were evaluated by using the criteria described in the chapter III.

Firstly, results obtained by feeding the reactor with a velocity equal to 30 m/s and a degree of dilution of 90% in nitrogen were presented. Moreover, lower and higher degrees of dilution were tested (85% and 95%) and a different main flow velocity was considered (35 m/s).

IV.1.1 - Main flow velocity: 30 m/s. Dilution degree: 90 %

Fig IV.1 shows temperature profiles obtained for three different initial temperatures (1263, 1313, and 1373K) and a value of feed ratio C/O of 0.05 as a function of the spatial coordinate of the reactor. The dilution degree has been set equal to 90 %, nitrogen was used as diluent species and main flow velocity equal to 30 m/s.

For the first temperature investigated (1263 K), the trend of the profile shows a small increase of temperature for a distance from the entrance of about 110 cm. The temperature rises slowly and reaches the value of 1287 K.

For T_{in}=1313 K the temperature profile is very similar to that obtained at lower temperature, even if a higher temperature increase at a shorter distance from inlet section is evident. In this case, the ignition delay time is shorter and the temperature reaches its maximum of 1370K.

For an initial temperature of 1373 K, ignition delay time significantly diminishes and there is an increase in temperature of 27 K. The mixture ignites immediately downstream of the inlet section of the tubular flow reactor and the temperature rapidly increases until it reaches a maximum value of 1397 K. It slowly decreased to a constant value of 1384 K.

The temperature profiles previously reported, can be used for summarizing system behaviors observed during the tests. Each single temperature profile acquired allows to fix a point on a (C/O -Tin) reactivity map as shown in Fig IV.2, where on a (C/O-Tin) plane the three red points are representative of the experimental conditions of temperature profiles reported in Fig. IV.1. The Fig also shows the stoichiometric condition ($C/O = 0.25$) with a dotted line. The delimited area at the bottom of the map has not been considered because of technical limitations due to flow controls used during the

experimental test. The species flow rates corresponding to these C/O are below the minimum value useful for the control system.

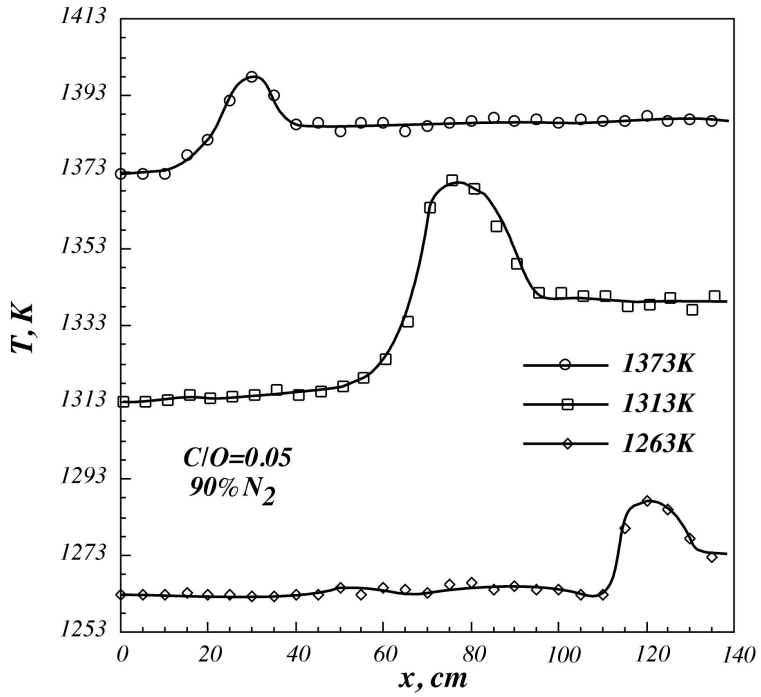

Fig IV.1 - Temperature profiles for three different initial temperatures obtained for C/O = 0.05 versus the spatial coordinate of the reactor.

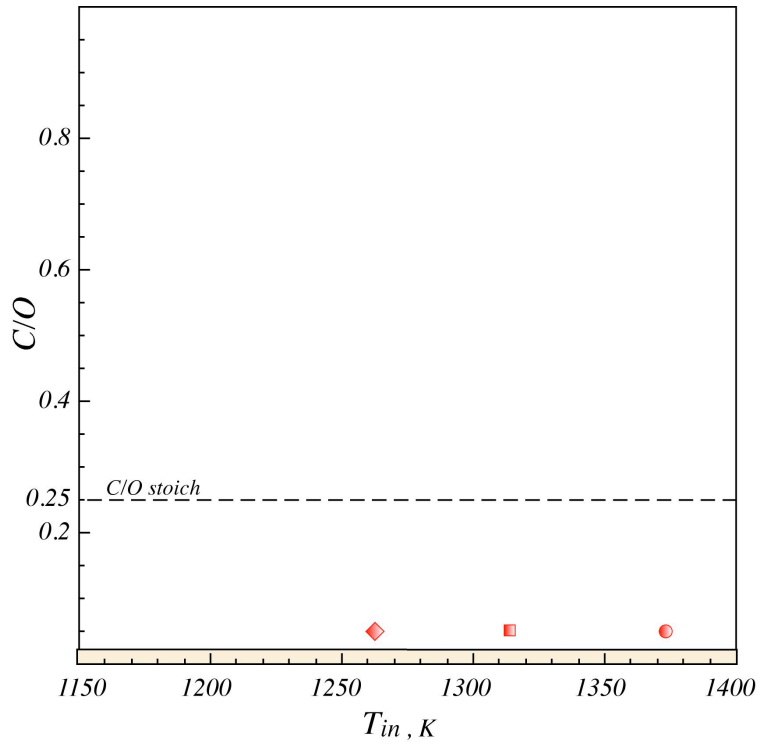

Fig IV.2 - Detail of the reactivity map. Three points correspond to the profiles presented.

Based on the temperature profiles obtained during the tests it was possible to obtain a reactivity map of methane for a specific working condition, showed in Fig. IV.3. It is possible to distinguish five areas according to different initial temperatures and feed ratios investigated. Each area was represented by a different color and is related to different observed phenomenologies.

For low temperatures (from 1150 K to about 1260 K) the system does not show any phenomenologies and does not ignite in the whole C/O range investigated. The area is reported in blue (*no-ignition zone*) and temperature profiles acquired for such conditions show no peak of temperature but just a linear trend corresponding to the initial temperature.

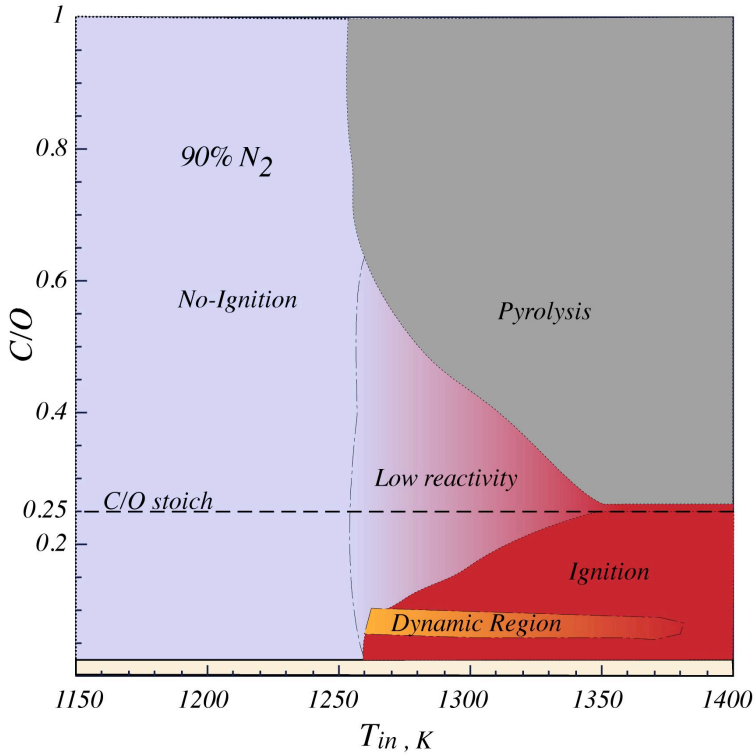

Fig IV.3 - Reactivity map of methane/oxygen mixture, diluted in nitrogen (90%) obtained for a main flow velocity equal to 30 m/s.

For temperature higher than 1260 K the system shows different phenomenologies. In the centre of the map is located a blue/red zone. This area is characteristic of working

conditions in which temperature profiles show a small increase of temperature, lower than the chosen auto-ignition criteria of ΔT=10K. Double colors of the area indicates an intermediate behavior between an ignition and no-ignition phenomenologies (*low reactivity zone*). Even though auto-ignition delay times in these conditions cannot be evaluated, it is significant to highlight that a chemical activity is present.

Moving from the *low reactivity zone* to higher temperatures and feed ratio values ($C/O > C/O_{stoich}$) there is a large gray zone denoted as *pyrolysis zone*. Such area extends for temperature values between 1350 K and 1400 K, just above the stoichiometric feed ratio C/O. For higher values of C/O, the pyrolysis area expands to lower temperatures. In particular, for a value of C/O equal to 1, the temperature range in which pyrolysis phenomena occur widens covering a temperature range from 1260 K up to 1400 K.

A temperature profile typical of that area is shown in Fig IV.4. This profile is indicative of a pyrolysis process with the formation of higher molecular weight hydrocarbons by means of endothermic reactions that lower the temperature. In particular, the Fig shows the temperature profile acquired by feeding the reactor with an initial temperature of 1358 K and C/O =0.8. It is evident a negative peak temperature at a distance of 15 cm from the entrance of the reactor. The temperature reaches a value of 1339 K with a negative difference in temperature of about twenty degrees.

The red region in the lower right part of the map of Fig. IV.3 is the *ignition zone*, The typical temperature profiles related to this zone are the one already shown in Fig IV.1, where a significant increment of temperature is present. The zone extends from 1260 K up to 1400 K and for values of feed ratio C/O up to stoichiometric condition. In this area it is possible to estimate the ignition delay time of the mixture, as it will be shown in the followings.

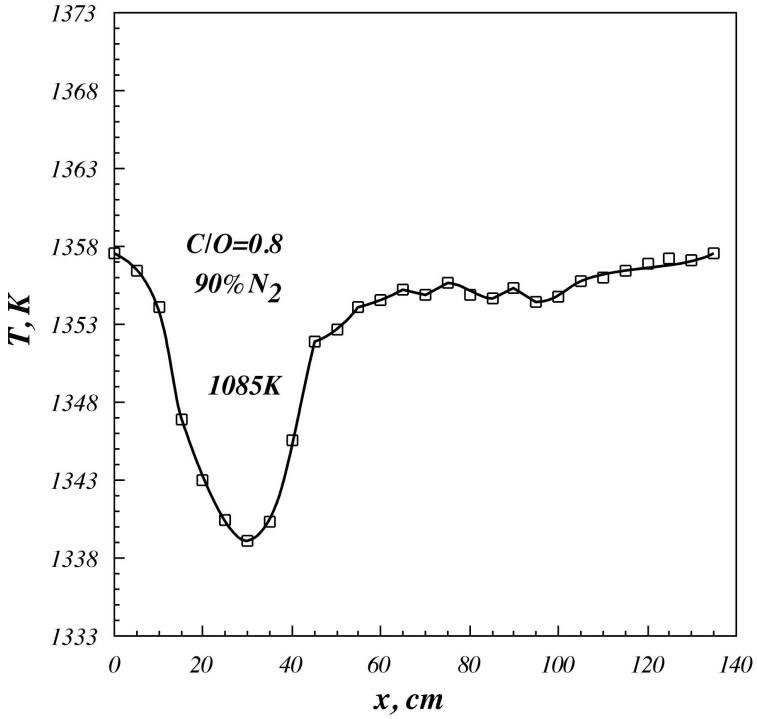

Fig IV.4 - Temperature profiles for Tin=1358 K obtained for C/O = 0.8 versus the spatial coordinate of the reactor.

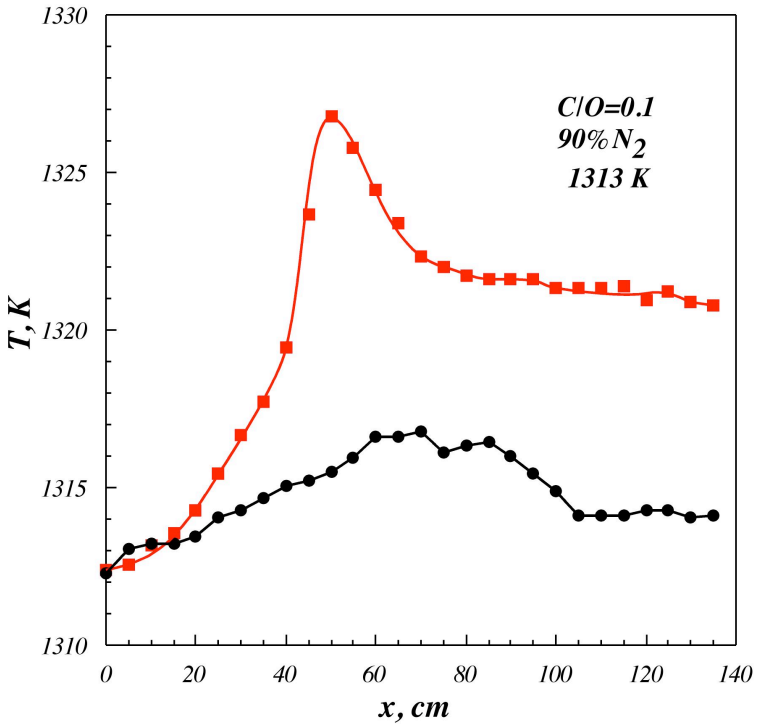

Fig IV.5 - Temperature profiles obtained for T_{in}=1313 K obtained for feed ratio C/O equal to 0.1 versus the spatial coordinate of the reactor.

A small orange zone is located within the ignition zone . It corresponds to C/O and T_{in} values where a non stable behavior was observed. These phenomena is shown in the reactivity map with the name of *dynamic region*.

In order to highlight this aspect in Fig IV.5 two temperature profiles representative of such a phenomenology are presented as a function of spatial coordinate of the reactor. These profiles have been collected for the same working conditions that are $T_{in} = 1313K$ and $C/O = 0.1$. The red curve is related to a reactive condition whereas the black one to a non-reactive conditions. In particular, in case of ignition, the temperature rises abruptly to the value of 1326 K and then lowers to a temperature of 1323 K. On the other side, black profile shows a slight increase in temperature (about two degrees). The temperature reaches the value of 1316 K and then undergoes a further decrease along the axial reactor coordinate.

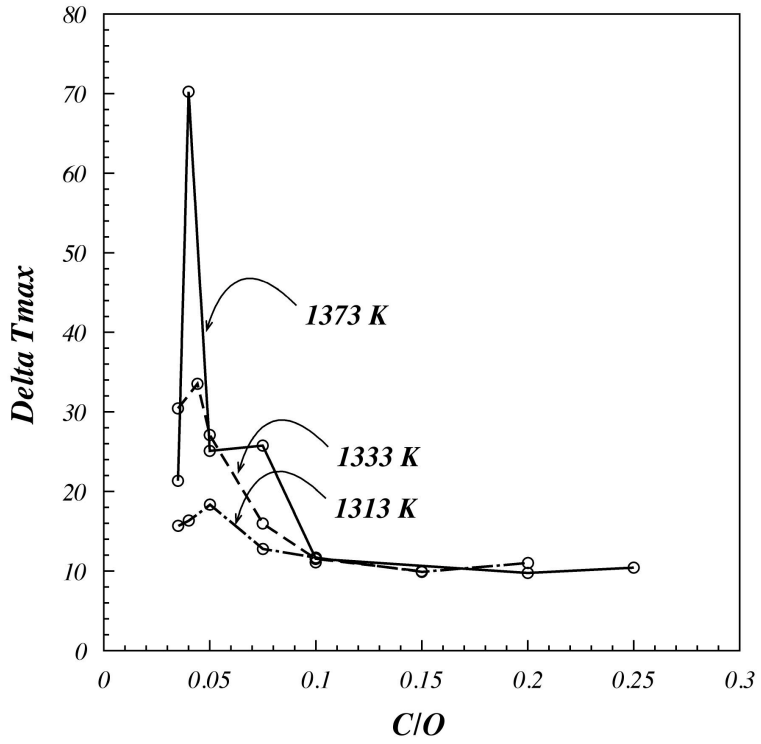

Fig IV.6 - Maximum temperature difference e as function of C/O for three initial temperatures (1313 K, 1333 K, 1373 K).

In order to highlight the main aspects of the experimental results Fig IV.6 shows the trend of maximum temperature difference acquired in the reactor (ΔT_{max}) as a function of C/O

Three curves are presented in the figure for different initial temperatures. All the curves show a maximum that depends on inlet temperature temperature and occurs for different values of C/O.

The dashed-dotted curve shows the ΔT_{max} obtained for the the initial temperature of 1313 K by varying C/O. For high values of feed ratio (from 0.1 up to 0.25) ΔT_{max} is equal to 10 K. A decrease in C/O leads to an increment of ΔT_{max} with a maximum of $\Delta T_{max} = 18K$ for C/O =0.05, then decreases to the values of 16 K.

A similar trend is observable for the dashed curve obtained for an initial temperature of 1333 K. As it is evident from the reactivity map for this T_{in} the mixture ignites also for a stoichiometric condition of feeding and shows a ΔT_{max} equal to 10 K. The same values are obtained for C/O up to 0.1. The difference of temperature then increases and reaches about 34 K for a C/O lower than the previous case ($C/O = 0.045$).

The last curve referring to an initial temperature of 1373 K shows the maximum ΔT_{max} . As it is shown in the figure this peak occurs for C/O lower than 0.05 and reaches 70 K.

On the basis of the ignition criteria **,** it was possible to evaluate the auto-ignition time for the all the working conditions in which ΔT transgresses 10K. As example, Fig IV.7 shows the ignition point on the profiles presented in Fig. IV.1. The red circle allows to locate the inception of the oxidation and hence the mixture ignition. In fact, in correspondence of these points a temperature rise of 10K corresponding to our criterion of ignition occurs.

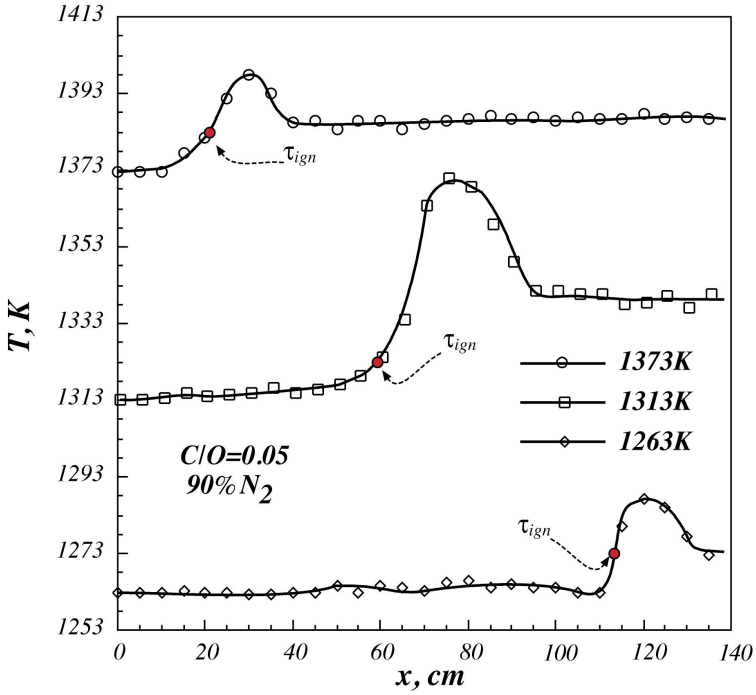

Fig IV.7 -Condition of ignition on the profiles presented previously.

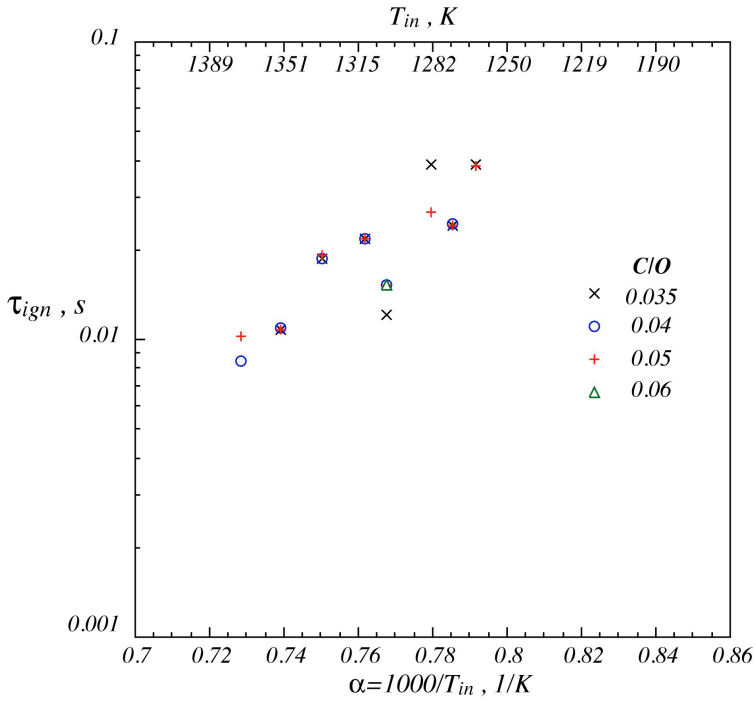

Fig IV.8 - Arrhenius plot of auto-ignition delay time of methane/oxygen blends diluted in nitrogen (90%) for different C/O .

Fig IV.8 shows in an Arrhenius diagram the auto-ignition delay times collected for four C/O , at v=30m/s and a dilution level of 90%. Some results were presented as an example

of all data collected. The parameter $\alpha = 1000 / T_{in}$ has been varied from 0.7 up to 0.86, corresponding to a range of temperatures from about 1162 K up to 1428 K. The times collected vary between a minimum of 0.008 sec, obtained for a value of C / O equal to 0.05 and an initial temperature of 1373 K, up to a maximum of 0.038 sec for $C / O = 0.04$ and $T_{in} = 1264 K$.

In particular, τ_{ign} for a value of C / O equal to 0.05 were shown in figure with cross-shaped points in red. It is worth noting that increasing the initial temperature implies decreases of auto-ignition times with an almost linear trend. For instance for $\alpha = 0.791$ the auto-ignition time of the mixture is equal to 0.038 sec then decreases to 0.027 sec for $\alpha = 0.779$. Finally the last experimental point is relating to $\alpha = 0.728$ with $\tau_{ing} = 0.01 \text{sec}$.

The experimental data are relating to fuel lean condition and are hence comparable. It is possible to highlight the same trend for all the C / O reported in the figure.

IV.1.2 - Main flow velocity: 30 m/s. Dilution degree: 95 %

One of the main peculiarities of MILD combustion mode is the higher dilution of the gases fed to the combustion system. So it is important to stress the dilution parameter in order to understand how it could alter oxidation pathways. In this sense several experimental tests were carried out with an higher dilution than the previous case. More specifically, the second session of tests were carried out by using higher dilution degree (95 %) while keeping constant the main flow velocity (30 m/s), the chemical nature of fuel and diluent.

As seen before, on the basis of the the temperature profiles obtained during the tests, it was possible to design a map of reactivity of methane in such a working conditions.

The temperature profiles acquired are similar to the previous case and were not presented again. However, the map obtained in a temperature range between 1150 K and 1400 K for a different feed ratio C / O (from 0.015 up to 1) is shown in Fig IV.9. Also in this case, the stoichiometric condition was indicated with a dashed line.

Five areas were located in the map. Each area corresponds to a different phenomenology observed during the experimental tests.

It is worth noting that the elevated degree of dilution has a great influence on the behavior of the system. The blue zone (*no-ignition zone*) extends its boundaries with respect to the previous case. The fuel/oxidant mixture ignites hardly and *no-ignition zone* is located from 1150 K up to 1350 K for every values of C / O investigated.

For temperature higher than 1350 K the system shows different phenomenologies. In the lower right part of the map is located the *ignition zone* (as usual in red color) in which the system shows profiles with a temperature rise equal to the chosen criterion. The zone is smaller than the previous case and extends for initial temperatures higher than 1350 K and for values of feed ratio C / O from 0.015 up to 0.1.

In the right upper part of the map, it is evident the presence of a *pyrolysis zone* in gray. Such area extends for temperature values between 1350 K and 1400 K and for all the feed ratio investigated starting from 0.45.

At the edge of the *ignition* and *pyrolysis* areas two more distinct zones defined as *low reactivity* (blue/red colors) and *dynamic zone* (in orange) were identified. Also in this case these areas were located close to the condition of mixtures ignition. Data acquired in the *low reactivity* region show slight increase of temperature (less than the chosen criterion) whereas the *dynamic* zone corresponds to a multiple temperature axial profiles.

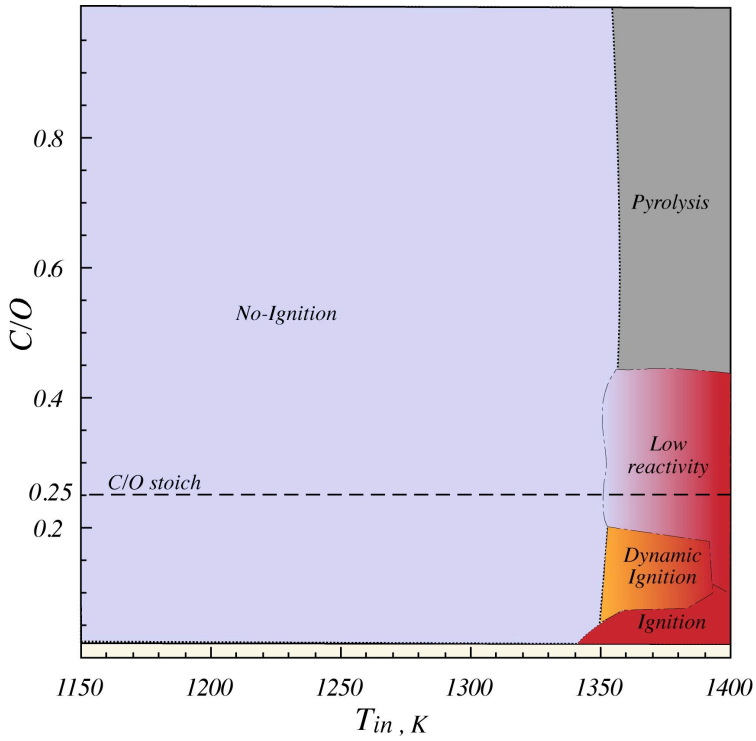

Fig IV.9 - Reactivity map of methane/oxygen mixture, diluted in nitrogen (95 %) for v=30 m/s.

However, the first phenomenology occurs in a range of temperature for feed ratio between 0.2 to 0.45, while dynamic zone were found from 0.1 to 0.2.

One of the peculiarities found at 95% of dilution is the overlap between the *dynamic* and *low reactivity zone*.

To highlight this aspect in Fig IV.10 two axial temperature profiles at a T_{in} =1363 K and $C/O = 0.1$ are presented. The red curve could be defined as a reactive condition while black one as a non-reactive condition. In the case of ignition of mixture, the temperature reaches the value of about 1398 K and then lowers to a temperature of 1358 K. In no-ignition condition the profile shows a slight temperature increase and could be categorized as a low reactivity condition (the difference of temperature is lower than 10 K).

In the literature that dynamic phenomena are justified with the competition of different oxidation pathways coupled with heat exchange processes. The different kinetic pathways

act in different ranges of temperatures and justify the observed temperature fluctuations in the experimental analysis (T. Wada ; M. De Joannon 2005; P. Sabia 2007; T. Wada 2011).

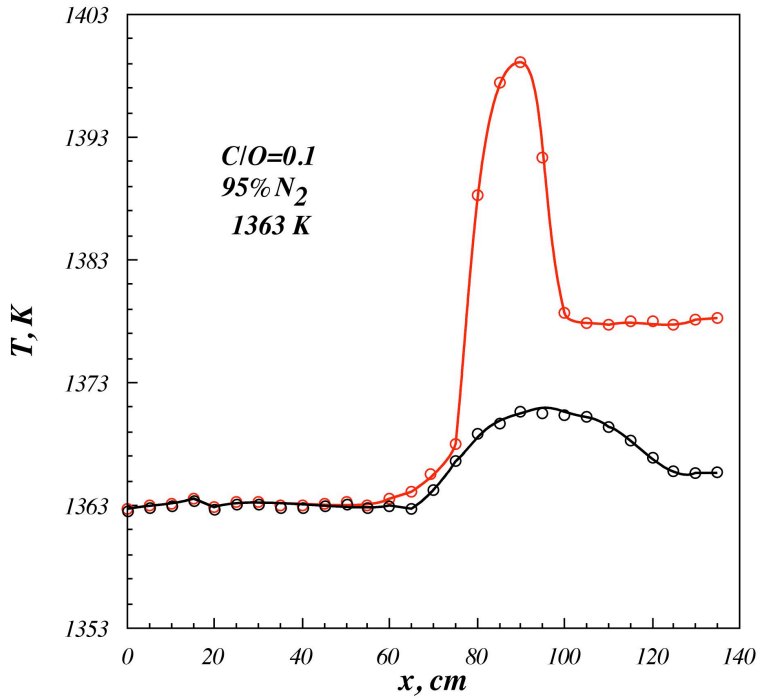

Fig IV.10 - Axial temperature profiles for T_{in}=1363 K and C/O =0.1

IV.1.3 - Main flow velocity: 30 m/s. Dilution degree: 85 %

Third session of tests were carried out by lowering dilution degree. In particular, a dilution equal to 85 % in nitrogen was fixed, keeping constant chemical nature of diluent and of fuel as well as the axial flow velocity.

In Fig IV.11 the reactivity map obtained in a temperature range between 1150 K and 1400 K by varying C / O from 0.015 up to 1 is shown.

As is evident from the figure, lower dilution degree implies higher global reactivity of the system in the same range of investigated parameter. As seen above, it is possible to classify different phenomenologies in the reactivity map with different colors. This means that a slavish characterization with respect to the previous case of the different behaviors was made in order to define the boundaries of the areas.

All the zones that identify a reactivity phenomenology are larger than that found in the previous cases. On the opposite, *no-ignition zone* extends from 1150 K up to 1200 K for lower values of C/O and is obviously smaller. The blue region widens for higher temperatures as soon as feed ratio increases. It is clear that for lean condition, mixtures ignite more easily.

In the upper right part of the map is located the *pyrolysis zone* (in gray) in which the system shows profiles with a negative temperature rise. The zone extends for initial temperatures higher than 1250 K and for values of C/O from 0.5 up to 1.

The *ignition zone* (in red in figure) was located in the right lower part of the map. Such area extends for temperature values between 1200 K and 1400 K for lean condition while its extension diminishes for higher feed ratio.

At its edge, in the upper left part of this area the *dynamic* zone(red/blue/orange colors) is located with an elongated shape from 1200 K up to about 1300 K.

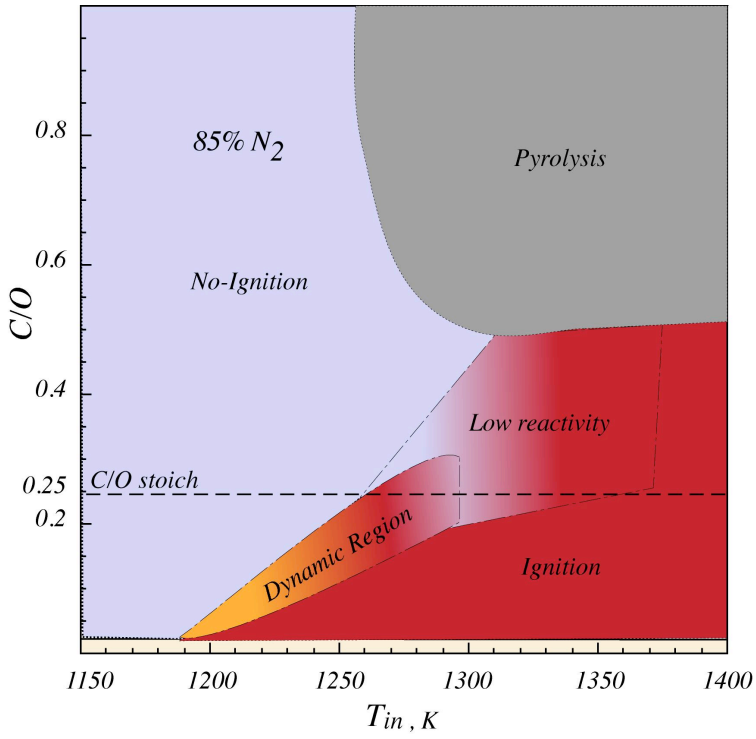

Fig IV.11 - Reactivity map of methane/oxygen mixture, diluted in nitrogen (85 %) for v=30m/s.

The location (as well as the colors) of this zone is indicative of the overlapping among this phenomenology and the *dynamic* and *low reactivity zone*. Sometimes it has been complicated to distinguish different behaviors in order to provide a definite characterization of the mixture oxidation processes.

Furthermore, it has been possible to find working conditions in which the mixture presents *low reactivity* behaviors. Such zone extends from 1300 K up to 1370 K and for C/O from about 0.2 to 0.5, at the edge of *pyrolysis zone*. Moreover pyrolysis profiles were observed for $1250 < T_{in} < 1400$ at $C/O = 1$ while the gray zone decreases its extension until it disappears for $C/O = 0.5$.

Fig IV.12 shows the trend of maximum difference of temperature in the reactor (ΔT_{max}) as a function of C/O .

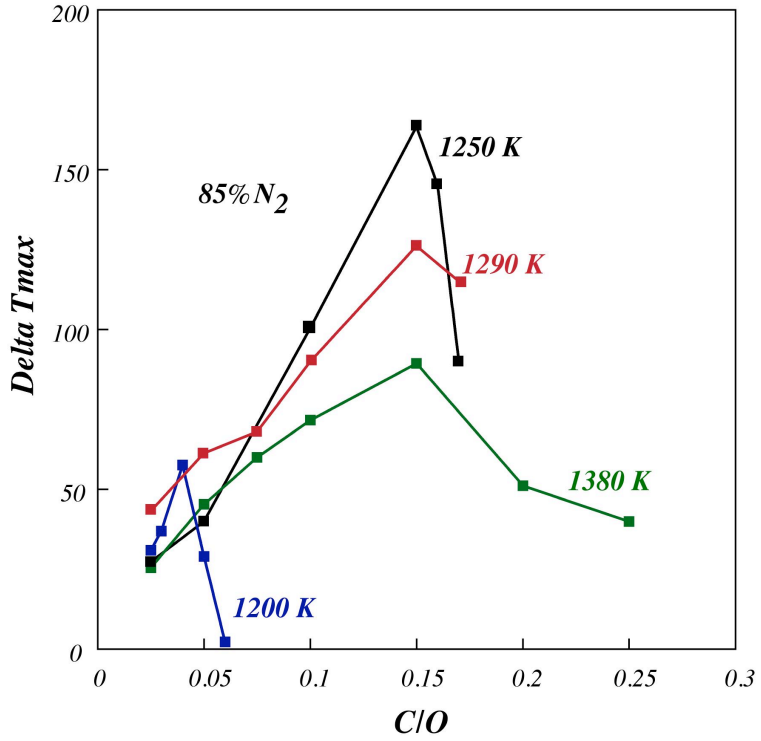

Fig IV.12 - Maximum difference of temperature as function of C/O for four initial temperatures (1200 K, 1250 K, 1290 K and 1380 K).

Four curves are presented in the figure for different initial temperature. The curves show a peak according to different value of C/O. The blue curve shows the ΔT_{max} trend obtained for the the initial temperature of 1200 K by varying C/O in the ignition zone of the reactivity map.

The estimated temperature difference is equal to 30 K for $C/O = 0.025$ and then increases for higher feed ratio. In fact, for $C/O = 0.03$, ΔT_{max} becomes equal to 36 K and afterward increases to a peak of fifty-seven degrees for $C/O = 0.04$. For higher C/O, ΔT_{max} decreases to the value of 28 K for the last ignition point $(C/O = 0.05)$. The blue curve is related to the first temperature in which the occurrence of ignition process of the mixture was revealed. For higher initial temperature (from 1250 K up to 1380 K) more experimental data were collected.

Black curve shows ΔT_{max} obtained for $T_{in} = 1250K$. Although the curve presents a similar trend to the previous one, ΔT_{max} obtained are higher and there is a peak for a different C/O value. In particular, peak was higher and shifted towards higher C/O. For $C/O = 0.025$ the temperature rises up to 1277 K with a $\Delta T_{max} = 27$ K. Higher values of ΔT_{max} were obtained for $C/O = 0.15$. In this working conditions the difference of temperature found was of approximately 163K. Subsequently, the differences diminishes to about 90K for $C/O = 0.17$.

For higher initial temperature ($T_{in} = 1290K$) ΔT_{max} further increases. At this T_{in}, the red curve shows a trend similar to the curve obtained at lower T_{in} with a peak for $C/O = 0.15$ with $\Delta T_{max} = 126K$.

A further increase in inlet temperature leads to a decrease in the absolute value of ΔT_{max} collected.

The green curve shows seven experimental data for an initial temperature of 1380 K. Although the peak was shown according to the same feed ratio ($C/O = 0.15$) as for $T_{in} = 1290 K$, the values of ΔT_{max} are lower in all the range of feed ratio investigated. For instance the maximum ΔT_{max}, obtained at $C/O = 0.15$ is of 90 K.

On the the Arrhenius diagram of Fig IV.13 auto-ignition delay times evaluated in these experimental conditions for various C/O as a function of $\alpha = 1000/T_{in}$ were shown. The auto-ignition time decreases with temperature increase for all the feed ratio investigated. In particular, several values of C/O are are reported in the figure, from fuel lean condition ($C/O = 0.017$) up to an almost stoichiometric ($C/O = 0.2$).

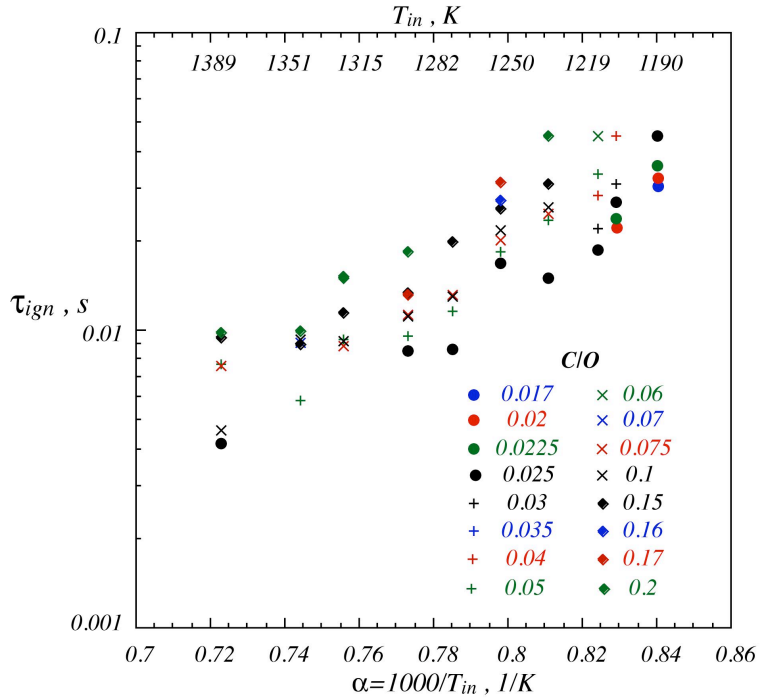

Fig IV.13 - Arrhenius plot of auto-ignition delay time of methane/oxygen blends diluted in nitrogen (85%) for different C/O versus $\alpha = 1000/T_{in}$.

The times collected vary from a minimum of 0.004 sec for $\alpha = 0.723$ up to a maximum of 0.045 sec for $C/O = 0.025$ and $\alpha = 0.084$.

In order to better follow the trend of τ_{ign}, in Fig IV.14 times obtained for $C/O = 0.025$ are shown (black circles in Fig IV.13). In addition to the experimental points a reference curve was indicated. It is evident an almost linear trend of auto-ignition time by varying initial temperature. For instance, for low temperature (Tin=1190 K) τ_{ign} is equal to 0.044 sec and then decreases to 0.027 sec because of an increment of Tin (Tin=1206 K). Afterwards, the black points show lower auto-ignition times obtained for lower α values.

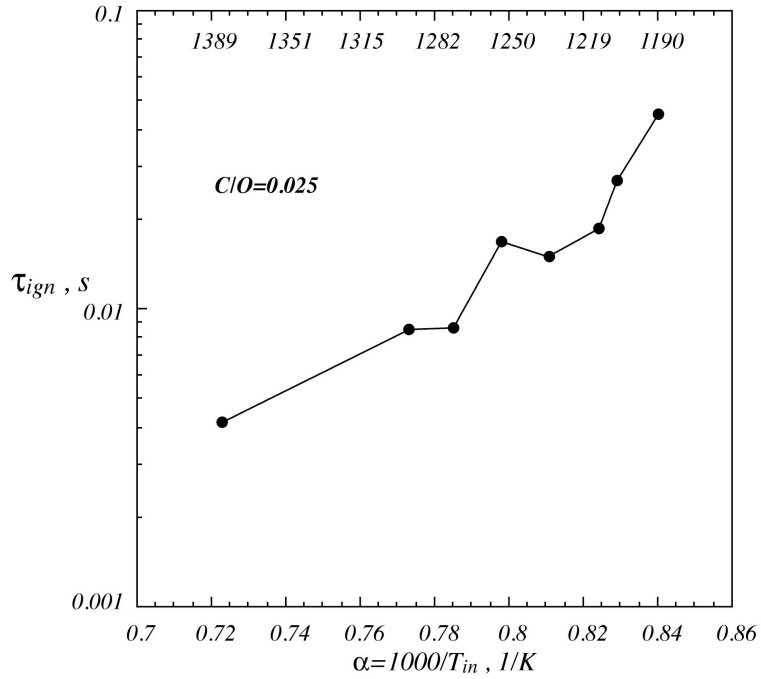

Fig IV.14 - Arrhenius plot of auto-ignition delay time of methane/oxygen blends diluted in nitrogen (85%) for C/O =0.025, versus $\alpha = 1000/T_{in}$.

Similar considerations could be also made for others C/O values. At this regard, in Fig IV.15, τ_{ign} for five feed ratios were shown with different colors. The auto-ignition times decrease by lowering C/O in the whole range of temperature investigated. In fact, the

black curve shows the greater times and is relating to $C/O = 0.2$. In particular, for the same initial temperature (T_{in}=1233 K), the mixture relating to $C/O = 0.2$ ignites after 0.083 sec while for $C/O = 0.15$ τ_{ign} is equal to 0.075 sec. Further decrease are shown for lower C/O with times collected equal to $\tau_{ign} = 0.07\,\text{sec}$ ($C/O = 0.075$), $\tau_{ign} = 0.069\,\text{sec}$ ($C/O = 0.05$) and $\tau_{ign} = 0.06\,\text{sec}$ ($C/O = 0.025$).

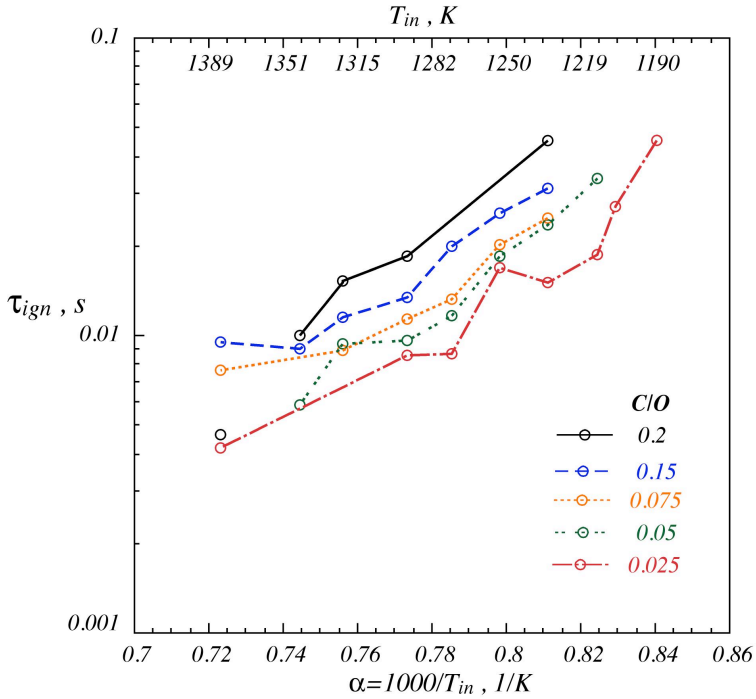

Fig IV.15 - Arrhenius plot of auto-ignition delay time of methane/oxygen blends diluted in nitrogen (85%) for C/O=0.025, versus $\alpha = 1000/T_{in}$.

IV.1.4 - Main flow velocity: 35 m/s. Dilution degree: 85 %

Fourth session of tests were carried out by varying main flow velocity. In particular, higher main flow velocity of 35 m/s was set, keeping constant the degree of dilution (85%), the diluent species as well as the chemical nature of fuel with respect to the previous case.

As it is described in detail above, on the basis of temperature profiles obtained along the axial coordinate of the reactor it was possible to design a reactivity map in this working

condition. Such map was reported in Fig IV.16. The same phenomenologies were observed as in the previous case, and it was possible to divide the reactivity map in different areas.

The mixture fed to the reactor does not show any phenomenologies in a range of temperature between 1150 K and 1220 K for lower C/O values. *No-ignition zone* (as usual in blue color) widens for higher temperatures as soon as feed ratio increases.

The first condition which shows a considerable increase of temperature equal to the ignition criterion is located for a temperature of 1225 K. Fuel lean mixtures ignite easily then the red zone widens towards higher feed ratios. In the lower right part of the map the *ignition zone* (red zone) is hence located.

In the right upper part, it is evident the presence of a *pyrolysis zone* in grey. Such area extends for temperature values between 1260 K and 1400 K for rich condition while its extension diminishes for lower feed ratio. In particular, for higher temperatures the zone becomes smaller until it disappears for C/O =0.35 where the mixtures follow the oxidation process.

In a range of Tin and C/O between the pyrolysis ad ignition zone a low reactivity area is located. As it is seen and described above, this area is typical of a little increase of temperature less than 10 K.

In addition, such zone highlight the change in the overall reactivity of the system, from the no-ignition towards a different process both pyrolytic or oxidative.

As in previous cases investigated, it was possible to appreciate working conditions in which the mixture presents phenomena of *dynamic reactivity* (orange zone). Such zone extends from 1240 K up to 1300 K and for C/O from about 0.2 up to 0.25. It is evident that this zone is smaller with respect to the previous cases.

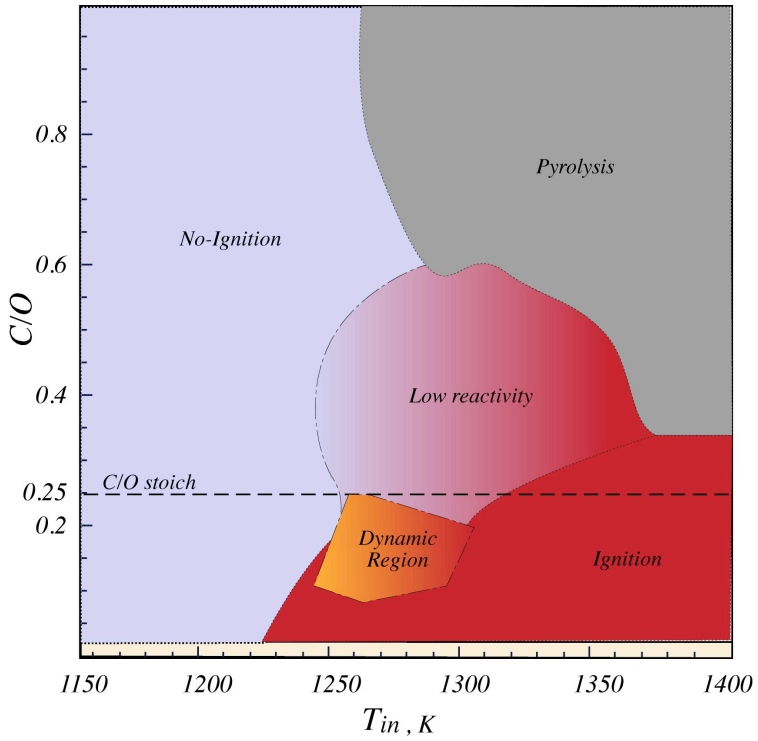

Fig IV.16 - Reactivity Map of methane/oxygen mixture, diluted in nitrogen (85 %) obtained for a main flow velocity equal to 35 m/s.

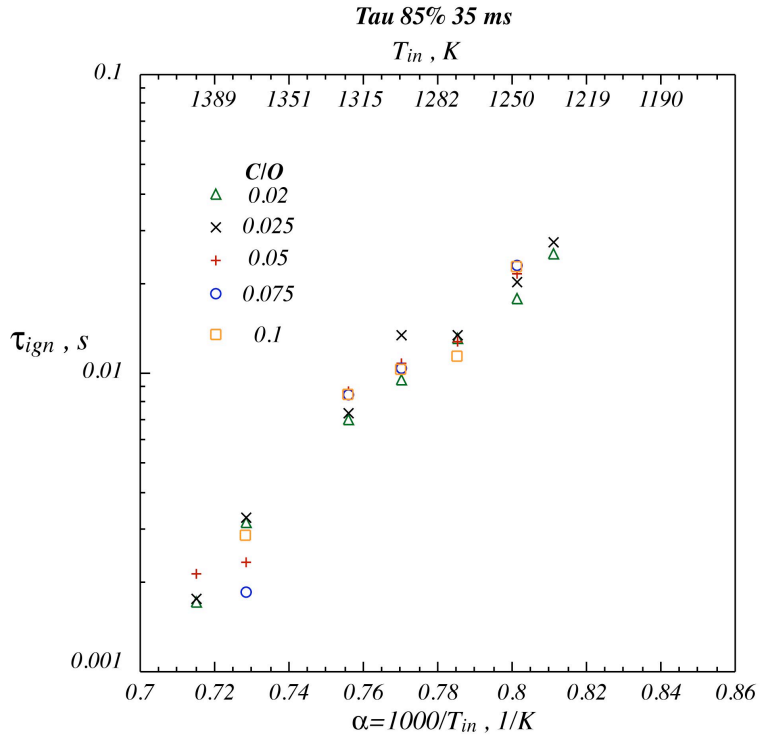

Fig IV.17 - Arrhenius plot of auto-ignition delay time methane/oxygen blends diluted in nitrogen (85%) for different C/O versus $\alpha = 1000 / T_{in}$.

The Fig IV.17 shows the auto-ignition times evaluated in the ignition zone for these working conditions. Range of temperatures (from 1219 K up to 1428 K) coincides with the ignition zone shown in Fig IV.16 and several C/O values were reported in the Arrhenius plot.

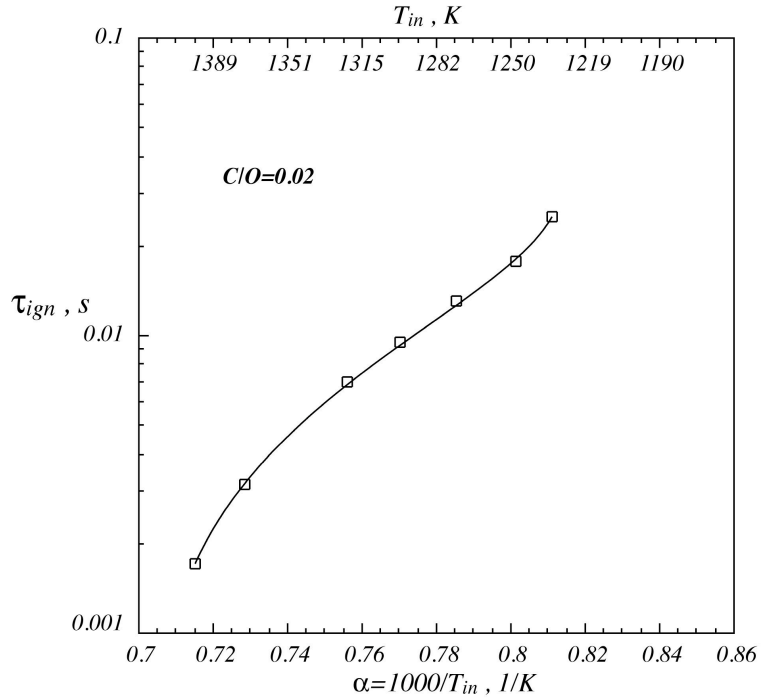

Fig IV.18 - Arrhenius plot of auto-ignition delay time methane/oxygen blends diluted in nitrogen (85%) for different C/O versus $\alpha = 1000 / T_{in}$.

Results show an increase of the auto-ignition times by lowering the initial temperature of the system. In particular all the times are comprised between a minimum of 0.002 sec ($C/O = 0.025$ and for $T_{in} = 1398K$) and a maximum equal to 0.027 sec ($C/O = 0.02$ and $T_{in} = 1233K$). As a matter of fact, in Fig IV.18 the times collected for $C/O = 0.02$ are shown with a reference curve. For low temperatures ($T_{in} < 1298K$) the mixture ignites with times higher than 0.01 sec. In particular for $T_{in} \cong 1233K$ $\tau_{ign} = 0.025\,\text{sec}$ and then becomes $\tau_{ign} = 0.013\,\text{sec}$ for $T_{in} \cong 1272K$. For higher temperatures ($T_{in} > 1298K$) all the

times are lower than 0.01 sec and in particular decrease to 0.003 sec for $\alpha = 0.729$ ($T_{in} = 1371K$).

IV.2 - Biogas

The growing interest in the gaseous mixtures obtained by biomass has led to explore the possibility of using these blends in combustion systems operating in MILD conditions. Indeed, the working conditions typical of MILD combustion, are in principle very suitable for biogas oxidation, because their low calorific value makes difficult the use of such fuels in conventional burner. Thus, it is crucial to build up a comprehensive experimental database to make easier design and efficiently manage practical systems using biogas. This is also needed by significant changes in the composition of mixtures, even depending on the procedure which the biomass was subjected.

In this thesis, a mixture with a composition typical of biogas deriving from a low temperature pyrolysis process of biomass has been chosen. With the aim of the characterization of phenomena associated with the oxidation of mixtures of biogas highly diluted and preheated, was selected a mixture of known composition (62 % CO_2, 25 % CO, 10 % CH_4, 1 % C_2H_6, 2 % C_2H_4). This composition is characteristic of a gaseous mixture obtained by subjecting the biomass to a slow combustion pyrolysis process. In the following it will be indicated with the generic term of *biogas*. As it is seen for methane, the dilution parameter was investigated. In particular, the mixtures were diluted in nitrogen from 90 % up to 95%. On the basis of the temperature profiles observed during the experimental tests it was possible to characterize the overall reactivity of the system. Two reactivity maps were designed and auto-ignition times were collected on the basis of the

chosen criterion. Several samplings at the exit of the reactor were made by means of a gas chromatography in order to understand the kinetic pathways follow by the mixtures.

IV.2.1 - Main flow velocity: 30 m/s. Dilution degree: 90 %

Note the composition of the fuel mixture using during the following experimental tests, it was necessary to define an additional parameter that would allow to determine the working conditions in terms of oxidant/fuel ratio. This is due to to the impossibility of using feed ratio C/O. In fact, as opposed methane, biogas has a composition in which are present oxygen species. Under these conditions the C/O would not be able to define the relationship between the fuel and oxidizer. Therefore on the basis of a study in literature, was decided to use *oxygen ratio* Ω that permits a slavish definition of the feed ratio (C. J. Mueller 2003).

A clear definition of Ω is: *"The oxygen ratio of a mixture is defined as the amount of oxygen in the mixture divided by the amount of oxygen required for stoichiometric combustion of the same quantity of fuel, where atoms bound in stable species are neglected. The oxygen ratio is a valid measure of mixture stoichiometry in any mixture for which the saturated stoichiometric products are CO_2, H_2O, N_2, and/or noble gases (NG)."*

The definition of the oxygen ratio requires the identification of stable reactant species. A stable reactant species is defined as one that is neither a fuel nor an oxidizer.

A mathematical definition of the oxygen ration is necessary in order to better understand the useful of this parameter.

Consider a general reactant mixture of the form:

$$\sum_i a_i C_{nC,i} H_{nH,i} O_{nO,i} Nn_{N,i} NG_{nNG,i} \tag{10}$$

where a is an index over all reactant species, a_i is the number of moles of the i^{th} species, and $n_{[element],i}$ is the number of atoms of [*element*] in the i^{th} species. The oxygen ratio of this reactant mixture is defined as:

$$\Omega = \frac{\sum_k a_k n_{O,k} + \sum_m a_m n_{O,m}}{\sum_r a_r \left(2n_{C,r} + \frac{1}{2} n_{H,r} \right)} \tag{11}$$

where k, m, and r are indices over all fuel, oxidizer, and fuel-plus-oxidizer reactant species, respectively. (In mathematical terms, if each species in the reactants has a unique index then indices k and m have no intersection and their union is the set of indices r.)

On the basis of this definition a mixture with an oxygen ratio Ω equal to 10 is considered an ultra-lean mixture (with a high ratio oxidant/fuel) while $\Omega = 1$ represents a stoichiometric mixture.

In Fig IV.19 are presented the temperature profiles obtained for eight different initial temperatures (1023, 1053, 1073, 1098, 1118, 1148, 1173, and 1198 K) and a value of oxygen ratio Ω equal to 10 as a function of the spatial coordinate of the reactor. The dilution degree has been set equal to 90 % and nitrogen was used as diluent species.

For the first temperature investigated (1023 K, curve in red), the trend of the profile shows an increase in temperature for a distance from the entrance of about 16 cm. The temperature rises slowly and reaches the value of 1045 K for $x = 40cm$. It is evident that a wide reaction zone extends from $x = 7cm$ until approximately 96 cm.

In the second case (T_{in}=1053 K, curve in blue) the trend of the temperature profile is very similar to that obtained for the previous temperature. The difference of temperature is quite similar and an extended reactive zone persists.

For an initial temperature of 1073 K, the temperature difference is slightly greater with ΔT equal to twenty-seven degrees. The mixture ignites immediately downstream of the mixing zone and the temperature rapidly increases until it reaches a maximum value of 1100 K and then decreased slowly up to a constant value of 1074 K.

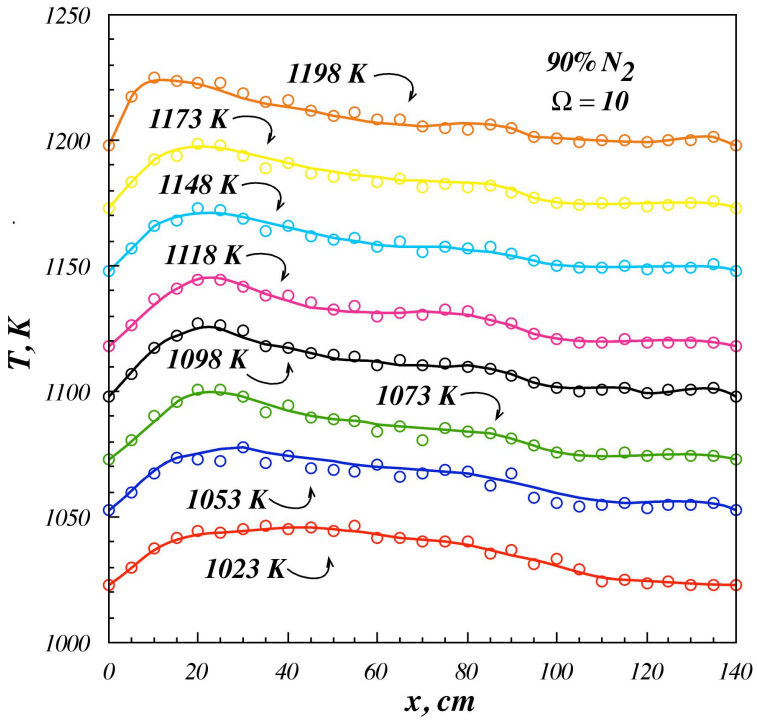

Fig IV.19 - Temperature profiles for eight different initial temperatures obtained for oxygen ratio $\Omega = 10$ *versus the spatial coordinate of the reactor (dilution degree equal to 90 % in nitrogen).*

It is possible to notice a slight shift of the reaction zone for smaller values of x. This phenomenology can be found for the following profiles obtained for highest initial temperature: the test region shifts, reduces its extension and shows a peak slightly higher. The following four curves (corresponding to 1098 K in black, 1118 K in pink, 1148 K in blue and 1173 K in yellow) show almost similar trends. As will be specified in detail later, the temperature increases will be the same with a small reduction in the time of ignition.

Based on the temperature profiles obtained during the tests it was possible to design a reactivity map for the mixture biogas\oxygen.

In Fig IV.20 is shown this map obtained in a range of temperature between 950 K and 1350 K for a different *oxygen ratio* Ω (from 0.02 up to 10). The white area at the bottom of the map is an area not investigated because of technical limitations due to flow control. It was highlighted the stoichiometric condition with a dotted line ($\Omega = 1$).

As shown in the figure has been possible to divide the reactivity map in different areas depending on the observed phenomenology obtained by acquiring different temperature profile.

In a first range of temperature (from 950 K up to 1000 K) the system does not show any phenomenologies and does not ignite for every *oxygen ratio* Ω investigated. This zone is indicated as *no-ignition zone* in blue.

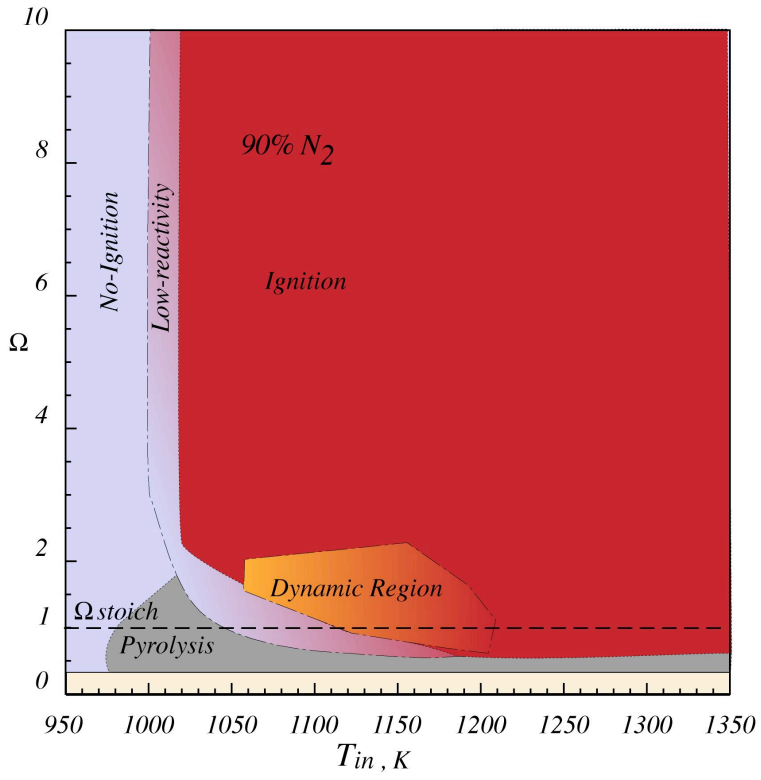

Fig IV.20 - Reactivity Map of biogas/oxygen mixture, diluted in nitrogen (90 %) obtained for a main flow velocity equal to 30 m/s.

For temperatures higher than 1000 K the system shows different phenomenologies. In the upper right part of the map is located the *ignition zone* in which the system shows profile

as these presented before. The zone extends from 1020 K up to 1350 K and for values of *oxygen ratio* Ω up to 0.5.

In this area it was possible to estimate the ignition delay time of the mixture on the basis of the evaluation criteria defined earlier and will be presented later. For temperatures between 1000 K and 1020 K a *low reactivity zone* was reported. As it is seen before for methane, this zone is representative of an incipient ignition. In fact the area in blue-red gradient color surrounds the ignition zone and shows working condition in which a small increment of temperature was observed. In addition, for lower values of Ω the low reactivity phenomenologies follows the edge of the red zone.

The map obtained for the biogas shows a pyrolysis zone. For small values of Ω profiles with negative ΔT were acquired.

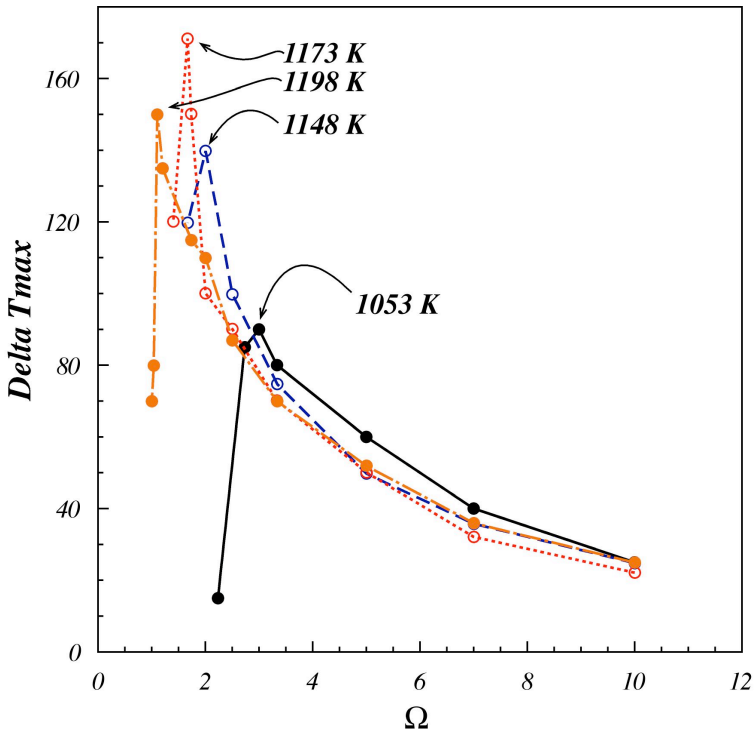

Fig IV.21 - Maximum difference of temperature as function of oxygen ratio Ω obtained for three initial temperatures (1053 in black, 1148 in blue, 1198 in orange, 1173 K in red).

The gray area starts from 980 K and low Ω (mixture fuel rich) and widens above the stoichiometric condition towards higher temperatures. Afterwards, pyrolysis phenomenologies disappear and the zone diminishes its extension only for low oxygen ratio.

For some values of Ω and T_{in} was observed a zone in which the system shows a non-stable behavior. This phenomena is shown in the reactivity map with an orange zone within the ignition area. Such area appears for temperatures comprises between 1060 K and 1200 K nearly stoichiometric condition. Results show that for higher temperatures such behavior disappears and stable ignition processes were observed.

In order to highlight the main aspects of the experimental results Fig IV.21 shows the trend of maximum difference of temperature in the reactor (ΔT_{max}) as a function of *oxygen ratio* Ω. Four curves are presented in the figure for different initial temperature. In particular, ΔT_{max} found for $\Omega = 10$ are the same for all curves, while for smaller values (from $\Omega = 10$ up to $\Omega = 3$) we can see a slight difference for each temperatures investigated.

The first curve (in black) shows the evolution of ΔT_{max} obtained for an initial temperature of 1053 K. Moving from lean conditions of fuel ($\Omega = 10$) up to rich conditions, ΔT_{max} collected grew. In particular, for $\Omega = 7$ we obtain a ΔT_{max} of 40 K. This value increases until it reaches a maximum at approximately $\Omega = 3$. In these conditions we obtain a ΔT_{max} of 90 K. For smaller values of Ω, ΔT_{max} becomes smaller until it reaches a value of 15 K for Ω equal to 2.2 (for lower values of Ω do not have the ignition of the mixture).

The dashed curve in blue in the figure shows ΔT_{max} obtained for an initial temperature of 1148 K. For high values of Ω (fuel lean condition) the differences in temperatures obtained

are almost similar to the previous case as described above. Moving towards lower values of omega parameter, ΔT_{max} increases exponentially until it reaches a peak for $\Omega = 2$ $(\Delta T_{max} = 140)$. Afterwards it decreases to 120 K for $\Omega < 2$.

A similar trend is shown for the red-dotted curve that presents ΔT_{max} for an initial temperature equal to 1173 K. It is worth noting that the maximum peak increases with increasing initial temperatures and shifts towards lower Ω values. This behavior is evident starting from the first temperature (1053 K) and until the last curve (referring to 1173 K). The last curve (dashed-dotted curve in orange) obtained for an initial temperature of 1198 K shows an inversion, with a lower peak (about 150 K) for a stoichiometric condition $(\Omega = 1)$.

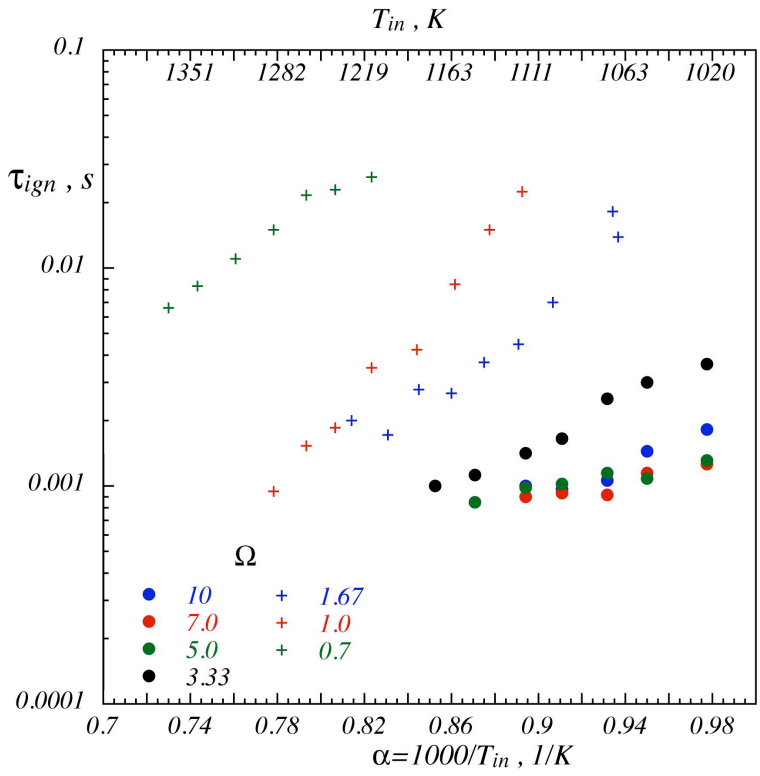

Fig IV.22 - Arrhenius plot of auto-ignition delay time biogas/oxygen blends diluted at 90% for different Ω

On the the Arrhenius diagram of Fig IV.22 auto-ignition delay times evaluated in these experimental conditions were shown for various Ω as a function of $\alpha = 1000 / T_{in}$. Seven oxygen ratios were plotted in a range of temperatures comprises between 1000 K and 1428 K and lean ($1 < \Omega < 10$), stoichiometric ($\Omega = 1$) and rich condition ($\Omega = 0.7$) were considered. The auto-ignition times evaluated show a reduction with temperature increase for all the oxygen ratio considered.

In particular, the trend of the ignition times are similar for all Ω and an almost linear reduction is shown.

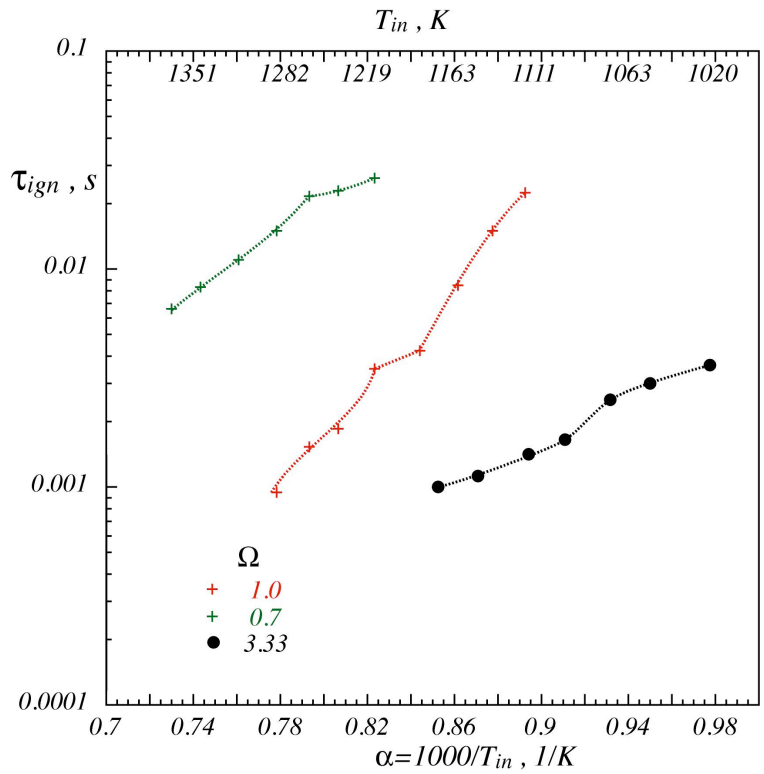

Fig IV.23 - Detail of auto-ignition times for three Ω values (0.7, 1 and 3.33).

As a matter of fact, in Fig IV.23 three Ω were selected and are shown with reference curves. Experimental data are indicated with circles (for $\Omega = 3.33$) and cross-shaped points (for $\Omega = 1$ and $\Omega = 0.7$). For lean condition ($\Omega = 3.33$) times are included between 0.004 and 0.0001 for α =0.853 and α =0.978 respectively. An higher slope is evident for

stoichiometric condition with τ_{ign} between 0.009 and 0.022 for $0.779 < \alpha < 0.893$. Last curve in green color shows auto-ignition times obtained for rich condition ($\Omega = 0.7$). The values of ignition time collected are $\tau_{ign} = 0.007$ for $\alpha = 0.824$ and $\tau_{ign} = 0.026$ for $\alpha = 0.731$.

IV.2.2 - Main flow velocity: 30 m/s. Dilution degree: 95 %

In order to a comprehensive study on the phenomena associated with the oxidation of mixtures of biogas in high diluted and preheated conditions further tests were performed by varying the concentration of the diluent, but maintaining constant its chemical nature (nitrogen). In particular, the concentration of diluent was increased from 90 % to 95 %.

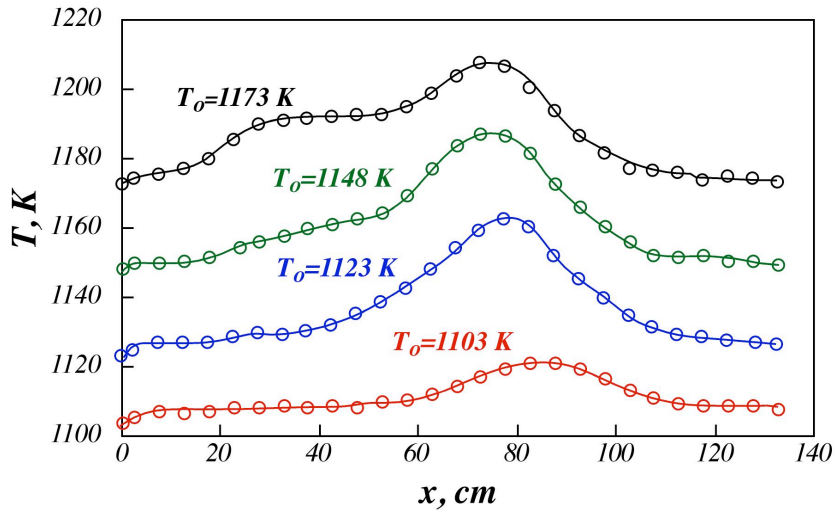

Fig IV.24 - Profiles of temperature along the axial coordinate of the reactor for a lean mixture of fuel ($\Omega = 3.33$) for four initial temperature.

As regards, in Fig IV.24 are shown the profiles along the axial coordinate of the reactor for different initial temperatures (1103 K, 1120 K, 1148 K and 1173 K) and for a lean mixture of fuel ($\Omega = 3.33$).

The first curve (in red) obtained for an initial temperature of 1103 K shows a modest increase in temperature up to 60 cm from the beginning of reactor. As a result, the temperature gradient increases until it reaches a maximum value equal to 1120 K.

For T_{in} = 1123 K, the trend is similar. The mixture ignites for an axial distance less than the first case and the maximum temperature value is higher. Furthermore there are two temperature increases, the first for $x = 25cm$, and the second, more pronounced for $x > 40cm$.

The same trend can be found for the other two initial temperatures shown in Fig IV.24. In particular, the first increase in temperature is more pronounced with increasing temperature of pre-heating of the reaction mixture. In addition, for T_{in} = 1173 K, the first increase in temperature is very pronounced and the maximum gradient of temperature is less than the experimentally profile found for T_{in} = 1148 K.

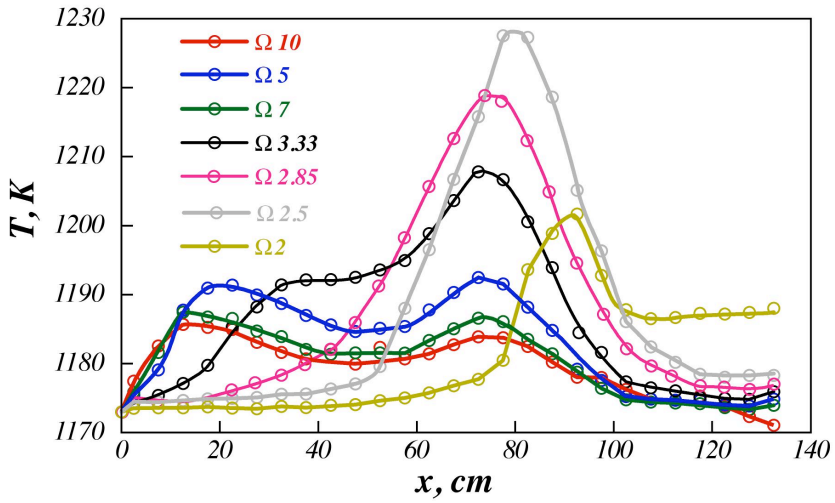

Fig IV.25 - Axial profiles of temperature Tin = 1173 K, parametric curves of the oxygen ratio Ω .

Focusing on these last profile was varied the concentration of oxidant in the mixture. The Fig IV.25 presented the profiles obtained at constant temperature (T_{in} = 1173 K) and parametric in the oxygen ratio Ω . In general, the fuel mixture is poor, the more the system

is highly flammable, and the lower the temperature gradients associated with the release of heat of oxidation reaction.

For fractions of oxygen between 10 and 5, the axial temperature profiles show two relative maxima. The trend are quite similar and the only difference is inherent to the differences of temperature obtained. In general, it is possible to notice an increase of ΔT_{max} observed, increasing the percentage of fuel in the mixture. In fact, although for $\Omega = 10$ and $\Omega = 7$ the ΔT_{max} are quite the same (about 12 K), for $\Omega = 5$ the profile shows a peak more marked of about 17 K. For $\Omega = 3.33$ the second maximum is relatively more pronounced than the first. As a result, an increase in the percentage of synthetic fuel in the mixture results in a single maximum much more pronounced than in mixtures characterized by a greater fraction of oxygen. This is evident for $\Omega = 2.85$ and $\Omega = 2.5$ in which a single maximum more pronounced is clear for axial coordinate up to 60 cm from the entrance of the reactor.

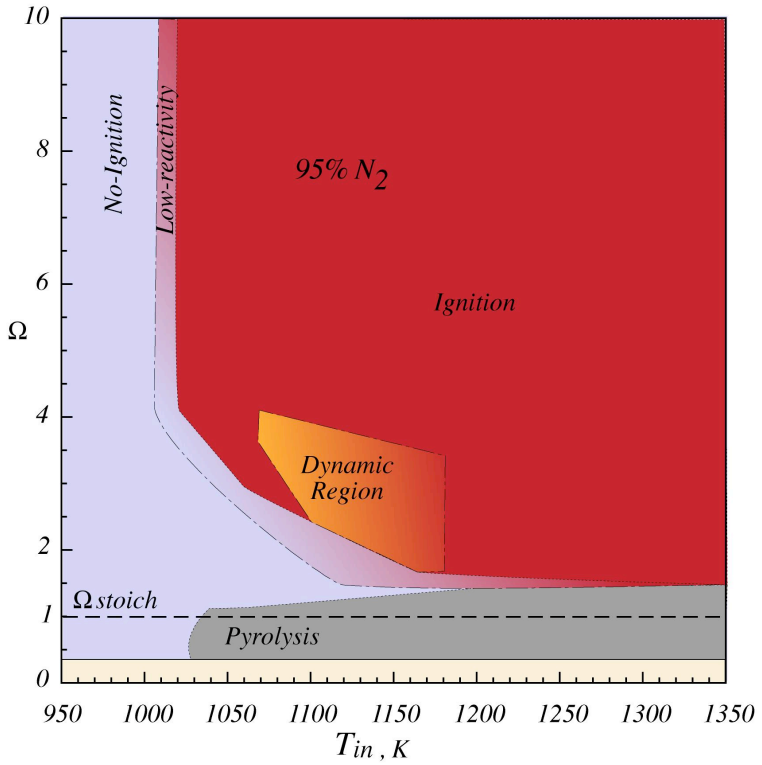

Fig IV.26- Reactivity Map for a mixture of biogas/oxygen, diluted in nitrogen (95 %) for a main flow velocity equal to 30 m/s.

For $\Omega = 2$, the mixture ignites for axial distance greater than the other cases, the maximum temperature value is smaller and the temperature of the mixture leaving the reactor is greater.

Based on the temperature profiles is possible to design a reactivity map for the flow velocity of 30 m/s and a dilution degree of 95 %. Fig IV.26 shows the map with the usual division into zones characteristics of different phenomenologies. The temperatures investigated are between 950 K and 1350 K and the concentration of oxidant was changed from 0.02 up to 10. The line corresponding to a stoichiometric concentration of the mixture is reported in the figure with a dashed line ($\Omega = 1$).

The map can be divided into five main areas; *ignition zone*, *no-ignition zone*, *dynamic region, pyrolysis zone* and *low reactivity zone* as usual. The area of *no-ignition* (blue color) extends from the temperature of 950 K up to about 1000 K. For higher temperatures and for high values of oxygen ratio Ω , the mixture ignites or shows a low reactivity with $\Delta T_{\max} < 10K$. In the first case the temperature profiles obtained allow to evaluate a time of ignition. The area of ignition (in red in figure) covers the entire range of temperatures between 1020 K and 1350 K for lean mixtures in fuel while for lower values of omega ($\Omega < 1.5$) are not achieved increases in temperature equal to chosen criterion of ignition and different phenomenologies are shown. The low reactivity zone surrounds , as usual the ignition zone and is located between 1010 K and 1020 K for higher oxygen ratios. For lower Ω the blue-red zone follows the trend of the ignition area and disappears for higher temperatures.

A dynamic region is located between ignition and no-ignition areas. This area (orange in the figure) covers initial temperature between 1070 K and 1175 K and Ω values between 1.5 and above 3.9.

For Ω valued below the stoichiometric conditions a pyrolysis zone is located. It starts from 1040 K (for fuel rich conditions) and widens for higher temperatures above $\Omega = 1$.

Based on the profile acquired it is possible to evaluate the auto-ignition time of the mixture.

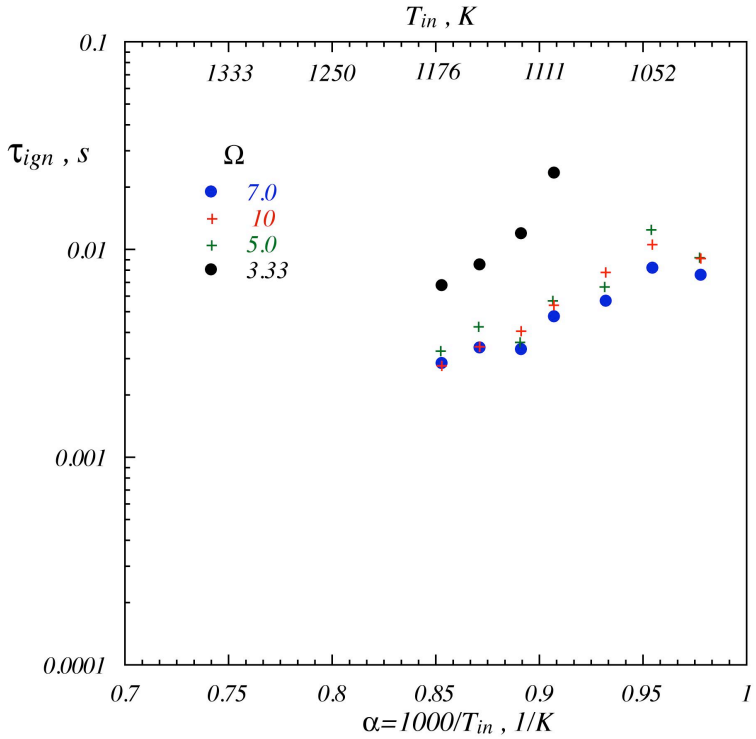

Fig IV.27 - Arrhenius plot of auto-ignition delay time biogas/oxygen blends diluted at 95% for different Ω .

In Fig IV.27 auto-ignition delay times for various Ω in function of $\alpha = 1000 / T_{in}$ are shown. Four oxygen ratios were plotted in a range of temperatures comprises between 1000 K and 1428 K and lean ($1.67 < \Omega < 10$) condition were considered. The auto-ignition times evaluated show a reduction with temperature increase for all the oxygen ratio considered.

In particular, the trend of the ignition times are similar for all Ω with a reduction observed for higher temperatures.

IV.2.3 - Gas-Chromatographic analyses

In this paragraph, the major species molar fractions are reported. They have been detected by means of a micro-GC supplied by the Agilent Technologies Company. It is equipped with two columns. The former is dedicated to the retention of H_2, N_2, O_2, CH_4, CO, while the latter to CO_2 and C_2 species (C_2H_2, C_2H_4, C_2H_6). By means of a thermal conductivity detector (TCD), species are analysed and their relative concentrations obtained. For an accurate description of the GC, see chapter III.

Exhausted gases have been sampled at the end of the reactor, throughout a dedicated pipeline. Gases are sucked out by means of a vacuum pump and sent to the micro-GC for analyses on-line. The sampling AISI 316 stainless steel pipeline is long enough to cool down the exhausted gases up to environmental temperature. A silica-gel trap has been placed along the sampling line to remove condensed water.

The analyses have been realised varying the inlet reference temperature of mixtures entering the TFR reactor from 800 K up to 1350 K. The reference oxygen equivalence ratios (Ω) are 3.33, 1.67, 1 and 0.7, so that the species distribution and concentrations are considered for fuel lean, stoichiometric and rich mixtures. The flow inlet velocity was 30 m/s, while the overall dilution degree is 90%.

Species	Mole fractions
O_2	8.18
N_2	82.00
CH_4	0.48
CO	1.2
CO_2	3.0
C_2H_4	0.045
C_2H_6	0.096

Tab. IV.2 - Reference mixture concentration for Ω = 3.33.

Figs IV.28-31 are relative to a very fuel lean mixture (Ω = 3.33). In such a case the inlet composition of the mixture is Tab. V.2.

Fig IV.28 shows the molar fraction of methane and hydrogen. Methane concentration remains equal to the inlet reference value for low temperature. In particular methane does not react before T_{in} = 1000 K. For higher inlet temperature its concentration becomes equal to zero. At the same time, H_2 is not formed before T_{in} = 1000 K. For such reference inlet temperature it reaches a maximum value, then it decreases to zero for higher T_{in} values.

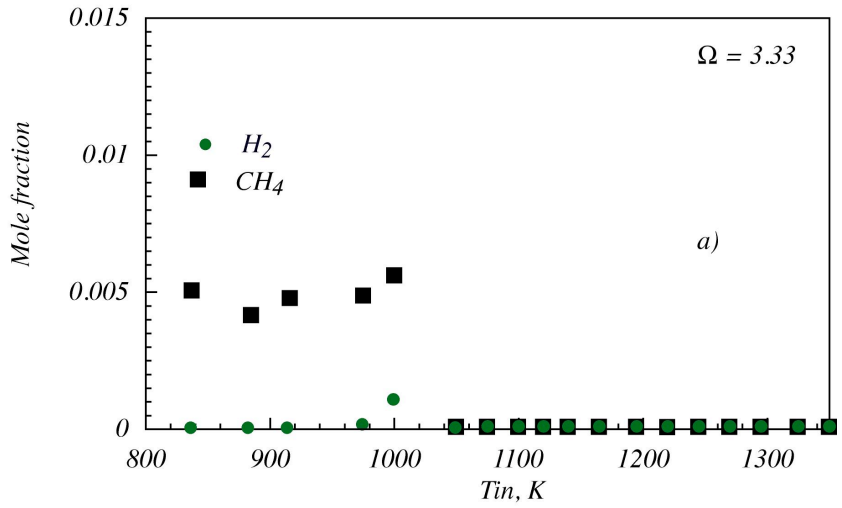

Fig IV.28 - CH_4 and H_2 mole fraction versus T_{in}.

Fig IV.29 is relative to C_2H_4 and C_2H_6. The ethane mole fraction remains constant up to T_{in} = 1000 K, then it decreases and for T_{in} equal to about 1040 K it becomes zero. Ethylene does not react up to T_{in} = 920 K, for T_{in} = 975 K its concentration shows a maximum value, than it decreases and for T_{in} equal to about 1040 K it is not detectable in the exhausted flue gases.

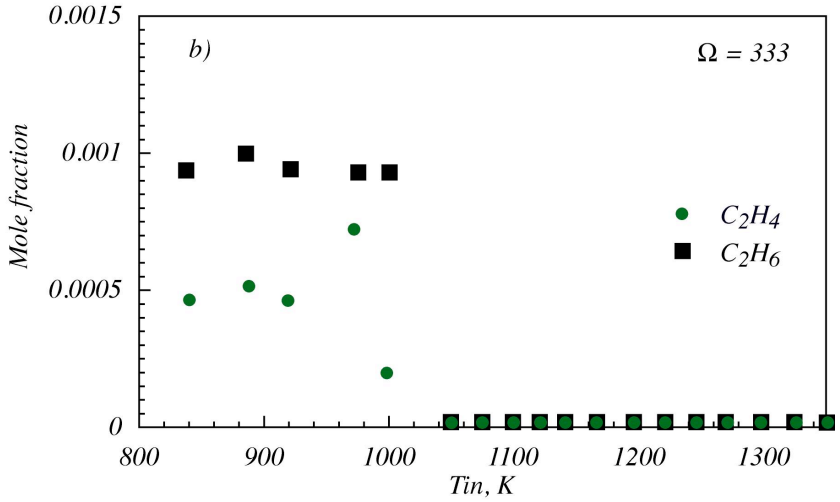

Fig IV.29 - C_2H_4 and C_2H_6 mole fraction versus T_{in}.

Fig IV.30 shows the molar concentration of CO and CO_2. It is worth noting that the mole concentration of both species remain constant up to T_{in} = 1000 K. For an inlet temperature of 1050 K the CO_2 concentration results to be equal to 5%, and remains constant for the higher considered inlet temperatures. The CO concentration at T_{in} = 1000 K becomes equal to 0.8%, then such species disappears from the exhausted gases flow.

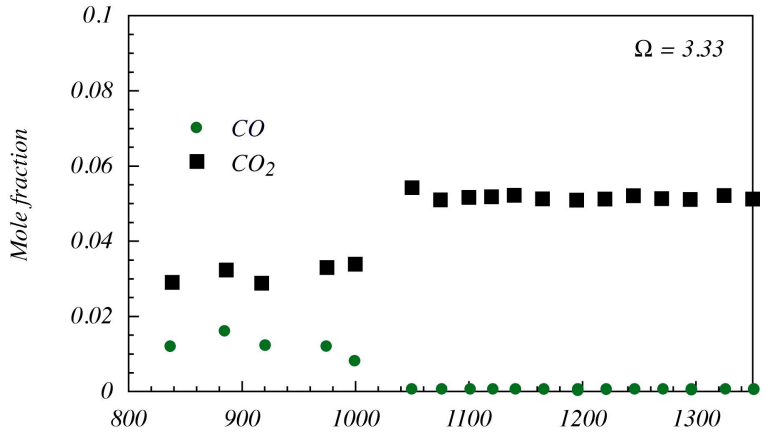

Fig IV.30 - CO and CO_2 mole fraction versus T_{in}.

The results for O_2 and water content are reported in Fig IV.31. The water concentration has been calculated on the basis of oxygen and hydrogen mass balances. While the carbon mass balance is respected by analytical calculation on the basis of species distribution, the

elementary hydrogen and oxygen amount inside the flow gases was not correct. The missing values are in the ratio of 2:1, so that it is plausible to account for water production during biogas oxidation. The validity of such assumption was confirmed by the closure of mass balances for such elements.

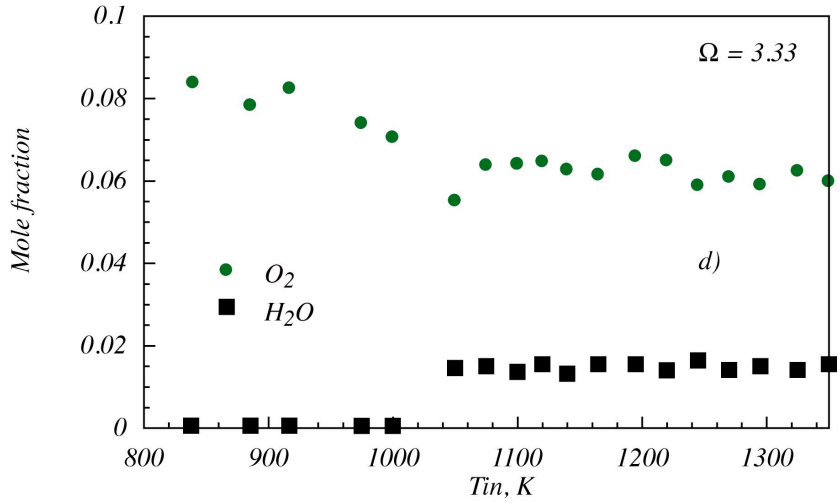

Fig IV.31 - H_2O and O_2 mole fraction versus T_{in}.

O_2 concentration in the flue gases remains equal to the inlet values up to T_{in} = 925 K. Afterwards, it starts decreasing and reaches a constant value of about 6% for T_{in} = 1080 K. Water is not present in the flue gases up to T_{in} = 1000 K, then its concentration increases and reaches a constant value of about 1.5%.

Species	Mole fractions
O_2	6.76
N_2	84.72
CH_4	0.85
CO	2.13
CO_2	5.3
C_2H_4	0.085
C_2H_6	0.17

Tab. IV.3 - Reference mixture concentration for Ω = 1.67.

Figs IV.32-35 show the species mole concentration versus the mixture inlet temperature for a fuel lean mixture ($\Omega = 1.67$). The inlet mixture composition is reported in table V.3.

Fig IV.32 is relative to methane and hydrogen. For both the considered species, for T_{in} < 1000 K, their concentrations remain equal to the inlet conditions, namely 0.85% for methane and zero for hydrogen. For T_{in} = 1000 K, the molar concentration of both species increases and at T_{in} = 1050 K their concentration reaches a maximum value. Afterwards, none of them is detectable in the flue gases.

Fig IV.33 shows C_2H_4 and C_2H_6 molar concentration versus T_{in}. For low inlet temperatures, their mole concentration is equal to the reference inlet values. For T_{in} = 975 K, ethane concentration starts decreasing while ethylene one increases. Increasing the inlet temperature, C_2H_6 concentration decreases and becomes zero for T_{in} = 1075 K, while ethylene concentration increases reaching a maximum value for T_{in} = 1000 K. Thereafter, it decreases down to zero for T_{in} = 1075 K.

Fig IV.34 reports the molar concentration of CO and CO_2. Up to T_{in} = 1000 K, their concentration remains constant. For higher inlet temperatures CO disappears, while the fuel conversion to CO_2 increases, and its concentration reaches a value of 9%.

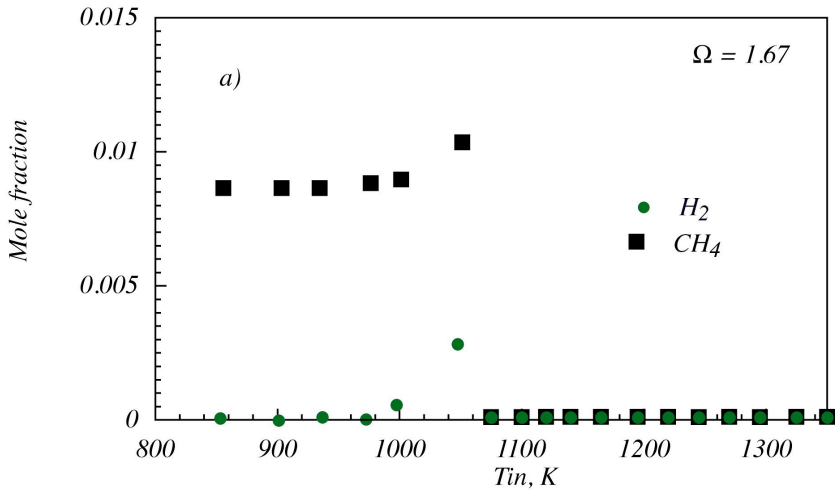

Fig IV.32 - CH_4 and H_2 mole fraction versus T_{in}.

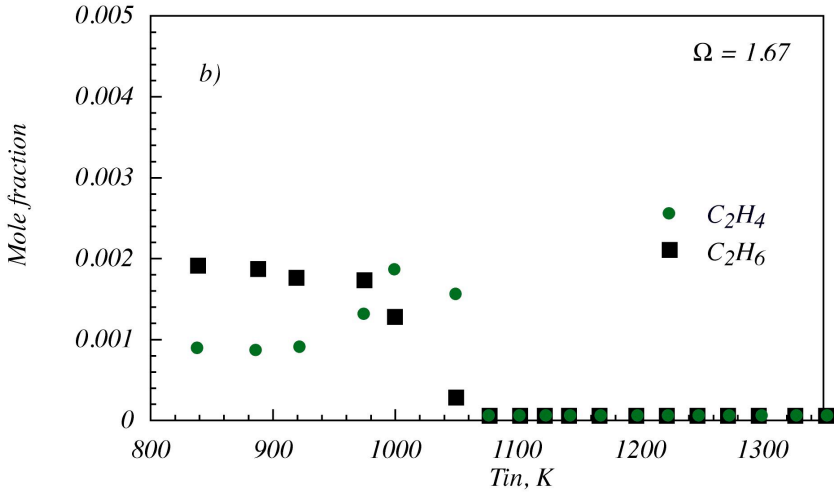

Fig IV.33 - C_2H_4 and C_2H_6 mole fraction versus T_{in}.

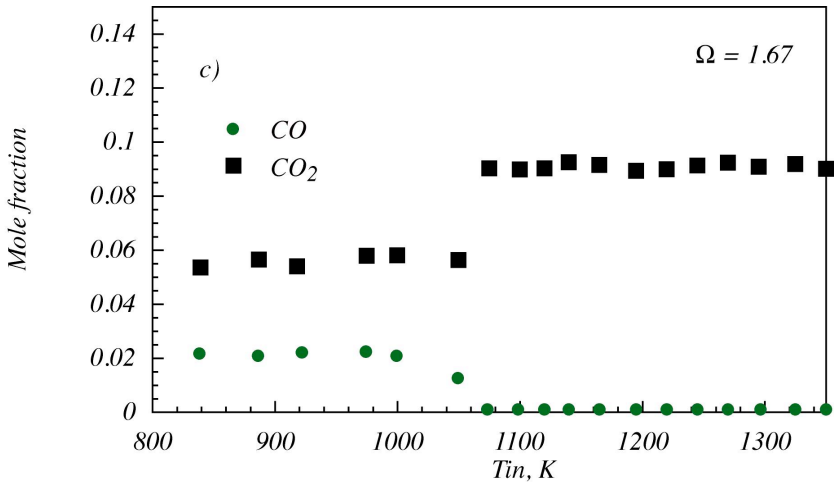

Fig IV.34 - CO and CO_2 mole fraction versus T_{in}.

Finally, Fig IV.35 is relative to O_2 and H_2O. The O_2 concentration decreases for T_{in} = 1050 K from the inlet reference value down to 3.5%. At the same inlet temperature, fuels conversion to water increases and steam mole fraction is equal to about 0.025.

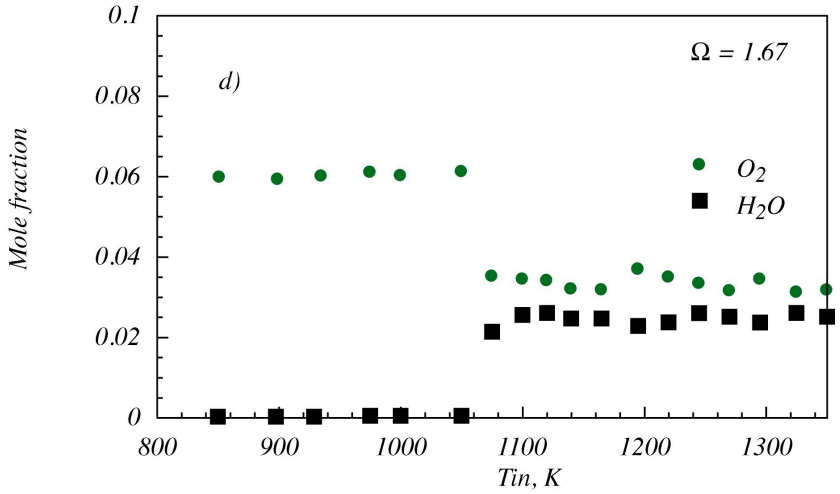

Fig IV.35 - H_2O and O_2 mole fraction versus T_{in}.

Figs IV.36-39 show the species mole concentration versus the mixture inlet temperature for mixture with a stoichiometric composition (Ω = 1). The inlet mixture composition is reported in table V.4.

Species	Mole fractions
O_2	5,28
N_2	82,3
CH_4	1,24
CO	3,10
CO_2	7,70
C_2H_4	0,124
C_2H_6	0,248

Tab. IV.4 - Reference mixture concentration for Ω = 1.

Fig IV.36 reports methane and hydrogen mole fractions as function of the mixture inlet temperature. For both the considered species, for T_{in} < 1000 K, their concentrations remain equal to the reference inlet conditions, For T_{in} > 1000 K, the molar concentration of both H_2 and CH_4 increases and at T_{in} = 1100 K their concentration reaches a maximum value.

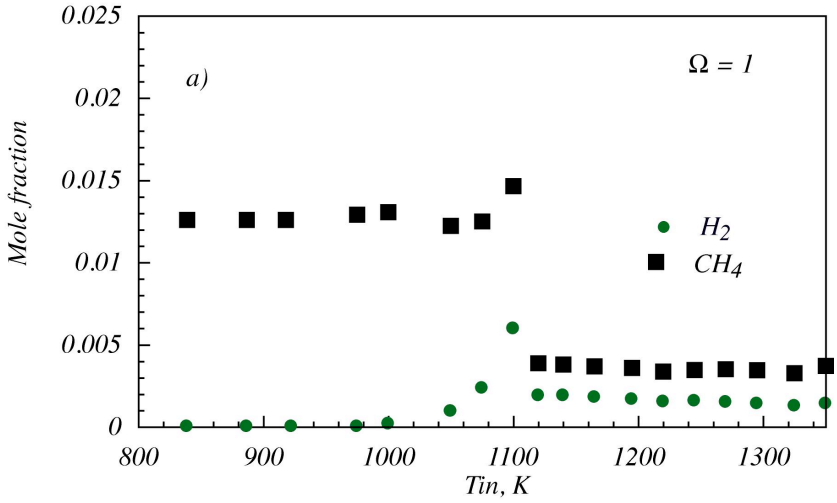

Fig IV.36 - CH_4 and H_2 mole fraction versus T_{in}.

Following, methane and hydrogen concentrations decrease to a constant value, respectively equal to about 0.003 and 0.0015. For the stoichiometric condition, methane conversion is not complete, and hydrogen is detectable in the flue gas stream at high inlet temperatures.

Fig IV.37 regards C_2H_4 and C_2H_6 molar concentration versus T_{in}. For low inlet temperatures, their mole concentration is equal to the reference inlet values. For $T_{in} > 975$ K, ethane concentration starts decreasing while ethylene one increases. For higher values of the mixture inlet temperature, C_2H_6 concentration monotonically decreases and becomes zero for $T_{in} > 1125$ K. On the contrary, ethylene concentration increases reaching a maximum value for $T_{in} = 1075$ K, then it decreases down to zero for $T_{in} = 1125$ K.

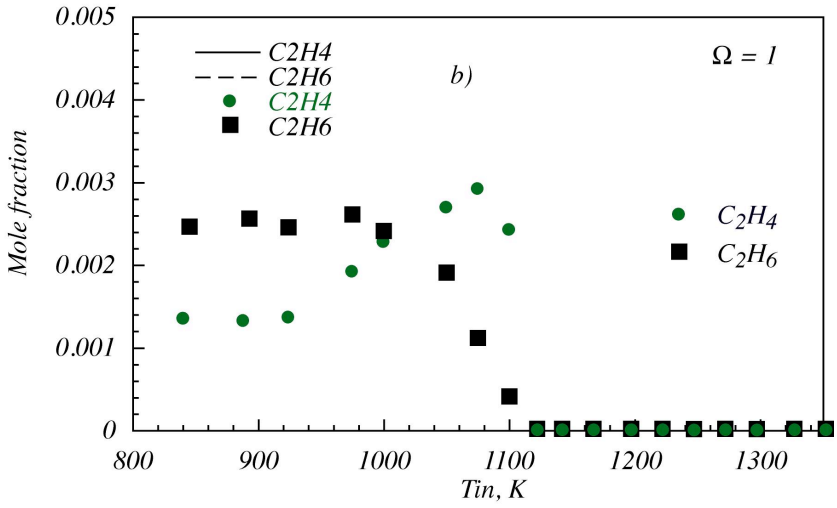

Fig IV.37 - C_2H_4 and C_2H_6 mole fraction versus T_{in}.

Fig IV.38 shows the molar concentration of CO and CO_2. Up to T_{in} = 1000 K, their concentration remains constant. For higher inlet temperatures CO monotonically decreases down up to disappears for T_{in} > 1100K, while CO_2 concentration reaches a constant value of 12%.

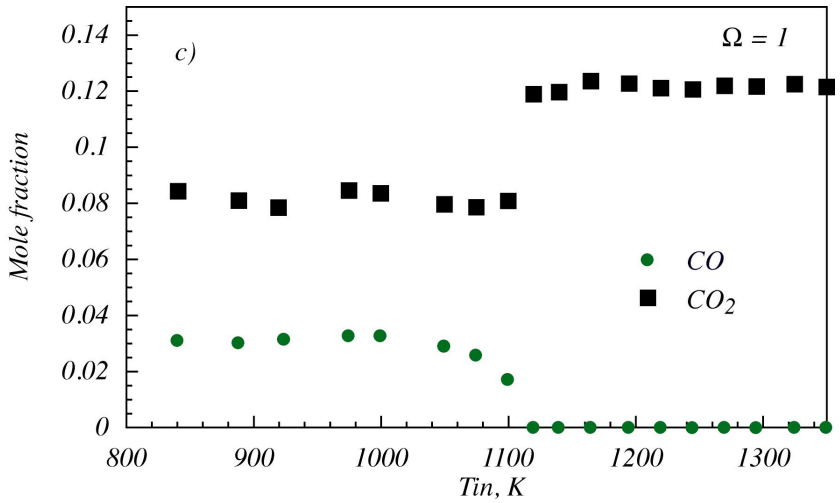

Fig IV.38 - CO and CO_2 mole fraction versus T_{in}.

Finally, Fig IV.39 is relative to O_2 and H_2O. The O_2 concentration decreases for T_{in} > 1075 K from the inlet value down to 3%, whereas water content reaches a constant value of about 1.3%.

In stoichiometric condition, the biogas conversion to CO_2 and H_2O is not complete, methane, hydrogen and oxygen are steel present in the exhausted flue gases for the inlet temperature considered.

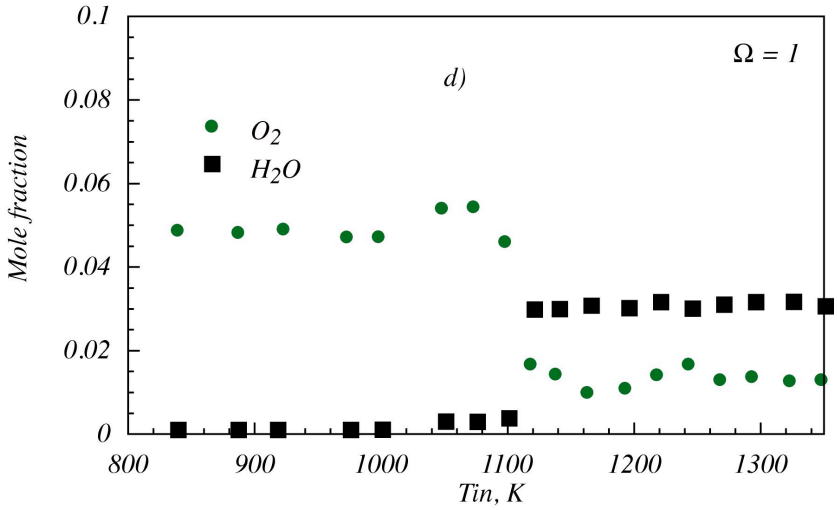

Fig IV.39 - H_2O and O_2 mole fraction versus T_{in}.

Figs IV.40-43 shows the species mole concentration versus the mixture inlet temperature for fuel rich mixture characterised by an equivalence ratio equal to 0.7. The inlet mixture composition is reported in table V.5.

Species	Mole fractions
O_2	4,06
N_2	80,3
CH_4	1,56
CO	3,90
CO_2	9,7
C_2H_4	0,156
C_2H_6	0,31

Tab. V.5 - Reference mixture concentration for Ω = 0.7.

Figs IV.30 reports methane and hydrogen mole fractions as function of the mixture inlet temperature. For both the considered species, for T_{in} < 1050 K, their concentrations remain equal to the reference inlet conditions. For T_{in} > 1050 K, their molar concentration increases and reaches a a maximum value at T_{in} = 1220 K for hydrogen and at T_{in} = 1240/1260 K. Following, their concentration slightly decreases.

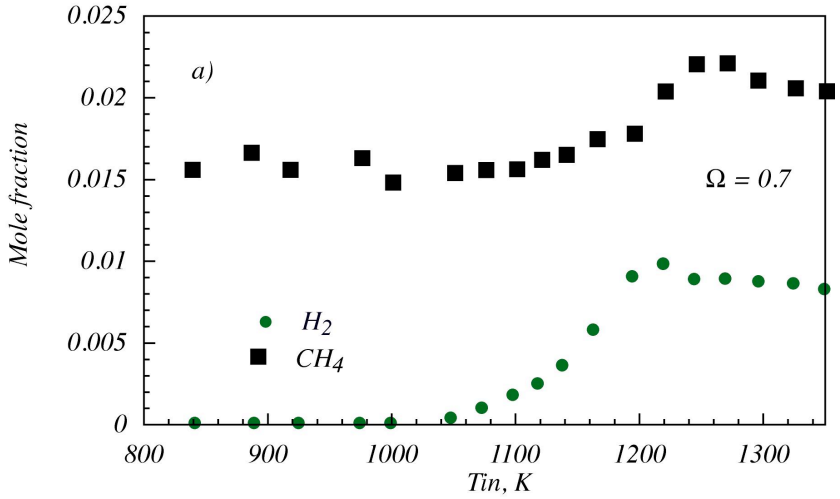

Fig IV.40 - CH_4 and H_2 mole fraction versus T_{in}.

Fig IV.41 concerns C_2H_4 and C_2H_6 molar concentration as function of T_{in}. For low inlet temperatures, their mole concentration is equal to the reference inlet values. For $T_{in} > 900$ K, ethane concentration starts decreasing while ethylene one increases. For higher values of the mixture inlet temperature, C_2H_6 concentration monotonically decreases and becomes zero for $T_{in} > 1225$ K. On the contrary, ethylene concentration increases reaching a maximum value for $T_{in} = 1175$ K, then it decreases down to zero for $T_{in} = 1125$ K.

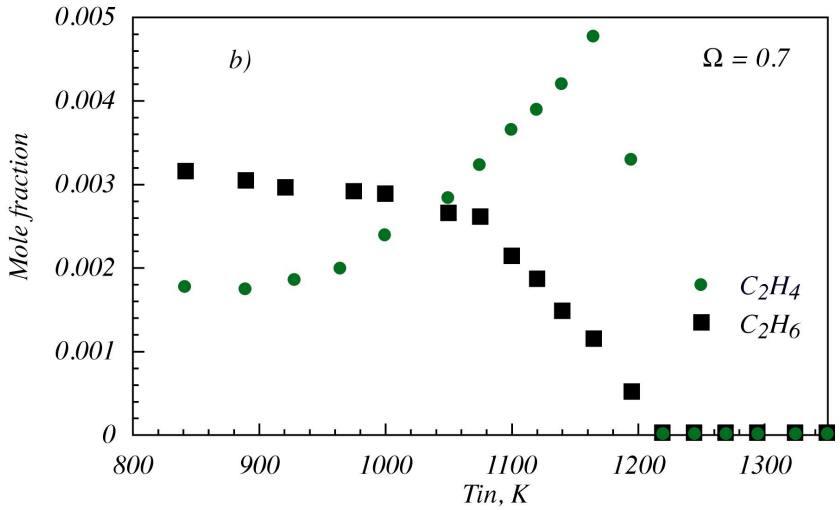

Fig IV.41 - C_2H_4 and C_2H_6 mole fraction versus T_{in}.

Figs IV.42 shows the molar concentration of CO and CO_2. Up to T_{in} = 1050 K, CO concentration remains constant.

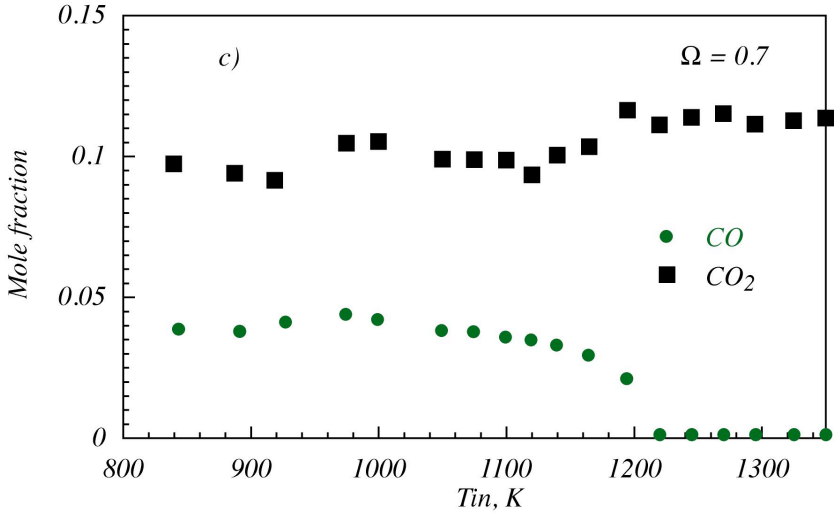

Fig IV.42 - CO and CO_2 mole fraction versus T_{in}.

Thereafter, it monotonically decreases down to for 1225 K. The CO_2 concentration remains constant for low temperatures and increases for T_{in} > 1120 K up to reach a constant value of about 11%.

Finally, Fig IV.43 is relative to O_2. The O_2 concentration decreases for T_{in} > 1075 K from the inlet value down to 3%, whereas water content reaches a constant value of about 1.3%.

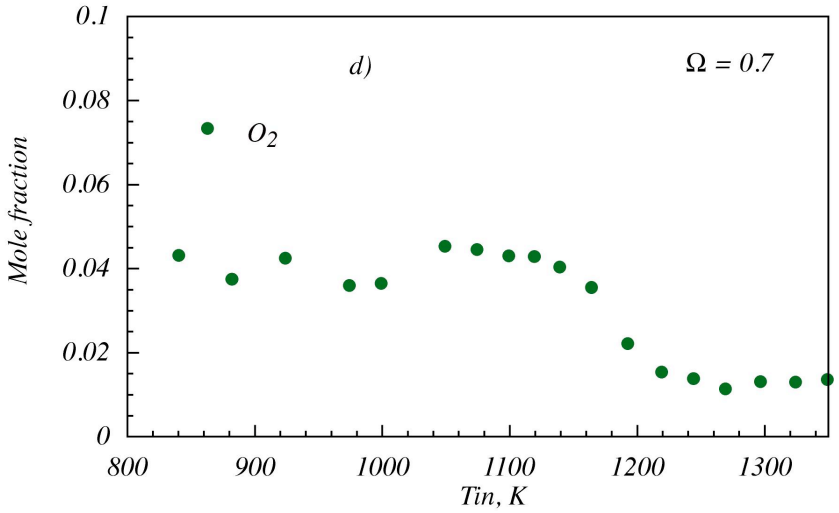

Fig IV.43 - O_2 mole fraction versus Tin.

In such operative conditions, it was not possible to calculate water content since the H elemental mass balance was respected while C and O mass balance were not. Therefore it was not possible to evaluate water content, and such consideration implies the presence of CO or of a greater amount of CO_2.

IV.2.4 - Optical Diagnostic

On the basis of temperature profiles acquired during different session of experimental tests it was possible to delineate the reactivity maps of the system. Such maps are shown in the previous paragraphs for each fuel blends used as well as different dilution degrees. The overall differences observed by varying the working conditions and the composition of the mixtures are highlighted and described in detail. Different phenomenologies were observed and for each of them a specific region was delineated on the map. The same phenomenologies are also shown for methane and biogas blends. In particular, there are some working conditions in which a dynamic behavior was founded within the ignition zone. Such behavior was presented in detail in the chapter relating to experimental results. and was described as a transition zone between no-ignition and ignition areas. The competition among different kinetic pathways are responsible of these behaviors.

In such working conditions several images were acquired by means of optical diagnostics system. Such system was implemented to make measurements of the light emitted spontaneously from the reaction volume and was described in detail in the chapter IV. For each test condition a 1000-frame sample was collected and also a background image was captured and then used to clean up the original images, reducing the electronic noise as well as the brightness of the bottom of the reactor, which operates at a very high temperature and emits a light beam similar to a blackbody at the same temperature. In fig.

IV.44 a typical original image (on the left side) and a background image (on the right side) were shown. The frames collected were stored and post processed by means of a Labview routine. The software also allows the representation of false color images by the application of appropriate look-up choices. The processing procedure is shown schematically in the chapter IV. In fig. IV.45 a typical image, results of such post-process was presented with a layout in false colors. In order to analyze the images, a region of interest was located on the frames with a square in black boundary.

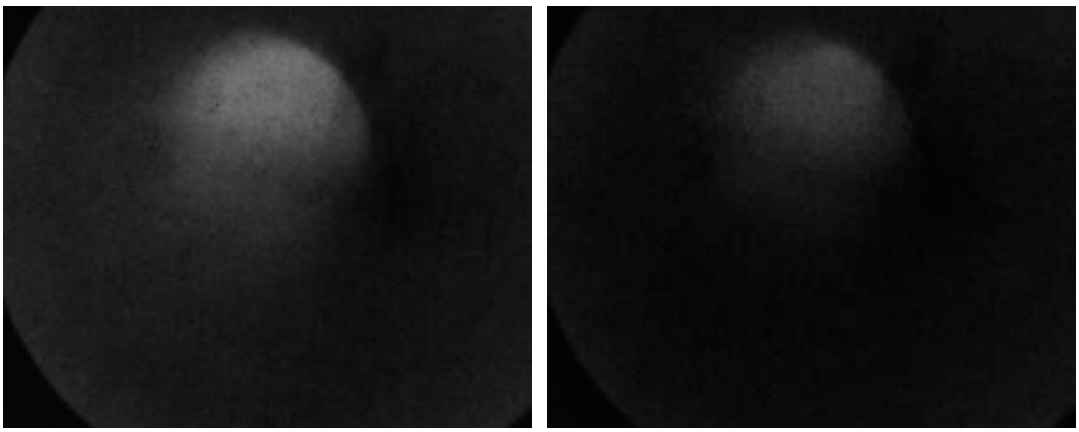

Fig IV.44 - Frames captured during the experimental tests: original image (on the left side) and background image (on the right side)

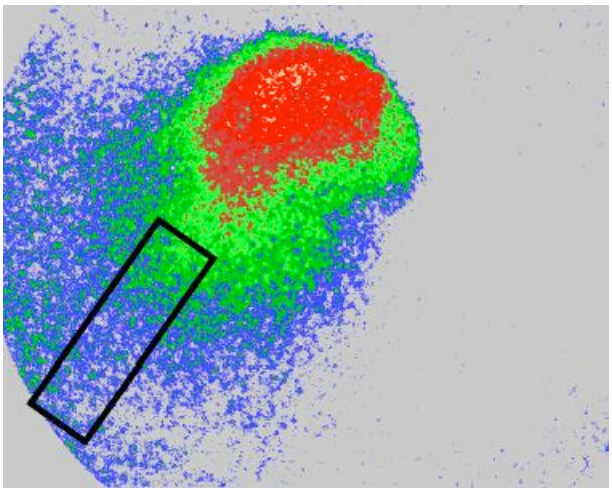

Fig IV.45 - Light intensity shown in a false colors layout.

In fig.IV.46 the average intensity of the radiation emitted by the system for wavelengths less than 400 nm in the region highlighted was shown as a function of time. Such intensity profile was obtained for Ω =1.2 and an initial temperature equal to 1150 K. The biogas blend was diluted in nitrogen at 90 % and the specific condition shown in such a figure are localized in the dynamic area of the reactivity map. As it is evident from the figure (Fig. IV. 46), the light intensity varies with a frequency less than 1 Hz, from a minimum to a maximum value, which are almost constant throughout the time period analyzed.

In particular, it varies between a maximum equal to 15 a.u. and a minimum of about 5 u.a. due to the emission of some excited intermediate species.

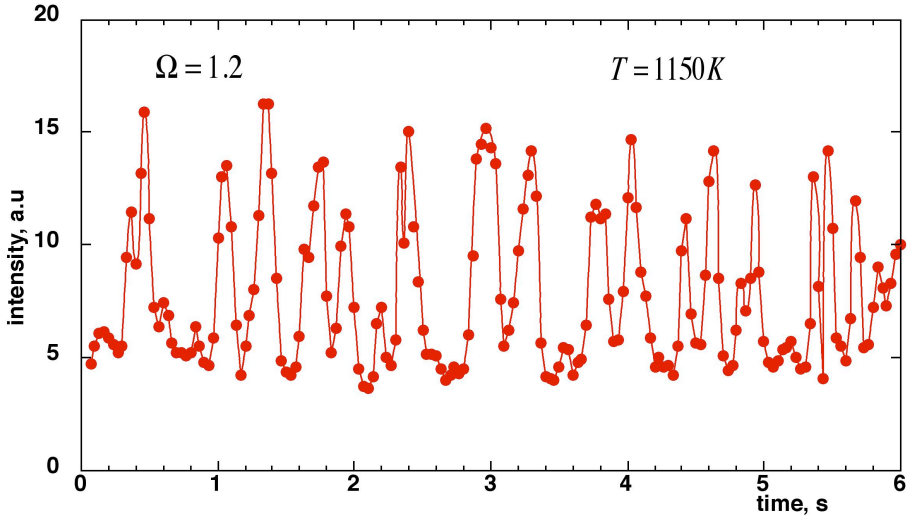

Fig IV.46 - Light intensity emitted from the reaction volume for wavelengths below 400 nm.

In order to understand the range of wavelengths of the light emission, several different filters were used. Figs IV.47 and IV.48 show the value of the light intensity captured by interposing two different filters between the amplifier and the light source. The first figure represents light intensity captured for $500nm \le \lambda \le 600nm$ in the region of interest, while the second one focuses the attention to $\lambda \le 400nm$. The trend of light intensity was reported along with some images relating to different instants of capture.

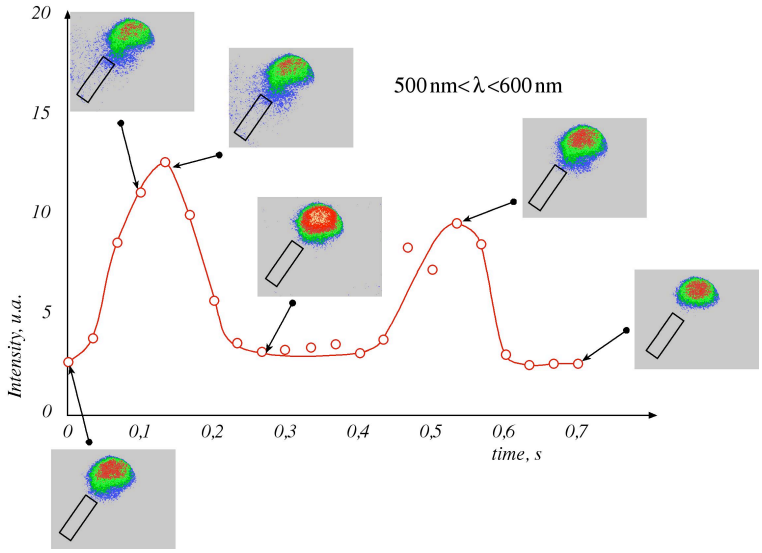

Fig IV.47 - Light intensity acquired for $500nm < \lambda < 600nm$.

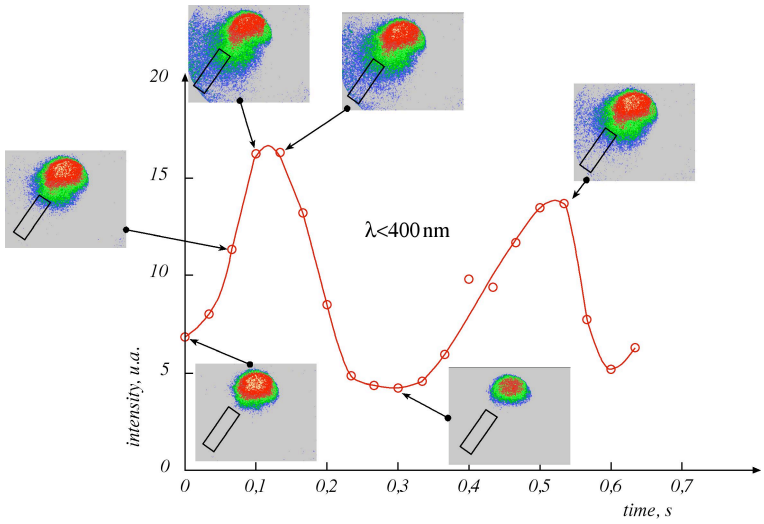

Fig IV.48 - Light intensity acquired for $\lambda < 400nm$.

Results show higher light emissions for ultraviolet wavelengths ($\lambda \leq 400nm$).

The analysis of the variation of light intensity measured under the operating conditions corresponding to dynamical systems are useful to give indications on the kinetic pathways responsible for these phenomena. In addition, to identify species that can be used as a marker to detect the onset of undesired phenomenologies. The light intensity collected for wavelengths below 400 nm may indicate the presence of oxygenated aldehyde type, characterized by an emission of light at about 320 nm. This hypothesis could be confirmed

by the formaldehyde concentration values obtained in these conditions, which are higher than those obtained in stable conditions.

Several samplings were performed in the same working conditions. In particular, the presence of oxygen species was evaluated by using a colorimetric technique developed for the identification of traces of formaldehyde in the atmosphere. (T. Nash 1953; T. Salthammer 2008) In the chapter IV the technique was described in detail.

Results are summarised in the fig. IV.49. The sampling tests were made for different omega values both in the dynamic and ignition zone. As it is evident from the figure, the concentration of formaldehyde increases as soon as dynamic behaviors occur. It changes from low concentrations (Mole fraction $< 2 \cdot 10^{-8}$) up to higher concentration (Mole fraction $= 1 \cdot 10^{-7}$) for Ω between 1 and 1.75. In particular, the mole fraction of formaldehyde reaches values of about one order of magnitude greater than the values measured in stationary conditions of ignition.

The formaldehyde is an intermediate species in the oxidation kinetic mechanism of hydrocarbons. Hence a lot of studies on the kinetic reaction of this species there have been realised. The larger amount of such a specie is hence necessarily relating to the occurrence of dynamic behavior. The non-stable behavior of the ignition process leads to the formation of such a species which afterwards do not react, and remain in the exhaust gases. Moreover, the higher light intensity observed during the occurrence of these behaviors are due to the emissions of excited formaldehyde molecules.

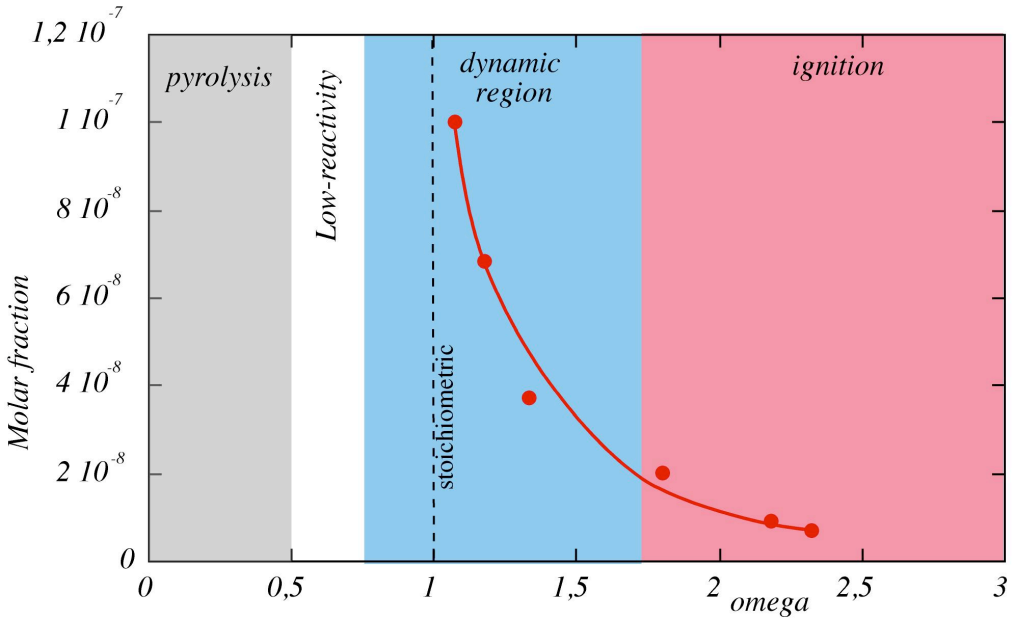

Fig IV.*49 - Mole fraction of formaldehyde in function of omega values.*

Chapter V

Numerical Results

The numerical analysis is an important tool for understanding the combustion process and should always be coupled with an experimental study.

This chapter presents the results obtained with the software CHEMKIN 3.7 and Cantera. As mentioned in previous chapters, the first was used to evaluate the ignition delays in different working conditions, to plot the temperature profiles, perform sensitivity analysis and assess the state of the production rate of a single species, while the second to get the paths of the main reactions.

Several kinetic mechanisms were selected in order to compare them and to assess the reproducibility of the experimental data collected. The ignition process in MILD combustion conditions, was analyzed numerically in a wide range of temperature at atmospheric and higher pressure, for different feed ratios and by varying the dilution degree, chemical nature of the diluent and fuel.

V.1 - Kinetic Mechanisms

Numerical simulations for studying the evolution of methane ignition process at atmospheric pressure in diluted conditions were performed by means of PLUG application of the Chemkin 3.7 software. PLUG simulates the behavior of plug-flow chemical reactor. Several oxidation kinetic mechanisms, freely available on the web, were considered. The names used to identify them in the chapter along with the relative reference and the numbers of involved species and reactions are reported in Table VI.1. All these

mechanisms were validated for a wide range of operative conditions and different reactor configurations in standard conditions, as well described in the literature. In the present work, from the computed temperature axial profiles auto-ignition delay times (τ_{ign}) (M. De Joannon 2002) were assessed in a wide range of parameters. Following a criterium described in details elsewhere τ_{ign} was defined as the time corresponding to a temperature increase of 10 K with respect to mixture inlet one (T_{in}). In addition to auto-ignition delay computation, PLUG application has also been used for reaction sensitivity and rate of production analyses, whilst Cantera was specifically used for automatically drawing net reaction path diagrams.

Mechanisms	*# Of species*	*# Of reactions*	*References*
Ranzi	***69***	***1134***	***(E. Ranzi 2010)***
GRI-Mech 3.0	***53***	***325***	***(C. Bowman 1999)***
Warnatz	***35***	***164***	***(J. Warnatz 2006)***
Huang	***40***	***194***	***(J. Huang 2004)***
RAMEC	***47***	***190***	***(E. Petersen 1999)***
Konnov	***127***	***1207***	***(A. Konnov 2010)***
San Diego	***46***	***235***	***(F. Williams)***
Zhukov	***209***	***1260***	***(V. Zhukov 2009)***

Tab. V.1 - Denomination, reference and numbers of involved species and reactions of the kinetic models used in this work.

V.2 - Numerical Results

V.2.1 - Methane

V.2.1.1 - Comparison of kinetic mechanisms

The prediction of the auto-ignition delay time (τ_{ign}) obtained with all the considered kinetic mechanisms have been reported in Figs. V.1 and V.2. Fig. V.2 shows the Arrhenius plots of numerical auto-ignition delay times versus $\alpha = 1000/T_{in}$ computed, at C/O = 0.2, with five of the seven selected mechanisms for a degree of dilution of 85 % in nitrogen. All of them shows that auto-ignition delay decreases monotonically with temperature increase, linearly or nearly linearly. It has to be noted that the values predicted at each temperature span over a wide range of values.

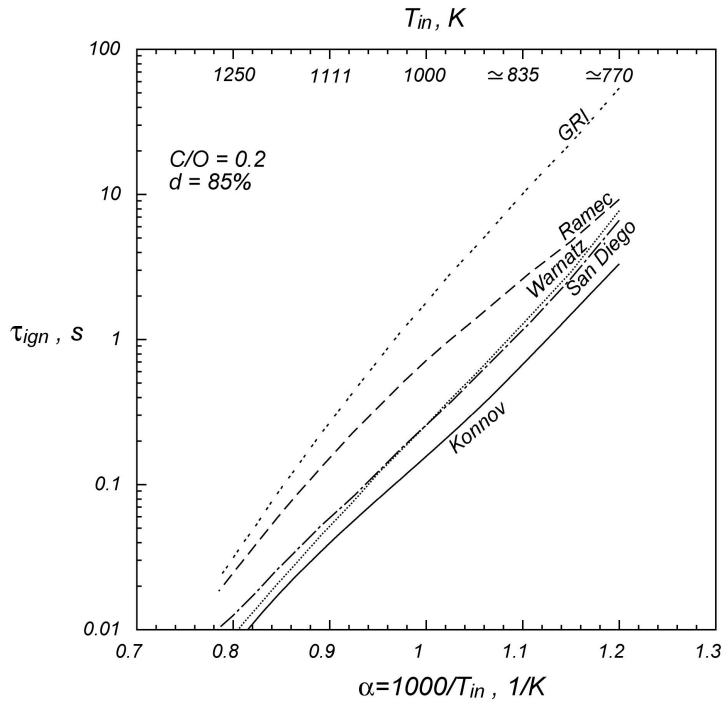

Fig. V.1 - Comparison of auto-ignition delay time computed with different kinetic mechanisms.

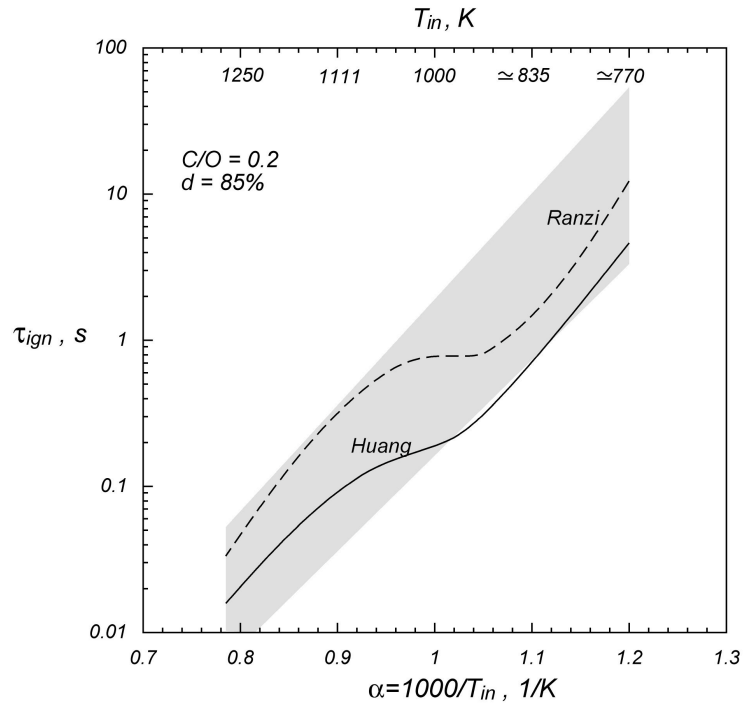

Fig. V.2 - Comparison of auto-ignition delay time computed with Huang and Ranzi mechanism. Gray area is the variation region of the ignition delay reported in Fig. V.1.

Auto-ignition delay time profiles computed with GRI-Mech 3.0 (double-dashed) and Konnov (solid line) envelop, upward and downward respectively, all the other profiles. For instance, at T_{in} = 830 K the values span over one order of magnitude, from the 50 s predicted by GRI-3.0 to the 3 s computed using Konnov mechanism. The variation is smaller at higher temperature. For T_{in} = 1250 K GRI-3.0 predicts a τ_{ign} = 0.02 s while Konnov mechanism gives a τ_{ign} = 0.008 s. Profiles obtained with RAMEC, Warnatz and San Diego mechanisms lie between GRI-Mech 3.0 and Konnov lines. Warnatz and San Diego profiles lie in the lower value range closer to the Konnov one than to the GRI-Mech 3.0 one. RAMEC profile is closer to GRI-3.0 one at higher inlet temperature whereas it bends toward Konnov profile at lower temperature. Fig. V.2 shows auto-ignition delay obtained using Ranzi and Huang mechanisms. The gray area, reported in the figure, represents the region delimited by the GRI-Mech 3.0 and Konnov profiles reported in Fig

V.1. It has been reported in order to facilitate the comparison among all the mechanisms. The two curves reported on the Arrhenius plot of Fig V.2 falls within or nearby such a region. Both mechanisms are able to predict the existence of temperature ranges related to different system reactivity. More specifically, both curves show that τ_{ign} decreases with temperature increase for temperature lower than 925 K and higher than 1050 K. For the intermediate range of inlet temperatures, between 925 K and 1050 K, the auto-ignition delay times curves show a change in slope which testifies a variation of system reactivity. Namely, for data obtained with Ranzi mechanism, τ_{ign} decreases of one order of magnitude, from 10 s to 1 s increasing T_{in} from 830 K to about 910 K, then it is nearly constant for a temperature change of about 120 K, from 910 K to 1010 K. There after, τ_{ign} decreases linearly from 0.7 s to 0.015 s, with increasing T_{in} from 1070 K to 1265 K. The Huang mechanism produces lower auto-ignition delay times and a much smoother transition between the two regions of linear dependence on T_{in} with respect to the Ranzi one.

The trend evidenced in Fig V.2 by both curves recalls the well known Negative Temperature Coefficient (NTC) largely characterized by paraffins larger than C4. Generally, in the literature NTC region always refers to a range of temperature where ignition delay time increase with temperature, i.e. the slope of τ_{ign} as a function of 1000/T_{in} in an Arrhenius plot from positive becomes negative. In most cases here reported the change in slope is drastic because from a positive value it becomes nearly equal to zero, but it does not assume negative values. In the same conditions Petersen et al. as well as Sokolov et al. referred this region as NTC. Following the available literature, NTC acronym has been used hereafter in order to easily associate it to a change in slope of τ_{ign}

as a function of $1000/T_{in}$ in a more general sense. Such a behavior is not fully characterized for low molecular weight hydrocarbon because there are very few experimental evidences showing a clear change in the reactivity of such hydrocarbons in any particular temperature range. This is most likely the reason why most of the mechanisms considered in this work are not able to predict its existence. As a matter of a fact, in the experimental facilities generally used for auto-ignition studies the fast ignition reactions hide the slower ones, characteristics of the intermediate temperature range, due to the non-uniform distribution of temperature typically occurring in those systems . It is clear that an NTC behavior of methane auto-ignition cannot be associated to the same kinetic pathway that determines the occurrence of an NTC in high molecular weight paraffins oxidation because no oxygen double addition occurs in methane oxidation. In order to understand the chemical pathways controlling the auto-ignition delay time dependence on T_{in}, the Ranzi mechanism has been used for carrying out reaction path diagrams, sensitivity and rate of production analyses. It has been preferred to Huang mechanism because it shows a more defined NTC region. In addition it has been validated in a wider range of conditions and reaction configuration at atmospheric pressure.

V.2.1.2 - Numerical Analysis: Reaction path diagrams

In order to clarify the prevailing methane oxidation kinetic pathways at different temperature ranges, an extensive numerical simulation activity was carried out by means of Cantera software. First, simulations were run in order to compare ChemKin and Cantera results on the basis of temperature axial profiles and auto-ignition delay times. The results show that the software predictions are practically coincident. The compatibility between the two software is already validated in the literature. Fig V.3 shows clearly that the results obtained from the two software are nearly coincident.

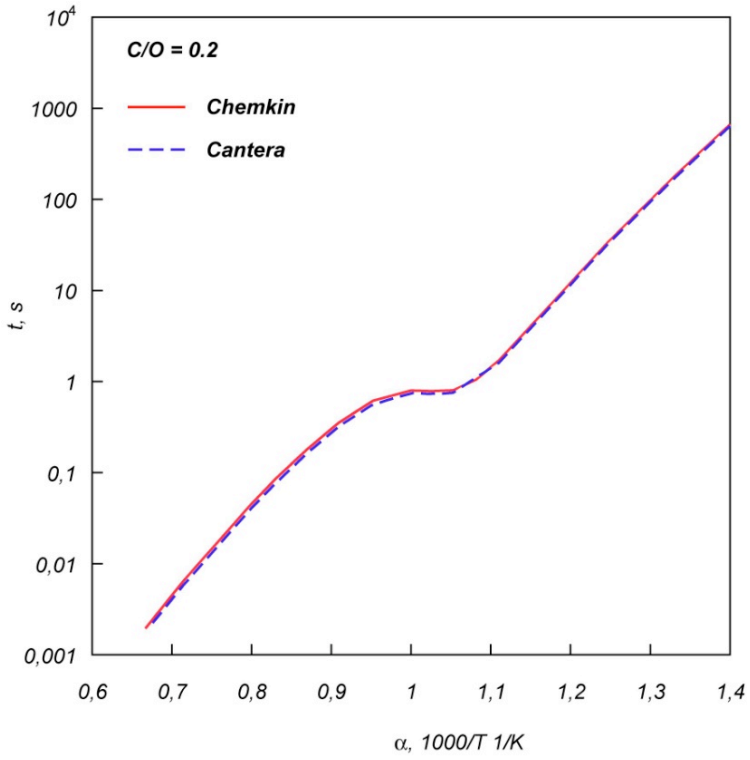

Fig. V.3 - Comparison of Chemkin and Cantera software. Comparison of auto-ignition delay times.

Path diagrams, freezing the reaction network at t = τ_{ign} , referred to carbon atoms for three different inlet temperatures and for C/O = 0.2 are shown in Figs V.4-5-6 . Inlet temperatures have been chosen as representative of the three different ranges of temperature previously identified. Arrow thickness is proportional to the net reaction rates and the plot scale is equal to 10^{-4} mol/s/cm3. The reaction path diagram of Fig V.4 shows that, at T_{in} = 850 K, methyl radicals, formed by dehydrogenation from methane, are then oxidized to CH_3O and CH_3O_2.

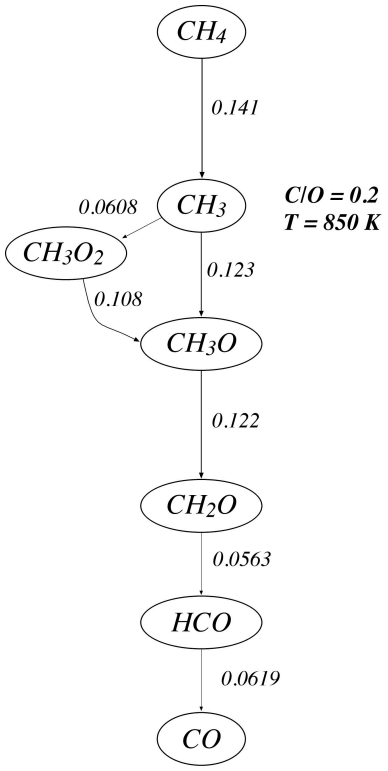

Fig. V.4 - Flow diagram computed with Ranzi mechanism at 850 K.

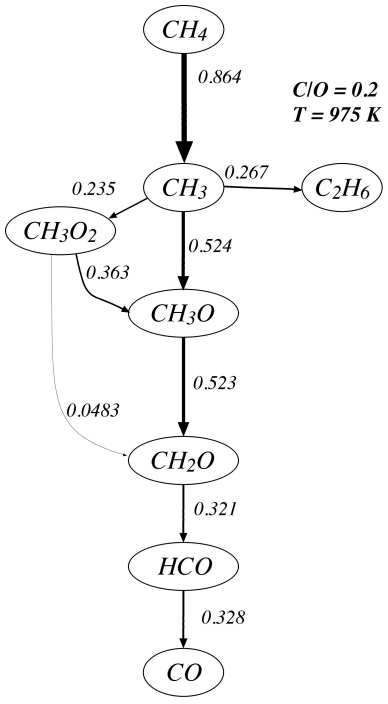

Fig. V.5 - Flow diagram computed with Ranzi mechanism at 975 K.

Later on, formaldehyde, formyl radical and CO are produced. At such an early stage of combustion the subsequent oxidation of CO to CO_2 is not active yet. The net reaction rates

are relatively low. At T_{in} = 975 K, in the temperature region where the results obtained using the Ranzi mechanism exhibit an NTC region, net reaction rates are higher with respect to the first case. In particular they result to be about six times the net rates relative to the previous considered temperature. Carbon main pathways are similar to the previous case even though two additional reactions routes are identifiable in the diagram reported in Fig V.5.

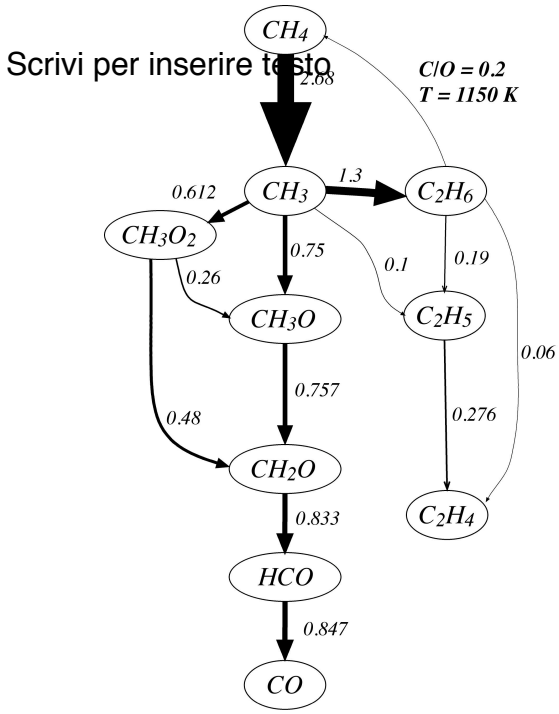

Fig. V.6 - Flow diagram computed with Ranzi mechanism at 1150 K.

Methyl radicals not only react following the oxidation channel to form CH_3O and CH_3O_2, but also recombine yielding ethane. Furthermore, methyl peroxide leads to the formation not only of CH_3O, as at lower temperature, but also of formaldehyde and OH radicals. It is worth noting that about 75% of formed CH_3 is transformed in either CH_3O_2 or CH_3O, while the remaining 25% follows the recombination pathway, which subtracts carbon and hydrogen from oxidative channels. A further increase of T_{in} beyond the NTC region strongly enhances the methane conversion and, as a consequence, the subsequent reactions,

as well shown in Fig V.6, obtained for 1150 K. As expected, the temperature affects also the relative weight of each channel. About 50% of methyl radicals feed the recombination channel. In addition, the formation of unsaturated hydrocarbons is set on. C_2H_5 radicals derive both by recombination from CH_3 radicals and by dehydrogenation from ethane. Then, they are dehydrogenated to ethene. The oxidation route follows the same channel reported for lower temperatures, even though the formation rate of CH_3O_2 and CH_3O from methyl radicals are, in this case, nearly equivalent. In addition the methyl peroxide radical decomposition to CH_2O and OH overcomes the metathesis of CH_3O_2 and CH_3 to form CH_3O. Similarly to the lower temperature cases, methoxy and methyl peroxide radicals are dehydrogenated to CO.

V.2.1.3 - Sensitivity and Rate of Production Analysis

Relevant information can be earned by sensitivity analyses diagram of Figs V. 7-8-9. obtained at 850 K, 950 K and 1150 K, respectively, at the relative ignition time.

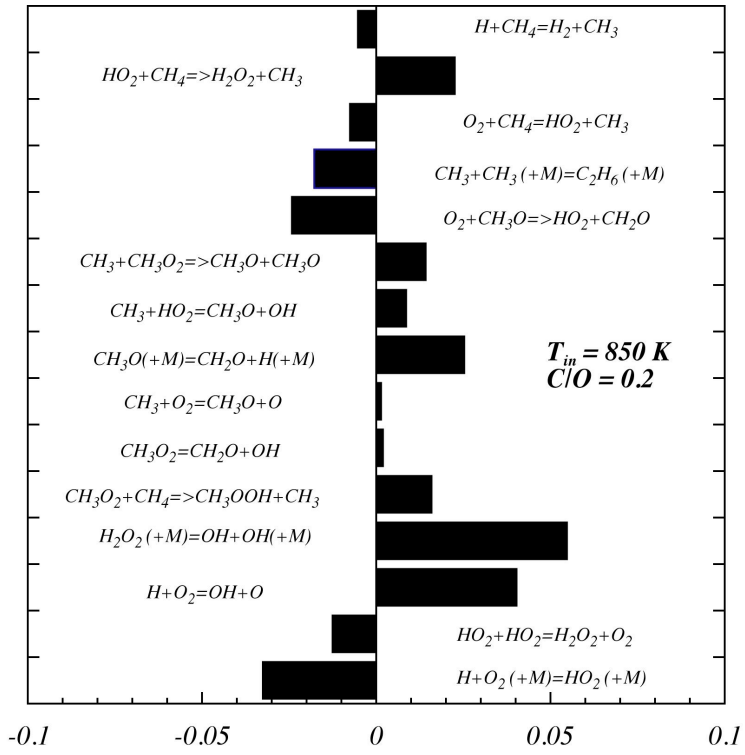

Fig. V.7 - Sensitivity coefficients obtained at 850 K and C/O = 0.2 with Ranzi mechanism.

Summarizing the results for the three temperatures, the most sensitive reactions involved in the methane auto-ignition for the operative conditions considered can be listed as follow.

For the H_2/O_2 system main reactions are:

(12) $H_2 + O_2 + M \rightarrow HO_2 + M$

(13) $HO_2 + HO_2 \rightarrow H_2O_2 + O_2$

(14) $H_2O_2 + M \rightarrow OH + OH + M$

(15) $H + O_2 \rightarrow OH + H$

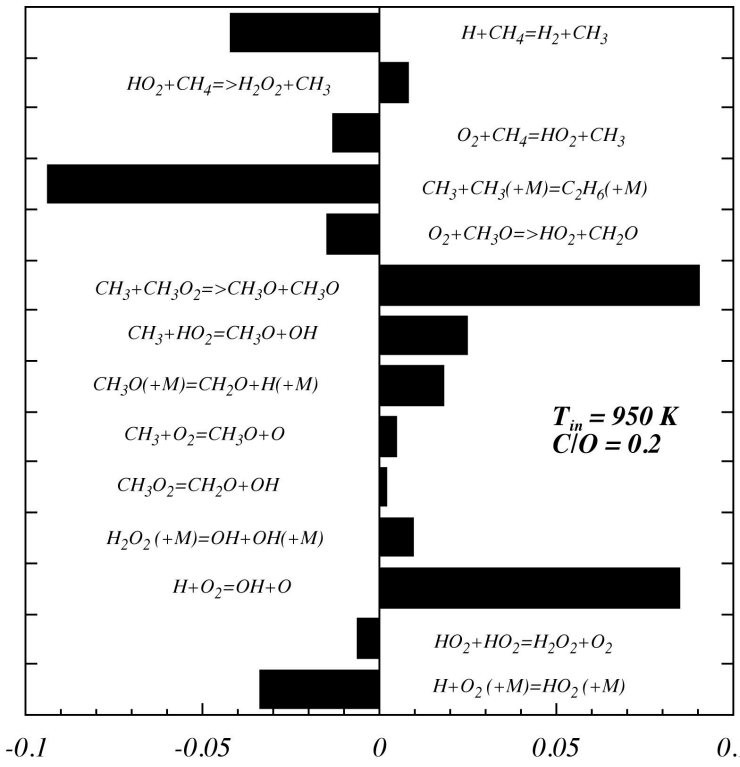

Fig. V.8 - Sensitivity coefficients obtained at 975 K and C/O = 0.2 with Ranzi mechanism.

while for methane:

(16) $CH_4 + H \rightarrow CH_3 + H_2$

(17) $CH_4 + HO_2 \rightarrow CH_3 + H_2O_2$

(18) $CH_4 + O_2 \rightarrow CH_3 + HO_2$

The most sensitive reactions involving methyl radicals are:

(19) $CH_3 + HO_2 \rightarrow CH_3O + OH$

(20) $CH_3 + O_2 \rightleftarrows CH_3O + O$

(21) $CH_3 + CH_3O_2 \rightarrow CH_3O + CH_3O$

(22) $CH_3 + O_2 \rightleftarrows CH_3O_2$

(23) $CH_3 + CH_3 + M \rightarrow C_2H_6 + M$

while CH_3O and CH_3O_2 most relevant reactions are:

(24) $CH_3O + M \rightarrow CH_2O + H + M$

(25) $CH_3O_2 \rightleftarrows CH_2O + OH$

(26) $CH_3O_2 + CH_4 \rightarrow CH_3OOH + CH_3$

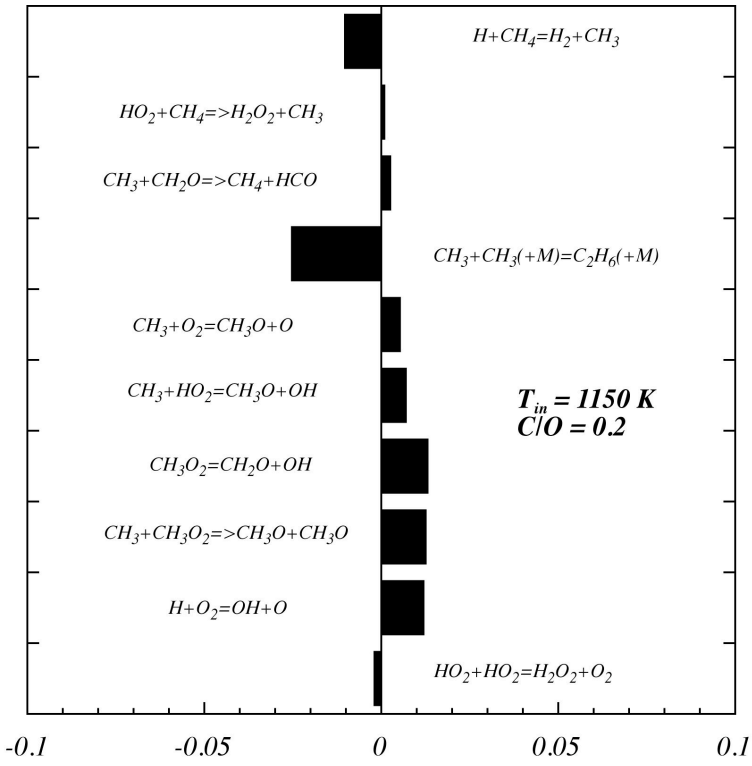

Fig. V.9 - Sensitivity coefficients obtained at 1150 K and C/O = 0.2 with Ranzi mechanism.

On the basis of information collected from path diagram and sensitivity analysis indications, the rate of production/destruction (ROP) of some key species involved in the most sensitive reactions has been analyzed as a function of temperature in Figs V.10 and VI.11. The secondary axis of Fig V.10 shows the net rates of destruction of methyl radicals through the recombination route (reaction (12)) with dashed line and the sum of net rates of reactions that lead from methyl radicals to CH_3O and CH_3O_2 (namely from reactions (8)–(11)) with dashed-dotted line. On the same diagram the auto-ignition times of Fig V.2 has been reported in order to make easier the comparison of the different curves. The gray area high-lights the temperature region of NTC. It is worth noting that for low inlet temperatures the sum of methyl oxidation reaction rate increases as T_{in} increases.

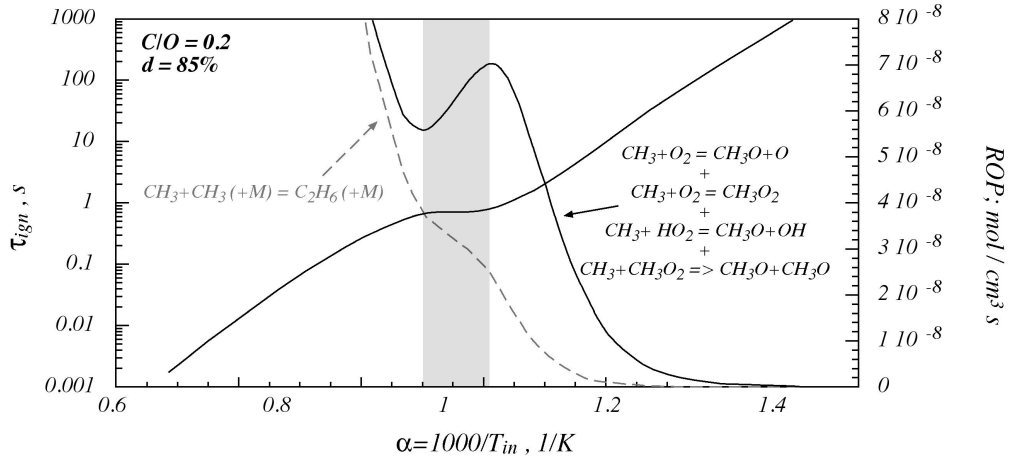

Fig. V.10 - Auto-ignition delay times and rate of production of CH3 through oxidation and recombination channel.

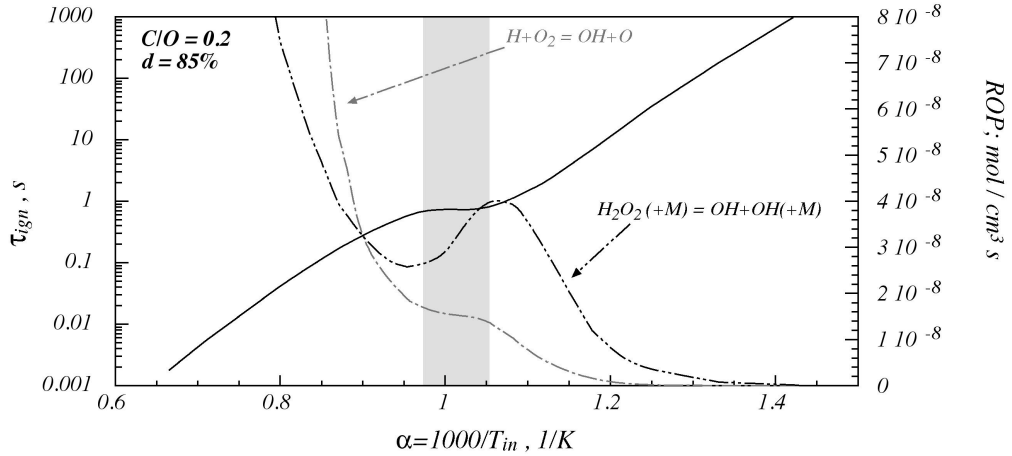

Fig. V.11 - Auto-ignition delay times and rate of production of OH reactions (3) and (4).

As soon as the recombination reaction becomes important, the oxidation reactions net rate increases with a lower slope, showing a maximum value just for the beginning of the NTC temperature range, then it decreases slowly down to a relative minimum value. Later on, just after the NTC temperature range, it increases again increasing the temperature. The net rate of recombination reaction monotonically increases in the whole temperature range considered. In order to identify the dominant branching reactions that lead to the main branching agent OH, relatively to the H_2/O_2 system, the rate of production of OH through

the reaction (3) (hydrogen peroxide decomposition) and reaction (4) have been reported as function of $1000/T_{in}$ in Fig V.11 along with the auto-ignition delay time of Fig V.2.

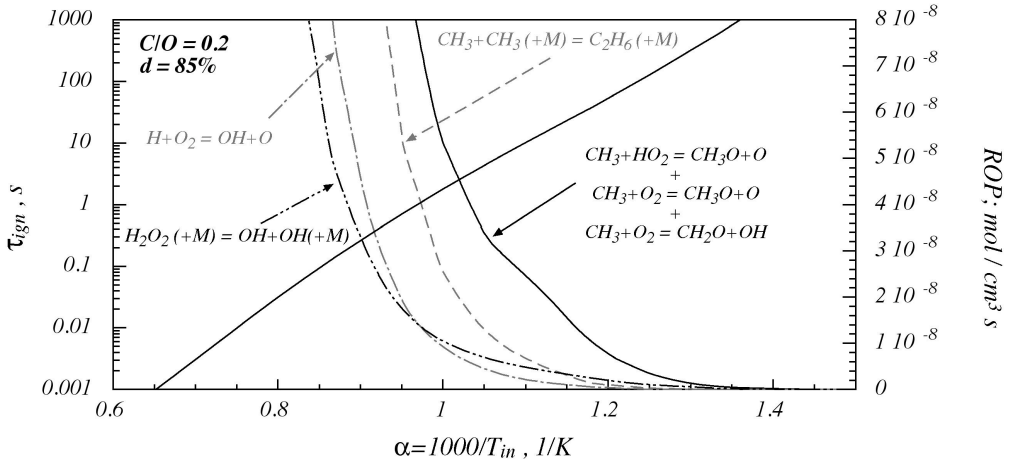

Fig. V.12 - Auto-ignition delay time and rate of production of specified reactions computed with GRI mechanism.

For low temperatures the main branching mechanism is the decomposition of H_2O_2, while in the NTC range, the ROP of the reaction **(3)** shows a maximum just for the low temperature side of the NTC region. Then, it decreases until the high temperature side of the NTC. Hereafter it increases due to the abruptly increase of reaction **(4)** that becomes the main branching reaction at high temperatures. The correspondent diagrams of Figs V. 10 and 11 obtained with GRI-Mech 3.0 have been summarized in Fig V.12. The rate of production of reactions (10) and (11) are missing because such reactions are not present in this mechanism. In consequence of their absence the rate of production of the other considered reactions show a monotonic increase with temperature with no remarkable trend. It has to be stressed that in this case the rates of production of reactions (3) and (4) do not differ as much as they do with the Ranzi mechanism.

V.2.1.4 - Effect of Mixture Composition

The analysis of NTC behavior has been extended in order to evaluate the effect of mixture composition on ignition delay. More specifically two aspects have been taken into account that concern the effect of carbon to oxygen ratio and the nature of inert gas present in the reactive mixture. Therefore, numerical simulations were carried on by changing the mixture composition from lean to rich mixtures and by substituting nitrogen with different diluent species of interest in new combustion technologies. Fig V.13 shows the auto-ignition time for three C/O, 0.1, 0.2 and 0.5.

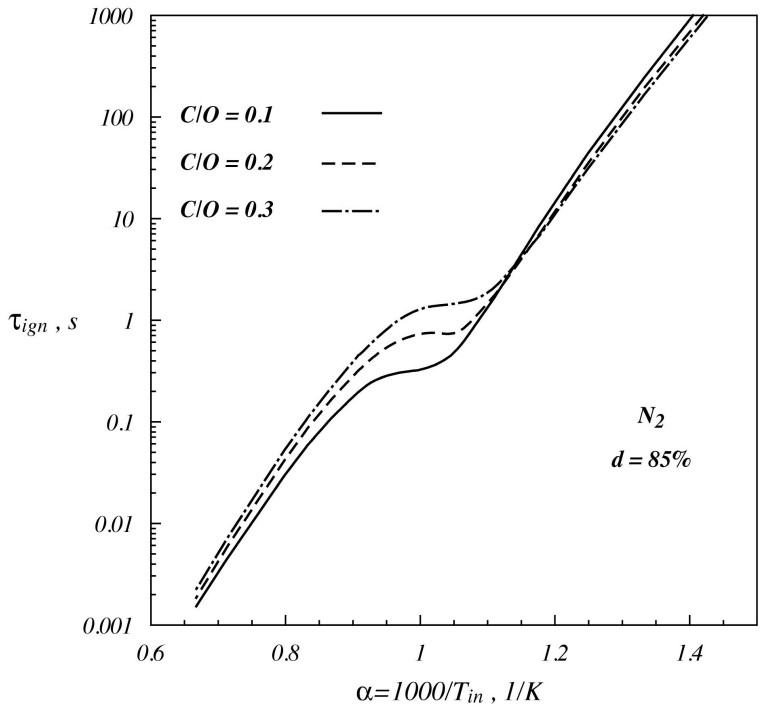

Fig. V.13 - Auto-ignition delay time computed for three C/O ratio.

All the profiles show a similar trend. For inlet temperature lower than 850 K, the ignition delay is almost independent on carbon to oxygen ratio, while at temperature higher than 850 K the richer the mixture, the longer the auto-ignition time is. In addition, it is worth noting than the temperature ranges where an NTC behavior can be observed, in all the three considered cases, shift toward lower temperature values with increasing C/O feed

ratio. At temperature above NTC regions ones differences among τ_{ign} values become more relevant.

Several numerical tests were carried out with different diluent species. Fig V.14 shows the auto-ignition delay times as function of $1000/T_{in}$ on curves parametric in the diluent, namely nitrogen, carbon dioxide and water vapor, for C/O = 0.2 and a dilution level equal to 85%.

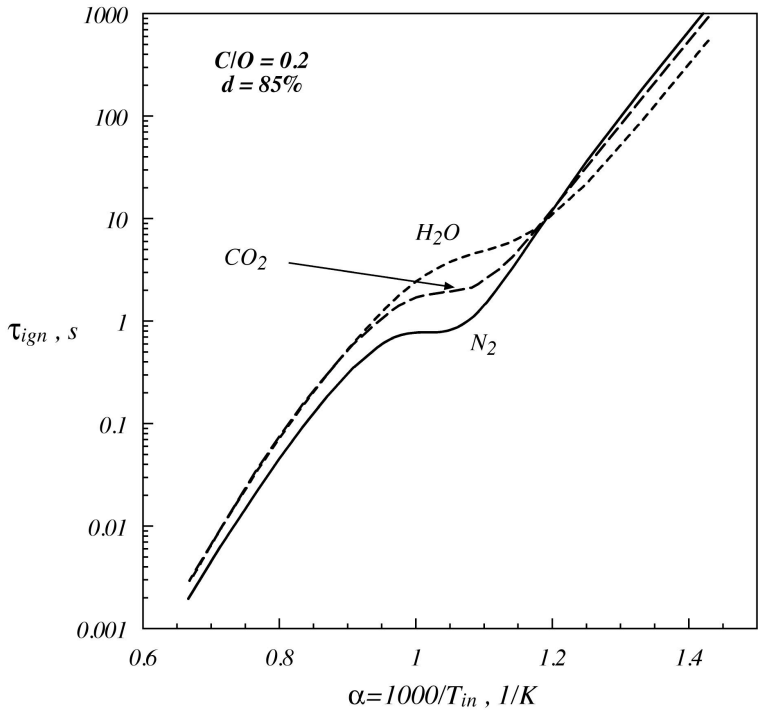

Fig. V.14 - Auto-ignition delay time obtained with different diluent species.

The trend of curves is similar for all the cases. At low temperatures, for T_{in} value comprised between 700 K and 850 K, the shortest auto-ignition times competes to H_2O diluted system, while nitrogen diluted system shows the longest ones. At T_{in} = 850 K curves intersect and, for T_{in} > 850 K, the trend is inverted and auto-ignition delay times computed using as diluents water and carbon dioxide are longer than those computed using N_2 as diluent. In particular, the longest auto-ignition times compete to the system diluted in

water. For instance, at T_{in} = 1000 K, τ_{ign} is equal to 0.74 s for N_2, 1.69 s for CO_2 and 2.42 s for H_2O. At T_{in} above 1100 K auto-ignition delay times computed for water and carbon dioxide diluted systems do not differ significantly.

Figs V.14 and V.15 show auto-ignition delay times versus α as function of C/O feed ratio, respectively for CO_2 and H_2O. The trend of the curves is the same as the one obtained with nitrogen dilution. For the systems diluted in CO2, at low temperatures a linear trend is observed up to α = 1.18. The richer the mixture, the lower the auto-ignition time is.

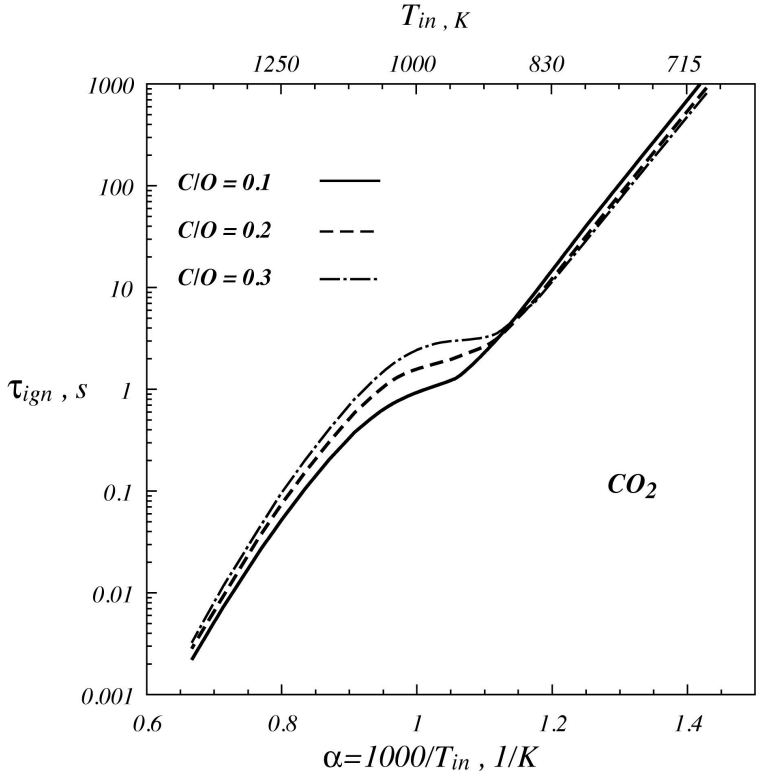

Fig. V.15 - Auto-ignition delay times computed for different C/O ratio and CO2 as diluent.

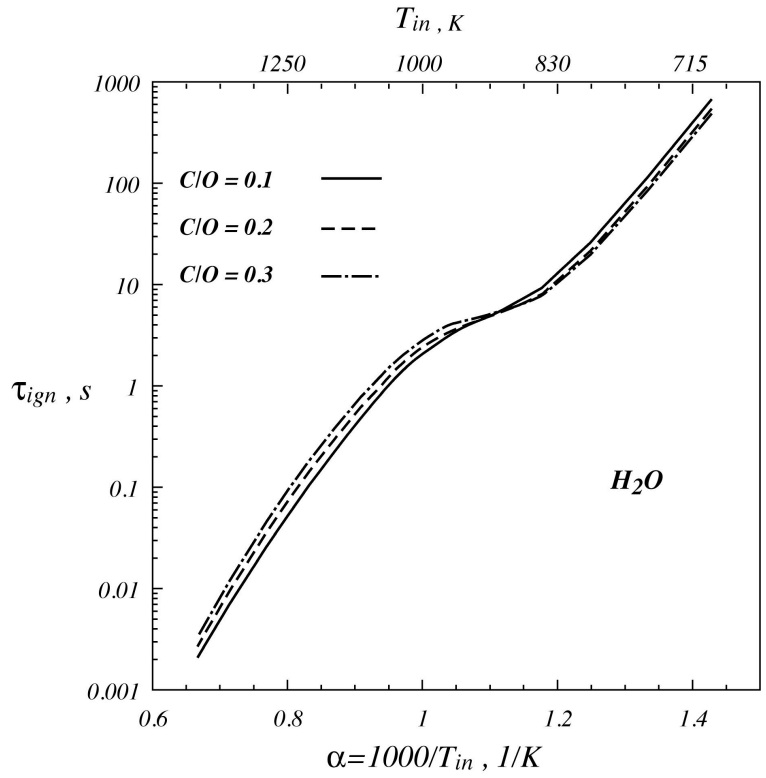

Fig. V.16 - Auto-ignition delay times computed for different C/O ratio and H2O as diluent.

The differences among auto-ignition delay values are lower with respect to nitrogen systems, showed in Fig V.13. In fact, at Tin =1000 K, τ_{ign} is equal to 0.962 s, 1.69 s and 2.54 s respectively for C/O = 0.1, 0.2, 0.3.

Similar considerations apply for water diluted systems. The NTC region is shifted to higher values of α and curves are very close to each other. As matter of fact, at α = 1, τ_{ign} is equal to 2.11 s, 2.42 s and 2.91 s, respectively for C/O = 0.1, 0.2, 0.3.

VI.2.1.5 - Numerical Analysis: CO_2 and H_2O Effect

Sensitivity analyses and reaction path diagrams have been realized also for methane/oxygen systems diluted in carbon oxide and water.

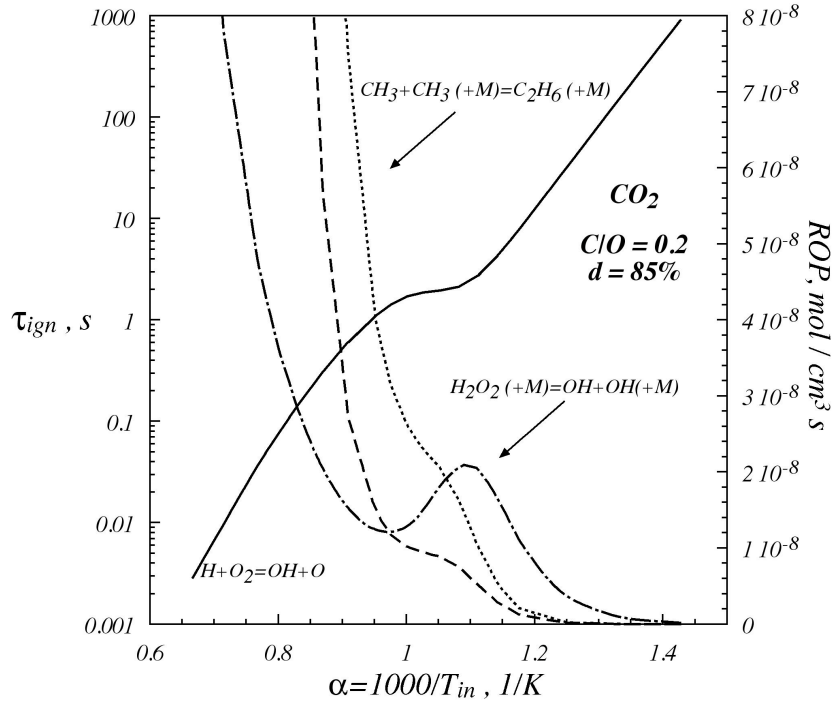

Fig. V.17 - Auto-ignition delay time and rate of production of specified reactions as a function of 1000/Tin for a mixture diluted in CO2 (85%).

Results fully confirm the role of reactions identified for the system diluted in nitrogen. In order to resume numerical outcomes and underline CO_2 and H_2O kinetic effects on the auto-ignition time, rate of production of the most influential reactions have been reported. Figs V.17 and V.18 reports the reaction rate of reactions 2, 4 and 12 for a system diluted respectively in CO_2 and H_2O at the auto-ignition time. For the system diluted in CO_2, at low temperatures the main branching reaction is the decomposition of hydrogen peroxide. At the beginning of the NTC region, it shows a relative maximum value, than the reaction rate diminishes. It reaches a relative minimum in correspondence of the end of the NTC, then it increases. The branching reaction 4 is relevant for high temperatures. The methyl recombination reaction becomes consistent just in occurrence of the NTC region, then, it increases increasing the temperature. Also in such a case, while the hydrogen peroxide decomposition reaction diminishes, reaction 4 and 12 show a slight change of the curve

slope. Same considerations apply for the water diluted system, even if in this case reaction 4 is negligible in the NTC region.

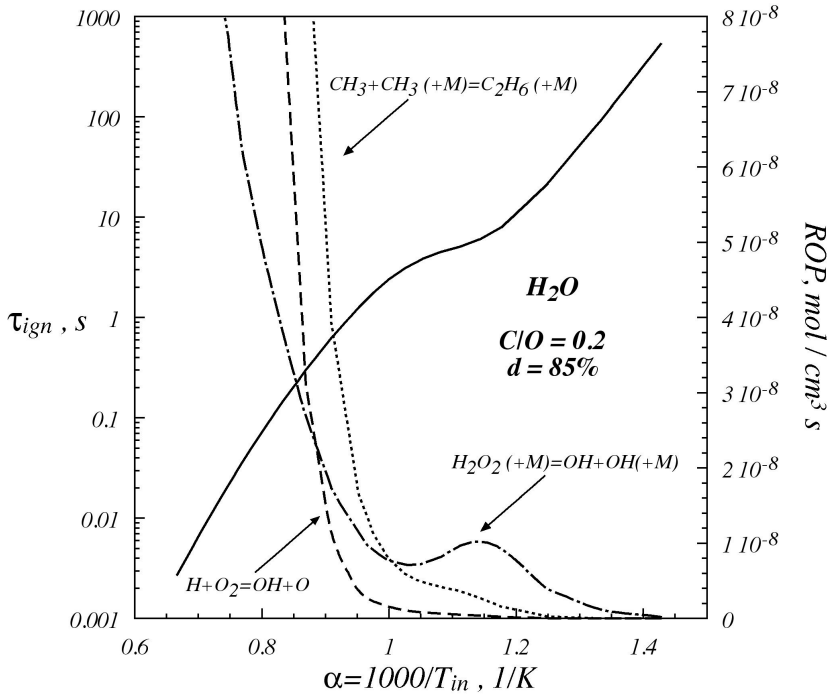

Fig. V.18 - Auto-ignition delay time and rate of production of specified reactions as a function of 1000/Tin for a mixture diluted in H2O (85%).

On the basis of literature suggestions, the role of CO_2:

(27) $$CO_2 + H \rightarrow CO + H$$

and H_2O:

(28) $$H_2O + O \rightarrow OH + OH$$

decomposition reaction have been investigated. In particular, further simulations have been realized modifying the c1-c3 mechanism by deleting such reactions from the detailed kinetic scheme. Results show that, in case of carbon dioxide diluted systems, CO_2 decomposition is active at high temperatures and leads to an increase of auto-ignition times, while auto-ignition times are not affected by H_2O decomposition in water diluted systems.

V.2.1.6 - Effect of pressure

Fig V.18 shows the auto-ignition delay times as a function of parameter α (=1000/ T_{in}) for a methane-oxygen system diluted in nitrogen up to 85 %. The mixture composition (C/O) has been fixed equal to 0.2 while six values of pressure (from 0.5 to 50 atm) are investigated.

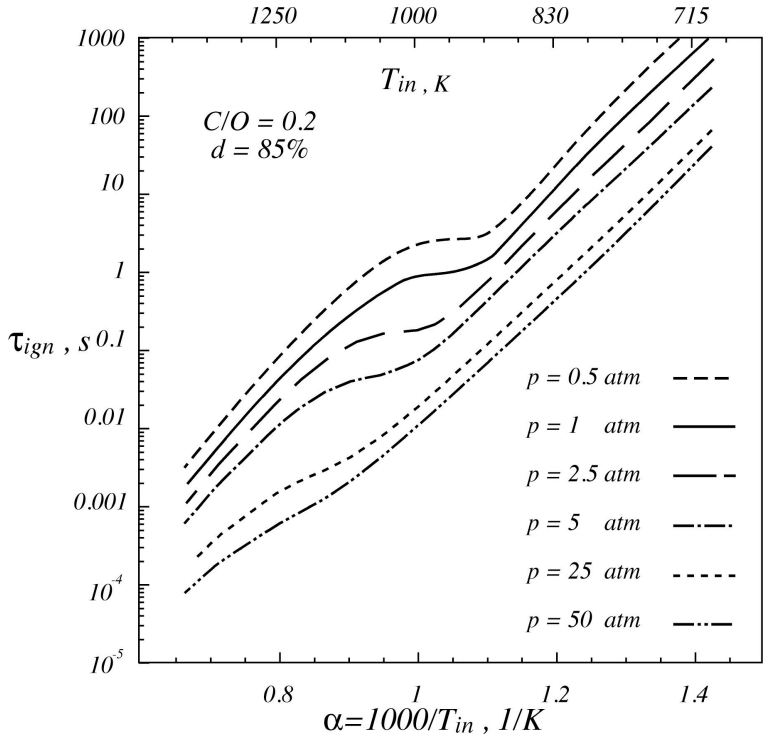

Fig. V.19 - Comparison among auto-ignition delay times at different pressure.

In general, the auto-ignition delay time decreases as the system pressure increases and it is less sensitive to pressure variation for high-pressure values. At sub-atmospheric pressure (0.5 atm), the trend is similar to atmospheric one, and the NTC behavior occurs in the same α range. Increasing the pressure up to 5 atm, temperature range of NTC behavior reduces and it shifts towards lower α values.

Such trend is confirmed for the last two curves obtained at 25 and 50 atm where only a smooth shoulder is present on the curves. Fig V.20 shows auto-ignition delay time versus

parameter α for several values of dilution degree while the pressure is fixed to 1 atm and the C/O feed ratio is 0.2. Solid-line represents auto-ignition delay times for a system diluted at 85 %, while dotted and dotted-dashed lines show respectively characteristic times for mixtures diluted up to 90 and 95% in nitrogen.

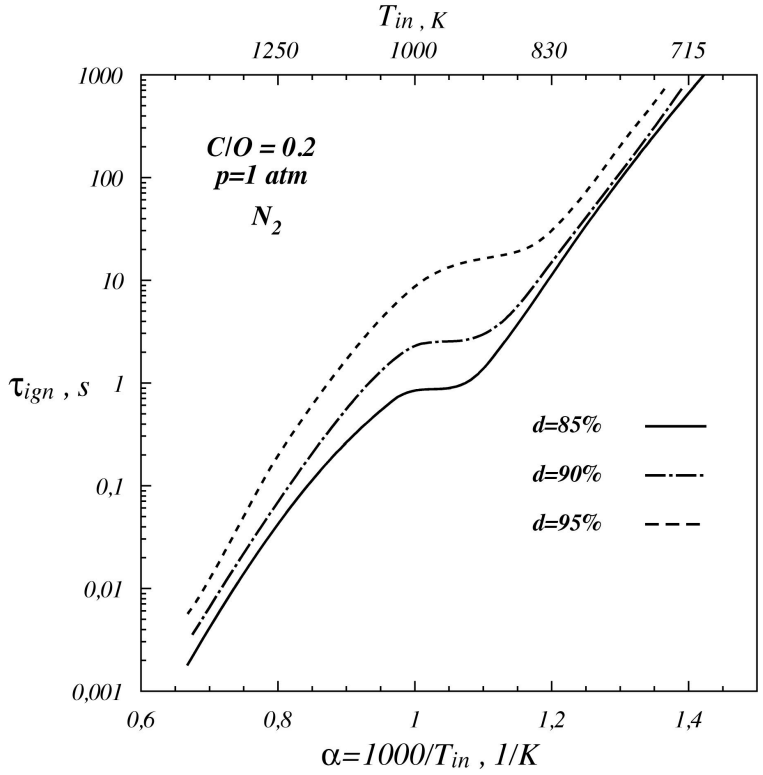

Fig. V.20 - Comparison among auto-ignition delay times for different dilution degree

General trend shows that auto-ignition time increases as mixture dilution degree increases. In instance, for α equal to 1 τ_{ign} is 0.831 sec while 2.2 sec and about 11 for the systems diluted respectively at 90 and 95%. Furthermore NTC behavior shifts towards α higher values and curve slope is almost similar in such range for all the considered mixtures.

It is worth noting that the effect of mixture dilution level variation on auto-ignition times is similar to the one relative to system pressure variations since modifying the mixture dilution degree means varying reactants partial pressure. In order to investigate kinetic pathways responsible of the NTC behavior path diagrams and sensitivity analyses were

performed previously at atmospheric pressure. Results allowed identifying methane oxidation main routes at different temperature. At low T_{in} methane is dehydrogenated to methyl radicals, then oxidized to CH_3O and CH_3O_2. They are dehydrogenated to formaldehyde. Later on, formyl radical and CO are produced. At intermediate temperatures, carbon main pathways are similar to the previous case but they have higher reaction rates. Two other main reactions pathways are identifiable at intermediate temperatures. Methyl radicals react to form ethane, while methyl peroxide radicals decompose to give rise to formaldehyde and OH radicals. For high temperatures, methyl radical recombination channel to ethane and methyl peroxide radical decomposition to CH_2O are significantly promoted. The most important reactions involved in the different sub-mechanisms active in methane oxidation can be summarized as follow.

For the H_2/O_2 system main reactions are:

(29) $$H + O_2 + M \rightarrow HO_2 + M$$

(30) $$HO_2 + HO_2 \rightarrow H_2O_2 + O_2$$

(31) $$H_2O_2 + M \rightarrow OH + OH + M$$

(32) $$H + O_2 \rightarrow HO + O$$

(33) $$O + H_2 \rightarrow HO + H$$

(34) $$HO + H_2 \rightarrow H_2O + H$$

Reactions 18, 19 and 20 represent the branching reactions at low temperature, those promote the formation and decomposition of H_2O_2 to OH radicals. At high temperature reaction 21, 22 and 23 are the set of chain branching reactions. They are initiated by reaction 21 .

In case of methane, the main reactions are:

(35) $CH_4 + H \rightarrow CH_3 + H_2$

(36) $CH_4 + HO_2 \rightarrow CH_3 + H_2O_2$

(37) $CH_4 + O_2 \rightarrow CH_3 + HO_2$

Methyl radicals, formed from methane dehydrogenation reactions, are involved in reactions:

(38) $CH_3 + HO_2 \rightarrow CH_3O + OH$

(39) $CH_3 + O_2 \rightleftarrows CH_3O + O$

(40) $CH_3 + CH_3O_2 \rightarrow CH_3O + CH_3O$

(41) $CH_3 + O_2 \rightarrow CH_3O_2$

(42) $CH_3 + CH_3 + M \rightarrow C_2H_6 + M$

while CH_3O and CH_3O_2 most relevant reactions are:

(43) $CH_3O + M \rightarrow CH_2O + H + M$

(44) $CH_3O_2 \rightarrow CH_2O + OH$

(45) $CH_3O_2 + CH_4 \rightarrow CH_3OOH + CH_3$

V.2.1.7 - Effect of pressure: Numerical Analysis

In order to fully understand the kinetic pathways involved in methane NTC behavior, on the basis of information collected from path diagram and sensitivity analyses indications, the rate of the most important reactions has been considered.

Fig VI.21 shows the net rate of production for methyl radicals recombination (reaction 32) and the sum of net rates of reactions that lead from methyl radicals to CH_3O and CH_3O_2

(reactions 27 to 31) versus the parameter α ($1000/T_{in}$) at atmospheric pressure. On the same diagram the auto-ignition times has been also reported.

For low inlet temperatures the sum of methyl oxidation reactions increases as T_{in} increases. As soon as the recombination reaction becomes important, the oxidation reactions net rates increase with a lower slope, showing a maximum value just in correspondence of the beginning of the NTC behavior temperature range and then it decreases Later on, just beyond the NTC temperature range, it increases again as soon as the inlet temperature is increased. The net rate of recombination reaction always increases.

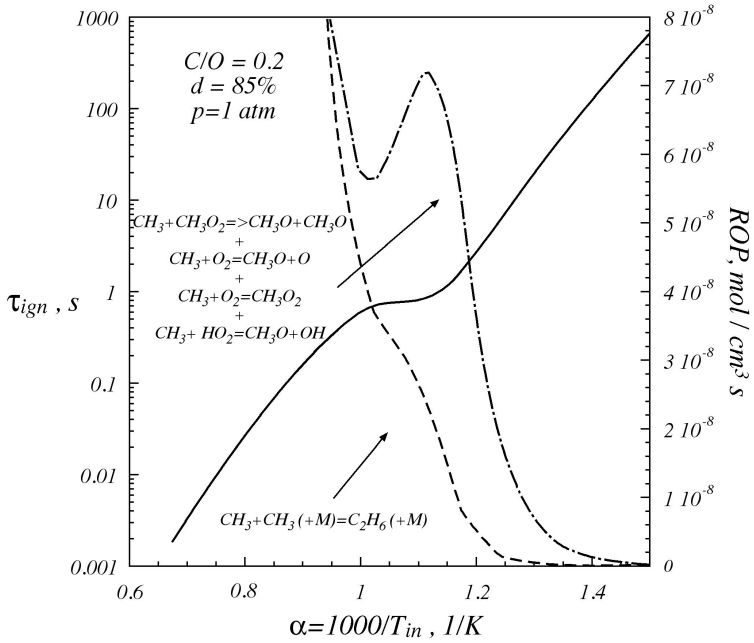

Fig. V.21 - Auto-ignition delay time and rate of production of specified reactions as a function of 1000/Tin at atmospheric pressure.

In order to identify the dominant branching reactions, relatively to the H_2/O_2 system, the rate of reaction 20 (hydrogen peroxide decomposition), reactions 18 and 21 have been reported in Fig V.22 as function of the parameter $1000/T_{in}$ along with the auto-ignition delay time for a mixture with a carbon/oxygen feed ratio equal to 0.2.

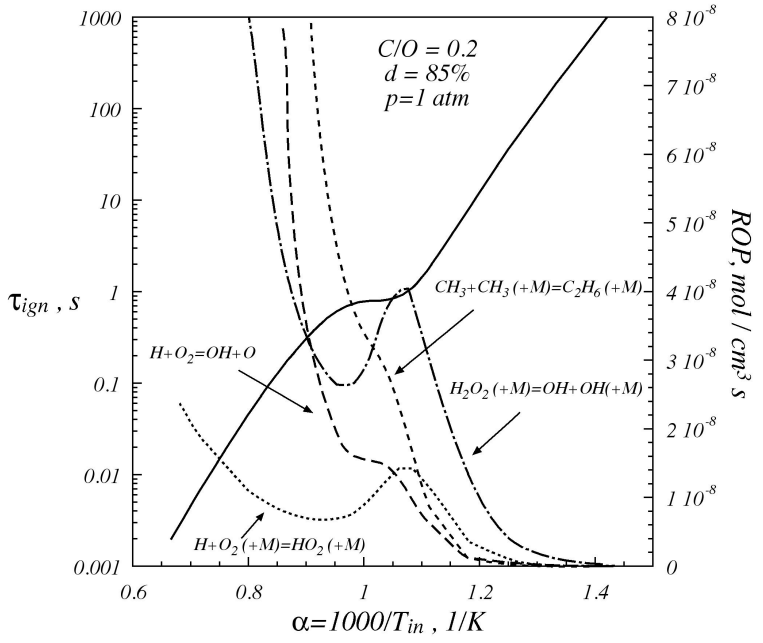

Fig. V.22 - Auto-ignition delay time and rate of production of specified reactions as a function of 1000/Tin at atmospheric pressure.

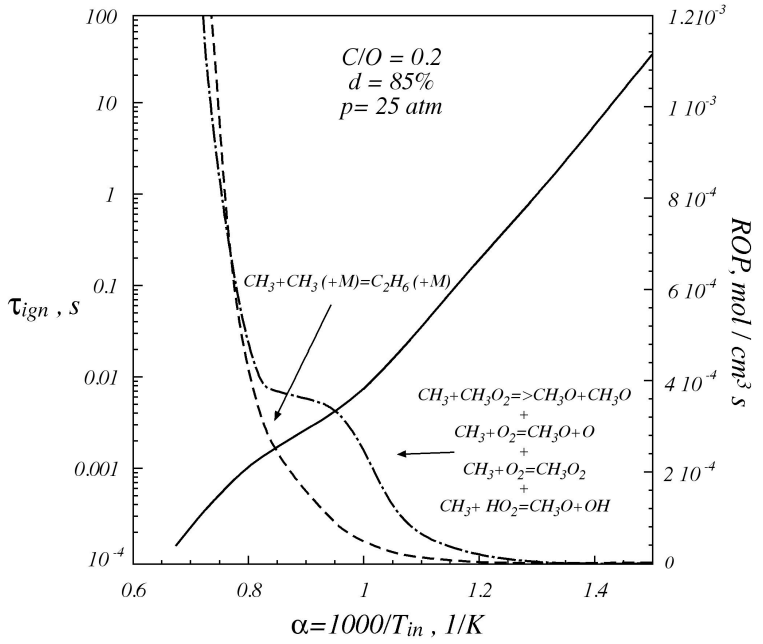

Fig. V.23 - Auto-ignition delay time and rate of production of specified reactions as a function of 1000/Tin.

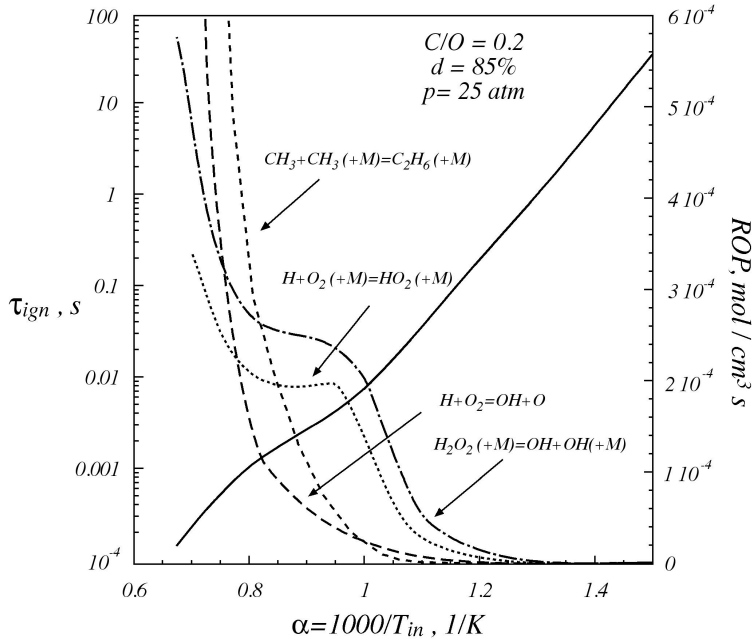

Fig. V.24 - Auto-ignition delay time and rate of production of specified reactions as a function of 1000/Tin.

In the same figure is reported also the methyl radical recombination reaction for a better understanding of kinetic reaction routes.

For low temperatures the main branching mechanism is the decomposition of H_2O_2, while in the NTC range, net rate of reaction 20 and 21 become almost equal, even if reaction 20 is still the fastest one. Reaction 20 shows a relative minimum just in correspondence of the end of the NTC behavior, then it increases abruptly whereas reaction 4 becomes the main branching reaction for higher temperature.

In the low and NTC regions mixture ignition is mainly supported by H_2O_2 decomposition. In the NTC region the recombination channel becomes active and removes CH_3 radicals from the oxidation route, as showed by the trend of sum of CH_3 net rates towards oxygenated compounds reported in Fig V.21, thus reducing system reactivity and relaxing auto-ignition delay times. At high temperature, reaction 21 becomes the main branching reaction, leading to higher system reactivity, thus decreases the auto-ignition delay times and causes the end of the NTC region.

The same analyses were performed for higher pressures. Fig V.23 reports the net rate of production for methyl radicals recombination route (reaction 31) and the sum of net rates of reactions that lead from methyl radicals to CH_3O and CH_3O_2 along with the auto-ignition times versus the parameter 1000/Tin for the mixture $CH_4/O_2/N_2$ diluted up to 85 %, with a C/O of 0.2 and 25 atm.

For low and high inlet temperatures the sum of methyl oxidation reaction rate increases as temperature increases. In the intermediate region the oxidation reactions net rates show a plateau-similar behavior. The net rate of recombination reaction monotonically increases in the whole temperature range considered. For $\alpha > 0.8$ the sum of methyl oxidation reaction rates is higher with respect to reaction 14, while for $\alpha < 0.8$ it results lower.

In the NTC region, the recombination channel acts similarly to the low-pressure case earlier discussed.

Fig V.24 shows the rate of reactions 18, 20, 21 and 31 for the system at 25 atm along with the auto-ignition delay times as function of the parameter α.

At low and intermediate temperatures the main branching reaction is the decomposition of hydrogen peroxide. It increases with temperature in all the temperature range considered but for the interval $0.8 < \alpha < 0.95$ the curve shows a plateau-similar behavior.

The branching reaction 4 is relevant only for high temperatures and overcomes the decomposition of H_2O_2 for a value of α greater than 0.75.

Net rate of methyl recombination reaction becomes consistent in intermediate temperature region. In particular it becomes equal to net rate of reaction 20 for $\alpha = 0.8$, corresponding to the end of NTC region, then it becomes lower.

The net rates of key reactions are significantly higher at elevated pressure; suggesting higher system reactivity, thus lower ignition delay times.

It is worth noting that the decomposition of hydrogen peroxide is the dominant branching reaction in a wider Tin range with respect to the atmospheric pressure system, taking effect from low to intermediate inlet temperatures.

Pressure significantly enhances the relative main pathways importance, in particular accelerates third-body reactions, namely reaction 18, 20 and 31.

The increase of reaction 1 induced by higher pressure leads to an enhancement of reaction 19 rates, promoting a faster formation of hydrogen peroxide. The third body reaction 20 is accelerated by pressure and by higher H_2O_2 concentration, leading to higher OH radical production by means of reaction 20.

At the same time, as soon as the pressure is increased, reaction 18 is advantaged with respect to reaction 21, so that the H_2/O_2 high temperature branching reactions become relevant for higher inlet temperatures with respect to low-pressure systems.

The increase of hydrogen peroxide decomposition rate implies lower auto-ignition delay time with respect to low-pressure cases and makes the system less sensitive to carbon and hydrogen storage in C_2 compounds induced by methyl radical recombination. Therefore the NTC behavior is less evident as soon as the system pressure is increased.

Furthermore the promotion of HO_2 radical formation by means of reaction 18, to the detriment of OH formation by reaction 21, inhibits the role of high temperature branching reaction mechanism in the intermediate temperature range causing the shift of the end of such phenomenology towards higher inlet temperature, where reaction 21 overcomes reaction 18.

V.2.2 - Biogas

A numerical study was also performed for biogas mixture. The prediction of the auto-ignition delay time (τ_{ign}) obtained with all the considered kinetic mechanisms have not been reported but Figs V.25-31 show time collected by means of Ranzi mechanism. The numerical simulations were carried out in a range of temperature between 800 K and 1450 K and for different oxygen ratios. Figs V.25-26 show auto-ignition times obtained for a mixture of biogas diluted in nitrogen at 90%. The range of feed ratios investigated allows to evaluate the characteristic time for lean, rich and stoichiometric composition. In particular, Fig V.25 shows times evaluated for three oxygen ratios in fuel lean conditions. Dotted-dashed line presents data for $\Omega = 10$ while continuous and dotted ones for $\Omega = 1.67$ and $\Omega = 5$ respectively.

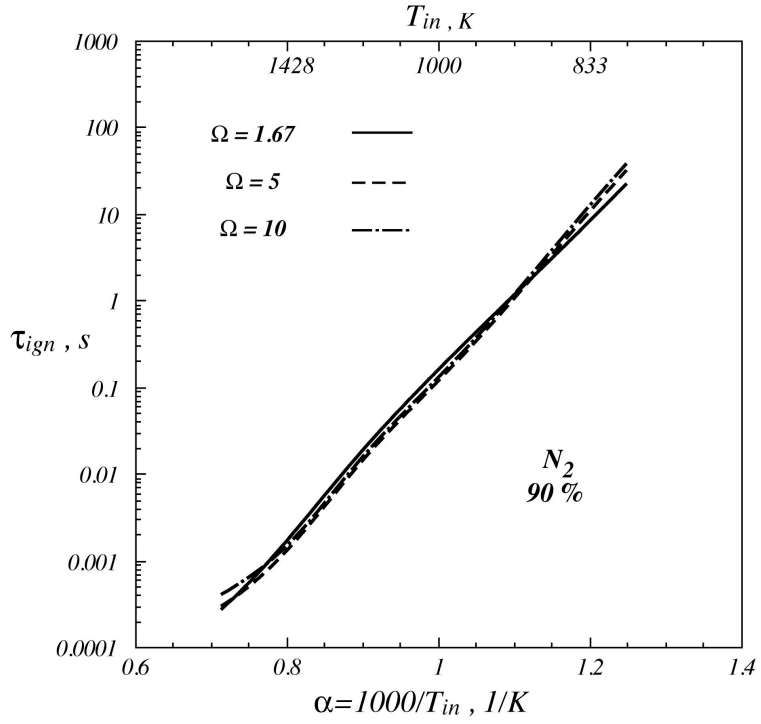

Fig. V.25 - Auto-ignition delay time computed for three Ω *ratios in fuel lean conditions.*

Results show that biogas auto-ignition times diminish with increasing temperature with a linear trend. In addition, τ_{ign} evaluated are little dependent on mixture composition for lean condition. As a matter of fact, all the times collected are almost coincident with slight differences in the whole range of temperatures investigated.

Afterwards, the numerical tests were extended for lower oxygen ratios both in stoichiometric and rich fuel conditions keeping constant chemical nature of diluent and its quantity in the mixture. Data collected are presented in Fig V.26 along with curve obtained for $\Omega = 10$. Continuous line shows auto-ignition times evaluated for rich feeding condition ($\Omega = 0.7$) while dotted curve presents data obtained for a stoichiometric condition ($\Omega = 1$). Although the linear trend of the curves shows for lean condition is still evident, the times collected are quite different. In particular, the differences are grater for high initial temperatures while then decrease until they disappear in correspondence of $T_{in} \cong 900K$.

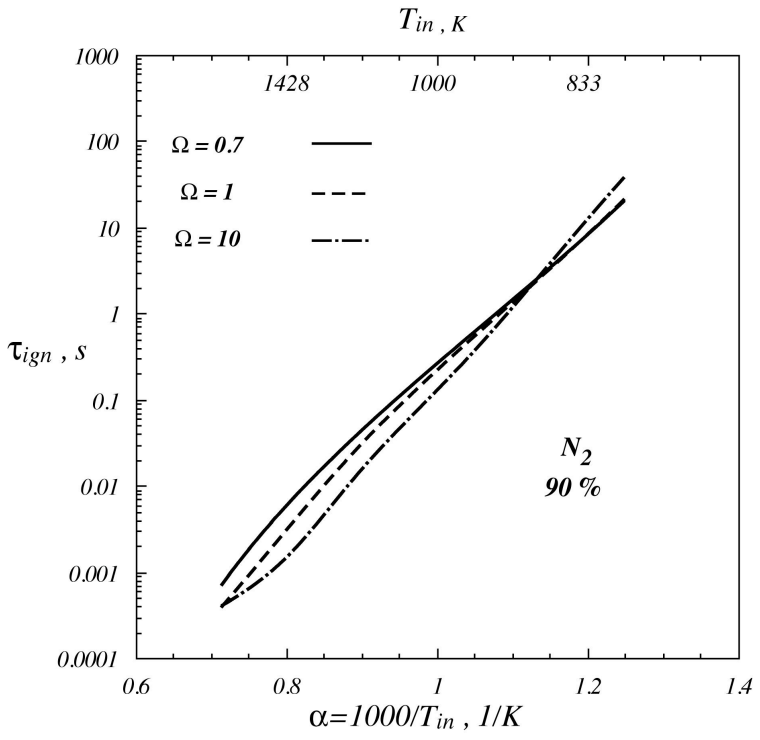

Fig. V.26 - Auto-ignition delay time computed for three Ω ratios; lean, rich and stoichiometric conditions for a dilution degree equal to 90% in nitrogen.

As a matter of fact, for an initial temperature of 1282 K the times computed are equal to $0.004\,\text{sec}$ for $\Omega = 0.7$, $0.002\,\text{sec}$ for stoichiometric condition and diminish to $0.001\,\text{sec}$ for $\Omega = 10$. For $T_{in} \cong 900K$ the auto-ignition times are coincident with slight difference that can not be appreciate from the figure ($\tau_{\text{ign}} \cong 1.781$). For initial temperatures lower than 900 K the curves show an inversion. with higher times collected for lean condition. The dotted and continuous lines are coincident and are not discernible. In particular, for $\alpha = 1.245$ the lean mixture ignites after $37.2\,\text{sec}$ while $\tau_{\text{ign}} \cong 20.7\,\text{sec}$ for stoichiometric and rich conditions.

The composition of the mixture is an important parameter in combustion system that evolves in MILD conditions. As it is described for methane, numerical tests were carried out by using different diluent species.

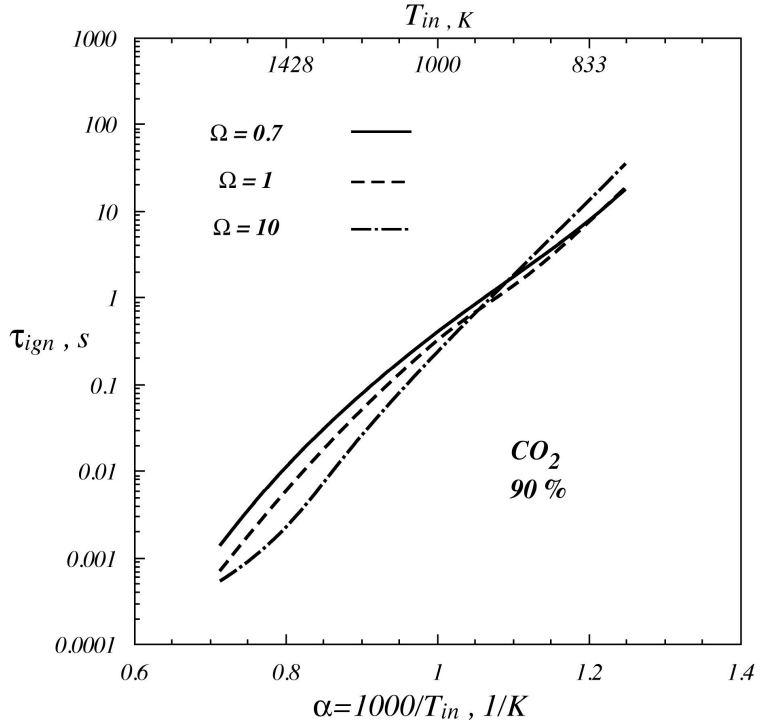

Fig. V.27 - Auto-ignition delay time computed for three Ω ratios; lean, rich and stoichiometric conditions for a dilution degree equal to 90% in CO_2.

Figs V.27-28 show the auto-ignition times computed for a mixture diluted in CO_2 and H_2O respectively in the same region of temperatures investigated for methane.

In particular, the curves show in Fig V.27 are representative of a mixture diluted in CO_2 for three oxygen ratios. The continuous line shows the τ_{ign} obtained for a fuel rich mixture ($\Omega = 0.7$) while dotted and dotted-dashed curves represent the trend of auto-ignition times for $\Omega = 1$ and $\Omega = 10$.

For high temperature, fuel lean mixtures show times lower than stoichiometric and rich ones. As a matter of facts for an initial temperature of 1383 K the τ_{ign} is equal to $0.002\,\text{sec}$ ($\Omega = 0.7$), $0.001\,\text{sec}$ ($\Omega = 1$) and $6.4 \cdot 10^{-4}\,\text{sec}$ ($\Omega = 10$). This behavior is evident also for lower temperatures although the differences diminish. For $T_{in} = 910K$ such discrepancy are almost disappeared with higher times computed for stoichiometric mixture. Lean and rich mixtures show almost similar auto-ignition times ($\tau_{ign} \cong 1.707\,\text{sec}$) while the dotted curve is located below the other two curves. For lower temperatures there is still an inversion as it is shown for nitrogen dilution. The fuel lean mixture ignites hardly then the stoichiometric and rich ones. In fact, for $\Omega = 10$ $\tau_{ign} \cong 31.6\,\text{sec}$ in correspondence of $T_{in} = 805K$ while is equal to 17.8 sec for $\Omega = 0.7$ and $\Omega = 1$.

Fig V.28 shows auto-ignition times computed for mixtures diluted in H_2O. The same comparison was made among three different oxygen ratios as described above for N_2 and CO_2. The trend is different from the previous cases and a singular behavior was observed.

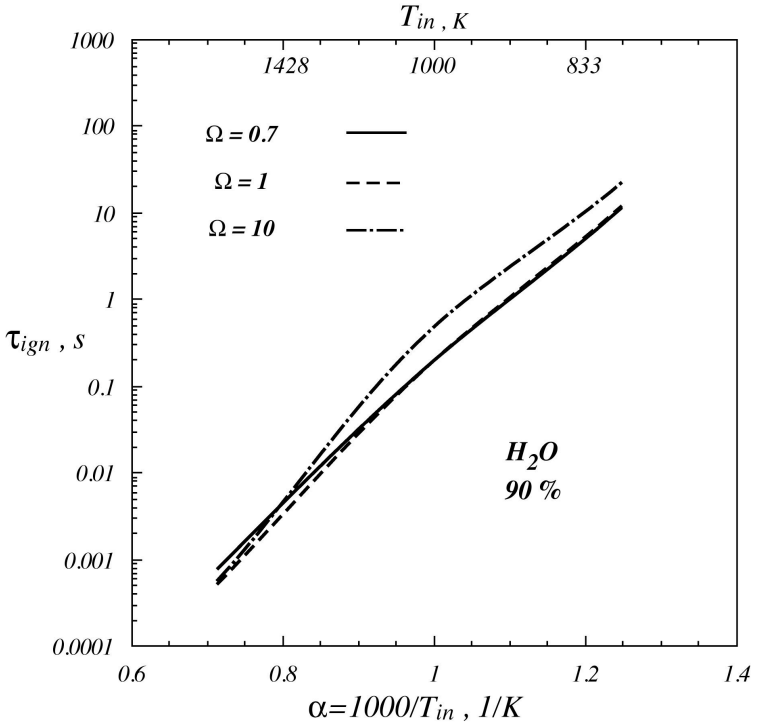

Fig. V.28 - Auto-ignition delay time computed for three Ω ratios; lean, rich and stoichiometric conditions for a dilution degree equal to 90% in H_2O.

The dotted-dashed curve that represents the times collected for a mixture fuel lean is above the other two curves for almost the entire range of temperatures investigated. For low temperatures the discrepancy is quite evident. For instance for $\alpha = 1.23$ ($T_{in} = 813K$) the fuel lean mixture ignites in correspondence of $\tau_{ign} \cong 15.7\,\text{sec}$ while the times collected for stoichiometric and rich mixtures are equal to about 9.2 sec and 8.14 sec respectively. These differences decrease for higher T_{in} and the curves become almost coincident

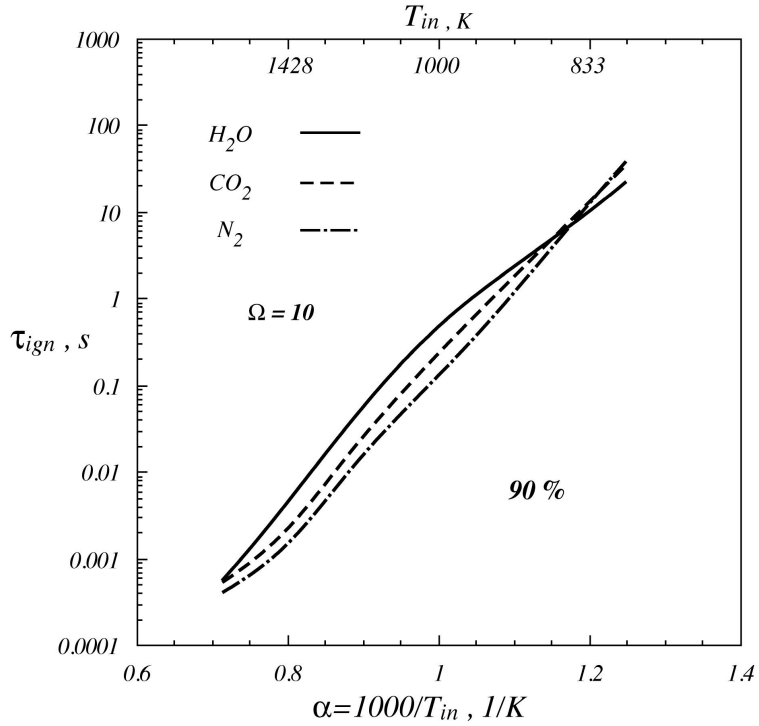

Fig. V.29 - Auto-ignition delay time computed for three Ω ratios; lean, rich and stoichiometric conditions for a dilution degree equal to 90% in H_2O.

In order to evaluate the time differences among different diluent species used, the Figs V. 29-31 show the trend of τ_{ign} in function of the initial temperature for three oxygen ratio, keeping constant the amount of diluent (90%).

The Fig V.29 shows three curves obtained for a fuel lean mixture. The continuous curve shows the trend of τ_{ign} for a dilution in H_2O while CO_2 and N_2 were used for plotting the dotted and dotted-dashed curves. Auto-ignition times computed by means of Chemkin software show a linear trend for all the diluent species used. In particular, only the continuous curve shows a little curve slope change for low temperatures. Times evaluated by using H_2O are higher in a range of temperatures comprise between 880 K and 1396 K. As a matter of facts, for an initial temperature equal to 1310 K τ_{ign} are respectively $0.002\,\text{sec}$ for H_2O, $0.001\,\text{sec}$ for CO_2 and $7.8 \cdot 10^{-4}\,\text{sec}$ for nitrogen.

Afterwards, for lower temperatures there is an inversion, τ_{ign} obtained by using CO_2 and N_2 become higher than ones obtained with H_2O. In addition, in this range of temperatures the dotted and dotted-dashed curves are comparable.

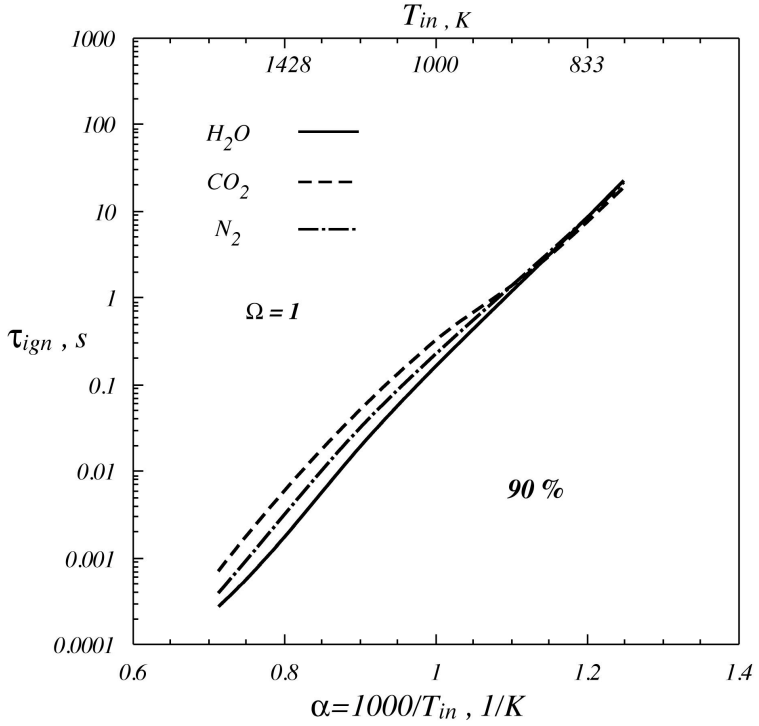

Fig. V.30 - Auto-ignition delay time computed for three Ω ratios; lean, rich and stoichiometric conditions for a dilution degree equal to 90% in H_2O.

A similar comparison was also made for a stoichiometric and rich mixtures. In Fig V.30 are shown three curves relating to $\Omega = 1$ for the different diluent species. Results show a different behavior by comparing the trend of the curves. For low temperatures the times computed are comparable and the curves are almost coincident (from 833 K up to 890 K). In correspondence of Tin=890 K, it is possible to distinguish different times for different dilution. In particular, the fuel mixture diluted in CO_2 ignites more easily and, the more high are the initial temperatures, the greater are differences among times computed.

For instance, for Tin=957 K the times collected are 0.636 sec , 0.518 sec and 0.388 sec relating to a dilution in CO_2, N2 and H_2O respectively. As it is described above, the

discrepancy among different curves are greater for higher temperatures. For $\alpha = 0.755$, auto-ignition times are equal to $0.002\,\text{sec}$ (CO_2), $0.001\,\text{sec}$ (N_2) and $6.629 \cdot 10^{-4}\,\text{sec}$ (H_2O).

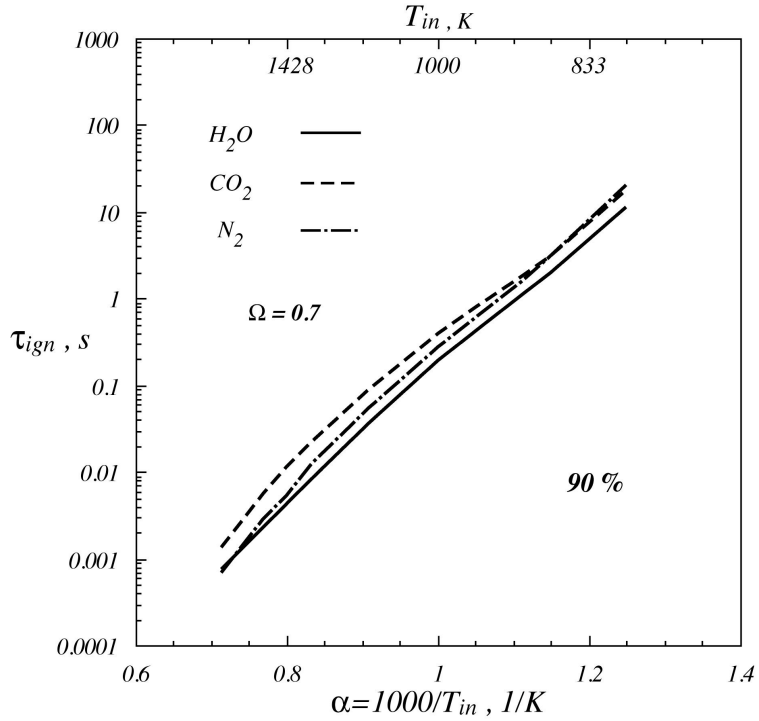

Fig. V.31 - Auto-ignition delay time computed for $\Omega = 0.7$ for a mixture diluted at 90% with three different diluent chemical species.

For fuel rich mixtures the same comparison was made, and results were reported in Fig V. 31. Arrhenius diagram show a linear trend for the auto-ignition times in function of the initial temperatures investigated.

The mixture diluted in CO2 shows higher τ_{ign} in the whole range of temperatures. Only in a small range of temperatures, from 833 K up to 874 K, the times are comparable with ones obtained with a dilution in nitrogen ($\tau_{ign} \cong 3\,\text{sec}$).Afterwards, for higher temperatures, the curves are distinct and it is possible to distinguish different times for different diluent

species. In particular for Tin=1240 K $\tau_{ign} = 0.014\,\text{sec}$ for a dilution in CO_2 whereas $\tau_{ign} = 0.006\,\text{sec}$, $\tau_{ign} = 0.005\,\text{sec}$ for N_2 and H_2O.

Chapter VI - Discussion

In this chapter the main experimental and numerical results obtained during this thesis are summarized and discussed. The experimental work, as well as the numerical simulations, were carried out with the aim to characterize the oxidation process of several fuels under typical conditions of MILD combustion.

Although in literature there are many works on this new combustion "mode", there is still the necessity to characterize the process by means of basic studies. The lack of fundamental investigations depends on the difficulty to realize a laboratory scale plants able to work with the extreme high inlet temperatures typical of MILD Condition. These extreme conditions imply a difficult choice of materials and problems of sealing of the reactor. These problems can be more easily overcome in pilot or industrial plant.

As matter of fact, the amount of data available in literature are relative to industrial or pilot scale furnaces. Such studies concerns the feasibility to run MILD combustion processes and they are devoted to the characterization of pollutant formations, furnaces performance and chemical-physical features of the process. The complex fluid-dynamic field, induced by the strong recirculation of exhausted gases, coupled with the kinetic evolution of the oxidation process make very difficult to characterize the process in terms of basic features.

Furthermore, in systems exercised in MILD operative conditions, the strong interaction between recirculated gases and fresh reactants induces longer kinetic characteristic times (due also to the mixture dilution level) and lower mixing times with respect to conventional combustion systems. Therefore the usual fluid-dynamic/chemistry models implemented to predict the evolution of the oxidation process in traditional systems are not suitable when MILD combustion systems have to be studied.

Basic studies are usually carried out on model reactors typical of chemical engineering. The strength of this approach is the opportunity to highlight particular features of combustion process using different elementary configurations.

In fact, the combustion process is characterized by very short characteristic time, i.e. for instance reaction time, and by the interaction between fluid-dynamic and chemistry. Model reactions allow simplifying the study of oxidation reactions since they permit to emphasize particular aspects of the process. Furthermore their complementary allow for a global and structured characterization of combustion process. These features justify their wide spread use in the scientific research field.

Moreover the behavior of model reactors has been widely modeled since the equations, such as mass or energy conservation, necessary to describe such systems, in ideal onditions, are function of a unique parameter, such as time or a spatial coordinate. In fact in literature they are also known as zero- or one-dimensional reactors. This aspect has promoted the development of numerous numerical codes able to simulate the behavior of ideal reactors and the development of a modeling activity of the oxidation process.

Hence they allow for a good comprehension of physical and chemical phenomenology and at the same time for a validation and tuning of predictive models supported by experimental data obtained in specific operative conditions.

The demand of experimental data is also stressed by the necessity to develop detailed kinetic mechanisms properly tuned in non conventional conditions. As matter of fact, they have been validated on the basis of experimental data obtained in several simple facilities excised in traditional conditions. Therefore, their trustability and robustness is questionable when they are used to predict the behavior of simple reactors exercised in MILD conditions.

This step is crucial also for the development of reliable reduced and/or global kinetic mechanisms to implement in CFD calculations.

In this thesis, the reactor used for the study of the evolution of the oxidation process is a Tubular Flow Reactor. Such configuration was properly chosen because it allows for studying the evolution of the combustion process as function of just one coordinate (axial coordinate of the reactor or time). So that, implementing the proper diagnostic techniques, it would be possible to resolve in time and/or space the oxidation process and obtain useful information on the effect of high dilution levels and high pre-heating on fuel oxidation.
The attention was focused on kinetic auto-ignition delay times of the oxidation process under MILD typical operative conditions for several fuels (hydrocarbons and bio-gas) and several mixtures dilution levels at atmospheric pressure. The auto-ignition time is a key parameter for the designing and dimensioning of lab-scale, pilot and industrial facilities.
It is worth noting that in the scientific literature ignition delay times are relative to pressurized systems (turbines), while at atmospheric pressure (furnaces) no data are available.

VI.1 - Velocity Analysis

The experimental tests were performed by varying some characteristic parameters to characterize the oxidation of different fuel blends in working conditions typical of MILD combustion processes. As described in a previous chapter, due to the experimental facility on purpose designed and set up, the working parameters can be varied independently from each other thus allowing to explore the effect of the single parameter on the whole process.

Several experimental tests were performed in order to investigate the effects of such variations on the system reactivity. The experimental data collected were presented in the chapter V and are described in detail in the following paragraphs.

Firstly, it was necessary a preliminary study on the performance of the experimental facility in order to characterize the fluid-dynamic and physical aspects related.

The experimental tests were focused on the study of the ignition process of the mixture fed to the reactor. Temperature profiles were acquired along the axis of the reactor by means of several thermocouples placed 2 mm from the inner wall. The auto-ignition times of the mixtures were evaluated on the base of a criterion on the increment of temperature. A detailed description of the experimental facility is reported in chapter IV and auto-ignition times is defined as the time needed by the system to increase its temperature of ten degrees with respect to the inlet one.

On the one hand, the quantification of the temperature in such condition could be affected by some inaccuracy due to axial and radial heat and mass dispersion. On the other hand, the velocity value used to calculate ignition time is necessarily dependent on the fluid-dynamic regime of the flow.

On the basis of these considerations, the velocity of the main flow gases is an important parameter in order to evaluate ignition time. The flow speed at 2 mm from the inner wall of the reactor was computed by means of Fluent software. Numerical simulations were reported and described in detail in the chapter IV. Results show that the velocity profile along the diameter of the reactor is less dependent from the initial speed fixed. In particular, the velocity computed at 2 mm from the reactor wall is practically equal to the initial speed, regardless of the value of T_{in} , which is of fundamental importance for the evaluation of the main characteristic times both chemical and physical. Moreover the simulation shows that the boundary layer affected by the presence of the wall and that

might be affected by catalytic effects is about 1 mm. For this reason, thermocouples placed at 2 mm are outside this layer.

A key parameter for the characterization of the flow is the Reynolds number, which represents the ratio between the forces of inertia and the viscous. Such dimensionless number depends on the velocity and temperature (through the density ρ, viscosity μ).

Data obtained and described in detail above show that Re number for the velocity investigated varies between 3540 and 2150 with little variation on the fluid dynamic regime of the flow. Higher velocity values were preferred in order to avoid the problem inherent the boundary layers at the wall of the reactor. On the other hand, velocity too high means low residence time of the flow in the reactor and high resolution time. Combustion process that evolves in MILD conditions are characterized by higher characteristic time of the oxidation process with respect to traditional ones. The large amount of diluent slows down the kinetics related to the ignition of the process and hence the entire combustion process. The choice of the main flow speed is hence an essential point in order to a feasible study of the MILD oxidation process in such a reactor.

In addition, the evaluation of the axial and radial dispersion was also described in detail in chapter IV. The results show that for a velocity equal to 30 m/s the dispersion time are negligible with respect to the convective one.

As a consequence, the optimal versatility of the facility has enabled to perform a preliminary study in order to evaluate the validity and reproducibility of the experimental data collected. Moreover, it has been possible to test the validity of the results obtained, by changing the speed of the main flow at the entrance of the reactor. It is obvious that the auto-ignition times are necessarily less dependent from the inner velocity of the flow.

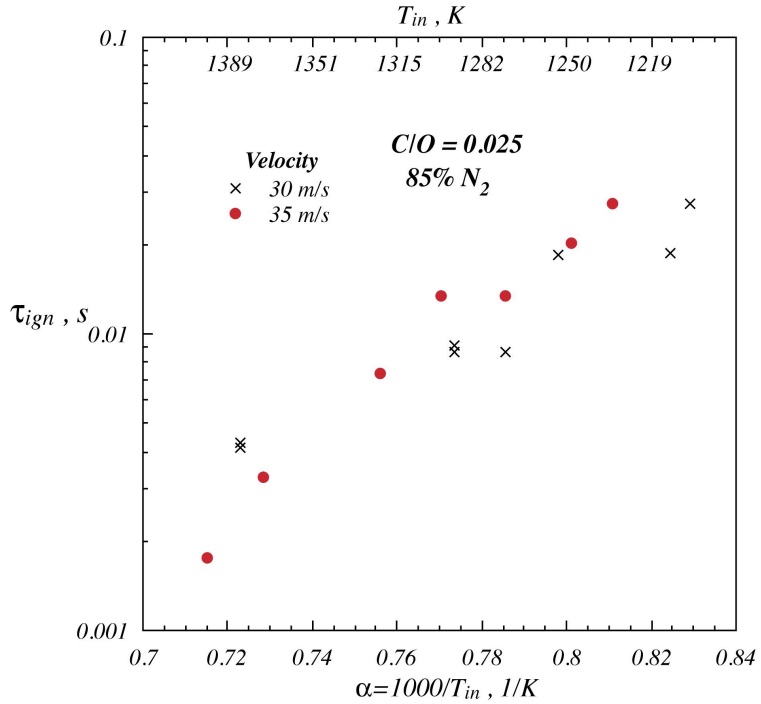

Fig. VI.1 - Auto-ignition delay times evaluated for two different main flow velocity (red circles for 35 m/s, points x-shaped for 30 m/s).

Firstly, tests were carried out by using mixtures of methane/oxygen highly preheated and diluted in nitrogen. In Fig VI.1, were shown the auto-ignition times evaluated in function of the parameter $\alpha = 1000 / T_{in}$. Times were collected for $C / O = 0.025$ in a range of temperature from 1190 K up to about 1430 K and a dilution set to 85 % in nitrogen. Red circles and points x-shaped are the experimental data collected for two main flow velocity equal to 35 m/s and 30 m/s.

Results show that the ignition times evaluated do not change significantly by varying the velocity in the whole range of temperatures.

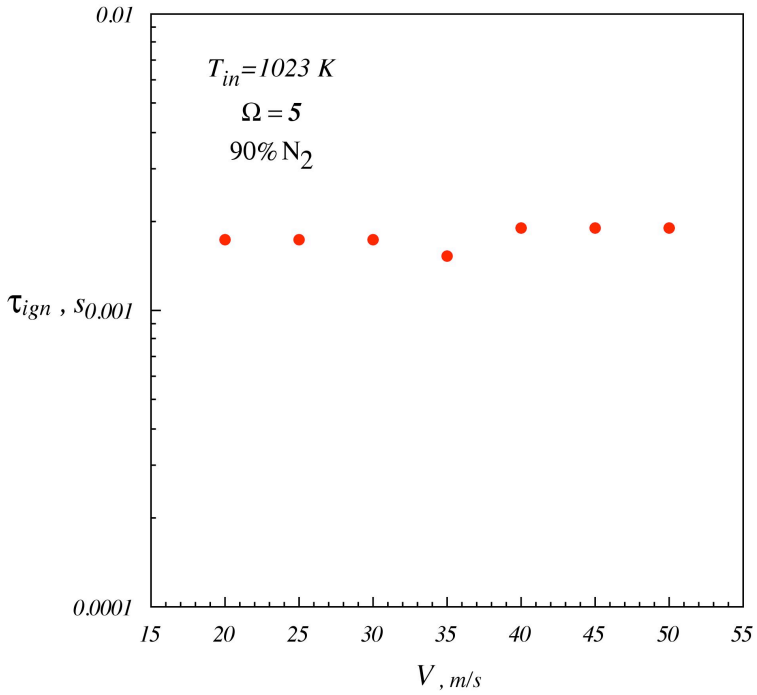

Fig. VI.2 - Auto-ignition delay times evaluated for different main flow velocity.

Afterwards, such investigation was repeated also for biogas and the flow velocities range was enlarged. Fig VI.2 shows data collected by varying the speed of the flow from 20 m/s up to 50 m/s. The dilution degree was set equal to 90 % in nitrogen for an initial temperature of 1023 K and $\Omega = 5$. Each points represent the times evaluated for a specific velocity and show little discrepancy between each measure. As a consequence, the validity and reliability of the information collected by means of tubular flow reactor were confirmed with good accuracy. Finally, the choice of the main flow velocity could be made on the basis of the optimal correspondence between the resolution and residence time. In the following, experimental results were presented for a main flow velocity equal to 30 m/s with $\tau_{res} \cong 0.05$ and a resolution time $\tau_{resolution} \cong 0.00167$.

VI.2 - Methane

VI.2.1 - Dilution Parameter

In combustion processes that evolve in MILD working conditions, it is necessary a deepen study on the effects of dilution (both in terms of chemical nature of diluent and degree of dilution) on the oxidation process.

Several experimental tests were made in order to investigate the importance of such parameter on the reactivity of the mixture. Experimental results were presented in detail in the chapter V, using two fuel blends diluted in nitrogen and by varying dilution degree from 85 % up to 95 %.

On the basis of the temperature profiles acquired, reactivity maps of the system were traced in each working condition.

In Fig VI.1, the reactivity map obtained for a dilution degree of 90 % is presented. It is possible to distinguish five regions showing the occurrence of different phenomenologies. For each values of T_{in} and feed ration C/O investigated it is possible to highlight the different behaviors. Such profiles, were shown in detail in the chapter V relating to experimental results.

Each area was represented by a different color and it is related to different observed phenomenologies. For low temperatures (from 1150 K to about 1260 K) mixtures do not ignite in the whole C/O range investigated. The area is reported in blue (*no-ignition zone*).

For temperature higher than 1260 K the system shows different phenomenologies.

For T_{in} comprised between 1250 K and 1350K and for C/O feed ratios lower than 0.6, the *low reactive* region is reported in a gradient blue/red zone. For such inlet operative conditions, the temperature increase is lower than 10 K. Even though auto-ignition delay

times in these conditions cannot be evaluated, because of the criterion used for the auto-ignition time evaluation, it is significant to highlight that a chemical activity is present. Such area diminishes in the CO coordinate range as soon as T_{in} is increased.

For $C/O > C/O_{stoich}$ and for temperature values between 1350 K and 1400 K, the map shows a large grey zone denoted as *pyrolysis zone*. For higher values of C/O, the pyrolysis area expands to lower temperatures. In particular, for a value of C/O equal to 1, the temperature range in which pyrolysis phenomena occur widens covering a temperature range from 1260 K up to 1400 K.

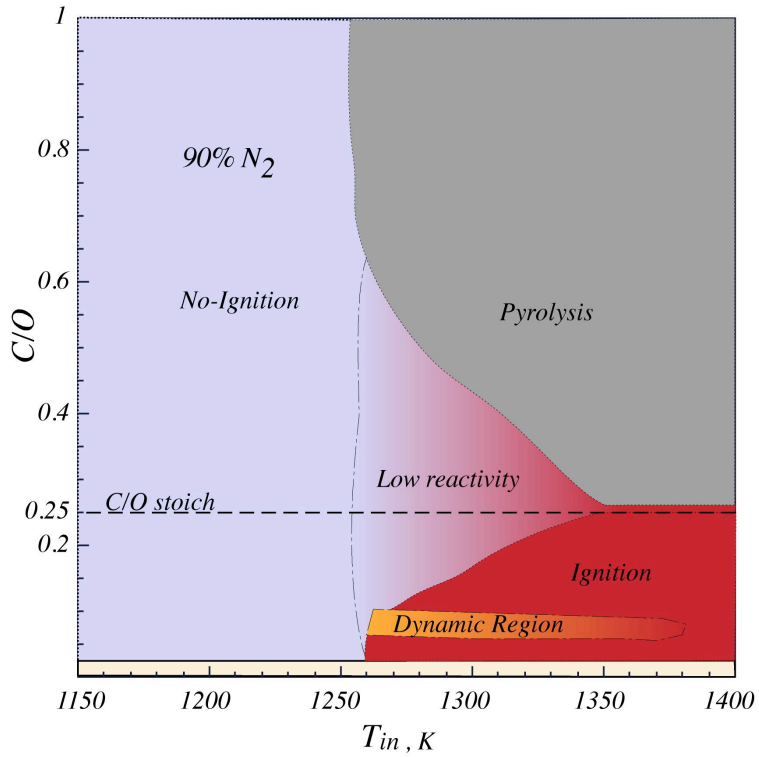

Fig VI.1 - Reactivity map of methane/oxygen mixture diluted at 90%, in function of the initial temperature.

The red region in the lower right part of the map of Fig. VI.1 is denoted as *ignition zone*. The typical temperature profiles related to this zone shows a significant increment of temperature. The zone extends from 1260 K up to 1400 K and for values of feed ratio C/O up to the stoichiometric condition. In this area it was possible to estimate the ignition

delay time of the mixture, as presented in chapter V. A small orange zone is located within the *ignition zone*. It corresponds to C/O and T_{in} values where a non stable behavior was observed. These phenomena is shown in the reactivity map with the name of *dynamic region*.

The same phenomenologies were observed by increasing the dilution of the system. In Fig VI.2 is shown the reactivity map obtained for a system diluted at 95 %.

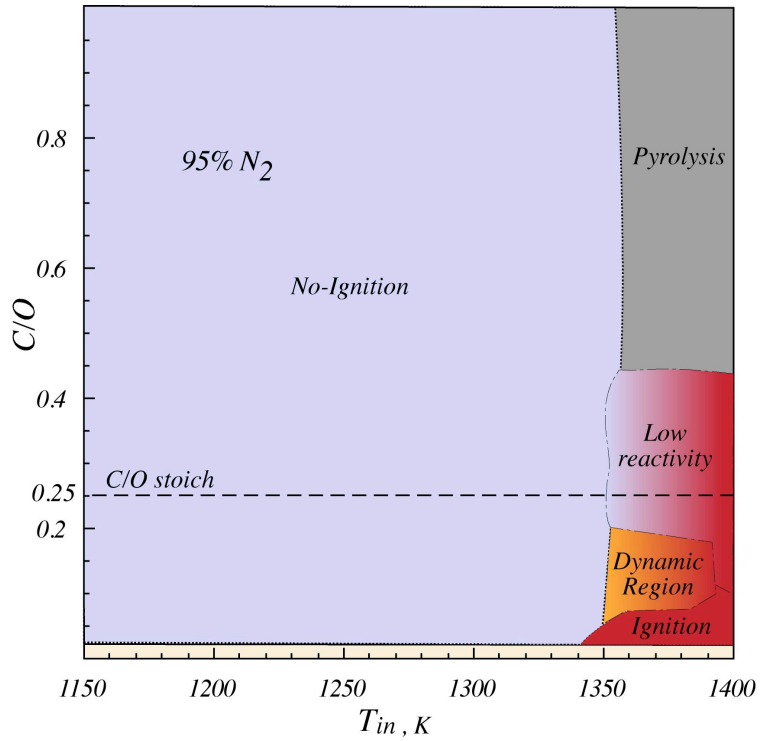

Fig VI.2 - Reactivity map of methane/oxygen mixture diluted at 95%, in function of the initial temperature.

A detailed description of the map was presented in the chapter V relating to experimental results. With the aim to compare the maps, in Fig. VI.3 an overlapping between two previous figures are presented. The layout of Fig. VI.3 was changed with respect of Figs VI.1 and VI.2 in order to allow an easy comparison between maps. The gray color represents the regions for a dilution equal to 95%, while the white areas are relative to the lower dilution level. As it is shown in the figure, a higher dilution level implies a lower

system overall reactivity. As matter of fact, all the phenomenologies are identifiable for T_{in} > 1350 K when the mixture dilution level is 95%, whereas from 1260 K up to 1400 K for a dilution degree of 90 %.

In particular, for a mixture dilution level equal to 95%, the ignition area extends from T_{in} = 1340 K up to T_{in} = 1400 K and for C/O < 0.15. The dynamic region occurs for 1350 K< T_{in} < 1390 K and for 0.1 < C/O < 0.2. The pyrolytic region extends for C/O > 0.45 and T_{in} > 1350 K, while the "low reactivity region" is comprised between the pyrolytic and the ignition zones.

The lower fuel concentrations and the higher mixture heat capacity with respect to the system diluted at 90%, implies higher inlet temperatures to promote the ignition/oxidation process and lower temperature gradient. Such aspects cause a reduction of the ignition region and an extension of the low reactivity zone.

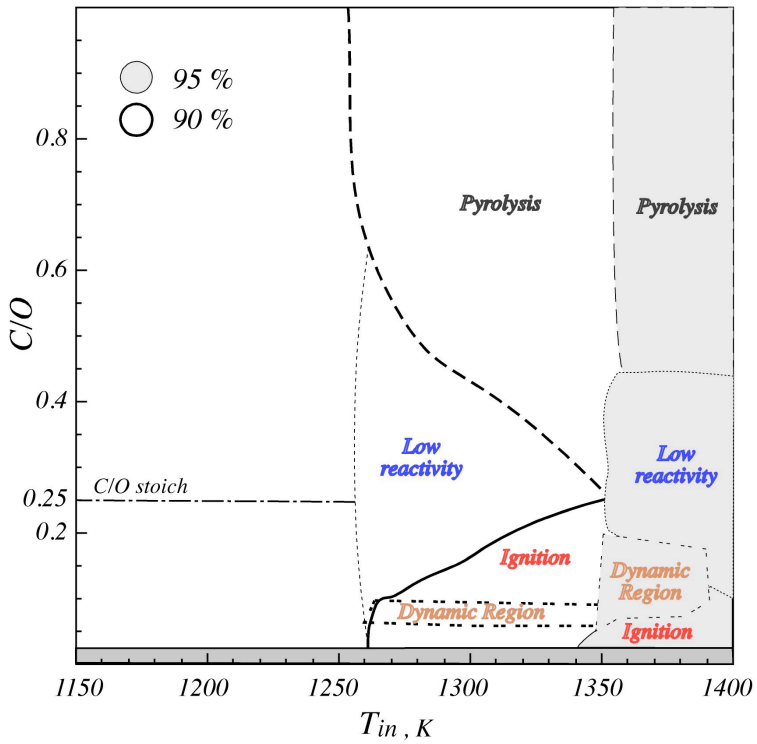

Fig VI.3 - Comparison between reactivity map of methane/oxygen mixture diluted at 95% and 90 %.

For instance, for T_{in} =1373 K and for C/O = 0.075, mixtures ignite for each dilution level and the ΔT_{max} is equal to 70 K for a dilution level equal to 90 %, while $\Delta T_{max} = 27K$ for a dilution level equal to 95 %.

Both the experimental maps suggest that the system goes from ignition to low reactivity, passing through a dynamic behavior as soon as the C/O feed ratio is increased. Increasing the C/O up to rich fuel conditions, methane pyrolysis reactions occur.

In Fig VI.4, the reactivity map for a dilution degree equal to 85 % is shown. The range of temperature investigated is the same of the previous cases and it is comprised between 1150 K and 1400 K by varying C/O from 0.015 up to 1.

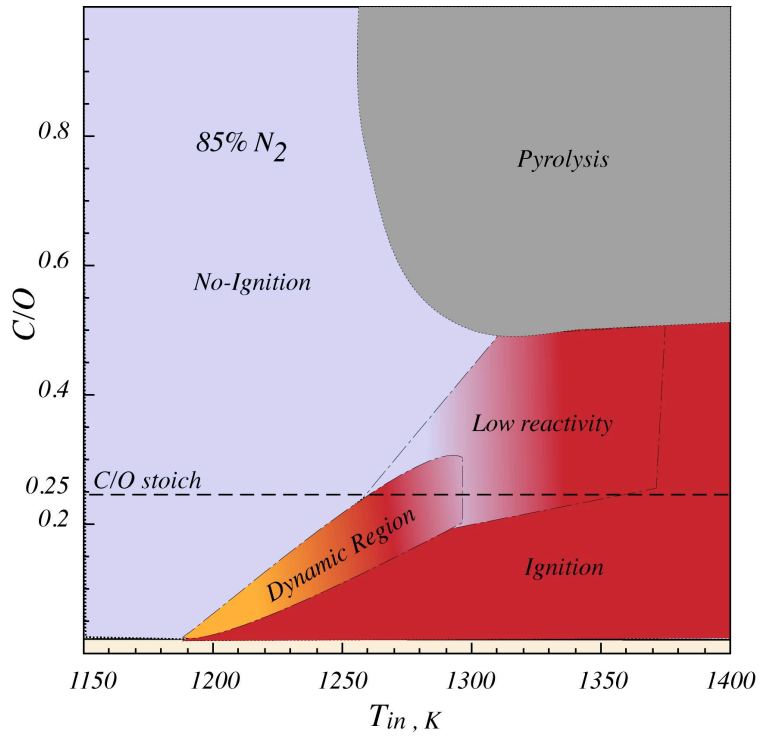

Fig VI.4 - Reactivity map of methane/oxygen mixture diluted at 85%, in function of the initial temperature.

As seen above, it is possible to classify different phenomenologies in the reactivity map with different colors. All the zones that identify a reactivity phenomenology are larger than that found in the previous cases. On the opposite, *no-ignition zone* extends from 1150

K up to 1200 K for lower values of C/O and is obviously smaller. The blue region widens for higher temperatures as soon as feed ratio increases. It is clear that for lean condition, mixtures ignite more easily.

In Fig VI.5, the same overlapping between two reactivity maps obtained for different dilution level was made. In this case, gray color shows regions for a dilution degree equal to 90 %, while white areas delineate zones for a lower dilution.

As it is evident from the figure, the overall reactivity of the system increases. Nevertheless this increment is lower than we could expected after the first comparison. In particular, each zone changes with different peculiarities.

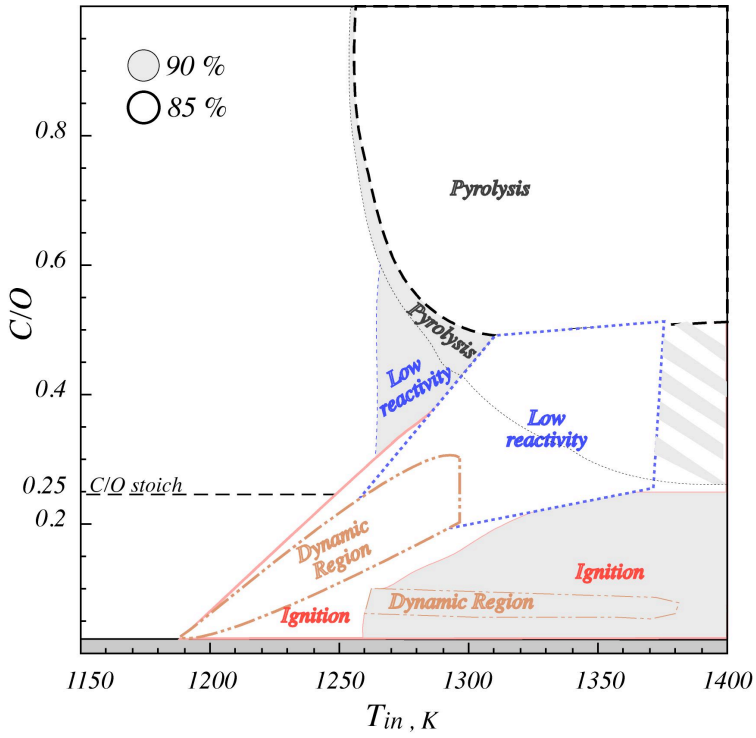

Fig VI.5 - Comparison between reactivity map of methane/oxygen mixture diluted at 85% and 90 %.

The pyrolysis zone undergoes an important decrease in terms of C/O rather than for temperatures investigated. As a matter of fact, the zone shows only a little decrease for $0.5 < C/O < 0.8$ and temperature comprises between 1260 K and 1270 K. Moreover, the

occurrence of pyrolysis phenomenology is replaced by the ignition of the mixture for 1370 K <T_{in}< 1400 K and $0.25 < C/O < 0.5$. This area is shown in figure with a gray striped layout.

The pyrolytic region is not significantly affected by the dilution level. Pyrolytic reactions are promoted mainly by system temperature.

As matter of fact, in the system with 90% of nitrogen the lower methane concentration in the system with 90% of nitrogen is balanced by the presence of higher concentration of nitrogen that promotes, in quality of third-body species, third body reactions, so that the formation of C_2 species and dehydrogenation reactions.

The ignition region expands covering an higher range of temperature and feed ratio. The first oxidation profile occurs for T_{in} = 1190 K and lean condition. Afterwards, the area widens towards higher C/O by increasing T_{in} and reaches $C/O = 0.5$ at the upper edge of the map.

The "low reactivity zone" is located between ignition and pyrolysis zone. It extends from 1260 K up to 1370 K and $0.25 < C/O < 0.5$. For T_{in} > 1370 K the mixture ignites with $\Delta T_{max} > 10K$.

Results suggest that the "dynamic region" is wider both in terms of C/O and temperature and shifts towards lower temperatures with respect to higher dilution. The region starts from 1190 K (C/O=0.015) up to 1300 K (0.2 < C/O < 0.3) and assumes an oblong shape for higher C/O.

The effect of a lower dilution is also evident in terms of ΔT_{max} acquired during experimental tests. In Fig VI.6 and VI.7, ΔT_{max} obtained for the analyzed dilution levels are presented. Overall, the maximum gradient of temperature observed increases because of lower dilution.

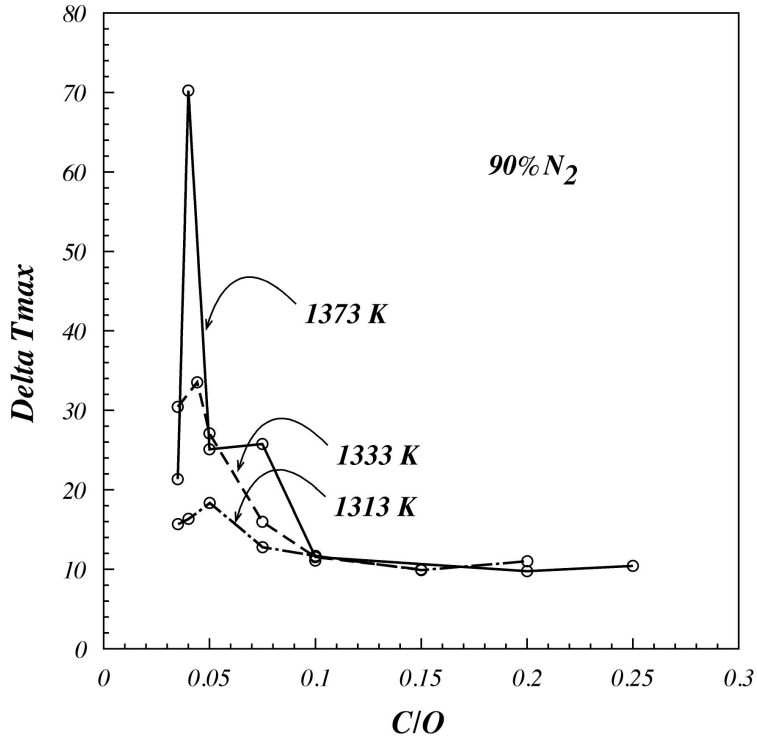

Fig VI.6 - Maximum difference of temperature obtained for three initial temperatures (1313 K, 1333 K, 1373 K) in function of C/O. Dilution is equal to 90 %.

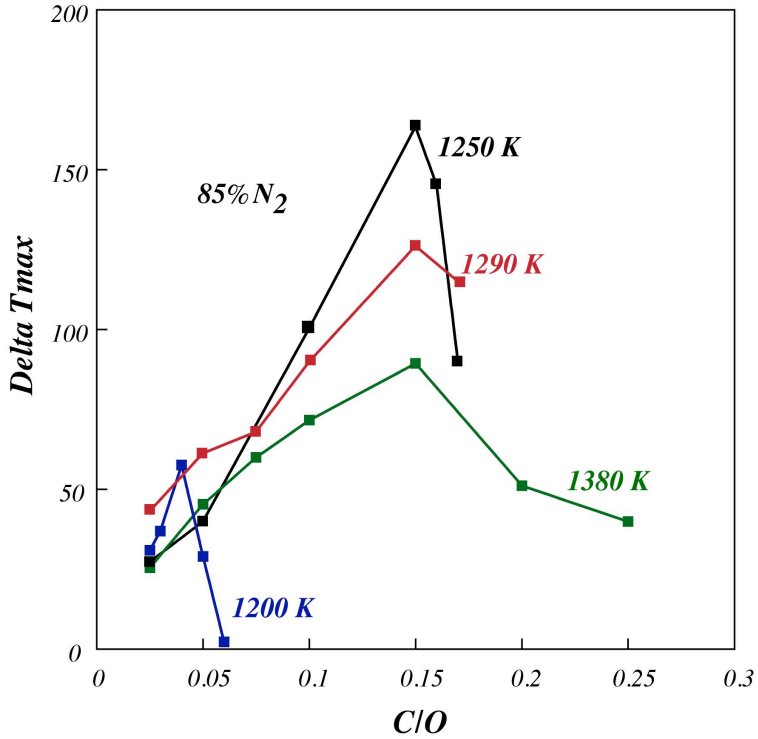

Fig VI.7 - Maximum difference of temperature obtained for four initial temperatures (1200 K, 1250 K, 1290 K and 1380K) in function of C/O. Dilution is equal to 85 %.

This result is coherent with previous consideration: the lower amount of diluent species leads to higher increment of temperature in the system.

As a matter of fact, for an initial temperature of 1373 K, $\Delta T_{max} = 70K$ at 90% while becomes $\Delta T_{max} = 90K$ for the mixture diluted at 85 %. This behavior is shown for the whole range of temperatures investigated. In particular, the maximum increment of temperature observed for mixtures diluted up 85% is higher than 150 K and it occurs for T_{in} = 1250 K and C/O = 0.15. For mixtures diluted up to 90% the maximum ΔT_{max} is about 70 K.

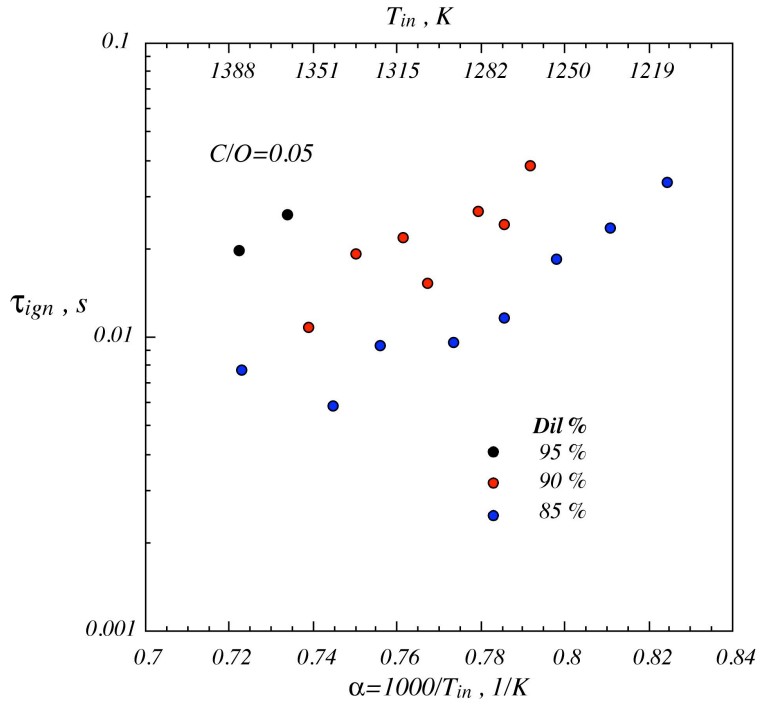

Fig VI.8 - Comparison among auto-ignition time evaluated for different dilution degree in an Arrhenius diagram for C/O=0.05.

Moreover, a singular trend was observed for the variation of ΔT_{max} as function of C/O. In general, for a fixed inlet temperature, the ΔT_{max} increases up to reach a maximum value and

then it decreases increasing the C/O feed ratio. The maximum ΔT_{max} increases enhancing the system inlet temperature up to T_{in} = 1250 K, then it diminishes for higher T_{in}.

Such peculiarity is not present for a system dilution level equal to 90 %. The disappearance of such behavior is probably due to technical impossibility of overcoming range of temperature investigated (T_{in} > 1400 K).

In Fig VI.8 the auto-ignition delay times evaluated for a C/O feed ratio equal to 0.05 are presented in an Arrhenius diagram. The experimental points with circles in different colors are displayed for different dilution levels. In particular, the blue circles represent τ_{ign} for a dilution equal to 85 %, red ones for 90 % and black circles for τ_{ign} at 85%.

The ignition process is clearly delayed as soon as the mixture dilution level is increased. The times obtained for a dilution equal to 85 % are comprise between a maximum of 0.034 sec (T_{in}=1212 K) and a minimum of 0.008 sec obtained for T_{in}=1383 K. For an higher dilution (90 %) the mixture ignites with $0.011\,\text{sec} < \tau_{ign} < 0.038\,\text{sec}$ while only two experimental points are reported in the figure for 95 %. In particular, for an initial temperature equal to about 1272 K τ_{ign} is 0.012 sec at 85 % and becomes 0.024 sec for a dilution equal to 90 % while for a higher dilution (95%) the mixture does not ignite. Finally dilution parameter affects the overall reactivity of the system so that higher dilution means lower reactivity and vice versa. Moreover the effect is also evident on auto-ignition times evaluated for the different dilution degrees.

VI.3 - Biogas

Further experimental tests were carried out by changing kind of fuel. With the aim to characterize the phenomena associated with the oxidation of mixtures of biogas in

highly diluted and preheated conditions, a mixture of known composition was chosen (62 % CO_2, 25 % CO, 10 % CH_4, 1 % C_2H_6, 2 % C_2H_4). The choice of such composition is made on the basis of literature evidence in order to investigate the characteristic oxidation times of a mixtures that can be classified as LCVG (Low Calorific Value Gases). The employment of such fuel blends in MILD combustion conditions implies to deepen the knowledge on the oxidation process of these mixture. For such a mixture the C/O values would not be able to define the relationship between the fuel and oxidizer at the entrance of the reactor. In fact, as opposed methane, biogas contains oxygen species. The feed ratio C/O was, hence, replaced by the oxygen ratio Ω that permits a slavish definition of the feeding ratio. Such parameter was already defined in detail in the chapter relating to experimental results.

Even for biogas blends, some important parameters were changed in order to study oxidation process of such mixtures. Dilution parameter was investigated in a wide region of temperature and Ω . Reactivity maps relating to different level of dilution were delineated as well as auto-ignition times that were evaluated by acquiring temperature profiles.

VI.3.1 - Dilution Parameter

Several experimental tests were carried out in order to investigate the effects of dilution parameter on the oxidation process of biogas.

Experimental results were presented in the chapter V, using fuel blends of biogas diluted in nitrogen and by varying dilution degree from 90 % up to 95 %. On the basis of the temperature profiles acquired, reactivity maps of the system were traced in function of parameter T_{in} and Ω .

In Fig VI.9 the reactivity map obtained for a mixture of biogas diluted at 90 % is shown. The range of temperature investigated is comprised between 950K and 1350 K and Ω varies from 0.025 up to 10.

It is possible to distinguish five regions in correspondence of different T_{in} and Ω investigated. The typical temperature profiles characteristic of each regions as well as a detailed description of the map were shown in the chapter V relating to experimental results.

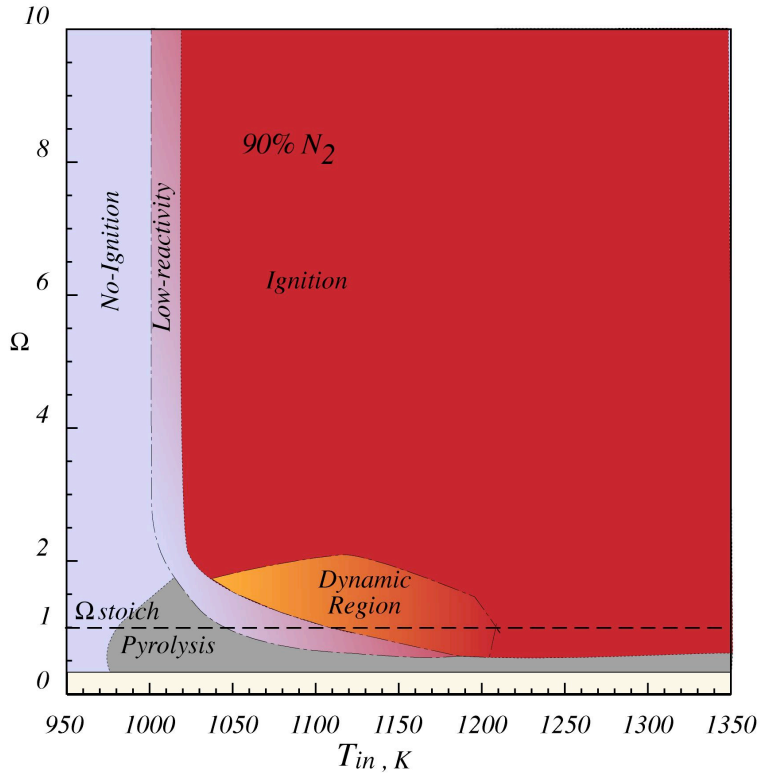

Fig VI.9 - Reactivity map of biogas/oxygen mixture diluted at 90%, in function of the initial temperature.

Each area was represented by a different color and is related to different observed phenomenologies. For temperature comprises between 1020 K and 1350 K the mixture fed to the reactor ignites. Within the ignition zone a dynamic behavior was observed and it was highlighted in the map with orange color.

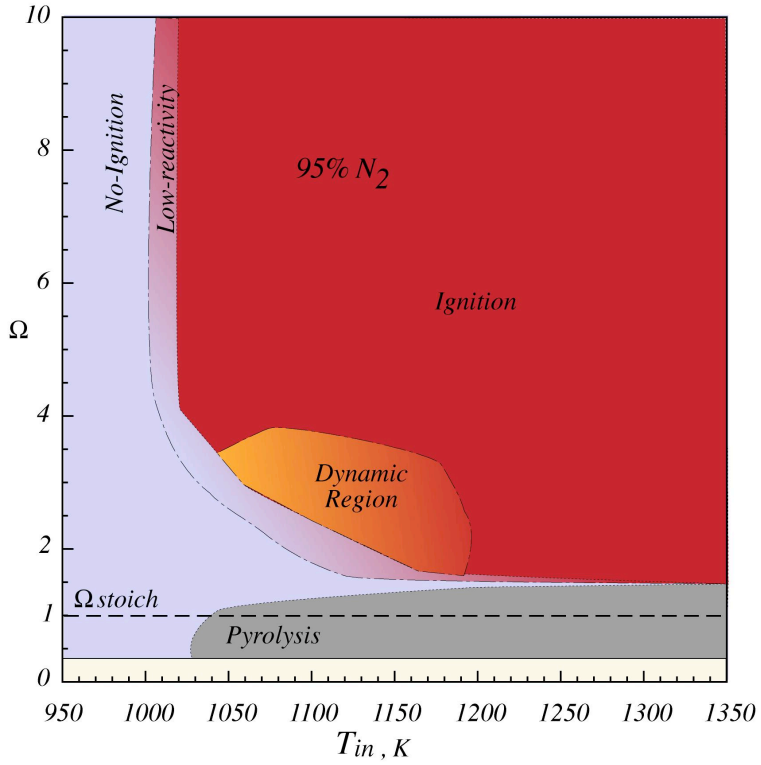

Fig VI.10 - Reactivity map of biogas/oxygen mixture diluted at 95%, in function of the initial temperature.

Under the stoichiometric condition ($\Omega < 1$) a grey zone is located explaining the occurrence of pyrolysis phenomenology. Between the ignition and no-ignition conditions, a small zone in blue/red color shows the presence of minor reactivity of the system with gradient of temperatures lower than 10 K.

The same phenomenologies were observed by increasing the dilution of the system. In Fig VI.10 the reactivity map obtained for a system diluted at 95 % is shown. In fact, dilution parameter was changed even for biogas, and results show similar trend observed for methane.

Moreover it is evident that an increase in the amount of diluent species leads to a decrease of the overall reactivity of the system. In order to compare the map relating to different dilution, an overlapping of two reactivity maps was made in Fig VI.11.

The layout of Fig. VI.11 was changed with respect of Figs VI.9 and VI.10 in order to allow an easier comparison. The gray color represents the regions for a dilution equal to 90%, whereas the white areas show higher dilution.

As it is described above, a higher dilution level implies a lower system overall reactivity. As a matter of fact the ignition zone diminishes its extension as it is evident from the figure. In particular, for low dilution the area in which it is possible to evaluate ignition times is larger in terms of oxygen ratios investigated. In fact, the first temperature in correspondence of the occurrence of ignition phenomenologies (or low reactivity) is the same for both the dilution degrees. For a Tin equal to 1000 K the temperature profiles observed show a little increase of temperature due to the onset of the exothermic chemical reactions.

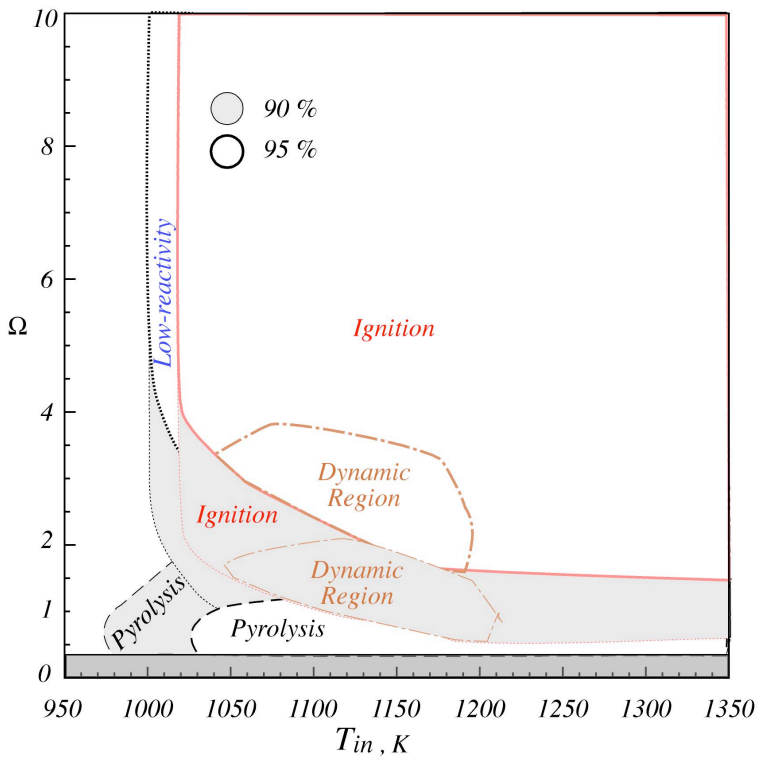

Fig VI.11 - Comparison between reactivity map of methane/oxygen mixture diluted at 90% and 95 %.

Afterwards, for Tin = 1020 K the gradient of temperatures observed is higher than the auto-ignition criterion chosen. It is hence evident that a greater amount of diluent in the mixture affects the overall reactivity of the system in terms of the oxygen ratios investigated. For a lower dilution the ignition zone is located in a range of Ω between 10 and 0.5 (for high temperatures). In fact, the mixtures ignite in correspondence of lean ($\Omega > 1$) condition for lower temperatures ($T_{in} < 1100K$), whereas rich ($\Omega < 1$) condition shows gradient of temperatures higher than the chosen criterion for $T_{in} > 1100K$. On the opposite, for a dilution equal to 95 % the mixture ignites only in correspondence of fuel lean condition. For stoichiometric and rich conditions the mixture does not ignite due to the presence of a larger amount of inert species. Such higher dilution affect the behavior of the system by promoting the occurrence of pyrolysis phenomenology.

The change in the overall behavior of the system is also evident for such a phenomenology. The extension of the grey zone in the map diminishes in particular, in terms of initial temperatures. The area shifted towards higher temperature from 980 K (90 %) to 1030 K (95 %). Moreover, it is evident that under lower dilution condition, the fuel blends follow an oxidation process rather than pyrolytic. The high initial temperature of the system along with the smaller presence of inert species promote the occurrence of oxidation reactions .In addition, the higher fuel concentrations and the lower mixture heat capacity with respect to the system diluted at 95%, implies lower inlet temperatures to promote the ignition/oxidation process and higher temperature gradient. Such aspects cause a decreases of the ignition region and an extension of the zone showing dynamic behavior of the system. Finally, by increasing the level of dilution of the system, the overall reactivity of the mixture diminishes in the whole range of temperature investigated. In addition, all the

phenomenologies observed remain evident although the occurrence conditions are different.

VI.4 - Comparison Methane-Biogas

The experimental data collected during the several tests gave an important results in terms of characterization of the global reactivity of the system. The experimental facility allows to appreciate different phenomenologies occurred during the tests. Two fuel blends were used in order to characterize different peculiarities, and similar behaviors are observed.

In order to compare the phenomenologies occurred during the oxidation of methane and biogas mixtures, it is important to set a relation between feed ratio C/O and oxygen ratio Ω. In particular, this relation for a mixture of methane is the following:

$$\Omega_{CH_4} = \frac{1}{4 \cdot C/O} \tag{46}$$

It is hence possible to add a second y-axis to each methane reactivity map in function of parameter Ω. This is shown in Fig VI.12. As it is evident from the figure the stoichiometric condition is located in correspondence of $C/O = 0.25$ and $\Omega = 1$. The simply relation shows clearly that all the reactivity maps traced for biogas are the reverse of these obtained for methane. Moreover the working condition are fuel lean condition when $C/O < 0.25$ and $\Omega > 1$, otherwise $C/O > 0.25$ or $\Omega < 1$ defines mixture fuel rich.

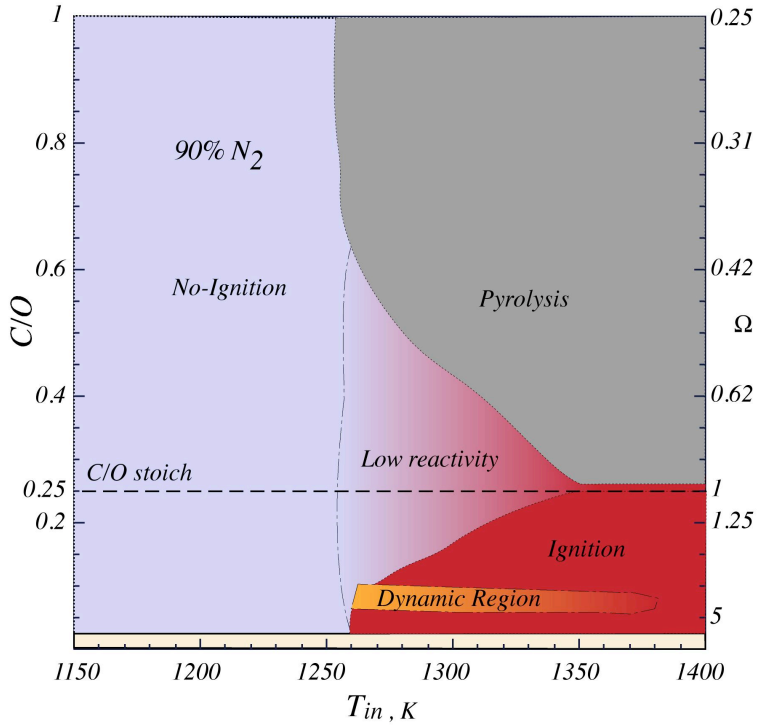

Fig VI.12 - Reactivity map of methane/oxygen mixture diluted at 90%, in function of the initial temperature, feed ratio C/O and oxygen ratio Ω .

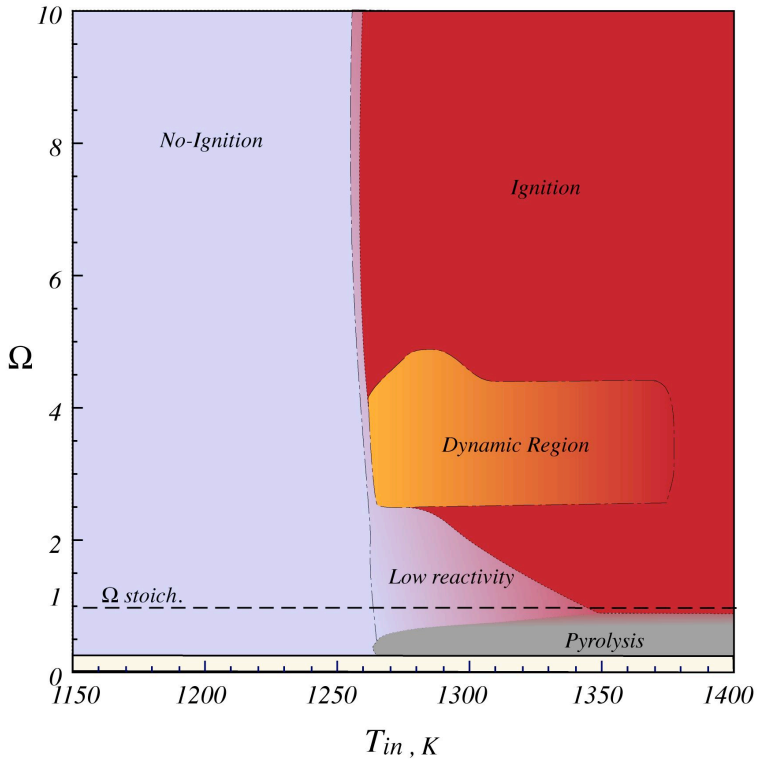

Fig VI.13 -Reactivity map of methane/oxygen mixture diluted at 90%, in function of the initial temperature and oxygen ratio Ω .

In other words, the inverse proportionality between two feed parameters reverse the reactivity map with respect of rich and lean fuel condition. In addition, it is possible to reshape the reactivity map in Fig VI.12 by obtaining Fig VI.13 in function of Ω for a mixture of methane.

This map makes easier a comparison between the reactivity of the system observe for methane (Fig VI.13) and biogas (Fig VI.14) in correspondence of a dilution degree equal to 90%.

It is possible to appreciate five different phenomenologies for each fuel, as described above. The ignition process for methane happens in a range of temperature between 1260 and 1400 K and a region of "dynamic behavior" is located within this area. This region extends from 1260 K up to 1370 K and for $2.5 < \Omega < 4.5$. Likewise, results show the presence of a low reactivity zone in which the gradient of temperature is lower than teen degrees. The area is located in proximity of the stoichiometric condition and represents the onset of the system reactivity which then leads to ignition conditions. The blue/red zone surrounds the ignition zone and extends for temperatures between 1260 K and 1340 K. By increasing the temperature, the low reactivity phenomenologies become rare and are replaced by ignition process. Below Ω_{stoich} and in a range of temperature between 1220 K and 1400 K, pyrolysis phenomena were observed with negative temperature profiles. The low concentration of oxygen lead to the formation of heavy hydrocarbon species.

It is worth noting, that biogas ignites in correspondence of lower temperatures than methane. The phenomenologies observed are similar to methane although the range of parameters are different. In particular, the ignition process of biogas happens 240 K earlier than methane and the mixtures show such phenomenology almost in the whole Ω range

investigated. In the same working condition methane does not ignite and just for a temperature 230 K higher shows a little increase of temperature ($\Delta T_{max} < 10K$).

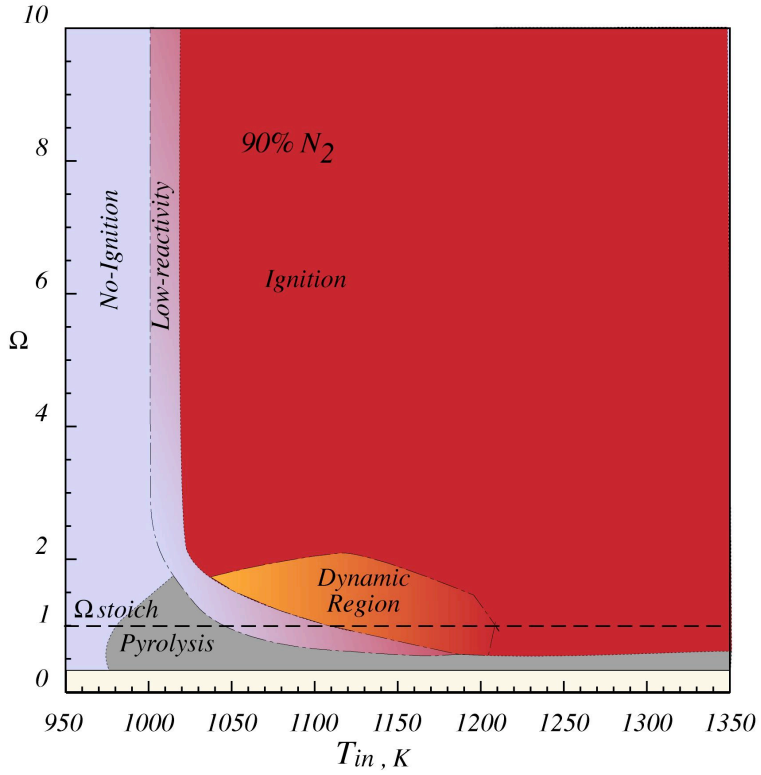

Fig VI.14 - Reactivity map of biogas/oxygen mixture diluted at 90%, in function of the initial temperature.

The composition of the two fuel blends allows to understand such behavior. Biogas could be considered as methane mixtures (in low concentration) with the addition of others light hydrocarbons (C_2H_6 and C_2H_4) and diluent (CO_2).

As it is shown in chapter V, the presence of such hydrocarbons changes the fuel oxidation pathways since they can undergo dehydrogenation reactions and give rise to radicals more easily then methane. So that mixture ignition is promoted by the the presence of C_2H_6 and C_2H_4.

The occurrence of first ignition evidence for methane blends is located for a temperature equal to 1255 K and for lean condition ($8 < \Omega < 10$). Biogas blends ignite more easily and there is a larger zone by going from oxidation through non-oxidation behavior. The low

reactivity zone is clear for biogas whereas is thin for methane and forecasts the beginning of the oxidation process in correspondence of higher temperature.

The pyrolytic region is also present in the biogas reactivity map. The grey zone is more evident for such a mixture and starts earlier as well as seen before for ignition zone. In particular, the first pyrolytic process occurs in correspondence of an initial temperature of 970 K and rich condition. On the opposite, methane pyrolysis happens for temperature 290 K higher and the zone does not comprehend stoichiometric working condition.

Even for biogas, not-stable ignition behavior was detected. The dynamic region is located on the map at the edge of the ignition zone between 1050 K and 1200 K. The working conditions characterized by these phenomenologies are located in proximity of the stoichiometric line ($0.5 < \Omega < 2$). The range of Ω interested by this behaviors is different with respect to methane. As a matter of fact, it occurs for methane for $2.5 < \Omega < 4.5$ and in correspondence of higher temperatures.

VI.5 - Comparison Experimental and Numerical Results

The wide availability of kinetic mechanisms in literature make necessary a deepen study on the singular peculiarities and on the range of validation of them.With this aim, a numerical study was carried out in order to investigate the oxidation of fuel mixtures in highly diluted and preheated conditions. Seven numerical mechanisms were chosen and characteristic oxidation times were evaluated by means of Cantera and Chemkin software.

The prediction of the auto-ignition delay time (τ_{ign}) obtained with all the considered kinetic mechanisms have been reported and described in detail in the chapter relating to numerical results.

The Ranzi mechanism has been used for carrying out a comparison between experimental ad numerical results in terms of auto-ignition delay times. It was chosen because it was validated in a wider range of conditions and reaction configuration at atmospheric pressure.

VI.5.1 - Methane

Several numerical tests were performed in order to appreciate how this mechanism allows to predict different phenomenologies observed during methane oxidation. In Fig VI.15 the reactivity map obtained by means of Ranzi mechanism is shown. The range of parameters investigated coincide with experimental ones, between 1150 K and 1400 K for T_{in}, and from 0.015 up to 1 for feed ratio C/O. The dilution level was set equal to 90 % and nitrogen was used as diluent species.

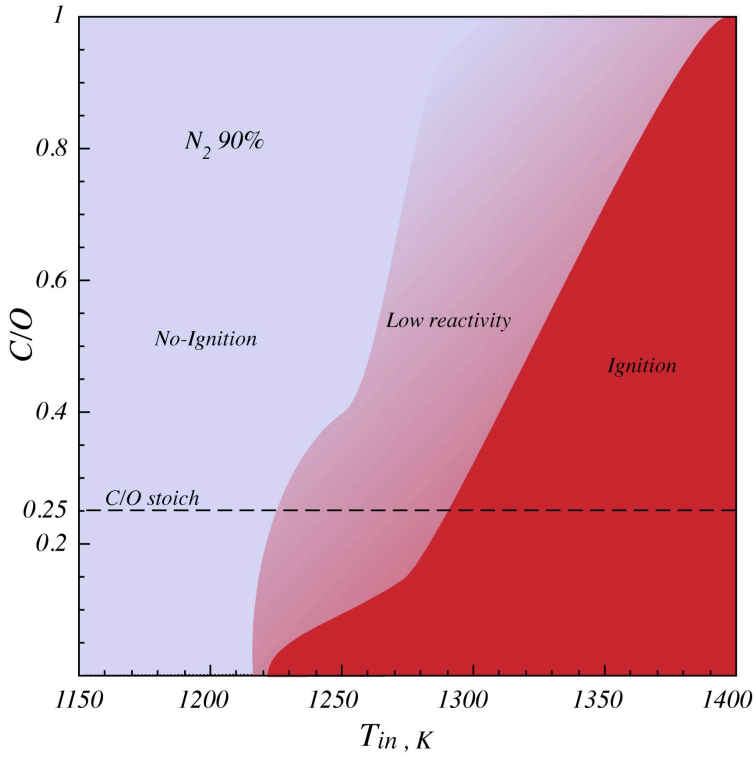

Fig VI.15 - Numerical reactivity map obtained by means of Ranzi mechanism for a dilution level equal to 90 % in nitrogen.

On the basis of temperature profiles computed by means of numerical software, three main zones were identified. For low temperatures (Tin<1225 K) the mixture does not ignite (blue zone) and does not show any gradient of temperature.

For lean conditions and initial temperatures higher than 1225 K a little increase of temperature (lower than the chosen criterion used for the experimental results) was shown and the zone was classified as low reactivity zone (with blue/red gradient color).

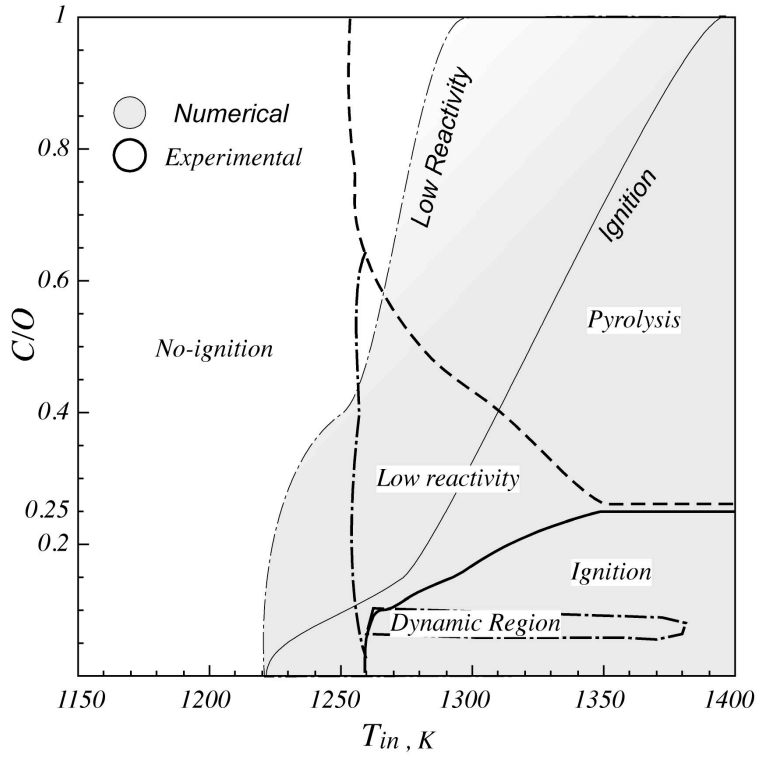

Fig VI.16 - Comparison between numerical and experimental auto-ignition delay times of a mixture diluted in nitrogen at 90% and C/O=0.05.

In Figs VI.17-18-19-20 the comparison between numerical and experimental τ_{ign} evaluated for different C/O and dilution degree are shown. Numerical τ_{ign} were computed by means of Ranzi mechanism and are shown with a red curve while circles in black represent experimental data.

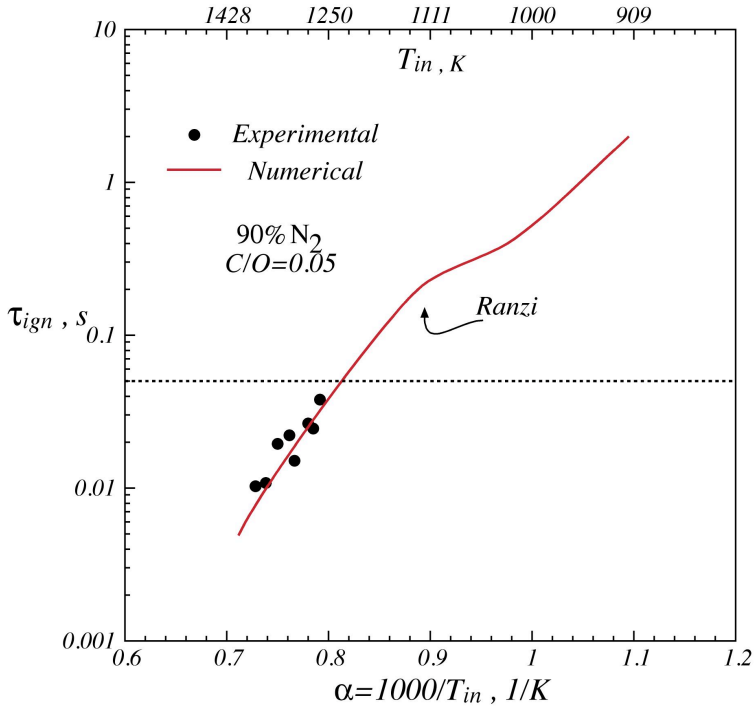

Fig VI.17 - Comparison between numerical and experimental auto-ignition delay times of a mixture diluted in nitrogen at 90% and C/O=0.05.

The numerical simulations comprehend a range of temperature from about 833 K up to 1428 K while experimental data are necessarily collected for higher temperatures (from 1250 K up to 1400 K). The auto-ignition times collected by means of the experimental facility are all below the dotted line that represents the experimental residence time for the chosen velocity.

An overall good agreement between experimental and numerical results are shown in the figures. In Fig VI.17 is shown a comparison for a dilution degree equal to 90 % and C/O=0.05. The times collected varying between 0.01 sec up to 0.038 sec and are similar to numerical ones. The red line is comprised among experimental results and black circles identify auto-ignition times with little discrepancy in the whole range of temperature investigated. The Ranzi mechanism seems to well predict the ignition times for fuel lean mixture.

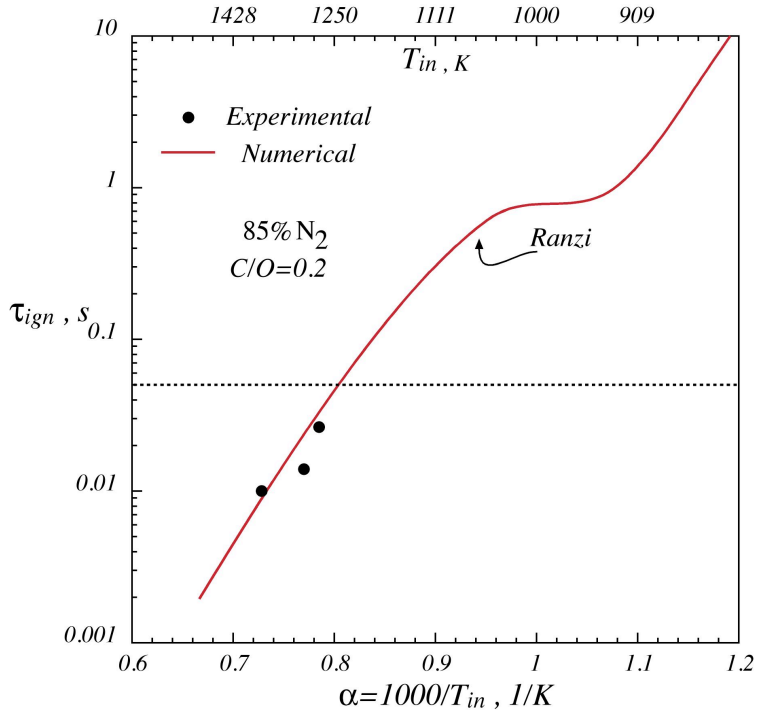

Fig VI.18 - Comparison between numerical and experimental auto-ignition delay times of a mixture diluted in nitrogen at 85% and C/O=0.2.

For higher fuel concentration (C/O=0.2), near stoichiometric condition and different dilution level (85 %) the comparison is shown in Fig VI.18. Likewise experimental and numerical results are comparable also for this case. Three experimental points are collected in this case and as it is seen before few differences are observable.

A similar trends are shown for the last two figures. The first case (Fig VI.19) shows a comparison related to a mixture in very lean condition ($C/O = 0.02$). Numerical times computed are almost coincident with experimental one although little discrepancy are shown for higher temperatures. These variations disappear for higher feed ratio ($C/O = 0.15$ and 85 % in Fig VI.20) with times nearly coincident in the whole range of temperature.

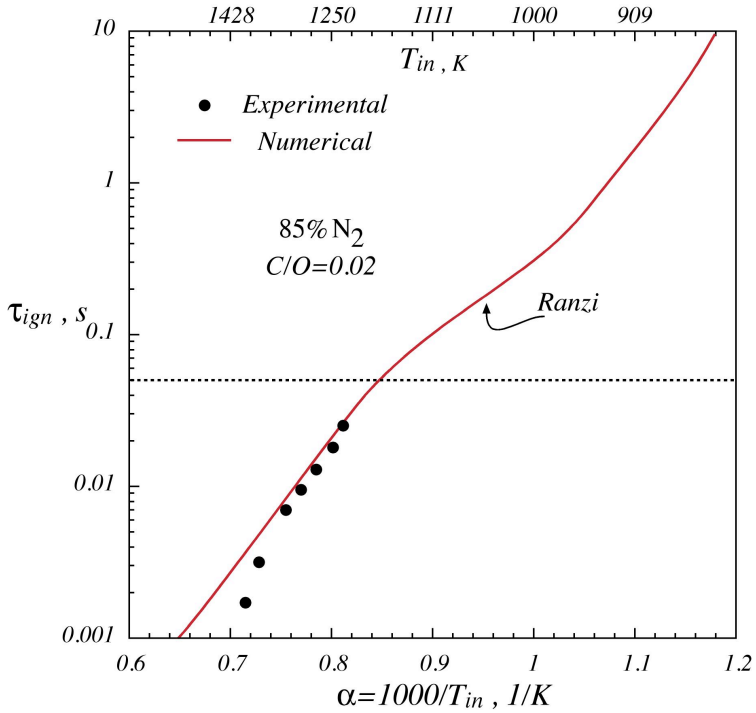

Fig VI.19 - Comparison between numerical and experimental auto-ignition delay times of a mixture diluted in nitrogen at 85% and C/O=0.02.

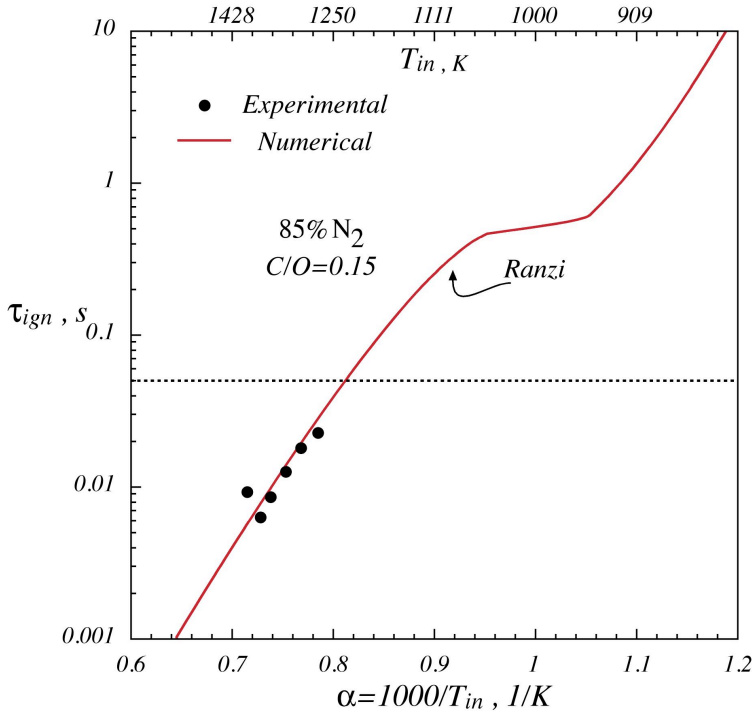

Fig VI.20 - Comparison between numerical and experimental auto-ignition delay times of a mixture diluted in nitrogen at 85% and C/O=0.15.

Finally, the Ranzi mechanism seems to correctly predict the experimental auto-ignition times even in conditions of mixture highly preheated and diluted. As described above, in the chapter relating to numerical results a curve slope change is evident for the curve shows in the figure.

This behavior was justified by different reaction pathways acting in different range of temperatures. Although several mechanisms were used to carry out numerical analyses, only two mechanisms were able to predict the trend and one of these is Ranzi mechanism. Nevertheless, the residence time of the experimental facility does not allow to appreciate the zone interested of such a behavior.

VI.5.2 - Biogas

As it is seen before the mechanism shows a good agreement with data collected for methane mixtures in highly and preheated conditions. The auto-ignition times are well predicted by the mechanism for different feeding conditions. With the aim to investigate the validity of the kinetic mechanisms available in literature, several numerical simulations were performed by means of Ranzi mechanism also for biogas. In fig. VI.21 the reactivity map obtained for biogas mixtures diluted at 90 % in nitrogen is shown. The application PLUG was used to evaluate the ignition conditions of the mixtures on the basis of the criteria described above. The map was divided in three different areas relating to ignition, no-ignition and low reactivity phenomenologies. The ignition zone (in red) is prominent and located in the right upper part of the map. It is comprised between 1040 K and 1350 K and starts from fuel lean (for Tin<1175 K) up to stoichiometric and rich conditions (for Tin >1175 K). A region in blue/red color between the ignition and no-ignition zone is located. Such zone shows working conditions in which low gradient of temperatures were observed.

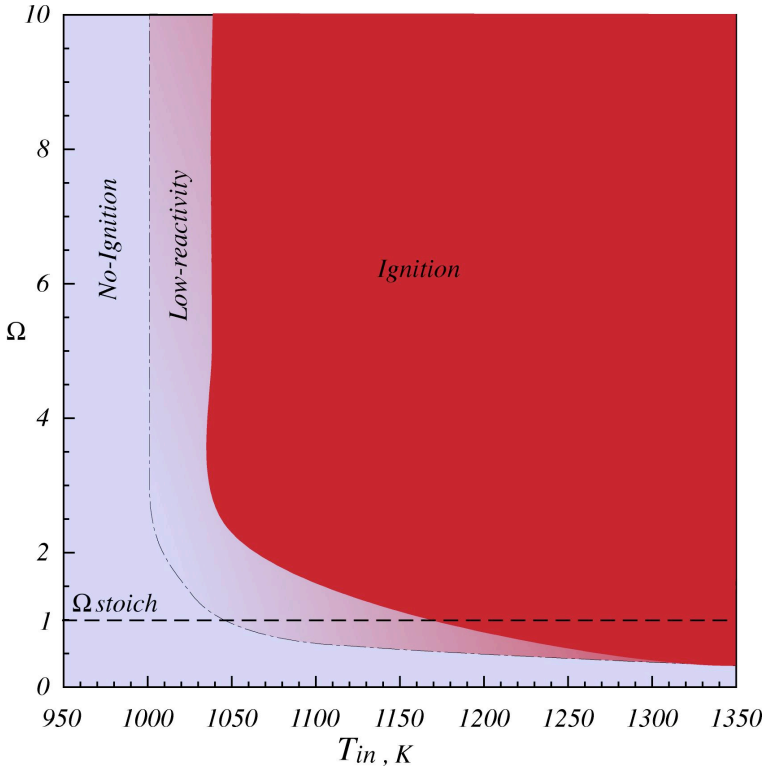

Fig VI.21 - Numerical reactivity maps obtained for biogas mixture diluted at 90 % in nitrogen.

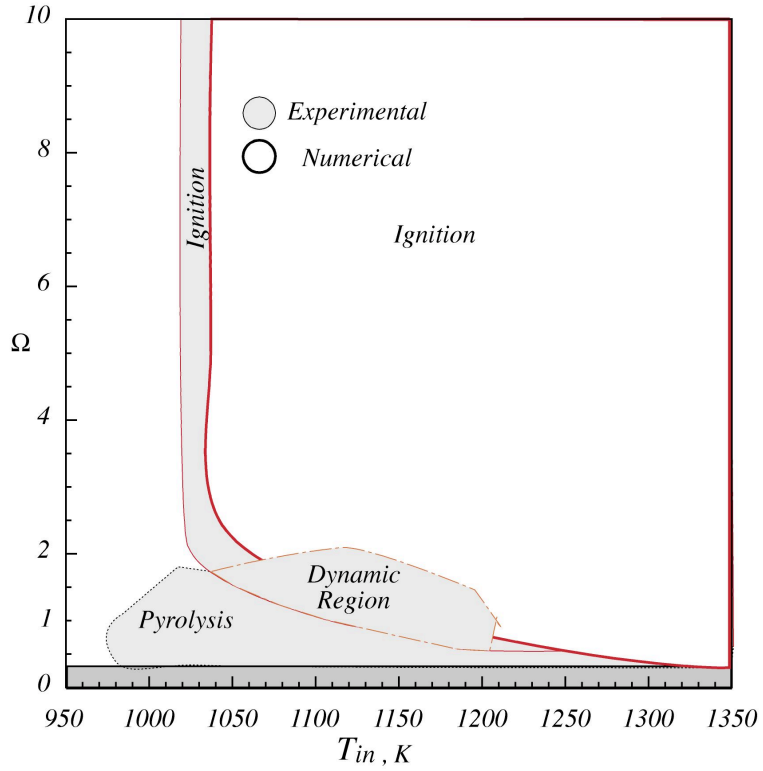

Fig VI.22 - Comparison between experimental and numerical reactivity maps for a dilution equal to 900 % in nitrogen.

In fig. VI.22 a comparison between the numerical and experimental map is shown. The low reactivity zones both for experimental and numerical maps are not reported to make easier the comparison.

A region with red boundary shows numerical (in white) and experimental ignition (in gray) zone. As described in details in the chapter relating to experimental results, a dynamic zone is located within the ignition zone This phenomenologies are unavailable in the numerical map. Similar considerations are evident for pyrolysis zone. Such a phenomenology is not present in the map obtained by means of numerical software.

Finally, numerical tests do not reproduce faithfully the experimental data even if the discrepancy is low. The mixtures ignite 25 K earlier in the experimental tests (from about 1025 K) and for oxygen ratios $\Omega > 1$. In this zone the simulations show increment of temperature lower than the chosen criterion (*low reactivity zone*).

The prediction of auto-ignition times by means of numerical software were performed in order to validate experimental data. Seven values of oxygen ration were chosen and are presented in different Arrhenius diagrams to compare experimental and numerical characteristic times. In Fig VI.23 τ_{ign} versus parameter α, for $\Omega = 10$ are shown. The blue line shows times obtained by means of simulations, while dots are relating to experimental τ_{ign}. Numerical simulation are not able to predict experimental times in the whole range of temperature. In particular for an initial temperature equal to about 1118 K the auto-ignition experimental time is $\tau_{ign} = 10^{-3} s$ while numerical simulation estimates that the mixture ignites with time one order of magnitude higher ($\tau_{ign} = 1.3 \cdot 10^{-2} s$). These variations increase towards lower temperatures. As a matter of fact, the last experimental point shows

an auto-ignition time in the order of millisecond and differs from numerical one equal to 0.089 sec.

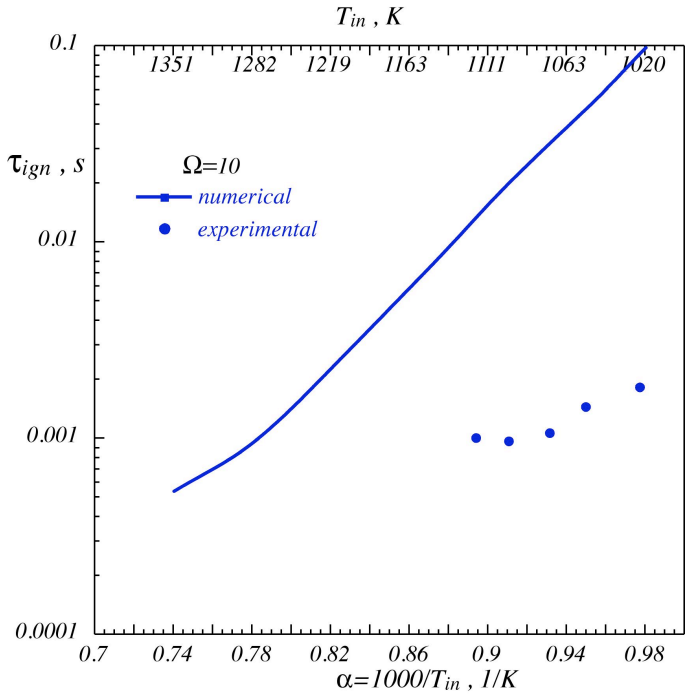

Fig VI.23 - Comparison between numerical and experimental auto-ignition delay times for $\Omega = 10$.

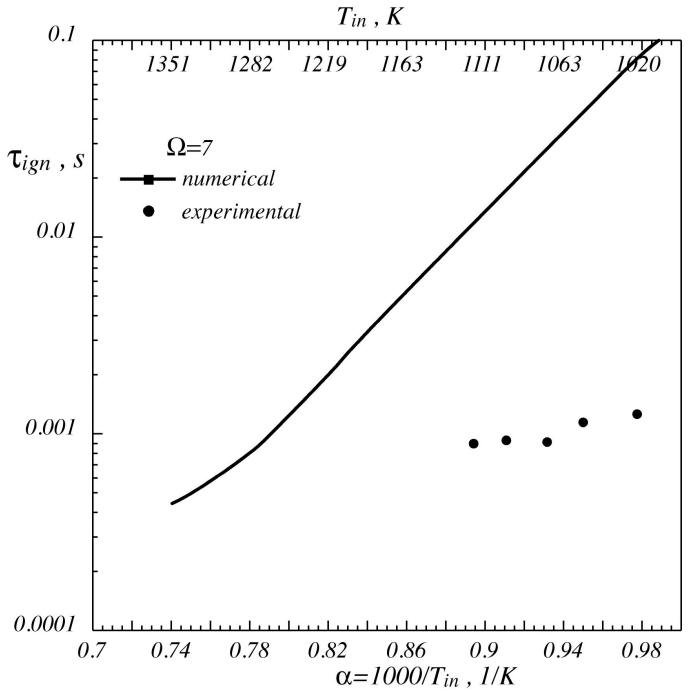

Fig VI.24 - Comparison between numerical and experimental auto-ignition delay times for $\Omega = 7$.

Fig VI.24 shows the comparison for lower oxygen ratio $\Omega = 7$ and consequently higher concentration of fuel.

The trend is similar to previous case, mixtures ignite faster in the experimental facility than in the numerical simulation. The black curve shows a linear trend versus parameter α with a little slope change between 1282 K and 1351 K.

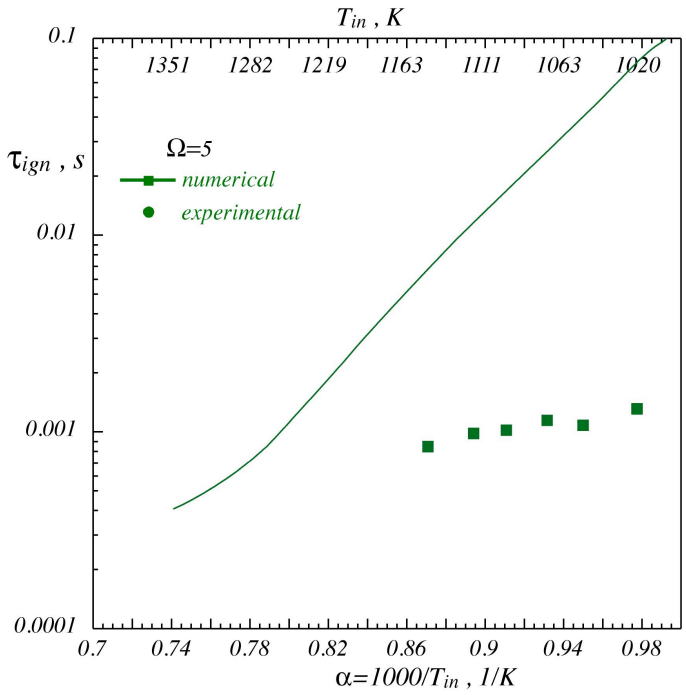

Fig VI.25 - Comparison between numerical and experimental auto-ignition delay times for $\Omega = 5$.

Experimental times are in the order of millisecond with slight difference for different initial temperatures.

This consideration is also evident in the following plot (Fig VI.25) that shows the ignition times for a richer condition. The oxygen ratio is set equal to 5 and data are displayed in green (line for numerical, squares for experimental). For lower Ω values the experimental times are similar to these obtained for $\Omega = 7$. In addition, there are similar differences with

numerical results as well as for the relative slope between numerical curve and experimental data.

The Fig VI.26 shows seven experimental τ_{ign} for $\Omega = 3.33$ and numerical results. Times predicted by means of tubular flow reactor are quite different from the previous Ω. Moreover τ_{ign} move closer to numerical data and the differences become lower in the whole range of temperatures investigated.

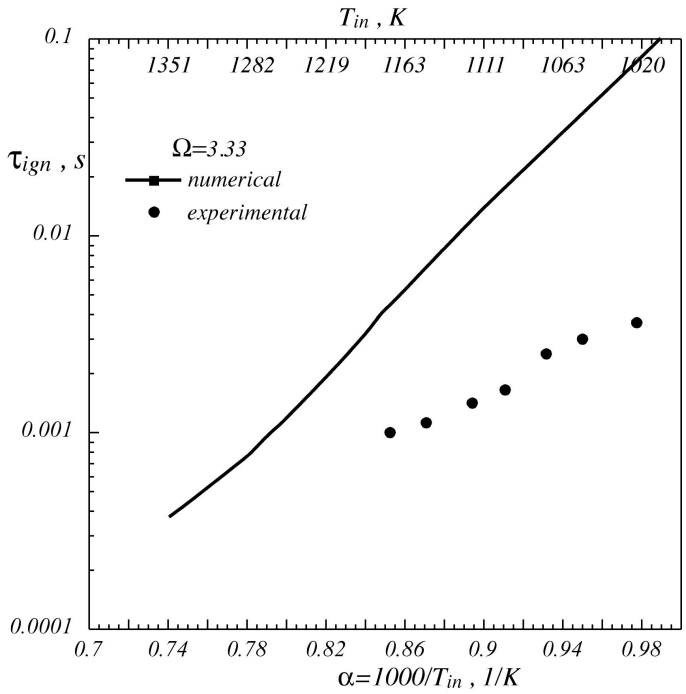

Fig VI.26 - Comparison between numerical and experimental auto-ignition delay times for $\Omega = 3.33$.

Such trend is also evident in the following plot (Fig VI.27) in which times were evaluated for a Ω equal to 1.67. The discrepancy between numerical and experimental data collected for the same initial temperatures decreases and in some cases they almost coincide.

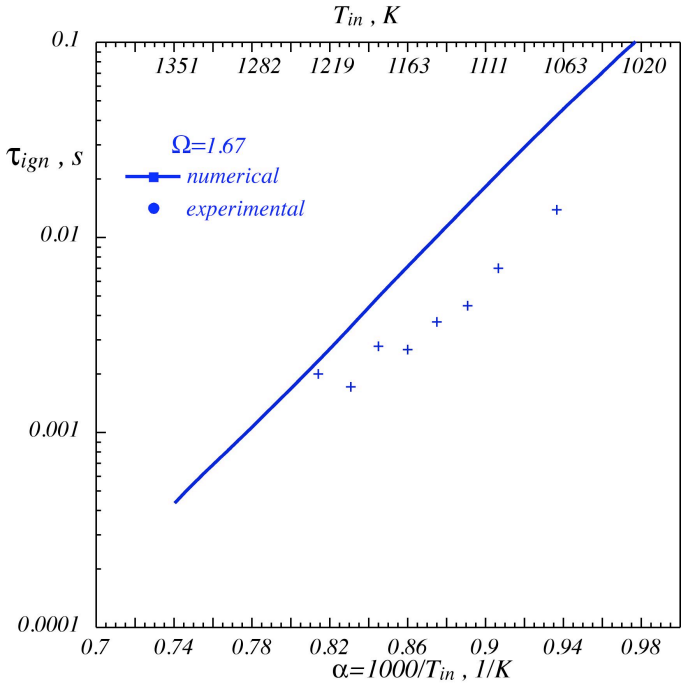

Fig VI.27 - Comparison between numerical and experimental auto-ignition delay times for $\Omega = 1.67$.

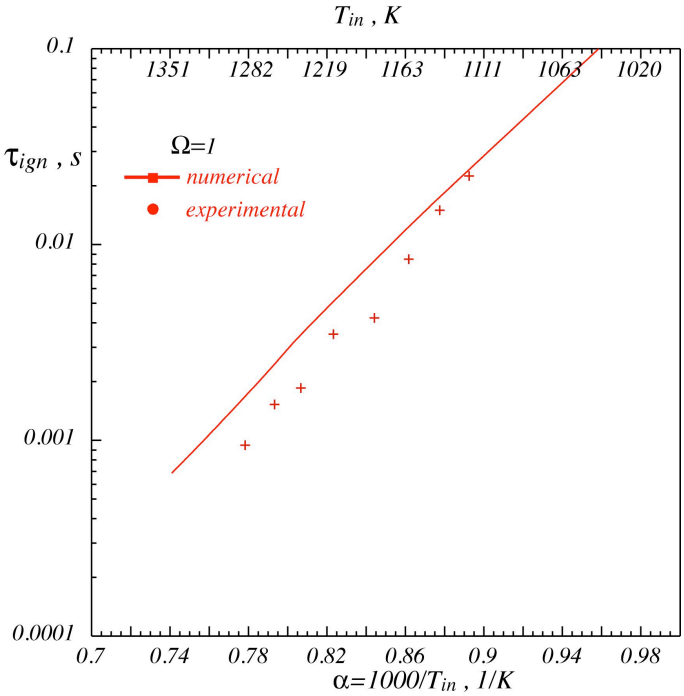

Fig VI.28 - Comparison between numerical and experimental auto-ignition delay times for $\Omega = 1$.

Although τ_{ign} experimental data show a trend almost parallel to numerical curve are quite different yet. For stoichiometric condition smaller discrepancy were shown between experimental and numerical results (fig. VI.28). As in the previous case, the curve (in red) shows numerical times that are all close to experimental ones. For instance, for a temperature of 1285 K ($\alpha = 0.778$) the experimental auto-ignition time is equal to $9.33 \cdot 10^{-4} s$ while for numerical test is 0.002s. The difference between numerical and experimental results become smaller for lower temperature until values are almost coincident. As a matter of fact, for $\alpha = 0.778$, experimental auto-ignition time is equal to 0.022 while $\tau_{ign}^{num} = 0.024 s$.

Finally, the kinetic mechanism is able to predict auto-ignition times in stoichiometric condition with a good accuracy, while it overestimates them for lean condition. The following Arrhenius diagram (Fig VI.29) shows the last comparison between numerical and experimental τ_{ign} for a rich condition ($\Omega = 0.7$). An inversion in the prediction of experimental times with respect to numerical ones is shown. The mechanism underestimates the auto-ignition time with large discrepancy. Numerical curve is almost parallel to the experimental trend and the difference increases for higher temperature. For example in correspondence of a $\alpha = 0.823$, the times evaluated are 0.025s and 0.009s respectively for experimental and numerical.

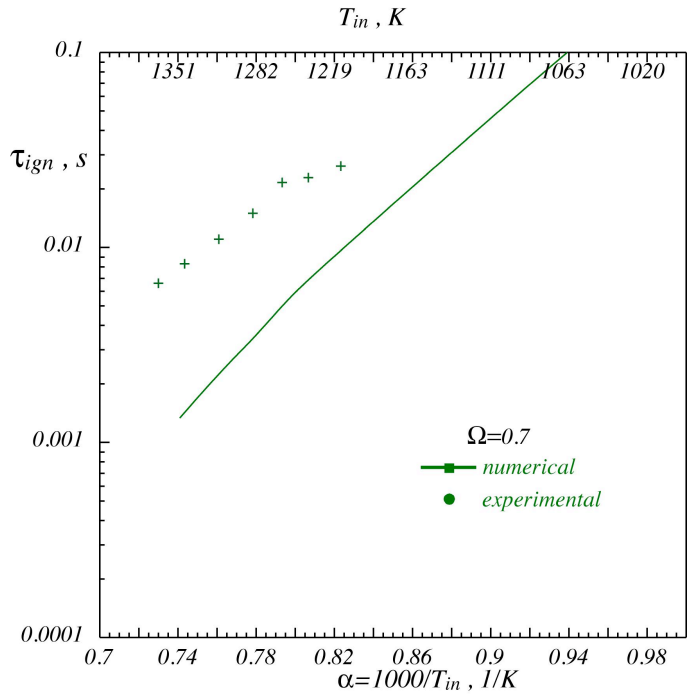

Fig VI.29 - Comparison between auto-ignition delay time evaluated for different dilution and main flow velocity

The major species mole fractions experimentally detected by gas-chromatographic techniques for different mixture compositions varying the inlet mixture temperature has been discussed in Chapter V. In this paragraph, the comparison between experimental and numerical species concentration is presented and discussed.

The prediction of the species produced during the biogas oxidation process under MILD operative conditions and of their relative concentration has been realized by means of the Chemkin package software and its application PLUG. The kinetic detailed model used is the c1-c3 mechanism.

Simulations were carried out in the same experimental operative conditions. Therefore, mixture inlet temperatures were changed from 800 K up to 1350 K while the reference oxygen equivalence ratios (Ω) were 3.33, 1.67, 1 and 0.7, so that fuel lean, stoichiometric and rich mixture composition are considered. The flow inlet velocity was 30 m/s, while the overall dilution degree is 90%.

In general, results will be presented considering that lines are relative to numerical results while points to experimental data.

Fig VI.28 is relative to a very fuel lean mixture (Ω = 3.33). In such a case the inlet composition of the mixture is reported in Tab. VII.1:

Species	Mole Fraction
O_2	8.18
N_2	82.00
CH_4	0.48
CO	1.2
CO_2	3.0
C_2H_4	0.045
C_2H_6	0.096

Tab. VI.1 - Reference mixture concentration for Ω = 3.33.

Fig VI.30 shows the molar fraction trend for methane and hydrogen as function of T_{in}. Hydrogen is numerically identified by the continuous line and experimentally by the red circle. Likewise, methane mole concentration trend is showed by the dashed line, while experimentally by black squares.

Experimental data clearly show that methane does not react before an inlet temperature equal to 1000 K. For higher inlet temperature its concentration becomes equal to zero. At the same time, H_2 is not formed before T_{in} = 1000 K. For such reference inlet temperature, it reaches a maximum value, then it decreases to zero for higher T_{in} values.

Numerical results predict experimental data quite well. It is worth noting that the kinetic model predicts both concentrations values and mole fraction trend as function of T_{in}. Nonetheless, the numerical data suggest that the biogas is oxidised for inlet temperature greater than 1050 K, while experimental data for T_{in} > 1000 K.

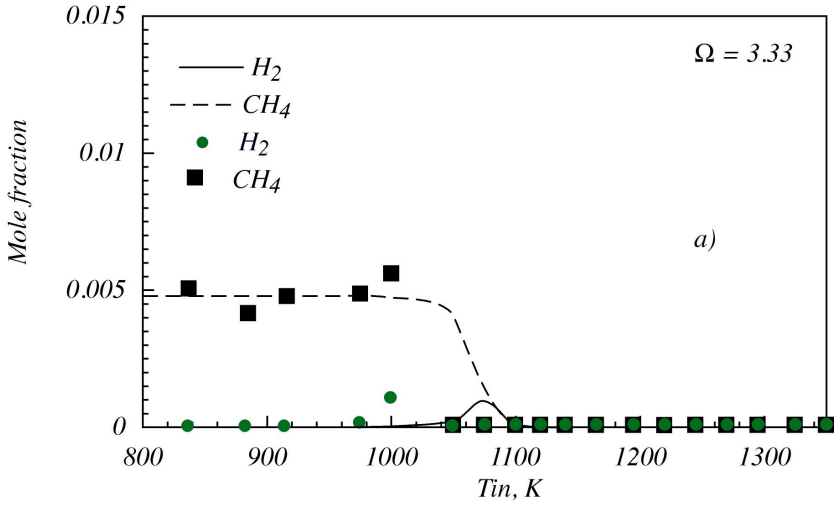

Fig VI.30 - Comparison between experimental and numerical CH4 and H2 mole fraction versus Tin.

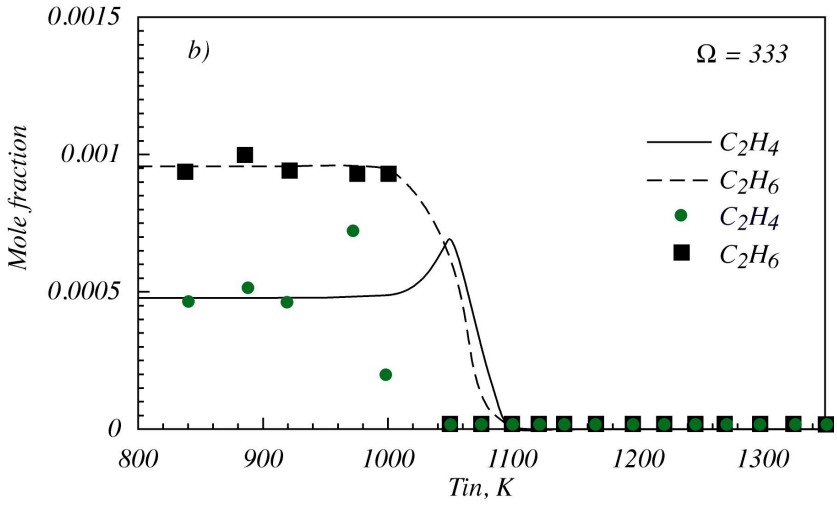

Fig VI.31 - Comparison between experimental and numerical C2H4 and C2H6 mole fraction versus Tin.

Fig VI.31 shows the molar fraction trend for C_2H_4 and C_2H_6 as function of T_{in}. In particular C_2H_4 is numerically identified by the the continuous line and experimentally by the red circle, while C_2H_6 mole concentration trend is showed by the dashed line, while experimentally by black squares.

Experimental data show that ethane mole fraction remains constant up to T_{in} = 1000 K, then it decreases and for T_{in} equal to about 1040 K it becomes zero. Ethylene does not react up to T_{in} = 920 K, for T_{in} = 975 K its concentration shows a maximum value, then it

decreases and for T_{in} equal to about 1040 K it is not detectable anymore in the exhausted flue gases.

Numerical results show that both ethane and ethylene do not react for $T_{in} < 1000$ K. Afterwards, ethane concentration monotonically decreases down and becomes 0 at $T_{in} = 1100$ K. In the temperature range $1000 \text{ K} < T_{in} < 1100$ K, ethylene mole fraction shows a maximum value, very similar to the experimental maximum one, then it is fully converted for $T_{in} > 1100$K.

Also for these two species, the trend and the mole fraction values are well predicted by the model, even if experimentally oxidation reactions occur for lower inlet temperatures.

Fig VI.32 shows the experimental and numerical molar concentration of CO and CO_2 as function of T_{in}. Carbon monoxide is identified by the red dot and by the continuous line, respectively experimentally and numerically, while carbon dioxide by black squares and the dashed line. From experimental tests, mole concentration of both species remain constant up to $T_{in} = 1000$ K. For an inlet temperature of 1050 K the CO_2 concentration results to be equal to 5%, and remains constant for the higher considered inlet temperatures. The CO concentration at $T_{in} = 1000$ K becomes equal to 0.8%, then such species disappears from the exhausted gases flow.

Simulations show that the CO_2 mole fraction trend is well-predicted by the model, even though experimentally the biogas complete oxidation occurs for lower inlet temperatures. In case of CO, the experimental data show a dissimilar behaviour with respect to numerical results. As matter of fact the CO concentration decreases monotonically from inlet conditions down to zero, while numerical integrations show that CO concentration increases from 1000 K and reaches a maximum value at about $T_{in} = 1080$ K, then it goes down to zero.

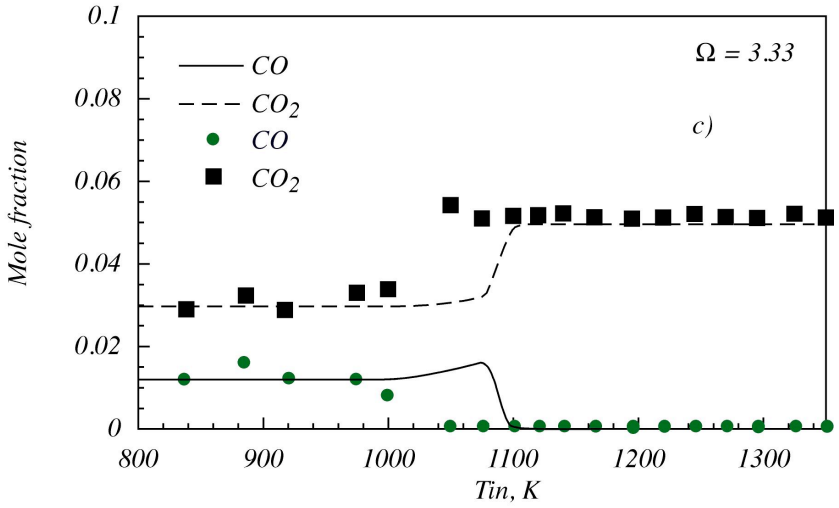

Fig VI.32 - Comparison between experimental and numerical CO2 and CO mole fraction versus Tin.

At last but not least, the comparison between experimental and numerical O_2 and H_2O molar concentration as function of T_{in} is reported in Fig VI.33.

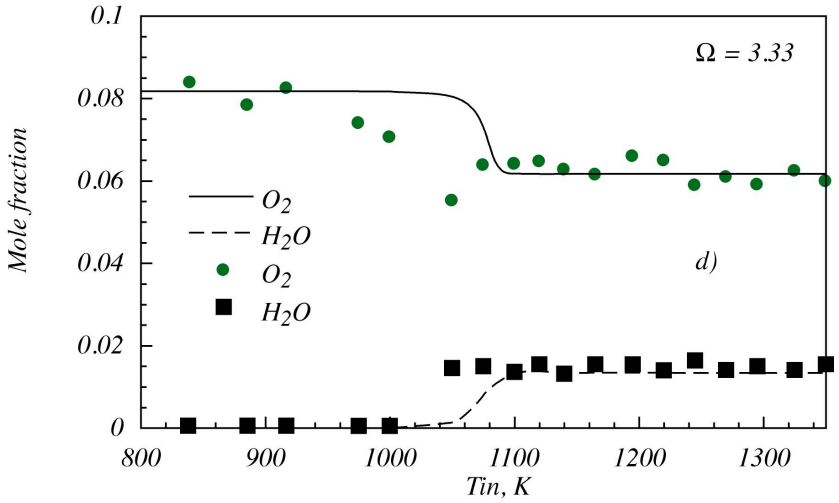

Fig VI.33 - Comparison between experimental and numerical H2O and O2 mole fraction versus Tin.

Oxygen molar fraction trend is indicated by means of the continuous line and the red dots, while steam by the dashed line and the black square.

Experimental tests show that O_2 concentration in the flue gases remains equal to the inlet values up to T_{in} = 925 K. Afterwards, it starts decreasing and reaches a constant value of

about 6% for T_{in} = 1080 K. Water is not present in the flue gases up to T_{in} = 1000 K, then its concentration increases and reaches a constant value of about 1.5%.

The steam content is numerically well predicted, but the inlet temperature where steam is formed is different from experimental conditions. Even oxygen concentration trend is numerically correct but oxygen reacts for higher inlet temperatures with respect to experimental data.

For a fuel rich mixture characterised by an oxygen equivalence ratio equal to 3.33, the agreement between experimental and numerical results is pretty good except for the inlet temperatures where oxidation reactions occur. As matter of fact, from experiments it results that ethene production occurs for T_{in} = 975 K, while numerically for T_{in} > 1050K.

Both experimental and numerical results suggest that ethane consumption corresponds to ethylene, hydrogen and methane production, so that it is plausible that dehydrogenation reactions occur for low inlet temperatures. Thereafter, fuels are fully oxidised to CO_2 and H_2O.

Figs VI.34-37 show the species mole concentration versus the mixture inlet temperature for a fuel lean mixture (Ω = 1.67). The inlet mixture composition is summarised in Tab. VII.2.

Species	Mole Fraction
O_2	6.76
N_2	84.72
CH_4	0.85
CO	2.13
CO_2	5.3
C_2H_4	0.085
C_2H_6	0.17

Tab. VI.2 - Reference mixture concentration for Ω = 1.67.

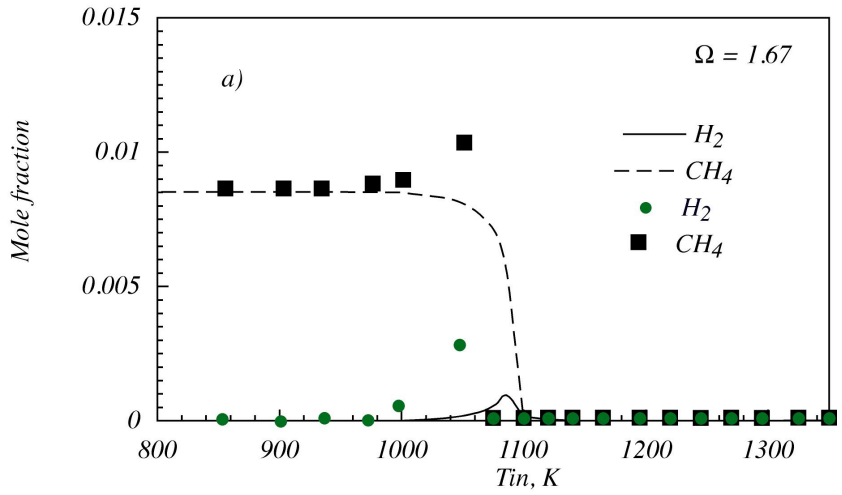

Fig VI.34 - Comparison between experimental and numerical CH4 and H2 mole fraction versus Tin.

Fig VI.34 shows the molar fraction trend for methane and hydrogen as function of T_{in}. Hydrogen is numerically identified by the continuous line and experimentally by the red circle. Likewise, methane mole concentration trend is showed by the dashed line, while experimentally by black squares.

Experimental tests show that both the considered species do not react for $T_{in} < 1000$ K. For $T_{in} = 1000$ K, the molar concentration of both species increases and at $T_{in} = 1050$ K their concentration reaches a maximum value. Afterwards, none of them is detectable in the flue gases. Numerical simulations show that methane mole fraction does not change up to $T_{in} = 1000$ K, than it decreases and becomes zero for $T_{in} = 1100$ K. For what concerns hydrogen, from the comparison between test data and numerical results, it comes out that the mole fraction trend is well kept, but neither the hydrogen mole fraction maximum value nor the reactive inlet temperature range is correct.

Fig VI.35 shows the molar fraction trend for ethane and ethene as function of T_{in}. Ethylene is numerically identified by the continuous line and experimentally by the red circle, while ethane mole concentration trend is showed by the dashed line, while experimentally by the black square.

Experiments show that for low inlet temperatures, their mole concentration is equal to the reference inlet values. For T_{in} = 975 K, ethane concentration starts decreasing while ethylene one increases. For higher inlet temperature, C_2H_6 concentration decreases and becomes zero for T_{in} = 1075 K, while ethylene concentration increases reaching a maximum value for T_{in} = 1000 K. Thereafter, it decreases down to zero for T_{in} = 1075 K. Apart of the consideration that the experimental and numerical oxidative reactions occur for different temperature ranges, the molar fraction trend for both the species is numerically well predicted. The experimental ethylene maximum value is not equal with the numerical one, but the discrepancy could be due to uncertainness in experimental data.

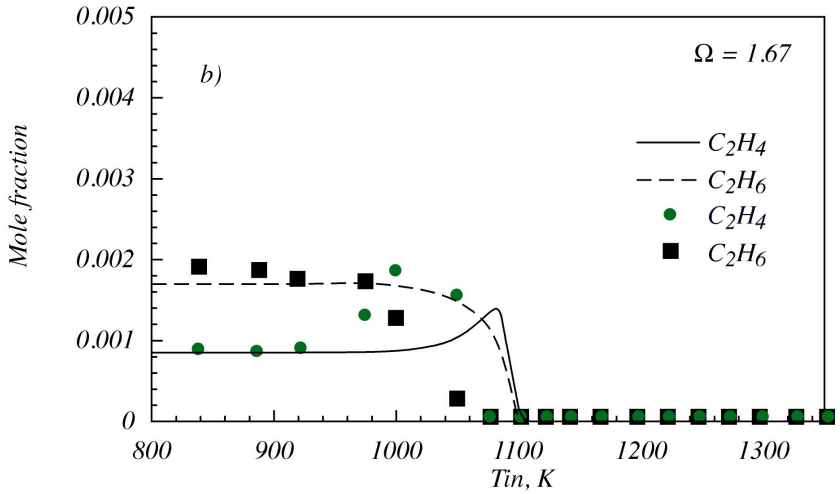

Fig VI.35 - Comparison between experimental and numerical C2H4 and C2H6 mole fraction versus Tin.

Fig VI.35 reports the experimental and numerical molar concentration of CO and CO_2 as function of T_{in}. Experimental data show that their concentration remains constant up to T_{in} = 1000 K. For higher inlet temperatures CO disappears, while the fuel conversion to CO_2 increases, and its concentration reaches a value of 9%.

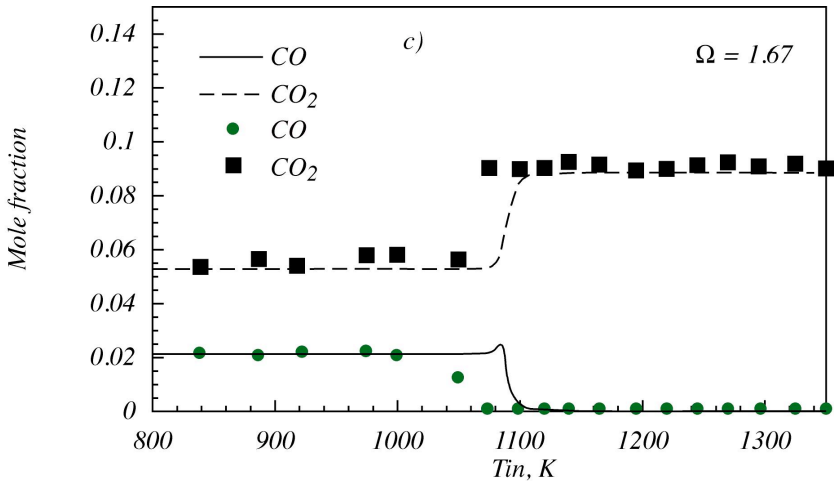

Fig VI.36 - Comparison between experimental and numerical CO and CO2 mole fraction versus Tin.

Numerical results well predict the CO and CO_2 concentration for low temperature and high temperature but not at intermediates temperatures. As matter of fact, the CO mole fraction profile shows a maximum value while experimentally the CO concentration decreases monotonically as soon as the inlet temperature is increased from T_{in} = 1000 K up to about T_{in} = 1080 K.

Finally, Fig. VI.37 is relative to O_2 and H_2O. From experimental data, it is worth noting that O_2 concentration decreases for T_{in} = 1050 K from the inlet reference value down to 3.5%. At the same inlet temperature, fuels conversion to water increases and steam mole fraction is equal to about 0.025.

For such species the model is able to predict well experimental concentrations and trends. Nevertheless model fails to predict the inlet temperatures where reactions occur with respect to experimental data.

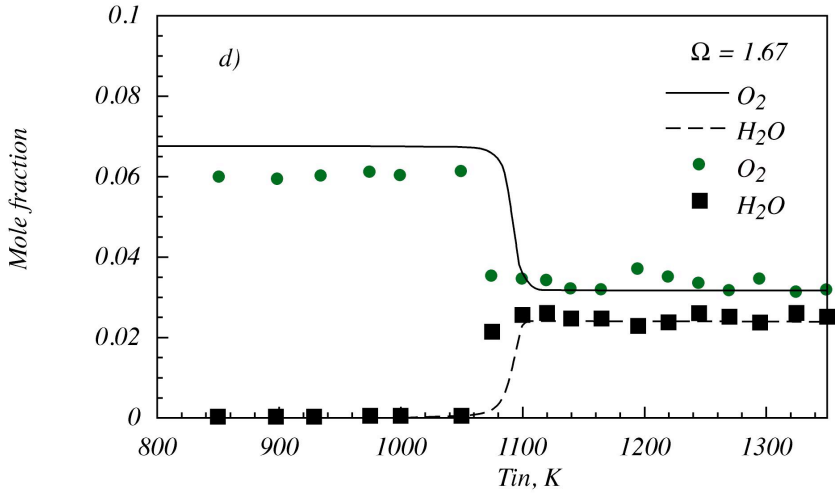

Fig VI.37 - Comparison between experimental and numerical H2O and O2 mole fraction versus Tin.

Fig VI.38-41 shows the species mole concentration versus the mixture inlet temperature for mixture with a stoichiometric composition (Ω = 1). The inlet mixture composition is reported in Tab. VII.3.

Species	Mole Fraction
O_2	5,28
N_2	82,3
CH_4	1,24
CO	3,10
CO_2	7,70
C_2H_4	0,124
C_2H_6	0,248

Tab. VI.3 - Reference mixture concentration for Ω = 1.

Fig VI.38 reports the numerical and experimental methane and hydrogen mole fractions as function of the mixture inlet temperature. Considering experimental data, it comes out that the concentrations of the considered species remain equal to the reference inlet conditions for $T_{in} < 1000$ K. For $T_{in} > 1000$ K, the molar concentration of both H_2 and CH_4 increases and at $T_{in} = 1100$ K their concentration reaches a maximum value.

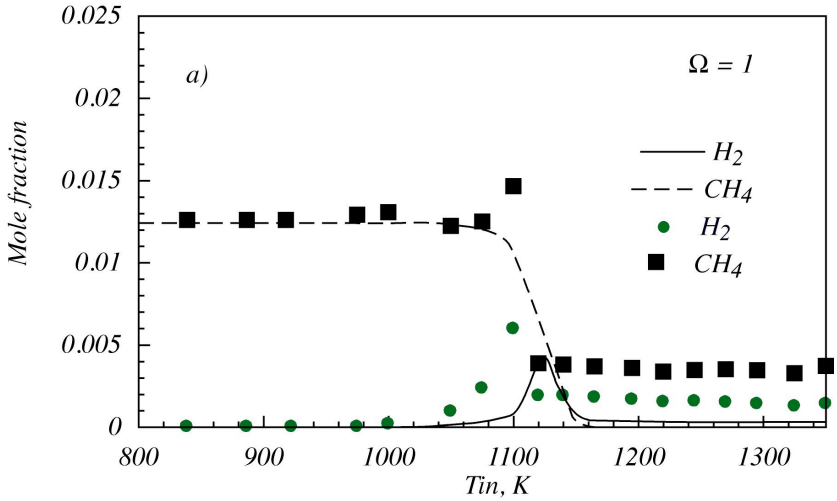

Fig VI.38 - Comparison between experimental and numerical H2 and CH4 mole fraction versus Tin.

Following, methane and hydrogen concentrations decrease to a constant value, respectively equal to about 0.003 and 0.0015.

Simulations show that methane concentration decreases monotonically with the inlet temperature for T_{in} > 1040 K, and for T_{in} > 1160 K it is completely consumed. For T_{in} > 1040 K, hydrogen is produced, its molar concentration increases up to reach a maximum value at T_{in} = 1120K, then it diminishes reaching a constant value equal to 3 10^{-4}.

Methane molar concentration profile and values at high inlet temperatures are not properly predicted by the model. In particular experimental data show that methane is formed, and also for high inlet temperature it not completely converted. Same considerations apply for hydrogen. For such species, the mole fraction is correct but maximum and high inlet temperature values are not.

Fig VI.39 shows the molar fraction trend for ethane and ethene as function of T_{in}. Analysing experimental data, it comes out that for low inlet temperatures, ethane and ethene mole concentration is equal to the reference inlet values up to T_{in} = 975 K. For T_{in} > 975 K, ethane concentration starts decreasing while ethylene one increases. For higher values of the mixture inlet temperature, C_2H_6 concentration monotonically decreases and

becomes zero for T_{in} > 1125 K. On the contrary, ethylene concentration increases reaching a maximum value for T_{in} = 1075 K, then it decreases down to zero for T_{in} = 1125 K.

Simulations are able to predict such trends, even if they underestimate ethylene production. Once again, numerical results envisage oxidation reactions for a different temperature range. As matter of fact, ethylene production experimentally is detectable for T_{in} = 925 K, while for simulations for T_{in} = 1050 K. At the same time, ethane consumption starts from 1000 K, while for numerical simulation for T_{in} > 1050 K.

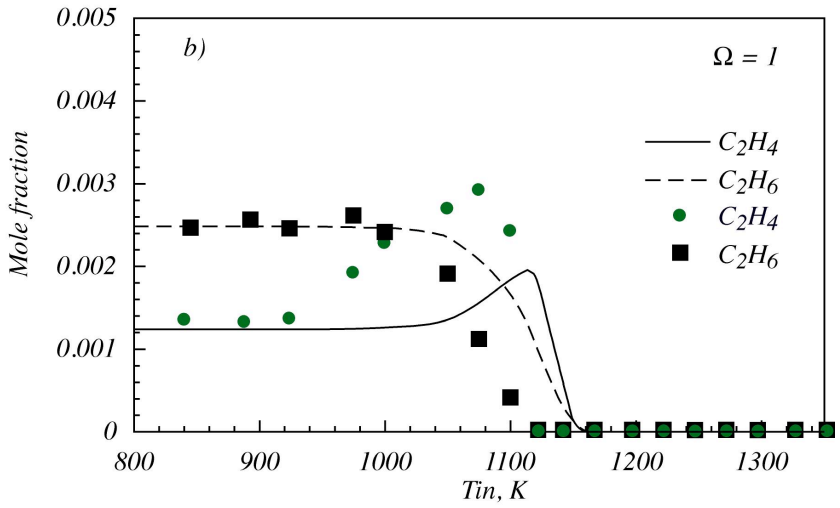

Fig VI.39 - Comparison between experimental and numerical C2H4 and C2H6 mole fraction versus Tin.

Fig VI.40 shows the molar concentration of CO and CO_2 both experimentally and numerically as function of T_{in}.

Experimental tests evince that CO and CO_2 concentration remains constant for T_{in} < 1000 K,. For higher inlet temperatures CO monotonically decreases down up to disappears for T_{in} > 1100K, while CO_2 concentration reaches a constant value of 12%.

Numerical results well predict CO_2 trend, while they fail for the CO trend. As matter of fact, numerical CO mole fraction trend show a maximum value, than it decreases down to a constant value while experimental data show that CO is completely converted.

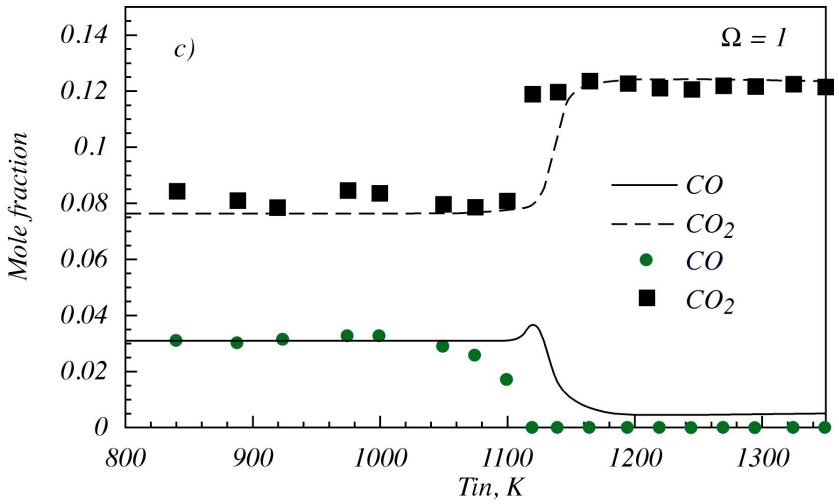

Fig VI.40 - Comparison between experimental and numerical CO and CO2 mole fraction versus Tin.

Finally, Fig VI.41 is relative to O_2 and H_2O. Experimentally it is possible to see that O_2 concentration decreases for $T_{in} > 1075$ K from the inlet value down to 3%, whereas water content reaches a constant value of about 1.3%.

In such a case, simulations are in agreement with experimental data, even though oxygen concentration at elevated temperature is not correct.

For stoichiometric conditions, oxygen it is not completely oxidized, while methane

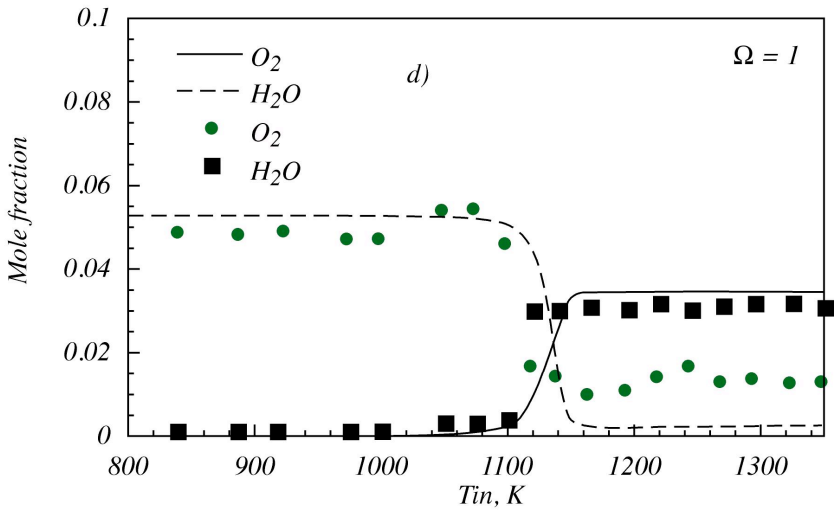

Fig VI.41 - Comparison between experimental and numerical O2 and H2O mole fraction versus Tin.

For stoichiometric conditions, experimental data suggest that oxygen is not completely consumed, as well as methane and hydrogen. They are produced but not completely converted at high temperature. Ethylene and ethane are completely oxidized to CO and water, as well as carbon monoxide. The main discrepancy with numerical results is that the kinetic model predicts a different trend of CO mole fraction as function of T_{in} and that CO is present also at elevated inlet temperature. Furthermore methane is fully converted at elevated temperatures for numerical simulations while a significative amount of methane is experimentally detected. Numerical hydrogen mole fractions are lower with respect to experimental data.

Fig VI.42-45 shows the experimental and numerical species mole concentration versus the mixture inlet temperature for fuel rich mixture characterised by an equivalence ratio equal to 0.7.

Species	Mole Fraction
O_2	*4,06*
N_2	*80,3*
CH_4	*1,56*
CO	*3,90*
CO_2	*9,7*
C_2H_4	*0,156*
C_2H_6	*0,31*

Tab. VI.4 - Reference mixture concentration for Ω = 0.7.

The inlet mixture composition is reported in Tab. VII.4. Fig VI.42 shows experimental and numerical methane and hydrogen mole fractions as function of the mixture inlet temperature. From experiments it comes out that the considered species concentration do not change with respect to inlet conditions for $T_{in} < 1050$ K. For $T_{in} > 1050$ K, their molar concentration increases and reaches a maximum value, at $T_{in} = 1220$ K for hydrogen and at $T_{in} = 1240/1260$ K. Following, their concentration slightly decreases. Simulations suggest

different mole concentrations trends. In particular, methane mole fraction remains constant up to T_{in} = 1100 K, then it decreases monotonically and is completely oxidised for T_{in} >1200 K. Hydrogen mole fraction is very similar to experimental values. As matter of fact, it is equal to zero up to T_{in} = 1050 K, then it increases up to a maximum value that occurs for T_{in} = 1220 K. Following, it slightly diminishes. Even though the hydrogen numerical molar fraction is not similar to the experimental values at high inlet temperature, the trend is well predicted.

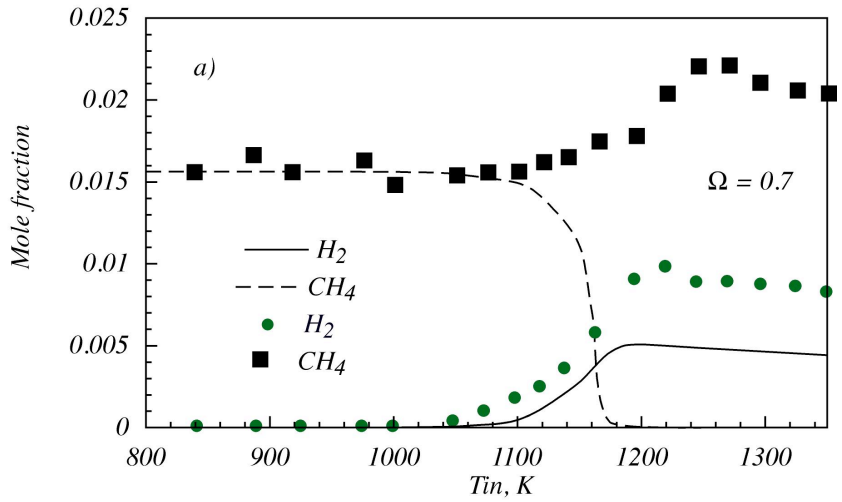

Fig VI.42 - Comparison between experimental and numerical CH4 and H2 mole fraction versus Tin.

Fig VI.43 concerns C_2H_4 and C_2H_6 molar concentration trend as function of T_{in}.

Experimental tests show that, their mole concentration is equal to the reference inlet values for T_{in} < 900 K. For T_{in} > 900 K, ethane concentration starts decreasing while ethylene one increases. For higher values of the mixture inlet temperature, C_2H_6 concentration monotonically decreases and becomes zero for T_{in} > 1225 K. On the contrary, ethylene concentration increases reaching a maximum value for T_{in} = 1175 K, then it decreases down to zero for T_{in} = 1125 K.

Simulations predict well the ethane and ethylene mole fraction trends, even though they underestimate ethylene values.

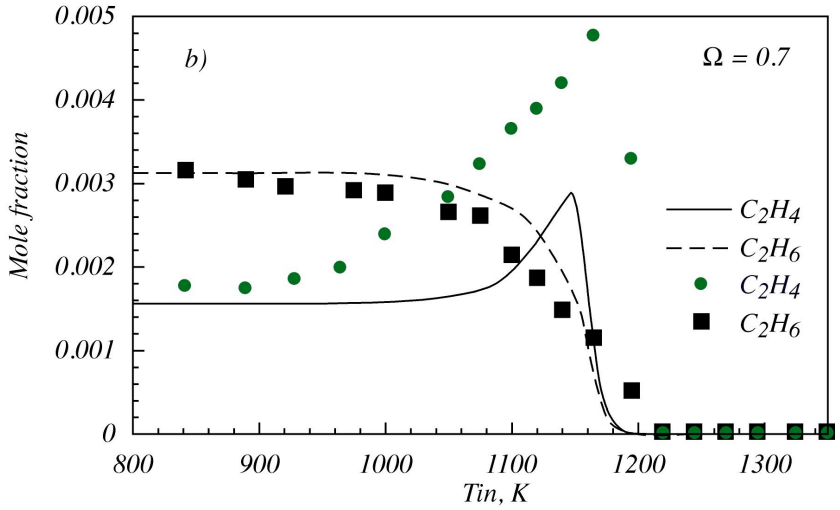

Fig VI.43 - Comparison between experimental and numerical C2H4 and C2H6 mole fraction versus Tin.

Fig VI.44 is relative to CO and CO_2 molar concentration. tests suggest that up to T_{in} = 1050 K, CO concentration remains constant. Thereafter, it monotonically decreases down to 0 for T_{in} = 1225 K. The CO_2 concentration remains constant for low temperatures and increases for T_{in} > 1120 K up to reach a constant value of about 11%.

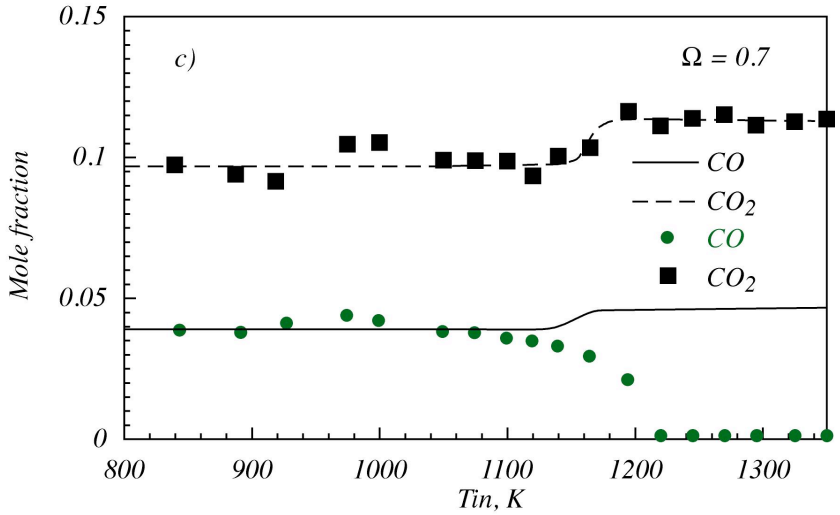

Fig VI.44 - Comparison between experimental and numerical CO2 and CO mole fraction versus Tin.

Simulations show that the CO_2 production is very well predicted. Numerical CO mole fraction increases as soon as T_{in} > 1140 K. Such trend is very different with respect to

experimental data. Finally, Fig VI.45 is relative to O_2. The O_2 concentration decreases for T_{in} > 1075 K from the inlet value down to 3%, whereas water content reaches a constant value of about 1.3%.

In such operative conditions, it was not possible to calculate water content since the H elemental mass balance was respected while C and O mass balance were not. Therefore it was not possible to evaluate water content, and such consideration implies the presence of CO or of a greater amount of CO_2.

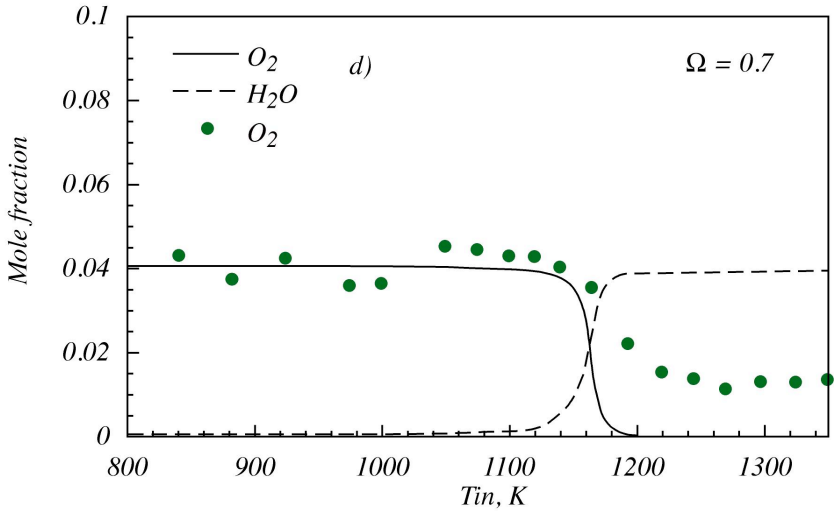

Fig VI.45 - Comparison between experimental and numerical O2 and H2O mole fraction versus Tin.

Simulations show that the oxygen concentration trend is well predicted by numerical integrations, even though oxygen mole fraction at elevated temperature is zero and does not correspond to experimental data.

For a mixture characterised by $\Omega = 0.7$, there is a good correspondence between experimental and numerical results for what concerns the temperatures that promote oxidation reactions, but the concentration trend as function of T_{in} of same species is very different. In particular methane and carbon oxide mole fraction trends are very dissimilar between experimental and numerical results.

In such case, on the basis on gas-chromatographic analysis, the chemical mass balances of C and O are not respected, so that higher concentrations of CO and/or CO_2 are plausible. Furthermore, the complete disappearance of CO at high inlet temperatures for a fuel rich mixtures is not reasonable.

In general it is possible to see that as the mixture composition is changed from lean to rich conditions, the onset of oxidation reactions occur for higher inlet temperatures and the shift from fuel no-conversion to fuel conversion conditions interests a wider inlet temperature range. The same behaviour is evident also from numerical simulations.

Chapter VII - Conclusion

In the context of academic and industrial research concerning combustion systems, the main targets are the achievement of a clean and efficient process. This means that, at the present time, the development of combustion systems strive to attain two different goals: the abatement or at least the reduction of pollutant emissions and the increase of the process efficiency, that implies the reduction of fuel consumption and hence CO_2 emissions.

The concurrent achievement of these targets is quite difficult to attain. In processes involving combustion, the abatement of pollutants often comes at the price of efficiency losses and vice versa. In other words, for the existing combustion systems it is to simultaneously satisfy these requirements (high efficiency and low pollution). In this context, the investigation on new combustion technologies is mandatory in order to respond to these issues.

In this field, MILD combustion is one of the most promising technology. It is characterized by an highly diluted and preheated working conditions. In particular, the mixture is diluted enough to be outside the flammability limits and preheated in order to exceed mixture auto-ignition temperature. These peculiarities allows to obtain an higher efficiency, lower pollutants emission as well as higher stability process with respect to traditional combustion process. One of the main important peculiarities of such technology is the high flexibility in terms of fuel blends used. High initial temperatures allow to exploit mixtures of different fuels such as methane as well as LCVG (Low Calorific Value Gases). The employment of fuels with low calorific value is conceivable in consideration of the high initial temperatures and the little gradient of temperature achieved in system which works in MILD combustion conditions. In addition, such fuel are frequently accompanied by a

large amount of diluent species (such as CO_2) and this characteristic makes it unusable in conventional system but suitable in MILD working conditions.

The massive employment of such technology in industrial plants is still, at the present time, not developed because of the lack of knowledge concerning the phenomenologies that occur in such non conventional combustion conditions. Therefore it is necessary a study on the basic aspects of the process in consideration of the huge difference with traditional combustion systems. The higher dilution of the mixtures used along with the high inlet temperatures lead to a reconsideration of the intrinsic characteristic of the oxidation process (such as oxidation time, auto-ignition time etc.). It does not occur in a restrict area of the combustion chamber, but evolves in the whole volume with homogeneous gradient of temperature through the chamber. This optimal characteristic prevents the occurrence of hot spot that in the long run could damage the plant and cause the loss of efficiency and increase pollutant formation. In this context, the task of this thesis has been to partially fill the need of experimental data on the oxidation process of fuel blends in highly diluted and preheated conditions at atmospheric pressure.

The ambient pressure is an another significant peculiarities of this thesis work in consideration of the lack of evidences in literature in such working condition. In fact, several data are available (both experimental and numerical) at high pressure because of the relevant importance in the majority of the industrial combustion systems. Nevertheless, the characterization of the combustion process at ambient pressure remains a crux point still unresolved. Although some industrial plants are already existent in the field of material treatment, the opportunity of a broad employment of combustion systems which work in MILD combustion conditions at ambient pressure is necessarily limited by this lack of knowledge. In this context, the contribution of the results presented is therefore essential in the development of awarenesses on the basic aspects related to this new combustion mode.

In particular, the experimental activities were focused on the ignition process of fuel blends and auto-ignition times were evaluated by means of a tubular flow reactor. Several criteria were defined and are available in scientific literature to detect the onset of the ignition process. On the basis of the temperature profiles acquired along the axial coordinate of the reactor, the auto-ignition time was defined as the time needed to observe an increment of temperature of ten degrees with respect to the inlet one. System highly diluted are characterized by low gradient of temperature, hence such criterion allows to highlight the different phenomenologies observed during the experimental tests.

Several working conditions were investigated and due to the experimental facility on purpose designed and set up, the working parameters can be varied independently from each other. Thus allowing to explore the effect of a single parameter on the whole process.

The assessment of the intrinsic peculiarities of MILD combustion process has allowed to focus the investigation tests on the crucial parameters of working. Moreover, the study was driven at filling the lack of experimental data relating to such parameters.

The high flexibility of such combustion system in terms of fuel used, has induced to explore the employment of two different energy carriers. Methane was chosen as a benchmark fuel because of its relevance in industrial field. In addition, methane blends is widely employed in scientific research even if the evidences available in literature are relating to different working conditions. Moreover, the study of the kinetic evolution of methane oxidation is the first step in order to deepen the knowledge on the oxidation process in MILD conditions. This is due to the relative simplicity of the methane molecule that acts as first guide to understand the oxidation process of heavy hydrocarbons as well as mixtures of them.

In this sense, further tests were performed with fuel blend named as *biogas*. The growing interest in different energy carriers alternative to fossil fuels emphasizes the scientific

research on gaseous fuel obtained by biomass treatments. The demand for experimental evidences concerning the oxidation of such alternative fuels is increasing on worldwide scale by now. In particular, the composition of the *biogas* employed during the experimental tests (62 % CO_2, 25 % CO, 10 % CH_4, 1 % C_2H_6 and 2 % C_2H_4 in volume) was chosen on the basis of literature evidences. This is relating to a typical mixture of gases obtained by subjecting biomass to a slow/conventional pyrolysis process. The choice was also made according to the features of such mixtures. On the one hand, the large amount of diluent species already existent in the mixture makes it suitable for the employment in MILD conditions. Moreover the low calorific value of such *biogas* make it as an ideal candidate in combustion system that works in non-conventional conditions. It is possible hence to include such fuel mixture in the class of LCVG (Low Calorific Value Gases).

The investigation on the different system behavior due to the variation of the dilution degree of the mixture is necessary according to the importance of such parameter in combustion system that evolves in MILD conditions. The degree of dilution was varied in a wide range both for methane and *biogas* and the phenomenologies observed are similar even though they occur in different working conditions.

For each dilution, it was possible to outline an overall reactivity map of the fuel blends. The map traces the phenomenologies observed in function of the feed ratio (C /O for methane, Ω for *biogas)* and the initial temperature T_{in} of the system. The range of temperatures investigated for a methane mixture varies between 1150 K and 1400 K and for feed ratios C/O comprise between 0.015 and 1. The variation of the initial temperatures of the system represents a further and important investigation because of the influence of such parameter on the system behavior. Moreover the feed ratio was considered and defined as C/O for methane and Ω for *biogas* mixtures. The characterization of the

oxidation process was hence made by varying the relative ratio between fuel and oxidant species and by exploring several conditions, from fuel lean to rich conditions.

Different phenomenologies were observed by acquiring temperature profiles. They were divided in five different areas in the reactivity map depending on feed ratio and T_{in}.

For low temperature the mixture does not show any phenomenologies and the range of parameters characterized by this absence of reactivity was named as *no-ignition zone*. As soon as the temperature increases, the reactions that lead to an increase of temperature and promote the onset of oxidation process start. The low presence of fuel in the mixture (fuel lean feed ratios) and hence, the high amount of oxygen encourages the beginning of such reactions. As a matter of fact, a *low reactivity zone* starts from these conditions and generally surrounds the real zone of ignition. This area was characterized by small increase of temperature ($\Delta T_{\max} < 10K$) and could be regard as a prelude of the *ignition zone*. In fact, the *ignition zone* defines the working conditions in which the mixture shows an increment of temperature equal to the chosen criterion.

In this zone, the characterization of the ignition process was deepened with the evaluation of the auto-ignition times of the mixtures.

Within the ignition region, a dynamic region was observed characterized by non-stable behavior. This zone is in general comprises between the area of low-reactivity and the occurrence of stable ignition. In such conditions the temperature profiles acquired show different behavior with subsequent ignition and no-ignition profiles. In order to deepen the study of such behaviors the intensity of the light emitted from the volume reactor was captured by means of an optical diagnostic system implemented at the end of the reactor. A small quartz window allows to appreciate such emission and different filters were used in order to capture a specific range of wavelengths. Moreover such analysis are relating to the presence of different species in the exhaust gases. These investigations were carried out

along with several samplings of the exhaust gases. In such a way, the presence of oxygen species was evaluated by using a colorimetric technique developed for the identification of traces of formaldehyde in the atmosphere. Results show that the presence of such species increases in the region of dynamic behaviours. The formaldehyde is an intermediate species in the oxidation kinetic mechanism of hydrocarbons and hence its presence is relating to the occurrence of dynamic conditions. Moreover, the optical analysis testifies such presence according to a higher light intensity captured for $\lambda \leq 320nm$.

Pyrolysis phenomenologies were also observed. The *pyrolysis zone* is always located in the fuel rich zone of the map whereas the low concentration of oxygen does not promote oxidative pathways. Moreover, the high temperature of the system decompose the first molecule of the fuel by means of dehydrogenation reactions. The pool of radicals formed afterwards lead to high molecular hydrocarbons with the occurrence of pyrolytic reactions and negative gradient of temperatures.

By varying dilution degrees it was investigated the importance of this parameter on the system behavior. In addition, different dilution levels (three for methane, two for *biogas*) were set and reactivity maps were compared in order to characterize the differences among them. The results have shown that by varying the amount of diluent in the initial mixtures, the overall reactivity of the system changes in terms of range of temperature and feed ratio in which different phenomenologies happen. In particular, a higher dilution decreases the reactivity of the system and delays the ignition times.

The effect of dilution is evident also on the maximum temperature acquired during the experimental tests. The comparison among the gradient of temperatures obtained by varying the dilution and keeping constant the initial temperature and C/O, shows a marked difference of the maximum temperature collected. In particular, for higher dilution level the ΔT_{max} are smaller because of the heat absorbed by the larger amount of inert species in

the mixture. On the opposite, lower dilution increases the reactivity of the system and leads to an easier ignition of the mixtures that show also higher gradient of temperatures. Finally, a different level of dilution of the mixtures feeding to the experimental facility implies different changes in the overall behavior of the system. An higher dilution decreases the overall reactivity of the system, reduces the ΔT_{max} obtained and retards the ignition of the fuel blends. On the opposite, a lower dilution leads to an easier ignition of the fuel with higher increase of temperature and lower delay of the ignition process.

Similar experimental works were also made for the *biogas* mixtures. The behavior of the system is similar with the possibility of observe similar phenomenologies by varying T_{in} and Ω.

The experimental tests show an higher tendency of the biogas to ignite with respect of methane. Mixtures show an increment of temperature equal to the described criterion 200 K earlier than methane blends. As a matter of fact, the range of initial temperatures investigated was shifted towards lower values and was between 900 K and 1350 K while $0.025 < \Omega < 10$.

In addition auto-ignition time evaluated are lower than methane and are compatible with industrial systems. It is evident that the feasibility of employing such mixtures as fuel under MILD conditions is hence proven.

In parallel with the experimental work, a deepen numerical analysis were carried out by means of commercial software. Chemkin and Cantera software were chosen as a valid tools to evaluate and test the several kinetic mechanisms available in literature. All of these mechanisms are validated in a wide range of working conditions and already represent an important means to face the challenges connected to the resolution of problems inherent combustion processes.

In particular, several mechanisms were chosen and tested in a wide range of parameters. A preliminary comparison was carried out in order to assess the times computed by means of the specific mechanism and the discrepancies among them. The temperatures investigated vary from 750 K up to 1400 K and auto-ignition times obtained show a linear trend by varying inlet temperature. The values computed are quite different and change significantly among the mechanisms. Only two mechanisms show a curve slope change for a specified range of temperature, know as NTC (Negative Temperature Coefficient) behavior. A deepen numerical study was made in order to understand the reason of this behavior typical of heavy hydrocarbons. Reaction path diagrams, rate of production of the main species and sensitivity analysis allow to understand the kinetic responsible of such behavior. Several tests were made also by varying the diluent species (CO_2, H_2O or N_2), the amount of diluent and the pressure of the system. Such simulations were carried out in order to understand the kinetic of methane and afterwards by choosing one mechanism a comparison between numerical and experimental τ_{ign} was made.

Results show an optimal correspondence between numerical and experimental ignition times for methane blends. Several comparisons were made for different feed ratios and by varying the initial temperature of the system. For each condition little differences were observed between numerical and experimental times. The mechanism is, hence able to predict the ignition times evaluated by means of tubular flow reactor at least at high temperature. The residence time of the experimental facility does not allow to appreciate the region of temperatures interested by the numerical NTC behavior. In particular, the experimental auto-ignition times evaluated were located in the high range of temperatures () whereas all the kinetic mechanisms show a linear trend.

Different considerations could be made for *biogas* mixtures. The numerical simulations were carried out also for such mixtures and the auto-ignition times were evaluated by varying the inlet temperature for different Ω values.

Results of the comparison shown a peculiar behavior. For high Ω (fuel lean condition) numerical times evaluated by means of Ranzi mechanism are higher than experimental ones.

The mechanism is not able to predict the auto-ignition times of the biogas mixture and the differences are quite large. A similar trend persist for lower Ω values even though the discrepancies become smaller. Close to stoichiometric condition ($\Omega = 1$), numerical and experimental τ_{ign} are similar with lower discrepancies. In particular, for $\Omega = 1$ the mechanism seems to well predict τ_{ign} of biogas blends, while for rich condition ($\Omega = 0.7$) the differences increase again. In this condition, in presence of a large amount of fuel, numerical times underestimated τ_{ign} evaluated experimentally. It is hence evident a reversal in the evaluation of ignition times. By passing through stoichiometric condition the mechanism, firstly overestimates and then underestimates the experimental auto-ignition times.

In order to deepen the knowledge of the oxidation pathways follow by the fuel blends, several samplings were made at the end of the reactor. Exhaust gases were sampled and analyzed by means of a gas chromatograpic that allows to verify the presence of some important species (such as CO_2, C_2H_4, CO, H_2, CH_4 etc.). A comparison between numerical and experimental species trend were made by varying initial temperature, with the aim to justify the discrepancy between auto-ignition times. The results of the comparison show clearly the reason of such differences.

For high Ω values the auto-ignition time evaluated by means of experimental reactor are shorter than numerical ones. In particular, for a value equal to 3.33 the experimental tests show that methane and hydrogen do not react, since after a concentration peak decreases and becomes equal to zero. A similar trend was shown for C_2 fuel species. Ethane mole fraction remains constant up to T_{in} = 1000 K, then it decreases and for Tin equal to about 1040 K it becomes zero. On the other hand ethylene does not react up to T_{in} = 920 K and for T_{in} = 975 K its concentration shows a maximum value, then it decreases and for Tin equal to about 1040 K it is not detectable anymore in the exhausted flue gases. Numerical simulation were carried out and similar trend for the species analyzed were shown in function of initial temperatures even if the the ignition process starts for higher temperature. The same behavior is observable for other species such as CO and CO2. Numerical results hence show a slower response to the increase of temperature and this influences auto-ignition time that becomes longer.

For stoichiometric condition the trend is similar but low differences were founded in the species profiles which move closer the ignition times evaluated.

Finally for a rich condition the behavior is quite different. The numerical auto-ignition times are lower than experimental ones and the reason was clearly shown by species profiles. Numerical simulations show a monotonically decreases for methane for a T_{in} equal to 1100 K. Experimental results shows instead a growth in the concentration of such species together with ethylene. The range of temperature in which the oxidation process happens is visibly larger from experimental evidences and methane does not decrease to zero. It is hence evident that kinetic mechanism is not able to predict auto-ignition time for biogas blends in MILD conditions. On the opposite, such mechanism is able to predict methane ignition time with good accuracy.

The composition of the two fuel blends allows to understand such behavior. Biogas could be considered as methane mixtures (in low concentration) with the addition of others light hydrocarbons (C_2H_6 and C_2H_4) and diluent (CO_2). Although the amount of such species is low in terms of volumetric composition, they change the oxidation pathways follow by the mixture.

As a result of such alteration, the global reactivity of the mixture change significantly as it is described above from the reactivity map outlined during the experimental work. The *biogas* mixture tends to ignite easily than methane although the phenomenologies observed are unvaried. Moreover the kinetic mechanism are not able to predict the auto-ignition times quite well.

All these considerations lead to asses that kinetic mechanism are not totally tuned in MILD combustion conditions. The auto-ignition times are well predicted since the mixture was made only by methane. As soon as light hydrocarbons were addicted to the blend mechanism fails and the discrepancies increase according to fuel rich condition.

This is hence evident that the highly preheated and diluted conditions affect the behavior of the system by changing the oxidative process both in terms of kinetic pathways follow by the mixture than in the auto-ignition times.

The rich database collected during the experimental works of this thesis represent a valid first step in the development of the required knowledge on these new combustion mode.

Although several data are collected, there is still the need to enlarge the range of parameters investigated. The variation of the chemical nature of the diluent (CO_2 and H_2O), the employment of different fuel, both gaseous or liquid as well as the extension towards heavy hydrocarbons are just some of the potential future challenges which scientific research has to face.

References

A. B. Bendtsen, P. G., K.D. Johansen. "Low temperature oxidation of methane: the influence of nitrogen oxides." Combust Sci Technol **151**(1): 31-71.(2000)

A. Burcat, K. S., A. Liftshitz. "Shock-Tube Investigation of Comparative Ignition Delay Times for C1-C5 Alkanes." Combust Flame **16**: 29-33.(1971)

A. Cavaliere, M. d. J. "Mild combustion." Progress in energy and combustion science **30**(4): 329-366.(2004)

A. Cavigiolo, M. A. G., A. Effugi, . "Mild Combustion in a Laboratory Scale Apparatus." Combust Sci Technol **175**(8): 1347-1367.(2003)

A. Effuggi, D. G., M. Derudi, R. Rota. "Mild combustion of methane-derived fuel mixtures: Natural gas and biogas." Combust Sci Technol **180**(3): 481-493. (2008)

A. G. Gaydon, I. R. H. (1963). The shock tube in high-temperature chemical physics, Reinhold Pub. Corp. (New York).

A. Gaydon, N. M., J. Simonson (1955). Chemical and spectroscopic studies of blue flames in the auto-ignition of methane. Proceedings of the Royal Society of London. Series A, Mathematical and Physical Sciences (1934-1990).

A. K. Gupta (17-18 January 2000). Flame characteristic and challenhges with high temperature air combustion. 2nd International Seminar on high temperature air combustion in industrial Furnaces, Stockholm, Sweden.

A. K. Gupta. "Thermal characteristics of gaseous fuel flames using high temperature air." Eng Gas Turbines Power **126**(1): 9-19.(2004)

A. Konnov (2010). "Mechanism ver. 0.5. <http://homepages.vub.ac.be/~akonnov/science/mechanism/main.html>."

A. Lefebvre (1999). Gas Turbine Combustion. T. F. P. Group.

A. Milani (17-18 January 2000). "Mild Combustion" techniques applied to regenerative firing in industrial furnaces" 2nd International Seminar on High Temperature Air Combustion in Industrial Furnaces, Stokholm, Sweden.

A. Milani, A. S. "Diluted Combustion Technologies." IFRF Combustion Journal **1**: 1-32.(2001)

A. Parente, C. G., L. Tognotti. "Effect of the combustion model and kinetic mechanism on the MILD combustion in an industrial burner fed with hydrogen enriched fuels." Int J Hydrog Energy **33**(24): 7553-7564.(2008)

A. Ponzio, S. S., W. Yang. "Nitrogen release during thermochemical conversion of single coal pellets in highly preheated mixtures of oxygen and nitrogen." Fuel **88**(6): 1127-1134.(2009)

A. Saponaro. Combustion & Environment Research Centre – Ansaldo Caldaie. 2009.(2009)

B. B. Dally, A. N. K., R. S. Barlow. "Structure of turbulent non-premixed jet flames in a diluted hot co-flow." Proc. Combust. Inst. **29**: 1147-1154.(2002)

B. B. Dally, E. R., N. Peters. "Effect of fuel mixture on moderate and intense low oxygen dilution combustion." Combust Flame **137**(4): 418-431.(2004)

B. B. Dally, S. H. S., R. A. Craig, P. J. Ashman, G. G. Szego. "On the burning of sawdust in a MILD combustion furnace." Energy Fuels.(2010)

B. L. Crynes, L. F. A. "Pyrolysis of Propane in Tubular Flow Reactors. Kinetics and Surface Effects." Ind. Eng. Chem. Res. **8**(1): 25-31.(1969)

B. Mullins. "Studies of the Spontaneous Ignition of Fuels injected into a hot airstream." Fuel **32**: 211-342.(1953)

B. Özdemir, N. P. "Characteristics of the reaction zone in a combustor operating at mild combustion." Exp Fluids **30**(6).(2001)

C. Aul, E. P. (2009). Early Ignition in Low-Temperature, High Pressure Shock-Tube Experiments for Non-Diluted Alkane Blends in Air. 6th U.S. Joint Combustion Meeting.

C. Bowman, M. F., W. R. Gardiner, G. Smith (1999). "The GRI 3.0 chemical kinetic mechanism."

C. Branca, P. G., C. Di Blasi. "GC/MS Characterization of Liquids Generated from Low-Temperature Pyrolysis of Wood." Ind. Eng. Chem. Res. **42**: 3190-3202. (2003)

C. Galletti, A. P., L. Tognotti. "Numerical and experimental investigation of a mild combustion burner." Combust Flame **151**(4): 649-664.(2007)

C. Galletti, A. P., M. Derudi, R. Rota, L. Tognotti. "Numerical and experimental analysis of NO emissions from a lab-scale burner fed with hydrogen-enriched fuels and operating in MILD combustion." Int J Hydrog Energy **34**(19): 8339–8351.(2009)

C. Goy, A. M., G. Thomas. "Autoignition characteristics of gaseous fuels at representative gas turbine conditions." ASME Paper – 2001-GT-0051. (2001)

C. J. Mueller, M. P. B. M., L. M. Pickett, W. J. Pitz, C. K. Westbrook (2003). The Oxygen Ratio: A Fuel-Independent Measure of Mixture Stoichiometry. 30th International Symposium on Combustion, Chicago, IL, United States.

C. K. Westbrook. "An Analytical Study of the Shock Tube Ignition of Mixtures of Methane and Ethane." Combust Sci Technol **20**(1-2): 5-17.(1979)

C. K. Westbrook, F. L. D. "Chemical kinetic modeling of hydrocarbon combustion." Progress in Energy and Combustion Science **10**(1): 1-57.(1984)

D. B. Spalding (1979). Combustion and Mass Transfer. Spontaneous Ignition, Pergamon Press. **15**.

D. Healya, H. J. C., S. Dooleya, J.M. Simmiea, D.M. Kalitanb, E.L. Petersenc, G. Bourqued. "Methane/propane mixture oxidation at high pressures and at high, intermediate and low temperatures." Combust Flame **155**(3): 451-461. (2008)

D. J. Beerer (2009). Autoignition of Methane, Ethane, Propane and Hydrogen in Turbulent High Pressure and Temperature Flows. Mechanical and Aerospace Engineering. California, UNIVERSITY OF CALIFORNIA, IRVINE. **Master of Science**.

E. Petersen, D. D., R. Hanson. "Kinetics modeling of shock-induced ignition in low-dilution CH4/O2 mixtures at high pressures and intermediate temperatures." Combust Flame **117**(1-2): 272-290.(1999)

E. Ranzi, T. F., A. Frassoldati, A. Cuoci (2010). "CRECK modeling. <http://creckmodeling.chem.polimi.it/C1C31006.CKI>."

E. Taback. "The Autoignition Characteristics of JP-4 at High Temperature and Pressure." Pratt & Whitney Aircraft.(1971)

F. C. Christo, B. B. D. "Modeling turbulent reacting jets issuing into a hot and diluted coflow." Combust Flame **42**: 117-129.(2005)

F. Dryer, M. C. "Ignition of syngas/air and hydrogen/air mixtures at low temperatures and high pressures: Experimental data interpretation and kinetic modeling implications." Combust Flame **152**: 293-299.(2008)

F. Williams. " <http://maeweb.ucsd.edu/~combustion.cermech>."

G. G. Szegö, B. B. D., G. J. Nathan. "Scaling of NOx emissions from a laboratory-scale mild combustion furnace." Combust Flame **154**: 281–295.(2008)

G. L. Agafonov, P. A. V. "Shock tube and modeling study of soot formation during the pyrolysis and oxidation of a number of aliphatic and aromatic hydrocarbons." Proc. Comb. Inst. **33**(625-632).(2011)

G. M. Choi, M. K. "Advanced low NOx combustion using highly preheated air." Energy Conv. Manag. **42**(5): 639-652.(2001)

G. Pang, D. D., R. Hanson. "Experimental Study and Modeling of Shock Tube Ignition Delay Times for Hydrogen-Oxygen- Argon Mixtures at Low Temperatures." Proc Combust Inst **32**: 181-188.(2009)

G. Schott, J. K. "Kinetics Studies of Hydroxyl Radicals in Shock Waves, II. Induction Times in Hydrogen-Oxygen Reactions." Journal of chemical physics **29**(5): 1177-1182.(1958)

G. Zhou, G. A. K. "An analytical examination of various criteria for defining autoignition within heated methane-air homogeneous mixtures." J Eng Resour Technol Trans **116**: 175-180.(1994)

G.G. Szegö, B. B. D., G.J. Nathan. "Operational characteristics of a parallel jet MILD combustion burner system." Combust Flame **156**: 429–438.(2009)

H. Stadler, D. R., M. Förster, A. Shuster, R. Kneer, G. Scheffknecht. "NOx-emissions from flameless coal combustion in air, Ar/O2 and CO2/O2." Proc Combust Inst **32**(2): 3131-3138.(2009)

H. Stadler, D. T., M. Foerster, R. Kneer. "On the influence of the char gasification reactions on NO formation in flameless coal combustion." Combust Flame **156**(9): 1755-1763.(2009)

H. Tsuji, A. K. G., T. Hasegawa, M. Katsuki, K. Kishimoto, M. Morita (2003). High temperature air combustion from energy conservation to pollution reduction.

H. Y. Qi, Y. H. L., C. F. You. "Emission on NOx in high temperature combustion with low oxygen concentration." J. Combust. Sci. Technol. **8**(1): 17-22. (2001)

H. Zhang, G. Y., J. Lu. "Development of high temperature air combustion technology in pulverized fossil fuel fired boilers." Proc. Combust. Inst. **31**(2): 2779-2785.(2007)

J. A. Wunning, J. G. W. "Flameless oxidation to reduce thermal NO-formation." Prog. Energ. Combust. **23**(1): 81-94.(1997)

J. de Vries, E. P. "Autoignition of Methane Based Fuel Blends under Gas Turbine Conditions." Proc Combust Inst: 3163 -3171.(2007)

J. Huang, P. G. H., W. K. Bushe, S. R. Munshi. "Shock-tube study of methane ignition under engine-relevant conditions: experiments and modeling." Combust Flame **136**(1-2): 25-42.(2004)

J. Koornneef, A. F. "Development of fluidized bed combustion—An overview of trends, performance and cost." Prog. Energ. Combust.(2007)

J. M. Simmie. "Detailed chemical kinetic models for the combustion of hydrocarbon fuels." Prog. Energ. Combust. **29**(6): 599-634.(2003)

J. Meyer, A. K. O. (1971). On the shock-induced Ignition of Explosive Gases. Thirteenth Symposium (International) on Combustion**:** 1153-1164.

J. Mi, P. L., C. Zheng. "Numerical Simulation of Flameless Premixed Combustion with an
Annular Nozzle in a Recuperative Furnace." Chinese J Chem Eng **18**: 10-17. (2010)

J. T. Wang, H. Y. Q., Y. H. Li. "Experimental study on heat transfer performance of honeycomb heat regenerator." J Eng Thermophys **24**(5): 897-899.(2003)

J. Warnatz, U. M., R. Dibble (2006). Combustion: physical and chemical fundamentals, modeling and simulation, experiments, pollutant formation. Berlin.

J. Yuan, I. N. "Effects of Air Dilution on Highly Preheated Air Combustion in a Regenerative Furnace." Energ Fuel **13**: 99-104.(1999)

L. Cowell, A. L. "Influence of Pressure on Autoignition Characteristics of Gaseous Hydrocarbon-Air Mixtures." SAE Technical Paper.(1986)

L. Spadaccini. "Autoignition Characteristics of Hydrocarbon Fuels at Elevated Temperatures and Pressures." Journal of Engineering for Power.(1976)

L. Spadaccini, M. C. "Ignition Delay Characteristics of Methane Fuels." Progress in Energy and Combustion Science **20**: 431- 460.(1994)

M. De Joannon, A. C., R. Donnarumma, R. Ragucci. "Dependence of autoignition delay on oxygen concentration in mild combustion of high molecular weight paraffin." Proc Combust Inst **29**(1): 1139-1146.(2002)

M. De Joannon, A. C., T. Faravelli, E. Ranzi, P. Sabia, A. Tregrossi. "Analysis of process parameters for steady operations in methane mild combustion technology." Proc. Combust. Inst. **30**(2): 2605-2612.(2005)

M. De Joannon, G. L., F. Beretta, A. Cavaliere, C. Noviello. "Mild Combustion: Process Features and Technological Constrains." Combustion Science and Technology **153**: 33-50.(2000)

M. de Joannon, P. S., G. Sorrentino, A. Cavaliere. "Numerical study of mild combustion in hot diluted diffusion ignition (HDDI) regime." Proc. Combust. Inst. **32**(2): 3147–3154.(2009)

M. de Joannon, R. R., A. Cavaliere. "Laser Excited Emission and Chemiluminescence from Autoigniting Spray." Combust Sci Technol **155**(1): 129-147.(2000)

M. Derudi, A. V., R. Rota. "Mild combustion of industrial hydrogen-containing byproducts." Ind. Eng. Chem. Res. **46**(21): 6806-6811.(2007)

M. Derudi, A. V., R. Rota. "Sustainability of mild combustion of hydrogen-containing hybrid fuels." Proc. Combust. Inst. **31**: 3393–3400.(2007)

M. Fantuzzi, L. B. "Industrial applications of Tenova FlexyTechÂ® flameless low NOx burners." Revue de Metallurgie Cahiers d'Informations Techniques **105**(4).(2008)

M. Frenklach, D. E. B. "Shock-initiated ignition in methane-propane mixtures." Combust Flame **56**(1): 1-27.(1984)

M. G. Zabetakis. "Flammability characteristics of combustible gases and vapors." Bureau of Mines Washington DC.(1965)

M. Galbiati, A. C., A. Effuggi. "Mild combustion for fuel-NOx reduction." Combust Sci Technol **176**(7): 1035-1054.(2004)

M. Holton, P. G., M. Klassen, R. Roby, G. Jackson (2009). Autoignition delay time measurements of methane, ethane, and propane pure fuels and methane-based fuels blends. SME Turbo Expo. Orland Florida.

M. Katsuki, T. H. (1998). The science and technology of combustion in highly preheated air. Twenty-Seventh Symposium (International) on Combustion/ The Combustion Institute**:** 3135–3146.

M. Mancini, P. S., R. Weber. "On mathematical modelling of flameless combustion." Combust Flame **150**(1-2): 54-59.(2007)

M. Mancini, R. W., U. Bollettini. "Predicting NOx emissions of a burner operated in flameless oxidation mode." Proc. Combust. Inst. **29**(1): 1155-1163.(2002)

M. Zieba, A. B., A. Schuster. "Ammonia chemistry in a flameless jet." Combust Flame **156**(10): 1950-1956.(2010)

N. Krishnamurthy, P. J. P., W. Blasiak. "Studies on low-intensity oxy-fuel burner." Proc. Combust. Inst. **32**(3139-3146): 3139.(2009)

N. Peters. "Principles and Potential of HICOT Combustion."(2000)

N. Shimo (2000). Fundamental Research of oil combustion with highly preheated air. 2nd International Seminar on high temperature air combustion in industrial Furnaces, Stokholm, Sweden.

N. Syred. "A review of oscillation mechanisms and the role of the precessing vortex core (PVC) in swirl combustion systems." Prog. Energ. Combust. **32**(2): 93-161.(2006)

O. Levenspiel (1958). Chemical Reaction Engineering.

O. T. Onsager, R. L., P. Søraker, A. Anundskaas, B. Helleborgc. "The homogeneous gas phase oxidation of methane and the retarding effect of basic/inert surfaces." Catalysis Today **4**(3-4): 355-363.(1989)

O. V. Sokolov, Y. V. P., V. S. Arutyunov, V. Ya. Basevich, V. I. Vedeneev. "Study of cool-flame phenomena during self-ignition of methane-oxygen mixtures." Russian Chemical Bulletin **45**(10): 2316-2320.(1996)

P. Giudicianni (2005). Composizione Chimica e caratteristiche di combustione dei liquidi derivati da pirolisi di biomasse. Department of Chemical Engineering. Naples, University of Naples "Federico II".

P. Gokulakrishnan, G. G., M. Klassen, R. Roby (July 2007). Autoignition of Aviation Fuels: Experimental and Modeling Studies. 43rd AIAA/ASME/SAE/ASEE Joint Propulsion Conference & Exhibit. Cincinnati.

P. J. Kim, U. S., G. Scheffknecht. "Comparison of different global reaction mechanisms for mild combustion of natural gas." Combust Sci Technol **180**(4): 565-592.(2008)

P. Li, J. M., B. B. Dally, R. A. Craig, F. Wang. "Premixed Moderate or Intense Low-Oxygen Dilution (MILD) Combustion from a Single Jet Burner in a Laboratory-Scale Furnace." Energ Fuel.(2010)

P. Papas (1994). An Additive Approach to Supersonic Combustion: Use of Silane in Hydrogen-Air Systems and Consideration of Pyrophoric Metals. Mechanical & Aerospace Department, Princeton University. **Master of Science**.

P. R. Medwell, P. A. M. K., B. B. Dally. "Simultaneous imaging of OH, formaldehyde, and temperature of turbulent nonpremixed jet flames in a heated and diluted coflow." Combust Flame **2007**: 48-61.(2007)

P. R. Medwell, P. A. M. K., B. B. Dally. "Imaging of diluted turbulent ethylene flames stabilized on a Jet in Hot Coflow (JHC) burner." Combust Flame **152**: 100-113.(2008)

P. S. Yarlagadda, L. A. M., N. R. Hunter, H. D. Gesser. "Direct conversion of methane to methanol in a flow reactor." Ind. Eng. Chem. Res. **27**(2): 252-256.(1988)

P. Sabia, M. d. J., S. Fierro, A. Tregrossi, A. Cavaliere. "Hydrogen-enriched methane Mild Combustion in a well stirred reactor." Exp Therm Fluid Sci **31**: 469-475.(2007)

R. Brokaw, J. J. (1955). Effect of Temperature, Pressure and Composition on Ignition Delays for Propane Flames. Fifth Symposium (International) on Combustion, New York.

R. Sawyer (1965). The Homogeneous Gas Phase Kinetics of Reaction in the Hydrazine-Nitrogen- Tetroxide Propellant Systems. Department of Mechanical & Aerospace Engineering, Princeton University.

R. Seyfioglu, M. O. "Investigation of air–water exchange of formaldehyde using the water surface sampler: Flux enhancement due to chemical reaction." Atmospheric Environ **40**(19): 3503-3512.(2006)

R. Swigart (1958). Study of the Kinetics of the Hydrogen-Oxygen Reaction in a New Flow Reactor. Aeronautical Engineering Department, Princeton University. **Master of Science**.

R. Weber, J. P. S., W. Kamp. "On the (MILD) combustion of gaseous, liquid, and solid fuels in high temperature preheated air." Proc Combust Inst **30**(2): 2623-2629.(2005)

R. Weber, S. O., N. Lallemant, A.D. Verlann (2000). Combustion of natural gas with high-temperature air and large quantities of flue gas. Proc. Combust. Inst.

S. Orsino, R. W. "Numerical simulation of combustion of natural gas with high temperature air." Combust Sci Technol **170**(1): 1-34.(2001)

S. R. Wu, W. C. C., J. Chiao. "Low NOx heavy fuel oil combustion with high temperature air." Fuel **85**(5-6): 820-828.(2007)

T. B. Hunter, H. W., T. A. Litzinger, M. Frenklach. "The oxidation of methane at elevated pressures: experiments and modeling." Combust Flame **97**: 201-224.(1994)

T. Nash. "The colorimetric estimation of formaldehyde by means of the Hantzsch reaction." Biochem J. **55**(3): 416-421.(1953)

T. Plessing, N. P., J. G. Wunning (1998). Laseroptical investigation of highly preheated combustion with strong exhaust gas recirculation. Twenty-Seventh Symposium (International) on Combustion/The Combustion Institute**:** 3197-3204.

T. Salthammer. "Comparison of analytical techniques for the determination of aldehydes in test chambers." Chemosp **73**(1351-1356).(2008)

T. Wada, F. J., D. Abel, N. Peters. "An Instability of Diluted Lean Methane/Air Combustion: Modeling and Control." Combust Sci Technol **183**: 1-19.(2011)

T. Wada, G. P., N. Peters. "Numerical Investigations of Highly Diluted Lean CH4/ Air Oscillations at Low Temperatures."

T. Wagner. "Task 200-Ignition Delay characterization."(1990)

T. Yasuda (1999). Dissemination project of high performance industrial furnace with use of high temperature air combustion technology. 2nd International High Temperature Air Combustion Symposium.

V. Zhukov. "Zhukov V. Kinetic model of alkane oxidation at high pressure from methane to n-heptane. Combust Theor Model 2009;13(3):427–42." Combust Theor Model **13**(3): 427-442.(2009)

W. Yang, A. P., C. Lucas. "Performance analysis of a fixed-bed biomass gasifier using high-temperature air." Fuel Process Technol. **87**(3): 235-245.(2006)

W. Yang, W. B. "Flame entrainments induced by a turbulent reacting jet using high-temperature and oxygen-deficient oxidizers." Energ Fuel **19**(4): 1473-1483.(2005)

W. Yang, W. B. "Mathematical modelling of NO emissions from high-temperature air combustion with nitrous oxide mechanism." Fuel Process Technol. **86**(9): 943–957.(2005)

W. Yang, W. B. "Numerical simulation of properties of a LPG flame with high-temperature air." Int. J. Therm. Sci. **44**(10): 973-985.(2005)

W. Yang, W. B. "Numerical study of fuel temperature influence on single gas jet combustion in highly preheated and oxygen deficient air." Energ **30**(2-4): 385-398.(2005)

X. J. Xing, Q. Z. L. "Research on NOx formation in normal temperature air flameless combustion." Acta Scientiae Circumstantiae **26**(10): 1671–1676. (2006)

Y. H. Song, W. B., D.W.Blair, V.J. Siminski (1981). Conversion of Fixed Nitrogen to N2 in rich Combustion. Symp. (Int.) Combust. (proc.).

Y. Yu, G. W., Q. Lin, C. Ma , X. Xing. "Flameless combustion for hydrogen containing fuels. ." Int J Hydrog Energy **35**(7): 2694–2697.(2010)

Z. Tang, M. A. P.-y., L.I. Yong-Ling, C. Tang, X. Xing, Q. Lin. "Design and experiment research of a novel pulverized coal gasifier based on flameless oxidation technology." Proc CSEE **30**(8): 50-55.(2010)